INVESTIGATING BIOFILM ADHESION AND COHESION FORCES IN RESPECT TO CLEANING APPLICATIONS

by

ARTEMIS TSIAPRAZI STAMOU

A Thesis

to

The University of Birmingham

For the degree of

DOCTOR OF PHILOSOPHY

School of Chemical Engineering College of
Engineering and Physical Sciences
The University of Birmingham
[May 2021]

ABSTRACT

Biofilms are complex microbial ecosystems formed by one or more bacteria species immersed in an extracellular matrix of different compositions depending on the environment and the colonizing species. While bacteria are beneficial for several technological bioprocesses, they could be catastrophic for our everyday lives as humans. In schools, healthcare facilities, food processing lines, our homes, we try to keep every surface clean and sterilized from our invisible "friends" in order to prevent ourselves from infectious diseases. Since biofilms are living communities, not traceable with the human eye, reliable methods are needed for the investigation of their attachment, growth and removal on surfaces, three different phenomena all regulated by forces. The goal of this PhD was to understand how the different material surfaces affect the above phenomena.

In the first study the initial biofilm growth as well as the removal of *Pseudomonas fluorescens* and *Pseudomonas putida* biofilms from different material surfaces was investigated. After 30 minutes of growth at 25 °C for *P. fluorescens* and at 30°C for *P. putida* it was found that *P. fluorescens* showed higher percentage of surface coverage comparing to *P. putida* on all surfaces. In terms of different materials, the percentage of the area covered by bacteria was significantly lower on plastic surfaces (PET, PTFE and polypropylene) than on more hydrophilic surfaces like glass, hydroxyapatite and stainless steel. The biofilm residual contamination was investigated using a parallel-plate flow chamber, developed for this thesis, where three different cleaning conditions were tested on stainless steel, polycarbonate and plasma-treated polycarbonate surfaces: 1) Water rinsing under shear stress conditions, 2) NaOH cleaning in static conditions and 3) NaOH cleaning under shear stress conditions. It was found that the procedure that combined NaOH and shear stress was more effective for all material surfaces. In terms of surfaces, it was seen that stainless steel was cleaned more efficiently compared to plastic surfaces. In terms of biofilm residual contamination, a more distinct biofilm removal was observed *for P. putida* than for *P. fluorescens*.

In the second study the removal of real mixed-microbial biofilm from common artificial surfaces was investigated using commercial enzymatic detergents and disinfectants used in the food industry. A mixed-microbial sample was sourced from a meat packaging line and biofilm was grown under high shear conditions on stainless steel and PET surfaces and the synergistic effect of enzymes in biofilm cleaning was studied. The cleaning effectiveness was evaluated in response to different

formulations containing non-foaming commercial surfactants among with amylase, protease and lipase at neutral pH. The microscopic observation of changes in biofilm structure using SEM and confocal analyses indicated that enzymes were very effective in biofilm removal, especially on stainless steel surfaces. It was observed that the combination of enzymes was more efficient than formulations based in a single enzyme regardless of surfaces. The treatment with formulation combining amylase, protease and lipase, effectively decreased the total biofilm mass, the bacteria viability and the polysaccharide content in the biofilm

The last chapter of this PhD was focused on the biofilm EPS and the role that the forces between EPS and the surrounding interphases play in biofilm cleaning. Regardless of the bacteria species, EPS is generally comprised of soluble, gel-forming polysaccharides, proteins and eDNA, as well as insoluble components such as amyloids, cellulose, fimbriae and pili. Thus, a polysaccharide and specifically alginic acid was chosen as an EPS-related material to be studied. Moreover, surface modification can play a significant role in the prevention of biofilm attachment and growth and consequently the achievement of more effective cleaning. For this reason, the goal of that study was to measure directly the adhesion and cohesion forces, developed between an EPS-related material and surfaces while in air or under simulations of cleaning conditions like water and different pH solutions. Several polymers were studied as material for polycarbonate surface modification under two different pH conditions (3 and 11) and the adhesion and cohesion forces of alginic acid were measured under air, water, NaOH and HCl solutions. Overall, it was seen that during acidic conditions the cohesive strength of alginic acid increases, while in water and in NaOH solution it decreases. Nonetheless, the adhesive strength showed decline during all cleaning conditions which depended highly on the surface. Furthermore, the polymer surface modification of the polycarbonate surfaces had a significant impact on the adhesive strength of the alginic acid in all cases. Of great interest were two polymers, Lupasol and Poly-(2-ethyl-2-oxazoline), as they caused the most important reduction in the adhesive strength of the alginic acid.

Since the results from all studies have been very interesting a future recommendation would be to expand the experiments through the combination of the relevant conditions. Thus, the technique used to measure adhesion and cohesion forces on alginic acid could be adjusted at the micron-mm scale to measure model *P. fluorescens* and *P. putida* biofilms under the optimal enzymatic conditions.

DEDICATION

This work is dedicated to my parents, Dimitri Tsiaprazi and Maria Stamou, for all their love, support and encouragement during this journey; to myself, as a reminder that we sometimes can find enough strength inside us in order to achieve goals that used to seem impossible; and to Dr. Konstantinos Tzaros, who was always showing interest in my work and, at some point in this life, "dragged" me into the amazing world of engineering.

ACKNOWLEDGEMENTS

First, I would like to enunciate my sincere gratefulness to Prof. Peter J. Fryer, School of Chemical Engineering, University of Birmingham, who was my supervisor for the completion of this Ph.D. thesis. He helped me, gave me important advice and encouraged me during the writing of this thesis.

I also want to express my gratitude to my first supervisor, Dr. Kostas Gkatzionis, who chose me for the BioClean project when he was teaching at the same School, now an Assistant Professor at the University of Aegean. Dr. Gkatzionis gave valuable advice during the first two years of this work and encouraged me throughout my Ph.D. journey.

Special thanks go to my industrial supervisors, Anju Brooker and Eric Robles from P&G Ltd, on Newcastle upon Tyne, who imagined and created the BioClean project and provided me with ideas and suggestions that broadened my horizones and strengthened my work.

Special thankfulness goes to Dr. Irene Ylla, Itram Hygiene, Vic, Spain, for her precious help during my secondment, both in terms of work and encouragement throughout my adaptation in a completely new environment. Her friendship and guidance were crucial for the accomplishment of this work.

My keen appreciation goes to Professor Anna Romani of the Institute of Aquatic Ecology in Girona, Spain, for her valuable support in the experiments during my secondment.

At this point, I wish to spend a few words for some people that made this Ph.D. work into a life journey. These are my BioClean friends and ESR colleagues, Helena, Hugo, Alessandra, Luca, Valeria, Silvia, Kamila, Gabrielle, Lukas, Osama, Abishek, Lili, Xavier and Joana. Together, we entered the amazing life of being a researcher, the experience of travelling around the world for conferences and working meetings, the fascinating journey of adapting in these multinational environments while sharing our different cultures. I want to thank them all for their support, love and friendship, which was crucial at times.

Finally, thanks to everyone who is, or was considered at a point, a BioClean person. I think I can speak for everyone among the 15 ESRs if I say that you changed our lives forever. Thanks for making it happen.

Table of Contents

List of Figures

of EPS (blue-colored), dead (red-colored) and alive (green-colored) singe cell bacteria of a mixed-microbial biofilm.

Figure 3.10: The average thickness (μm) is the average height of all columns taken together. The average thickness is presented for the entire observed area of the biomass containing columns.

Figure 3.11: Micromanipulation stage that consists of: 1) Power supply and signal conditioner, 2) PC monitor for data collection, 3) Force transducer, 4) T-Shaped probe and 5) Microscopic camera for sample visualization and adjustment.

Figure 3.12: (Left) Representation of rectangular samples mounted on the micromanipulation stage. (Right) The development of 100μm thick alginic acid films using the micromanipulation stage.

Figure 4.1: Average work of adhesion (mN/m) of Hydroxyapatite (HA), Stainless steel (SS), Borosilicate glass (BG), Polycarbonate (PC), Nylon, Polytetrafluoroethylene (PTFE), Polypropylene (PRP) and Polyethylene Terephthalate (PET). The error bars are the standard deviation of the triplicate repeats for the work of adhesion.

Figure 4.2: Average work of adhesion (mN/m) of non-modified polycarbonate coupons (PC_NonModified) and plasma-treated polycarbonate coupons for different 5 (PC_PlasmaTreated_5min), 10 (PC_PlasmaTreated_10min) and 30 (PC_PlasmaTreated_30min) minutes. The error bars are the standard deviation of the triplicates work of adhesion. Capital letters indicate statistically significant different groups at each cleaning step (Tukey's test, $p<0.05$). The same letter indicates no significant difference, i.e., A‡A: no significant difference, one similar letter indicates partial difference, i.e., A‡AB: slightly different and different letter indicates significant difference, while the furthest from control letter A, the most significant the difference, i.e., A‡B: significant difference and A‡C: more significant

difference.

Figure 4.3: $Log_{10}(CFU/cm^2)$ of *P. fluorescens* and *P. putida* biofilm initial attachment on Hydroxyapatite (HA), Stainless steel (SS), Borosilicate glass (BG), Polycarbonate (PC), Nylon, Polytetrafluoroethylene (PTFE), Polypropylene (PRP) and Polyethylene Terephthalate (PET). The error bars are the standard deviation of the triplicate's biofilm concentration in $log_{10}(CFU/cm^2)$. Capital letters indicate statistically significant different groups at each cleaning step (Tukey's test, $p<0.05$). The same letter indicates no significant difference, i.e., A‡A: no significant difference, one similar letter indicates partial difference, i.e., A‡AB: slightly different and different letter indicates significant difference, while the furthest from control letter A, the most significant the difference, i.e., A‡B: significant difference and A‡C: more significant difference.

Figure 4.4: Area covered by *P. fluorescens* and *P. putida* bacteria after 30 minutes of fouling for on Hydroxyapatite (HA), Stainless steel (SS), Borosilicate glass (BG), Polycarbonate (PC), Nylon, Polytetrafluoroethylene (PTFE), Polypropylene (PRP) and Polyethylene Terephthalate (PET). The error bars are the standard deviation of the triplicate's biofilm surface area (%). Capital letters indicate statistically significant different groups at each cleaning step (Tukey's test, $p<0.05$). The same letter indicates no significant difference, i.e., A‡A: no significant difference, one similar letter indicates partial difference, i.e., A‡AB: slightly different and different letter indicates significant difference, while the furthest from control letter A, the most significant the difference, i.e., A‡B: significant difference and A‡C: more significant difference.

Figure 4.5: Confocal laser scanning microscopy images of the effect of CIP with NaOH (Cleaning Process C) on *P. fluorescens* NCIMB 9046 biofilm grown on stainless steel,

polycarbonate and plasma-treated polycarbonate surface coupons before cleaning and after 10, 20 and 30 minutes of cleaning. Biofilm was stained with Acridine Orange (1%w/w). Three replicates were measured at three different spots. One replicate is shown in this case.

Figure 4.6: Biofilm surface area (expressed as a % of the total surface area) of *P. fluorescens* grown on stainless steel, polycarbonate and plasma-treated polycarbonate surface coupons before cleaning and after 5, 10, 15, 20 and 30 minutes of a) Mechanical rinsing with water (Cleaning Process A), b) Immersion in NaOH (Cleaning Process B) and c) CIP with NaOH (Cleaning Process C). Three replicates were measured at three different spots. The error bars are the standard deviation of the triplicate's biofilm surface area (%). Capital letters indicate statistically significant different groups at each cleaning step (Tukey's test, $p<0.05$). The same letter indicates no significant difference, i.e., A⫲A: no significant difference, one similar letter indicates partial difference, i.e., A⫲AB: slightly different and different letter indicates significant difference, while the furthest from control letter A, the most significant the difference, i.e., A⫲B: significant difference and A⫲C: more significant difference.

Figure 4.7: Biovolume (μm^3) of *P. fluorescens* grown on stainless steel, polycarbonate and plasma-treated polycarbonate surface coupons before cleaning and after 5, 10, 15, 20 and 30 minutes of a) Mechanical rinsing with water (Cleaning Process A), b) Immersion in NaOH (Cleaning Process B) and c) CIP with NaOH (Cleaning Process C). Three replicates were measured at three different spots. The error bars are the standard deviation of the triplicate's biovolume x 10^4 (μm^3). Capital letters indicate statistically significant different groups at each cleaning step (Tukey's test, $p<0.05$). The same letter indicates no significant difference, i.e., A⫲A: no significant difference, one similar letter indicates partial difference, i.e., A⫲AB: slightly different and different letter indicates significant difference, while the furthest from control letter A, the most significant the difference, i.e., A⫲B: significant difference and A⫲C:

more significant difference.

Figure 4.8: Absolute values of up) Biovolume (μm^3) and down) the biofilm surface area covered (%) of *P. Fluorescens* before cleaning and after 30 minutes of all cleaning processes on stainless steel (SS), polycarbonate (PC) and plasma treated polycarbonate (PT-PC) surfaces. Capital letters indicate statistically significant different groups at each cleaning process (Tukey's test, $p<0.05$). The error bars are the standard deviation of the triplicate's a) biovolume $x10^4$ (μm^3) and b) biofilm surface area (%). The same letter indicates no significant difference, i.e., A‡A: no significant difference, one similar letter indicates partial difference, i.e., A‡AB: slightly different and different letter indicates significant difference, while the furthest from control letter A, the most significant the difference, i.e., A‡B: significant difference and A‡C: more significant difference.

Figure 4.9: Effectiveness of cleaning (%) of *P. fluorescens* according to up) Biovolume (μm^3) and down) the biofilm surface area covered (%) data before cleaning (BC) and after 30 minutes of all cleaning processes on stainless steel (SS), polycarbonate (PC) and plasma treated polycarbonate (PT-PC) surfaces. Three replicates were measured at each of three different spots. The error bars are the standard deviation of the triplicate's effectiveness of cleaning for a) biovolume $x10^4$ (μm^3) and b) biofilm surface area (%). The same letter indicates no significant difference, i.e., A‡A: no significant difference, one similar letter indicates partial difference, i.e., A‡AB: slightly different and different letter indicates significant difference, while the furthest from control letter A, the most significant the difference, i.e., A‡B: significant difference and A‡C: more significant difference.

Figure 4.10: Confocal laser scanning microscopy images of the effect of CIP with NaOH (Cleaning Process C) on *P. putida* biofilm grown on stainless steel, polycarbonate and plasma-

treated polycarbonate surface coupons before cleaning and after 10, 20 and 30 minutes of cleaning. Biofilm was stained with DAPI (1%w/w). Three replicates were measured at three different spots. One replicate is shown in this case.

Figure 4.11: Biofilm surface area (expressed as a % of the total surface area) of *P. putida* grown on stainless steel, polycarbonate and plasma-treated polycarbonate surface coupons before cleaning and after 5, 10, 15, 20 and 30 minutes of a) Mechanical rinsing with water (Cleaning Process A), b) Immersion in NaOH (Cleaning Process B) and c) CIP with NaOH (Cleaning Process C). Three replicates were measured at three different spots. The error bars are the standard deviation of the triplicate's biofilm surface area (%). Capital letters indicate statistically significant different groups at each cleaning step (Tukey's test, $p<0.05$). The same letter indicates no significant difference, i.e., A⫲A: no significant difference, one similar letter indicates partial difference, i.e., A⫲AB: slightly different and different letter indicates significant difference, while the furthest from control letter A, the most significant the difference, i.e., A⫲B: significant difference and A⫲C: more significant difference.

Figure 4.12: Biovolume (μm^3) of *P. putida* grown on stainless steel, polycarbonate and plasma-treated polycarbonate surface coupons before cleaning and after 5, 10, 15, 20 and 30 minutes of a) Mechanical rinsing with water (Cleaning Process A), b) Immersion in NaOH (Cleaning Process B) and c) CIP with NaOH (Cleaning Process C). Three replicates were measured at three different spots. The error bars are the standard deviation of the triplicate's biovolume x 10^4 (μm^3). Capital letters indicate statistically significant different groups at each cleaning step (Tukey's test, $p<0.05$). The same letter indicates no significant difference, i.e., A⫲A: no significant difference, one similar letter indicates partial difference, i.e., A⫲AB: slightly different and different letter indicates significant difference, while the furthest from control letter A, the most significant the difference, i.e., A⫲B: significant difference and A⫲C: more significant

difference.

Figure 4.13: Absolute values of up) Biovolume (μm^3) and down) the biofilm surface area covered (%) of *P. Putida* before cleaning and after 30 minutes of all cleaning processes on stainless steel (SS), polycarbonate (PC) and plasma treated polycarbonate (PT-PC) surfaces. Capital letters indicate statistically significant different groups at each cleaning process (Tukey's test, $p<0.05$). The error bars are the standard deviation of the triplicate's a) biovolume $x10^4$ (μm^3) and b) biofilm surface area (%). The same letter indicates no significant difference, i.e., A‡A: no significant difference, one similar letter indicates partial difference, i.e., A‡AB: slightly different and different letter indicates significant difference, while the furthest from control letter A, the most significant the difference, i.e., A‡B: significant difference and A‡C: more significant difference.

Figure 4.14: Effectiveness of cleaning (%) of *P. putida* according to a) Biovolume (μm^3) and b) the biofilm surface area covered (%) data before cleaning and after 30 minutes of all cleaning processes on stainless steel, polycarbonate and plasma treated polycarbonate surfaces. The error bars are the standard deviation of the triplicate's effectiveness of cleaning for a) biovolume x 10^4 (μm^3) and b) biofilm surface area (%). Capital letters indicate statistically significant different groups at each cleaning step (Tukey's test, $p<0.05$). The same letter indicates no significant difference, i.e., A‡A: no significant difference, one similar letter indicates partial difference, i.e., A‡AB: slightly different and different letter indicates significant difference, while the furthest from control letter A, the most significant the difference, i.e., A‡B: significant difference and A‡C: more significant difference.

Figure 5.1: Bacterial viability measured by flow cytometry as a ratio of LIVE/DEAD bacteria/cm^2 during cleaning steps on a) stainless steel (SS) and b) polyethylene terephthalate

The same letter indicates no significant difference, i.e., A‡A: no significant difference, one similar letter indicates partial difference, i.e., A‡AB: slightly different and different letter indicates significant difference, while the furthest from control letter A, the most significant the difference, i.e., A‡B: significant difference and A‡C: more significant difference.

Figure 5.6: Effectiveness of Cleaning (%) calculated from the data obtained for the biovolume and the percentage of surface area covered by biofilm during the enzymatic cleaning with the different enzymatic formulations and after the disinfection step for a) stainless steel (SS) surfaces and b) polyethylene terephthalate (PET) surfaces. Capital letters indicate statistically significant different groups at each cleaning step (Tukey's test, $p<0.05$). The same letter indicates no significant difference, i.e., A‡A: no significant difference, one similar letter indicates partial difference, i.e., A‡AB: slightly different and different letter indicates significant difference, while the furthest from control letter A, the most significant the difference, i.e., A‡B: significant difference and A‡C: more significant difference.

Figure 5.7: Scanning electron microscopy images of 25-days-old biofilm grown on a) stainless steel b) and polyethylene terephthalate surface coupons before cleaning.

Figure 5.8: Scanning electron microscopy images of the effect of different enzymatic formulations on 25-days-old biofilm grown on stainless steel and polyethylene terephthalate (PET) surface coupons. a) stainless steel before cleaning, b) PET before cleaning, c) control on stainless steel, d) control on PET, e) formulation A on stainless steel, f) formulation A on PET g) formulation B on stainless steel, h) formulation B on PET, i) formulation C on stainless steel and j) formulation C on PET.

Figure 5.9: Scanning electron microscopy images of the effect of the disinfection step after cleaning with different enzymatic formulations on 25-days-old biofilm grown on stainless

steel and polyethylene terephthalate (PET) surface coupons. a) stainless steel before cleaning, b) PET before cleaning, c) control – surfactants without enzymes on stainless steel, d) control – surfactants without enzymes on PET, e) amylase/lipase/protease on stainless steel, f) amylase/lipase/protease on PET, g) amylase/protease on stainless steel, h) amylase/protease on PET, i) amylase/lipase on stainless steel and j) amylase/lipase on PET.

Figure 6.1: Chemical structure of a) Poly-(2-ethyl-2-oxazoline), b) DADMAC and c) Lupasol

Figure 6.2: Visualization of polycarbonate tiles surface modification with polymers.

Figure 6.3: (Up) Schematic of the T-shaped probe, fouling sample and stainless-steel disc. (Down) Schematic of the Micromanipulation rig. (Taken from Liu et al., 2002).

Figure 6.4: a) Side view of the probe pulling the sample from the surface and b) Alginic acid on coupon surfaces before and after adhesion measurement.

Figure 6.5: Average work of adhesion (mN/m) for modified and unmodified surfaces under different pH conditions. Three replicates were examined for each material surface at each pH condition. The error bars are the standard deviation of the triplicates work of adhesion. Capital letters indicate statistically significant different groups at each cleaning step (Tukey's test, $p<0.05$). The same letter indicates no significant difference, i.e., AłA: no significant difference, one similar letter indicates partial difference, i.e., AłAB: slightly different and different letter indicates significant difference, while the furthest from control letter A, the most significant the difference, i.e., AłB: significant difference and AłC: more significant difference.

Figure 6.6: Adhesive and cohesive strength for modified and unmodified surfaces (at pH 3 and pH 11 solutions) under air. The error bars are the standard deviation of the triplicates' adhesive and cohesive strength respectively. Capital letters indicate statistically significant

different groups at each cleaning step (Tukey's test, $p<0.05$). The same letter indicates no significant difference, i.e., AłA: no significant difference, one similar letter indicates partial difference, i.e., AłAB: slightly different and different letter indicates significant difference, while the furthest from control letter A, the most significant the difference, i.e., AłB: significant difference and AłC: more significant difference.

Figure 6.7: a) Cohesive strength (J/m^2) of alginic acid measured on all surfaces of interest as a function of the weight of deposit left on the probe (10^{-1}-kg). b) Cohesive strength (J/m^2) of alginic acid measured on stainless steel as a function of the probe height over the surface (μm).

Figure 6.8: Adhesive strength for modified and unmodified surfaces (under different pH conditions) under water, HCl and NaOH solutions. The error bars are the standard deviation of the triplicates' adhesive and cohesive strength respectively. Capital letters indicate statistically significant different groups at each cleaning step (Tukey's test, $p<0.05$). The same letter indicates no significant difference, i.e., AłA: no significant difference, one similar letter indicates partial difference, i.e., AłAB: slightly different and different letter indicates significant difference, while the furthest from control letter A, the most significant the difference, i.e., AłB: significant difference and AłC: more significant difference.

List of Tables

List of Symbols and Abbreviations

AFM	Atomic Force Microscopy
CER	Cation Exchange Resin
CDC	Centre for Disease Control
CIP	Cleaning-in-Place
CFU	Colony forming unit
CLSM	Confocal laser scanning microscopy
CT	Computerized Tomogrpahy
DLVO	Derjaguin, Landau, Verwey and Overbeek
XDLVO	Extended-DLVO
EPS	Extracellular Polymeric Substances
HCL	Hydrochloric Acid
HA	Hydroxy Apatite
MRI	Magnetic Resonance Imaging
PBS	Phosphate Buffer Saline
PT	Plasma Treated
PC	Polycarbonate
PET	Polyethylene Terephthalate
PRP	Polypropylene

PTFE	Polyterepthalate	
PI	Propidium Iodide	
SAXS	Small Angle X-Ray Scattering	
SEM	Scanning Electron Microscopy	
NaOH	Sodium Hydroxide	
SS	Stainless Steel	
H_2SO_4	Sulphuric Acid	
A	Hamaker Constant	N
d	Separation distance between cell-substratum	m
D	Diameter of rectangular pipes	m
dx	distance	m
E_f (%)	Effectiveness of Biofilm Reduction	-
F	Force	N
h	Height of Chamber	μm
L	Length of Chamber	cm
p	Hyrdodynamic Pressure	N/m^2
Q	Volumeric Flow rate	m^3/s
Q_{AC}	Parameter Measured After Cleaning	According to Parameter
Q_{BC}	Parameter Measured Before Cleaning	According to

		Parameter
r	Radius	m
Re	Reynolds Number	-
t	Time	s
v	velocity	m/s
V_A	Attractive Force	N
V_R	Repulsive Force	N
V_{TOT}	Total Force	N
W	Work	J
w	Width of Chamber	μm
W_a	Work of Adhesion	N/m
γ_c	Critical surface tension	N/m
γ_{lv}	Surface tension between liquid and vapor interphase	N/m
γ_{sl}	Surface tension between solid and liquid interphase	N/m
γ_{sv}	Surface tension between solid and vapor interphase	N/m
ΔGAB	Lewis Acid-Base Interactions	
ΔG_{adh}	Lifshitz-van der Waals Interaction	
ΔG_{dl}	Electric Double Layer Interaction	

ΔG_{vdW}	Van der Waals interactions	
ΔP	Pressure drop	N/m^2
μ	Fluid viscosity	kg/(ms)
ρ	Fluid density	kg/m^3
σ	Adhesive/Cohesive Strength	J/m^2
τ_w	Shear Stress	N/m^2

1 INTRODUCTION

1.1 Motivation and background

Bacteria can attach to hard surfaces, and, if the environment is optimum, they can flourish and grow bacterial colonies, known as biofilms. Bacteria living in biofilms show much higher resistance to agents with antimicrobial properties than single planktonic bacteria (Sharma et al., 2019). This happens as bacteria living within the biofilms are protected from the varieties of environmental stresses, such as desiccation, antimicrobials attack by the immune system and ingestion by protozoa hence this architecture makes the biofilm communities advanced when compared to planktonic cells (Sharma et al., 2019). Over the years bacterial biofilms have developed the ability to tolerate antibiotics, as well as increased tolerance to disinfectant chemicals (Sharma et al. 2019; Høiby et al. 2010). This special bacteria skillfulness is of great concern for various sectors, including industrial, domestic and health-related fields. Biofilms can proliferate everywhere, from the dental plaque formed in our oral cavities and medical stethoscopes, to reverse osmosis desalination membranes and industrial pipes. Especially on industrial environments, where the moisture and nutrients conditions are optimum, biofilms will grow gradually. Increased concerns in microbial contamination and infection risks in the food industry due to poor disinfection practices and ineffective cleaning products have been raised. Thus, it is of great importance to understand biofilm-biofilm interactions and biofilm-surface interactions in order to create the technologies for effective prevention and removal. Hence, it is extremely important to develop new effective methods to study the biofilm cohesion forces inside its matrix as well as the biofilm adhesion forces that interact with the underline surface of its development.

This research project is a contribution to the BioClean Marie Sklodowska-Curie Innovative Training Network. BioClean is the acronym of "BIOfilm management and CLEANing by leveraging fundamental understanding of biological, chemical and physical combined approaches".

BioClean was a Horizon2020 Marie Curie funded project worth € 3.9 MM led by Procter & Gamble, in partnership with 10 universities and 15 Ph.D. students (http://www.biocleanh2020.eu/). The aims of BioClean were, to develop mechanistic understanding into achieving deep down and long-lasting clean surfaces via surface modification and photocatalytic approaches(http://www.biocleanh2020.eu/). In parallel, research was also being carried out to develop novel naturally derived polymers technologies for malodour control and polymer brushes for soil repellence (http://www.biocleanh2020.eu/). The project was also working on developing cutting edge visualization techniques such as 4D Micro CT, MRI, SAXS and surface measurement techniques such a Micromanipulation for studying impact of surface and bulk chemistry on adhesive and cohesive forces in biofilms (http://www.biocleanh2020.eu/). The goal is the learnings from this research project will feed into various industrial applications(http://www.biocleanh2020.eu/). The BioClean network addressed the urgent need to find innovative ways to manage biofilm, using physics, chemistry and engineering approaches. BioClean's coordinator was Procter & Gamble (Technical Centres Limited, Newcastle, UK), while the participants and associated partners were (http://www.biocleanh2020.eu/):

Participants

(i) IMPERIAL COLLEGE OF SCIENCE TECHNOLOGY AND MEDICINE -

United Kingdom

(ii) THE UNIVERSITY OF BIRMINGHAM - United Kingdom

(iii) UNIVERSITY OF BRISTOL - United Kingdom

(iv) CONSORZIO INTERUNIVERSITARIO PER LO SVILUPPO DEI SISTEMI A GRANDE INTERFASE - Italy

a. Bari Unit, Local Coordinator: G. Palazzo

b. Florence Unit, Local Coordinator: E. Fratini

c. Roma Unit: Local Coordinator: C. Crestini

d. Siena Units, Local Coordinators: C. Rossi, R. Rossi

(v) KATHOLIEKE UNIVERSITEIT LEUVEN - Belgium

(vi) UNIVERSITEIT GENT - Belgium

(vii) FRAUNHOFER GESELLSCHAFT ZUR FOERDERUNG DER ANGEWANDTEN FORSCHUNG E.V. - Germany

(viii) PROCTER & GAMBLE SERVICES COMPANY NV - Belgium

Associated Partners

(i) Itram Higiene – Spain

(ii) Akzo Nobel - United Kingdom

In the project 15 Ph.D. students worked on several subjects concerning the visualization and manipulation of biofilms, the interaction with 2D-surfaces and 3D-porous media, as well as with the modification of surfaces using both physical and chemical ways. More specifically:

(i) Luka Pellegrino worked at Imperial College, on “developing methods, models and mechanistic understanding of adhesion and removal from model

surfaces for consumer relevant substrates".

(ii) Gabrielle Cimmarusti worked at University of Birmingham, on "Visualizing via MRI the Increase in Flow Through Channels in Biofilms".

(iii) Silvia Ruscino worked at the University of Bristol, on "Responsive Polymer Brushes to Prevent Adhesion of Biopolymers".

(iv) Xabier Villanueva worked at the Katholieke Universiteit Leuven, on "The effect of surface modifications on biofilm structure and community organization".

(v) Abishek Shastry worked at the Katholieke Universiteit Leuven, on "Identifying Contrast Agents for 3D Imaging of Biologically Derived Soils in Porous Organic Substrates".

(vi) Helena Mateos Cuadrado worked at the University of Bari, on "Understanding the interaction between surfaces coated with polymers and model biopolymers".

(vii) Hugo Matias Duarte worked at the University of Florence, on "Understanding the Mode of Action of Different Chemistry on the Microstructure of Bacteria".

(viii) Valeria Angarano worked at the Katholieke Universiteit Leuven, on "Develop a light treatment approach to enhance removal of biological soils on surfaces".

(ix) Lili Zhen worked at the University of Rome, on the "Interaction of Natural wood extracts with biofilms".

(x) Osama Hussein Bekhet worked at the University of Siena, on the "Mechanistic understanding of oxidative processes at the cellular level".

(xi) Kamila Jankowska worked at the University of Siena, on "Understanding the

interaction between surfaces coated with polymers and biofilms".

(xii) Lukas Kriem worked at the Fraunhofer Institute for Interfacial Engineering and Biotechnology IGB, on the "Development of In-Vitro Oral Biofilm Models for screening surface modification and other Oral Care technologies".

(xiii) Alessandra Valentini worked at P&G Newcastle, on the "Impact of surface modification on biofilm adhesion and growth on real consumer substrates".

(xiv) Joana Pinheiro Da Silva Pinto worked at P&G Brussels, on "Delivering deep down cleaning in Hand Dish Formulation".

As a part of their Ph.D. research referred as a "Secondment", all the above students exchanged places between their Universities and the two P&G hubs, in Newcastle and Brussels, while Abishek Shastry performed part of his Ph.D. in Akzo Nobel.

The contribution of this Ph.D. thesis to the BioClean project was to investigate new ways to measure biofilm cohesion and adhesion forces in relation with the surface characteristics of the different modified and non-modified surfaces. The quantification of adhesion and cohesion forces is crucial in understanding, predicting and modelling biofilm removal and cleaning from surfaces. The secondment for this thesis took place in Itram Higiene, in Spain, a company that focuses its activity in hygiene in the food and agricultural food industry. They manufacture a wide range of specialty chemicals, detergents and disinfectants, for biofilm control, and they offer services of technical advisory and consultancy, specialized in the field of food hygiene (https://www.itramhigiene.uk/).

For this thesis, two common bacteria strains have been chosen as a starting point, *Pseudomonas fluorescens* NCIMB 9046 and *Pseudomonas putida* ATCC 700008 that were

grown on various material coupon surfaces. Initially the biofilm removal was investigated by using simple chemical agents using a customed Cleaning in Place (CIP) method. The genus of *Pseudomonas* species is wide and diverse, while it includes separate species in various types of ecological and non-ecological environments (Quintieri et al., 2020). They can be found in water or in soil, as well as in aquamarine niches, but also in foods, medical devices and consumer products (Raposo et al., 2017). It comes as a natural result that even until today its taxonomy is being constantly revised and frequently updated (Quintieri et al., 2020). As reported by Ichinose et al. in 2013, the few *Pseudomonas* species that are recognized as human pathogens are:

(i) *Ps. aeruginosa*

(ii) *Ps. syringae*, and

(iii) *Ps. cichorii*

A significant number of *Pseudomonas* strains that do not express human pathogenicity have displayed multiple drug resistance, a concerning issue that can become a great threat to global health (Guzel et al., 2018; Quintieri et al., 2020). Furthermore, increased human clinical cases, derived from the isolation of non-pathogenic *pseudomonas* strains have been lately reported (Quintieri et al., 2020). Thus, it is observed, *P. fluorescens* and *P. putida* strains colonize several environments like the human lung airway, the urinary tract, our blood or even cells, which shows that the average body temperature does not create an obstacle to the development of *Pseudomonas* species (Chapalain et al., 2008; Quintieri et al., 2020).

Quantification of bacterial detachment on common artificial surfaces is of great importance to determine the effectiveness of several biofilm cleaning agents. For evaluating the effectiveness of biofilm cleaning from the surfaces, a parallel-plate flow chamber has

been designed and used for this thesis in order to evaluate the biofilm residual contamination from the different surfaces under CIP conditions (Tsiaprazi-Stamou et al., 2019). Furthermore, a combination of microscopy techniques has been used to measure and characterize the biofilm residual contamination over cleaning. In order to find a correlation between the techniques, a cell detachment quantitative method was required and thus the effectiveness of cleaning has been tested in all cases.

After gaining fundamental knowledge on the cleaning behaviour of single-species biofilm, a mixed-microbial biofilm was collected from the "real world". An industrial environment of a meat-packaging line in Spain was the place of interest in order to collect samples from common everyday surfaces and grow a real case biofilm. At this point the biofilm removal was investigated by using commercial, ecologically friendly enzymatic cleaning products, provided by Itram, as a substitute for the chemical agents.

Finally, after collecting information on the biofilm cleaning behavior the goal was to manipulate biofilms and measure adhesion and cohesion forces in the biofilm matrix. As biofilm is a sensitive and challenging study material to measure forces, alginic acid was chosen as a biologically relevant soil that is abundant in extracellular polymeric substances of *Pseudomonas* biofilms. Micromanipulation technique is well-known for the use of direct measurement of biofilm-surface interactions and bacteria cell-bacteria cell interactions in the biofilm. The availability of micromanipulation can help academics and researchers to create a targeted strategy for the reduction of biofilm growth and the enhancement of biofilm removal. The work performed in this PhD thesis basically aimed to develop new understanding in the application of biofilm removal via the investigation of their adhesive and cohesive strengths on different substrates and the effects of surface modification on them

and their cleaning behaviour in all cases.

1.2 Layout of thesis

This thesis is being presented in 7 chapters (including this chapter) and shows the research results obtained from January 2017 until October 2019. The thesis focuses on the investigation of biofilm cleaning behaviour on surfaces that are usually found on industrial premises, using a parallel-plate flow chamber in combination with various microscopy techniques (Tsiaprazi-Stamou et al., 2019). The surface materials used throughout this study are (i) stainless steel 316L, (ii) polyethylene terephthalate (PET), (iii) polycarbonate (PC) and polycarbonate surfaces that have been chemically modified as it will be explained in detail in the next chapters. In Chapter 2, a literature review presents the various reasons for bacterial adhesion including the initial biofilm development, the theory of adhesion, the DLVO theory, the factors that is believed to affect biofilm adhesion as well as the application of the available up-to-date instrumentation that helps us observe and study bacterial adhesion.

In Chapter 3, the materials and the methods that used during the thesis along with the equipment are described. The first results are presented in Chapter 4 which comprise of *P. fluorescens* and *P. putida* biofilm residual contamination measurements after different cleaning in place applications. By using confocal microscopy in combination with fluorescence microscopy, the biofilm thickness, biofilm surface coverage and biovolume have been measured. In Chapter 5, the synergistic effect of commercial enzymatic formulations against bacterial cells and extracellular polymeric substances (EPS) of a real, mixed-microbial biofilm sourced from a meat packaging line was studied for its cleaning

performance (Tsiaprazi-Stamou et al., 2019). This study was conducted in Itram Higiene in collaboration with the Institute of Aquatic Biology of the University of Girona and lead to the publication of the paper “The synergistic effect of enzymatic detergents on biofilm cleaning from different surfaces” (Tsiaprazi-Stamou et al., 2019). Additionally, in Chapter 6 a micromanipulation technique was used for the investigation of the difference in adhesion and cohesion forces of alginic acid in terms of different surfaces and different environmental conditions. Finally, in Chapter 7 overall investigations and conclusions are discussed, while several next steps are reported for further investigation.

2 LITERATURE REVIEW

2.1 Summary

In this chapter mainly the phenomenon of biofilm adhesion and growth on surfaces as well as the cleaning methods studied in theory and applied in industry for its elimination will be reviewed. First, the theory of bacterial adhesion and the theoretical models and mechanisms are presented. In theory, biofilm adhesion is governed by both physicochemical and molecular/cellular interactions that can be studied as two distinct phases. The measurement of the energy required for bacterial adhesion to occur has been discussed by three main theories: The “DLVO theory”, the “Thermodynamic theory” and the “Extended DLVO theory”. Secondly, the main factors that affect surface bacterial adhesion and removal are shown. Surface topography, i.e., roughness, surface chemistry and surface energy are three basic parameters that influence bacterial attachment and proliferation. Nonetheless, chemical surface modification is also presented as a factor that changes the substrate’s cleanability against biofilm.

Next, the basic methods used to determine the bacterial cell-surface and bacteria cell-bacteria cell interactions are discussed, as they can be categorized in two main chapters: *macroscopic-conventional* methods that include shear stress flow methods and the *microscopic-advanced* methods that use single-molecule force spectroscopy. In the first category microfluidic and macrofluidic methods are used, such as the parallel-plate flow chamber and the cone-and-plate viscometer. In the second one, the “mother” of all methods is the Atomic Force Microscopy (AFM) technique; a fundamental method that operates in the atomic scale for measuring forces. With several transformations that include the

modification of AFM cantilevers or by using spherical, colloidal probes, this technique is very useful for measuring the mechanical properties of biofilm or single bacteria, such as Young's modulus and the elasticity. Furthermore, with this technique, adhesion and cohesion forces can be calculated in an atomic scale, to estimate the balance between bacteria growth and detachment.

However, as the perspective of this thesis was more industrially-oriented and the approach followed was focused on measuring macroscopic scale data, the method used was the micromanipulation technique which is discussed here. Finally, the different Cleaning-in-Place methods that have been studied for biofilm removal are presented in detail, as they act as a first step in the application of industrial cleaning protocols.

2.2 Introduction

Microorganisms live and thrive either as individual bacteria cells or they attach to any surfaces to grow into highly organized multicellular communities (Otto et al, 2008). These communities, known as biofilms, are now considered as the major type of microbial life in nature and in diseases and are studied as adaptive multi-population colonies (Tsiaprazi-Stamou et al., 2019). Biofilms are formed since bacteria generally choose to grow on available substrates rather than in the surrounding media in order to decrease their energy (Katsikogianni and Missirlis, 2004; Otto et al, 2008). Biofilms are considered the major type of microbial life in nature and exist as microorganism associations embedded in self-produced matrix of extracellular polymeric substances (EPS), which gives them consistency and resistance to antibiotics and disinfectants (Katsikogianni and Missirlis, 2004; Flemming et al., 2016; Tsiaprazi-Stamou et al., 2019).

Over the last years in research, much improvement has been achieved in understanding both the mechanisms occurring in the molecular level of initial attachment of bacteria to substrates and the proliferation of biofilm development. It is generally accepted that biofilm growth is ruled by several complex physicochemical as well as biological mechanisms. The attachment of a bacteria-cell to a surface is called adhesion while the attachment of a bacteria cell with another in a continuous medium is called cohesion. The progresses that rule these types of attachment eventually control the adhesive and cohesive properties that a biofilm will develop, depending always on the surrounding system (Katsikogianni and Missirlis, 2004; Herrera et al., 2007; Garrett et al., 2008; Otto et al, 2008; Stoodley et al., 2013). For example, biofilms in nature are exposed to various environmental conditions with gradients of nutritious media established in all directions. Biofilms growing in highly varied environments from hot springs to urinary catheters appear to utilize similar strategies to attach and grow on surfaces, and can also show remarkable structural similarity suggesting a selective advantage that surface association offers (Stoodley et al., 2013). Biofilms create microcolony gradients and form various architectures, from hemispherical colonies (height more than 100 mm), to extra thin bacterial films only 10 μm in depth (Doyle et al., 2016).

To understand the mechanisms that determine the phenomena of bacterial adhesion and cohesion, various measurement techniques have been introduced. These techniques are separated into two basic categories: those counting the number of the bacteria detached using fluid flow against the attached biofilm surface, and those that manipulate microbes in several formations by applying specific forces to the bacteria, and analysing the bacteria-material interactions (Katsikogianni and Missirlis, 2004; Herrera et al., 2007; Garret et al, 2008;

Angeloni et al., 2016). The techniques in the second category can be further characterized to “active” and “passive” techniques, hence the methods that deform the cells by applying force on them and the methods that sense the mechanical forces that are generated by the cells (Addae et al., 2008).

Understanding the mechanisms that determine bacterial adhesion and bacterial cohesion phenomena will contribute in the development of a reliable model that can describe and predict the bacterial attachment onto surfaces (Angeloni et al., 2016). Despite the continuous efforts that have been made by many researchers until now there is no accurate model, but three major theoretical models have been introduced for the estimation of biofilm development on different substrates. These models are:

(i) the DLVO

(ii) the thermodynamic theory and

(iii) the extended DLVO theory.

Although work has been done to explore the dominant parameters that regulate bacterial adhesion to different surfaces over the years, the complex variety of biofilm composition, in combination with the changes that occur in the dynamic environmental conditions (nutrients and their concentrations) can explain much of the inconsistency observed in experimental studies of biofilm attachment. (Katsikogianni and Missirlis, 2004; Stoodley et al., 2013).

2.3 Biofilm Adhesion Mechanisms and Theoretical Models

When microorganisms approach several substrata, physicochemical interactions are developed. These interactions, either attractive or repulsive, are predominant in the initial bacteria attachment and biofilm formation, a phenomenon that is generally described as biofilm adhesion (Katsikogianni and Missirlis, 2004; Garret et al, 2008). In general, bacteria adhesion to surfaces consists of two separate steps, the reversible ant irreversible step. Biofilm bacteria coordinate their behaviour by cell-cell communication using secreted chemical signals which allow the bacteria to sense and respond to their environment by assessing cell density or environmental cues, resulting in modification of gene expression (Stoodley et al., 2013). This ability to adapt to and modify micro-niches at a surface interface allows bacteria in biofilms to facilitate survival at a population level. When planktonic cells adhere to a surface, they exhibit behaviours that have been divided into “reversible” and “irreversible” patterns that is dominated by biochemical mechanisms (Katsikogianni and Missirlis, 2004; Garret et al, 2008; Stoodley et al., 2013). Bacterial adhesion on surfaces can be divided in the “initial attachment” of the bacteria cells on the surface that is governed by the physicochemical interactions among bacteria and substrates, followed by adsorption and attachment relations entre microbes and substrates become predominant, leading to “biofilm proliferation” (Ong et al., 1999). The last step of proliferate adhesion on a substratum is the colonisation or growth of the bacteria that forms a “mature biofilm” while after some time detachment of the biofilm starts naturally as a result of the detachment kinetics of the biofilm environment (Herrera et al., 2007; Harriott M., 2019). Attachment of a cell to an abiotic substrate is adhesion, while live cell-to-live cell attachment is cohesion (Garrett et al., 2008). Biofilm’s steps of deposition are shown in **Figure 2.1**.

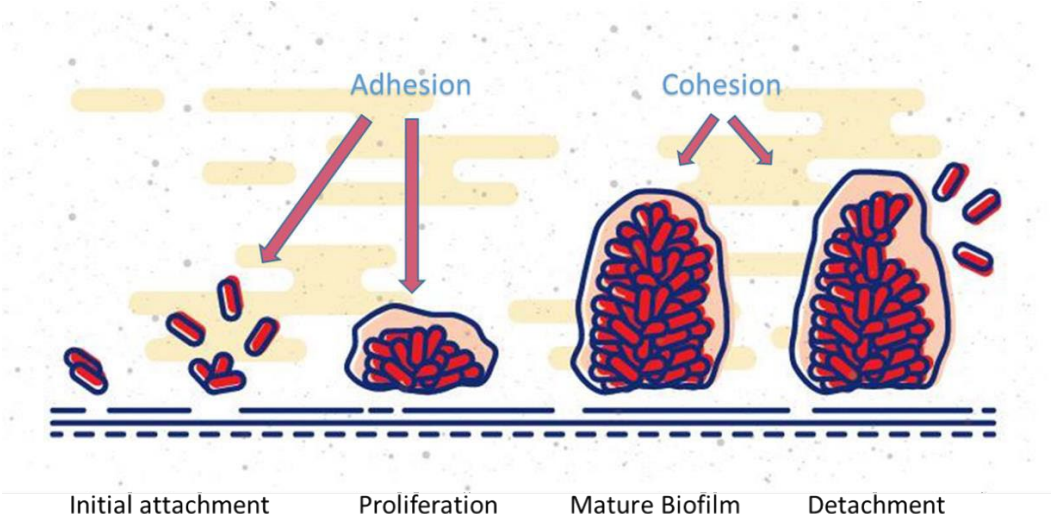

Figure 2.1: Schematic model of the phases involved in biofilm formation.

Adhesion is mediated by both non-specific interactions and specific microbial factors. In fungal biofilms for example, including *Candida albicans* and *Aspergillus fumigatus*, the attachment phase requires morphogenesis, the development of hyphae and subsequently mycelia from conidia which initially adhere to the surface. Once a monolayer has formed, the microorganisms aggregate, and form clusters referred to microcolonies. The biofilm then enters the maturation phase which is characterized by growth and the production of the EPS; this extracellular matrix, also known as glycocalyx, is the hallmark of biofilm communities. The mature biofilm is a complex and elegant three-dimensional structure. The final phase of development involves dispersion of microorganisms from the mature biofilm thereby facilitating the genesis of new biofilms (Beauvais et al., 2007; Harriott M., 2019).

2.3.1. Physicochemical Interactions: Phase One

Bacteria are attracted by a biotic or abiotic substrate through and by the effect of

physical interactions, i.e., gravitational forces, van der Waals forces, Brownian motion, electrostatic charge effects and hydrophobicity, while the phenomena of chemotaxis and haptotaxis are also believed to contribute to this process (Katsikogianni and Missirlis, 2004; Garret et al., 2008). The material surface where a biofilm grows can be any conditioning layer, composed of several organic and/or inorganic particles. Anything present in the bulk fluid can sit onto a surface and change it so as bacteria accessibility will be facilitated. For example, biofilm growth under high fluid shear often exhibits filamentous streamers, while biofilms grown in low shear environments form towers or mound-like structures which vary according to different nutrient conditions or mass transfer-determined localized growth patterns. These observations suggest that bacteria in biofilms can rapidly adapt to their local environment, to an extent not possible with multicellular eukaryotic organisms (Stoodley et al., 2013). Surface charge, potential or tensions can be changed by the layer-substrate interactions and eventually cause the augmentation of bacteria-favourable nutrients that will lead to biofilm formation and growth (Garret et al., 2008). To separate the phenomena that occur between the bulk and the surface, two terms have been introduced, "Chemotaxis" and" Haptotaxis" (Kirov, 2003). "Chemotaxis" is referred as the bacterial directive motion that is affected by concentration gradients of chemo-attractants, diffusible chemical factors like amino acids, sugars, oligopeptides etc. "Haptotaxis" is the bacterial directive motion dominated by the same chemical factors that are now found on the surface (Katsikogianni and Missirlis, 2004).

As distance plays an important role in the forces developed between two bodies, the physical relations are additionally characterised into long-range interactions and short-range interactions (Gottenbos et al., 2000; Katsikogianni and Missirlis, 2004). Long-range interactions (>50nm) entre bacteria and substrates can be explained by common forces

developed as a function of (i) distance and (ii) free energy. Similarly, short-range interactions (<5nm) are present once the bacteria and the surface approach to each other and are further subcategorised to covalent chemical bonds, ionic interactions, dipole forces and hydrophobic phenomena (Mayer et al., 1999; Katsikogianni and Missirlis, 2004). Cells approaching the substrate which are affected by long-range forces and at smaller distance, "short-range interactions" are more important into leading the initial biofilm attachment and further proliferation. This initial attachment of cell-surface is the first phase of adhesion, while the second phase, governed by complex molecular and cellular reactions (Katsikogianni and Missirlis, 2004). **Figure 2.2** shows the typical force-distance curve between interatomic and intermolecular forces.

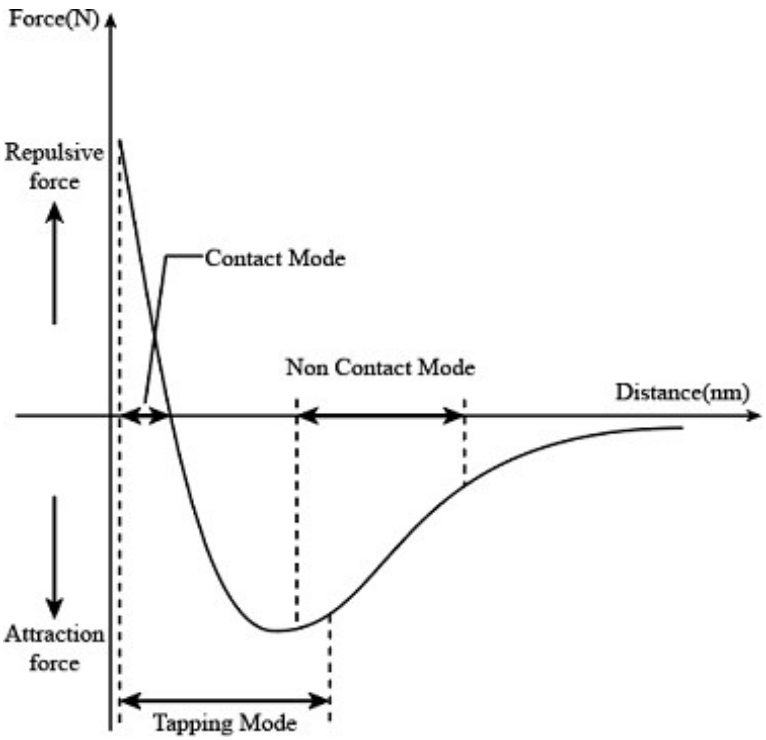

Figure 2.2: Typical force-distance curve between interatomic and intermolecular forces. Obtained by (https://study.com/academy/answer/distinguish-between-interatomic-and-intermolecular-forces-on-the-basis-of-the-force-distance-graph.html)

For example, motile organisms like *P. aeruginosa* may use their flagella for initial attachment, followed by type IV pili for twitching motility that allow them to form elaborate structures. However, surface appendages and motility are not required for biofilm formation, staphylococci and streptococci are both capable of forming biofilms in vitro and in vivo, although in these cases it is assumed that biofilm structures develop from clonal growth. When a bacterial cell colonizes a surface, the pattern of gene expression is profoundly different from the previous planktonic phenotype, resulting in a distinct biofilm phenotype that may differ by as much as 70% in the proteins expressed. Among the first genes that are upregulated in adherent cells are those involved in the production of molecules associated with the EPS that forms the biofilm matrix and anchors the cell irreversibly to the surface (Stoodley et al., 2013).

2.3.2. Molecular and Cellular Interactions: Phase Two

During the second adhesion step, molecular and cellular interactions between microbes and surfaces govern the phenomenon (Katsikogianni and Missirlis, 2004). In this phase, the bacteria attach to the surfaces through capsules, pili or fimbriae, the polymeric substances of microbial surfaces. Most importantly, the inhabitants of biofilm communities are social and communicate with one another via quorum sensing, a coordinated and sophisticated mechanism. In brief, quorum sensing involves the production and subsequent release of diffusible signal molecules by the microbe into the surrounding environment. Once the signal molecules surpass the threshold concentration, the signal is recognized by specific receptors resulting in changes in gene expression (Harriott, 2019). Adhesion proteins are expressed on the surface of planktonic organisms and eventually cells that are

not washed away enter a non-reversible attachment to the surface. There is a plethora of surface proteins and these will vary based on the microbe and the substratum (Harriott, 2019). Moreover, adhesion could be governed as a result of polysaccharide adhesins (Mack et al., 1999). Some of the most important adhesins that facilitate the adhesion of common microbes or cells to surfaces are composed of acetyl-glucosamines and proteins (Yuehuei et al., 1998).

Not all genes are activated at the same density; different genes are activated at different densities. Changes in gene expression modulated by quorum sensing often result in increased pathogenicity. Environmental biofilms and human associated biofilms are rarely monomicrobial and instead are comprised of multiple species which must interact with each other. Dental plaque, a well characterized biofilm community, may contain up to 700 different species of bacteria (Kuramitsu et al., 2007). Polymicrobial biofilms may also contain mixed kingdoms of microbes including bacteria and fungi. The architecture of mixed species biofilms may vary compared to monospecies biofilms, and microorganisms within polymicrobial biofilms can exist as separate microcolonies, co-aggregate with one another or different species may be layered within the biofilm (Elias and Banin, 2012). Microorganisms within polymicrobial biofilms can impact each other often resulting in detrimental outcomes (Peters et al., 2012). Polymicrobial interactions can also contribute to antimicrobial resistance. Resistant organisms within a polymicrobial biofilm can transfer resistance genes to other organisms within the biofilm, leading to the development of multi-resistant organisms and therefore more resistant biofilms (Weigel et al., 2007). While gene transfer does play a substantial role in resistance, resistance of polymicrobial biofilms is more likely to be attributed to cooperation between species (Harriott, 2019).

In the case of mucoid *P. aeruginosa*, the upregulation of *algC*, which is a part of the alginate synthesis pathway, occurs within 18 minutes of initial cell adhesion, and there is a secretion of bacterial biofilm matrix material by these cells within 30 minutes. Once attached, cells which have triggered the conversion to the biofilm phenotype and the formation of a multicellular community on the colonized surface begin to accrete larger numbers of cells through growth. As they increase in numbers and produce more EPS matrix material, the attached cells form microcolonies which constitute approximately 10% of the volume, with the EPS matrix occupying approximately 90% of the biofilm. Recent data suggest that the structure of the EPS is much more sophisticated than previously thought, with confocal and SEM images showing features such as "honeycombs" and 3D networks in *P. aeruginosa* and staphylococcal biofilms grown in vitro (Stoodley et al., 2013).

Several studies so far have attempted to understand the governing interactions of bacterial adhesion. Some have tried to identify whether the microbial adhesion to substrates is dominated by the physicochemical forces that initiate the non-living-colloid deposition. Thus, three theoretical models have been proposed so far: the "DLVO theory", the "thermodynamic theory" and the "extended DLVO theory" (Bowen et al., 2001; Katsikogianni and Missirlis, 2004; Garret et al, 2008; Addae-Mensah et al., 2008; Stoodley et al., 2013; Angeloni et al., 2016).

2.4. Theory of bacterial adhesion

2.4.1. The "DLVO Theory"

Derjaguin and Landau suggested a theory in 1941 that the instability of colloidal

dispersions was caused by strong but short-ranged van der Waals forces governed by the stabilizing influence of electrostatic repulsions (Derjaguin and Landau, 1941). In 1948, Verwey and Overbeek came up with the same result in one independent research (Verwey and Overbeek, 1948). This "DLVO theory" contributed in explaining the lack of the Levine–Dube theory to take into account the stability of colloidal dispersions affected by the electrolyte ionic strength (Levine and Dube, 1940). Furthermore, while studying the lyophobic sols and the adhesion of charged particles in electrolyte solutions, Derjauin and Landau (1993) considered the particles' interaction as the summation of two individual terms: (i) Van der Waals forces attraction between the micelles molecules, and (ii) electrostatic forces repulsion between the particle's ions of the electric double layers.

The "DLVO theory" as a theory to explain microbial attachment was first proposed in 1971 by Marshall et al. This theory implies that the net force interaction (V_{TOT}) between an attached bacterium and a surface is the balance between two separate forces, attractive (V_A) and repulsive (V_R) as shown in equation 2.1.

$$V_{TOT} = V_A + V_R \tag{2.1}$$

V_A is calculated:

$$V_A = -\frac{Ar}{6d} \tag{2.2}$$

Where A represents the Hamaker constant, d the cell-substratum separation distance and, r the cell radius (Hermansson, 1999). The assumption that cells are spherical has to be made. Attractive forces are observed due to Van der Waals forces while repulsive forces are because of Coulomb interactions (Marshall et al., 1971; Hermansson, 1999; Katsikogianni and Missirlis, 2004). Marshall et al., (1971) showed that during marine bacteria sorption to

surfaces, an immediate and reversible phase, and a time-dependent and irreversible phase occurred, that depended on the electrical double-layer repulsion energies at different electrolyte concentrations and the van der Waals attractive energies. Choi et al. (2017) explained the detachment of *P. putida* during transport in terms of the DLVO theoretical model, showing that an energy barrier was formed and disappeared as the ionic strength slowly decreased.

The initial DLVO theory described the probability of a bacterium overcoming an electrostatic barrier and could explain low amounts of cell adhesion to negatively-charged substrata. However, it failed to give an explanation for the wide variety of adhesion phenomena to different surfaces or in electrolytic solutions as well as the effect of the distance between the cell and the surface and the specific kind structure-molecule interactions on bacterial surfaces like the roughness or the surface charge of the surface (Katsikogianni and Missirlis, 2004). Bowen et al. (2001) used the atomic force microscopy (AFM) and specifically the "colloid probe" technique to study the adhesion forces measured in aqueous environment for yeast cells with electrophoretic as well as hydrophobicity experiments of the accounted surface. They concluded that the yeast cell-surface adhesion was affected by a component that indicated serial bond breakage, cell elongating, and a "peeling" of the cell abandoning the surface, a result that could not be explained just with the hydrophobicity and/or DLVO theory. Nevertheless, some crucial parameters like hydrophobic interactions, proven to be crucial in biofilm adhesion, are not taken into account, leading to inconsistency between "DLVO theory" and experimental data. Furthermore, The DLVO theory works on perfect, smooth surfaces, not existing in real life (Hermansson, 1999). Subsequently, in order to include the hydrophobic interactions between the surfaces and the bacteria, the thermodynamic theory was introduced (Busscher

et al., 1984; Morra et al., 1996; Katsikogianni and Missirlis, 2004).

2.4.2. The "Thermodynamic Theory"

The "Thermodynamic theory" next has tried to explain adhesion of bacteria on substrata (Busscher et al., 1984; Morra et al., 1996). From a qualitative point of view, it takes into account the interactions that are present in the "DLVO theory", but it quantifies them in the thermodynamic term of 'surface free energy'. The cell surface energy and the substratum surface energy as well as the suspending solution surface energy are calculated to evaluate the Gibbs adhesion energy for microbial adhesion. Adhesion is favoured when the free energy (per unit surface area) is negative as a result of adhesion, which, as predicted by 2nd thermodynamic law, that spontaneous attachment causes a decrease in the system's free energy (Katsikogianni and Missirlis, 2004; Angeloni et al., 2016).

In general, the thermodynamic theory falsely considers microbial adhesion as possibly reversible. Furthermore, it does not take into account the kinetics and the dependence of the distance ("long-range" and "short-range" interactions), as it is an equilibrium. Nonetheless, due to the complex chemistry of bacterial surfaces it is difficult to measure the precise values of their free energies and thus energy calculations during adhesion may be incorrect, as it is a highly dynamic parameter. Moreover, despite the fact that microbes are live organisms that produce energy, the above theory refers to closed systems with no energy input. However, adhesion may be affected by the synthesis of adhesins or energy consuming physiological mechanisms. As a result, the thermodynamic theory has not led to entirely successful results, concerning the explanation or the prediction of microbial adhesion.

Nonetheless, the thermodynamic theory contributed to the explanation of a common observation, where the increasing surface hydrophobicity resulted to an increased percentage of bacterial adhesion for some bacterial species. Since both the "DLVO theory" and the "thermodynamic theory" failed to explicate bacterial adhesion, there was a need for a new approach (Katsikogianni and Missirlis, 2004; Stoodley et al, 2013; Angeloni et al., 2016).

2.4.3. The "Extended DLVO Theory"

A new theoretical, presented as the "extended DLVO theory" – XDLVO (Jucker et al., 1998) that includes the hydrophobic/hydrophilic forces, has been developed. So, the total energy of adhesion is calculated (Araújo et al., 2009):

$$\Delta G_{adh} = \Delta G_{vdW} + \Delta G_{dl} + \Delta G_{AB} \quad (2.3)$$

Where, ΔG_{vdW} and ΔG_{dl} are the van der Waals (vdW) and double layer (dl) forces, and ΔG_{AB} refers to acid-base forces (Araújo et al., 2009). Acid-base forces describe attractive hydrophobic forces as well as repulsive hydration causes, 10-100 times stronger than the van der Waals forces. ΔG_{vdW} and ΔG_{dl} interactions explain from the initial "DLVO theory" the distance-dependence, a highly important parameter in the total adhesion energy calculation. The surface energy term, ΔG_{AB} declines at close contact in an exponential way. The "extended DLVO theory" has a greater aspect in studying bacterial adhesion, as it involves the term of acid-base interactions (Katsikogianni and Missirlis, 2004; Angeloni et al., 2016).

Sharma and Hamumantha Rao (2003) examined the *Paenibacillus polymyxa* bacteria adhesion behaviour on pyrite/chalcopyrite using the thermodynamics of the surface and the 'extended DLVO' theory models. They found that the 'extended DLVO' theory was more accurate in the adhesion behaviour prediction than the thermodynamic one. The significant difference was that the thermodynamic theory yielded zero adhesion on mineral surfaces, an inconsistency that resulted in insufficient description of the electrostatic forces. Predicting the adhesion by the 'DLVO approach' partially explained the bio-flotation results of pyrite/chalcopyrite, while 'XDLVO', considering the electrostatic interactions also which were attractive, was effective as it predicted the different *P. polymyxa* attachment on the surfaces. XDLVO also predicted the stable water microbial suspension caused by highly repulsive acid-base and electrostatic repulsion.

Baydouh et al., (2009) studied *Pseudomonas stutzeri* and *Staphylococcus epidermidis* attachment to glass and indium tin oxide (ITO)-coated glass surfaces, using the 'DLVO' and 'XDLVO' theories to predict the interaction energies among bacteria and surfaces at long and short distances. The comparison of the two different energy profiles derived from the above theories, showed that the Acid-Base interaction energy showed a highly significant difference between 'DLVO' and 'XDLVO' predictions at close approach, while 'XDLVO' approach predicted more accurately both the adhesion and its reversibility than 'DLVO' theory.

Chia et al. (2011) studied the bacterial attachment of two *Salmonella enterica* strains on different material surfaces and compared it with the stochasticity and predictability by the 'XDLVO' theory. They concluded that bacterial attachment to different materials was likely to be non-stochastic when the bacteria physicochemical properties were significantly

different ($P < 0.05$) from each other. 'XDLVO' theory could model the isolates attachment to particular materials but could not be used to predict the likelihood of stochasticity in pairwise attachment experiments.

2.5. Factors influencing bacterial adhesion and removal

As biofilm formation and proliferation affect many aspects both of public health and industrial processes, including contamination in the food and beverage industry (Johansen et al. 1997; Palmer et al., 2007; Goode et al., 2013; Tsiaprazi-Stamou et al., 2019), its elimination is of great importance. In a review paper about the role of surfaces in the cleaning processes, Detry et al. (2010) refer first in the importance of hygiene in industrial surfaces. More specifically, they state "Hygiene is a permanent concern for food industries since they must commercialize high quality products in order to comply with the legislation and the expectations of the consumers". Because of this concern, it is well accepted that the hygienic level of a surface is an important aspect that affects immediately, firstly, the production-line process and, secondly, the final product quality (Detry et al., 2010). However, biofilms adapt and change their structure according to the environmental conditions, and are unpredictable and challenging to study and control (Johansen et al., 1997; Otto, 2008; Flemming et al., 2016; Tsiaprazi-Stamou et al., 2019). Thus, the study of biofilm removal at the optimum conditions is of great importance.

To control biofilm formation, food industries use routine cleaning processes, including cleaning-in-place (CIP) and cleaning-out-place (COP) systems mainly comprising shear stress generated by fluid flow or mechanical action together with chemical agents (Lécrigny-Nolf et al., 2000; Antoniou and Frank, 2005; Keener, 2005; Bel et al., 2007; Li et

al., 2017; Tsiaprazi-Stamou et al., 2019). Effective biofilm cleaning comprises of two distinct phenomena: biofilm removal and biofilm deactivation through disinfection. However, apart from bacteria removal, a key component involved in biofilm elimination is removal of the EPS matrix, which is mostly water (up to 97%) and contains the structural and functional components of the matrix: soluble, gel-forming polysaccharides, proteins and eDNA, as well as insoluble components such as amyloids, cellulose, fimbriae, pili and flagella (Flemming et al., 2016; Tsiaprazi-Stamou et al., 2019). From a physicochemical point of view, the removal of biofilms is achieved by using substances that induce detachment by diminishing the cohesiveness of the EPS matrix (Xavier et al., 2005; Tsiaprazi-Stamou et al., 2019). Thus, understanding the microbial and polymeric interactions with surfaces is essential for the optimum biofilm elimination and removal. Additionally, knowing the biofilm EPS composition is key in order to choose the appropriate agent for its elimination. Regardless of the bacteria species, the EPS composition will depend on the medium that the biofilm is grown (Molobela et al., 2010). Moreover, the EPS compounds that will be found in biofilms will strongly depend on the method essay used for their extraction. For *P. fluorescens* biofilms for example, in some studies it was indicated that carbohydrates are the main constituents of the EPS while some studies found proteins to dominate (Liu et al., 2003; Orgaz et al., 2006). Hung et al., (2005) found that the main components in the EPS were rhamnose, fucose, ribose, arabinose, xylose, mannose, galactose and glucose. The acidic groups in the EPS were mainly composed of carboxylic acid and other minor polyanionic groups, e.g. sulphate and phosphate. Up to 70% of total carbohydrates were uronic acids, and total carbohydrates made up 26–31% of organic carbon. Besides the neutral and acidic sugars in the EPS, EPS also contained 2% of proteins in terms of carbon. On the contrary, Molobela et al. (2010) found proteins to be dominant rather than carbohydrates similarly to Simoes (2003) who found total protein=217,7mg/g

and total carbohydrate = 63.3mg/g in the EPS produced by *P. fluorescens* biofilms under specific growth conditions.

Therefore, the understanding of the interphases between microbes and surfaces is a multidimensional problem that needs to take into account several parameters. The physicochemical properties of the surfaces, like the roughness, the chemistry of the surface, i.e., its composition, and the surface energy are essential starting parameters that affect their cleanability.

2.5.1. Roughness

Various research studies have focused on the cleanability of a surface depending on the surface roughness. The two main parameters that are usually studied over the literature are the 2D roughness descriptors, the arithmetic average height, Ra, and the more promising, difference between the average height of the five highest and the five lowest points through the surface, R_z. Arithmetical mean height R_a indicates the average of the absolute value along the sampling length and it is calculated as described below:

1. Measure height across the microscopic peaks and valleys.
2. Calculate the SQUARE of each measurement value.
3. Calculate the MEAN (or average) of those numbers (squared).
4. Find the square ROOT of that number.

As concluded by many studies, the effect of the surface abnormalities on their cleanability can only be partially characterized by the arithmetic average, Ra. Frank and Chmielewski (2001) found a difference between the effect of surface roughness on biofilm removal and of bacteria spores. In the latter case they observed low cleanability for high R_z values, whilst for the biofilm the roughness showed no effect on its removal.

Since no simple correlation among the 2D roughness descriptors with the cleanability of the surfaces is available, the characterization of the 3D surface topography is essential and can be achieved with the concept of fractal dimension, D. Although it may sound reasonable that the surface topography will affect its cleanability, it is hard to find a clear relationship between the two parameters (Detry et al., 2010; Tsiaprazi-Stamou et al., 2019).

2.5.2. Surface Chemistry & Surface Energy

The surface chemical composition is affected by the functional groups that cause the physicochemical reactions that will occur on the surface or the interface. However, it is hard to correlate the surface chemical composition with the surface cleanability or its fouling susceptibility (Frank and Chmielewski, 2001; Tsiaprazi-Stamou et al., 2019), as any change that may be held on the surface composition will modify its physicochemical properties, and more likely its wettability or as defined by the Zisman Plot, the critical surface tension, γ_c (Zisman, 1964). In contrast to the chemical composition, the wettability is related to the surface energy. Solid surface energy can be calculated by various methods, i.e., direct-force-measurement (Drehlich et al., 2004), powder column capillary penetration (Siebold et al., 1997), inverse gas chromatography or contact angle (theta) measurement technique

(Planinsek et al., 2001).

When a liquid and a solid are in direct contact, there is a work required for their separation. This work, which is exerted perpendicularly from both the interfaces, is known as the work of adhesion. It is the reversible work per unit area due to the adhesion forces developed between the two interfaces and it is calculated from the equation (Good, 1993; Michalski et al., 1998; Detry et al., 2010; Tsiaprazi-Stamou et al., 2019):

$$W_{sl} = \gamma_{sv} + \gamma_{lv} - \gamma_{sl} \tag{2.4}$$

Where, γ_{xy} represents the surface tension between two interfaces, s-v the solid and the vapor phase, l-v the liquid and the vapor phase, and s-l the solid-liquid phase. When a small amount of liquid is dropped on a solid-surface it takes a different form according to the three interfaces. The drop-shape will be sculptured to reach a minimum energy state. In a gas-solid-liquid system, the surface-force-equilibrium is expressed by Young's equation, which includes the angle formed between the drop (known as the contact angle, theta θ), the surface energy of the solid (γ_{sv}), the surface energy of the liquid (γ_{lv}), and the interfacial energy between the solid and the liquid (γ_{sl}).

$$\gamma_{sv} = \gamma_{sl} + \gamma_{lv} \cos\theta \tag{2.5}$$

From equations (2.4) and (2.5) the Young-Dupre equation (2.6) is formed, which implies that the solid liquid work of adhesion can be calculated from liquid surface tension and contact angle values (Michalski et al., 1998; Detry et al., 2010; Tsiaprazi-Stamou et al., 2019).

$$W_{sv} = \gamma_{lv} \cdot (1 + \cos\theta) \tag{2.6}$$

A theory that establishes an empirical association between the critical surface tension γ_c and the bioadhesion strength is the Baier curve (Baier, 2006; Zerhiou et al., 2019). Among the initial work on the surface-composition on fouling-behaviour effect, Baier and Zisman compiled data on the bacteria-fouling-surfaces and concluded that when in a surface energy-release plot, two minima were observed; one concentrated at low surface energy characteristic of silicone surfaces and the other at higher energies associated with hydrogels (Ober, 2017).The Baier curve demonstrates the relative amount of biofouling versus critical surface tension of the substrate, as it is shown figuratively in Figure 2.3.

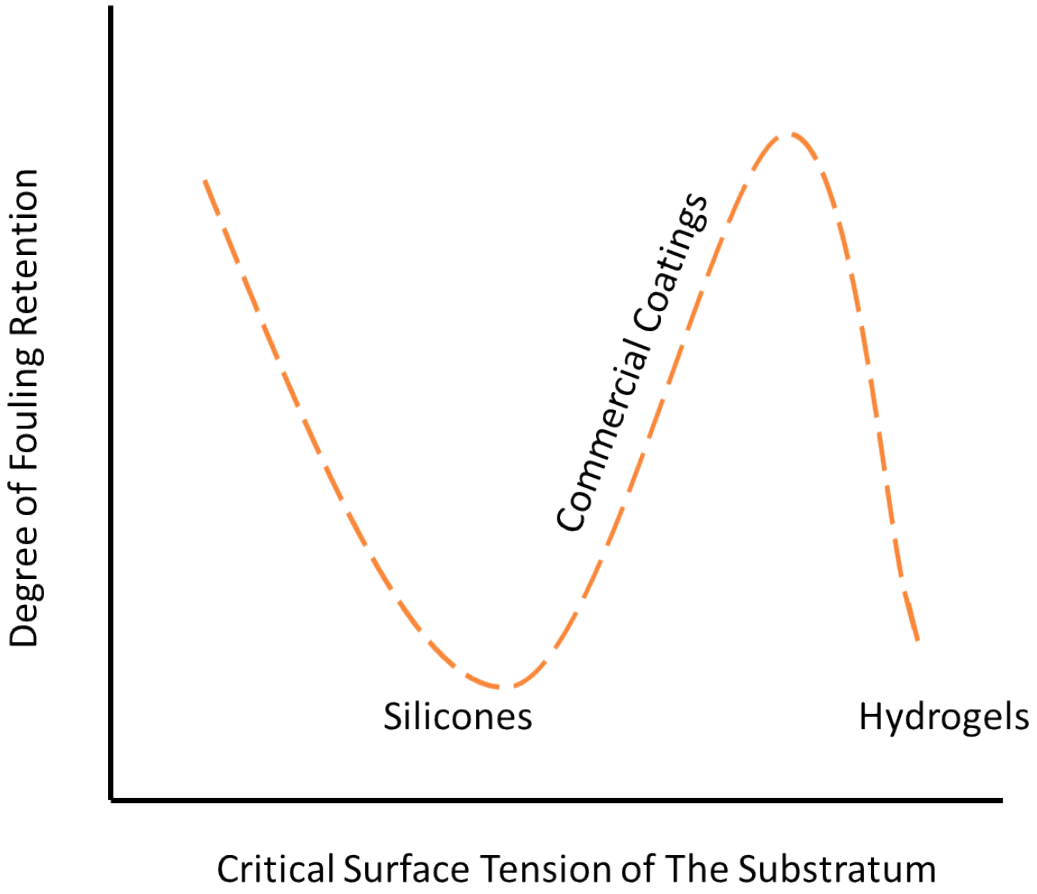

Figure 2.3: The Baier curve – Relationship between biofouling and critical surface tension

Biofouling is an entirely natural process that occurs in domestic, industrial or marine systems and costs society as it causes fuel consumption and CO_2 production increase. Today marine coatings include copper-toxic components, which might reduce bacteria fouling but simultaneously are harmful for the environment. Anti-fouling coatings are of great interest because of their unique wettability and self-cleaning properties, but their widespread applications are limited so far because of low stability and complicated production processes (Dong et al., 2021). Understanding and controlling the coating surface physical structure that interacts with its environment can lead to non-toxic 'anti-fouling coatings' (Ober et al., 2017). The current approach of ablative paints loaded with copper, while effective, leads to accumulation of copper in the environment, thus new concepts of surface composition that inhibit fouling and fouling release have been studied.

The interpretation of the Baier Curve today is that there are important parameters in biofouling and biofouling release beyond surface energy. These parameters include the mechanical properties and the surface composition of coatings. According to the Baier curve, PDMS coatings show the minimum fouling properties combine surface-energy effects with low modulus. Equally, hydrogels with very low modulus are the highest surface energy coatings. Arguments can however be made that the low modulus effect on fouling release because a cracking false can propagate more easily in the bacteria-coating interphase (Chaudhury et al., 2005; Ober et al., 2017). While a coating achieves highly elastomeric properties and the appropriate surface energy and chemical composition, then a fouling resistant, fouling release coating is a possibility (Krishnan et al., 2006; Ober et al., 2017).

Today's research focuses on these facts and is searching for fresh ideas of chemical composition that prevents 'fouling and fouling release'. Among these ideas are amphiphilic surfaces with a dynamic character (Weinman et al., 2009), zwitterionic surfaces of equal numbers of negative vs positive charges (Jiang and Cao, 2010) and developing studies of 'active groups' that reverse the biofilm adhesion mechanisms. The introduction of effective surfaces against a wide spectrum of biofilm relevant foulants, including those that facilitate attachment to surfaces of both negative or positive charge is the real challenge (Ober et al., 2017). Simultaneously, those surfaces should have the ability to repel biofilm relevant adhesives while using a variety of curing mechanisms and have various critical dimensions and mechanical properties (Ober et al., 2017). Given the variety and diversity of biofoulants this goal becomes a real challenge (Ober et al., 2017). Yin et al., (2016) created antifouling surfaces with self-cleaning properties using slippery liquid-infused technique (SLIPS), to prevent dental biofilm/plaque formation. The SLIPS inspired by the leaves of a pitcher plant, exhibits remarkable properties such as liquid repellence, smoothness and self-healing and antibiofouling activities. A stable SLIPS, which consists of a film of lubricating liquid locked in place by a micro/nanoporous substrate, is designed based on three important criteria: (i) the solid should preferably be roughened to increase the surface area for adhesion of the lubricating fluid and its immobilization; (ii) the chemical affinity between the lubricating fluid and solid should be higher than that between the ambient fluid and solid; and (iii) the lubricating fluid and ambient fluid must be largely immiscible. To satisfy the first requirement in constructing the slippery liquid-infused enamel surface, a micro/nanotextured rough surface with a large surface area was obtained by acid etching, which is a commonly used technique in clinical dentistry. The micro/nanotextured rough surface facilitated wicking the lubricating liquid into the enamel surface. To satisfy the second criterion, the acid-etched hydrophilic rough surface was functionalized using

hydrophobic low-surface energy polyfluoroalkyl silane to match the chemical nature of the infiltrated lubricant chosen to be immiscible with the ambient fluid. Roughness analysis confirmed that the lubricating fluid overcoated the surface topographies of the porous enamel surface, forming a nearly molecularly smooth surface. Water contact angle measurements indicated that the silanized surface and SLIPS became hydrophobic, but the FC-70 directly adsorbed surface and acid-etched enamel surface remained hydrophilic. Wang et al. (2016) managed to create a surface with both recyclable, bactericidal and 'self-cleaning antimicrobial' properties by using a temperature-responsive terpolymer through surface-initiated 'reversible addition–fragmentation chain-transfer' (RAFT) polymerization. Other surfaces that show antifouling properties and cleanability features, easy-to-clean, or self-cleaning properties, are Lotus-Effect surfaces and surfaces that have photocatalytic coatings (Detry et al., 2010; Tsiaprazi-Stamou et al., 2019). Dong et al., (2021) introduced a new kind of smooth anti-fouling coatings based on methyltrimethoxysilane that show high stability and excellent anti-fouling properties against several fluids. The transparent and environmental friendly coatings were prepared by simple hydrolytic condensation of methyltrimethoxysilane in isopropanol, followed by wiping the slides with the non-woven fabric that sucked the stock solution. It is a quite promising step in terms of anti-fouling coatings but the issue of antibacterial properties needs to be further studied (Dong et al., 2021).

2.6. Determination of cell- surface and cell- cell interactions

2.6.1. Conventional Methods

2.6.1.1. Shear Stress Flow Methods

Shear stress flow methods use fluid flowing against the adhered bacteria cells and count the cell-percentage that manages to detach and consists of two basic configurations (Missirlis and Spiliotis, 2002). The first one is a parallel-plate flow chamber that generates laminar flow and the second one a cone-and-plate viscometer with a static flat plate and a spinning inverted cone available to create either laminar or turbulent flow (Missirlis and Spiliotis, 2002; Addae-Mensah and Wikswo, 2008) The parallel-plate flow configuration has a simple design and the developed flow in the chamber can be easily analysed. In the most common configuration (Figure 2.4), a laminar flow is generated, the fluid enters in one side and exits from the other side in a four-sided chamber. A glass coverslip consists the upper plate while the bottom 'plate' is the biofilm-treated surface. The flow causes wall shear stress, τ_W, that can be calculated as described in equation 2.7 below (Missirlis and Spiliotis, 2002; Martines et al., 2004; Otto, 2008).

$$\tau_w = \Delta P \frac{h}{2L} \tag{2.7}$$

Where, ΔP is the pressure drop (while outlet-inlet pressure is calculated as $\Delta P=(12L/h^3W)\mu Q$), h is the height of the chamber, L is the length of the chamber, W is the width of the chamber, μ is the fluid viscosity and Q is the volumetric flow rate (Missirlis and Spiliotis, 2002).

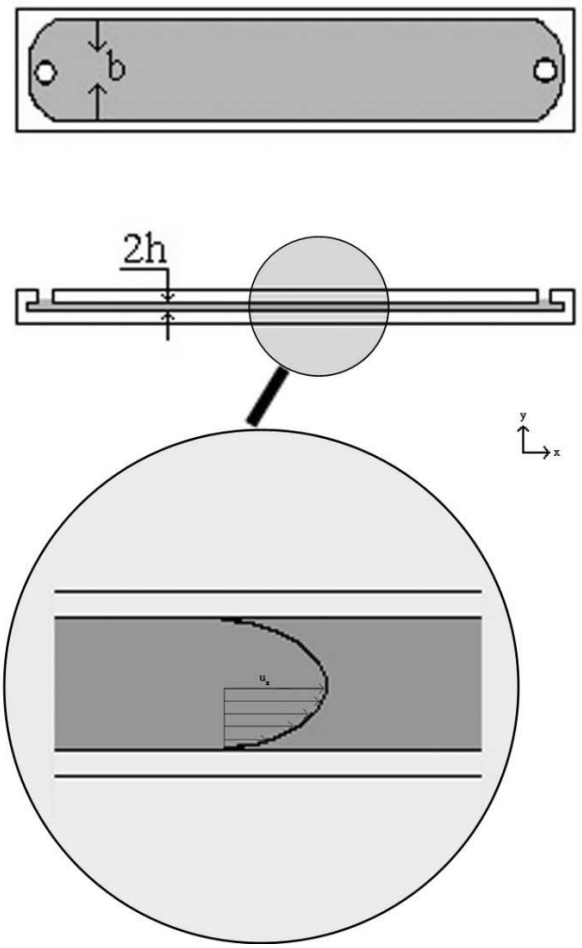

Figure 2.4: Schematic diagram of the upper view, the side view and the flow profile inside the flow chamber.

In the second type of flow chamber, a simple example is a rotating disc device, where linearly varying shear stresses can be generated inside the plates along different sections of the chamber. Either way the shear stresses that are developed at the bottom of the chamber are affected by parameters of the chamber like channel width and height and the fluid properties as the flow rate and its viscosity (Missirlis and Spiliotis, 2002; Katsikogianni et al., 2004; Addae-Mensah and Wikswo, 2008).

To measure the erythrocytes elastic shear modulus attached to a glass slide, Hochmuth et al. (1973) used a parallel-plate flow chamber with a constant shear stress, while Wang et al. (2016) used a similar configuration to evaluate the effect of exercise-induced τ_W

on endothelial cells. As this parallel-plate flow chamber with a constant shear stress could mimic the τ_W acquired from the carotid artery both in resting and exercise-induced state, they concluded that it is suitable for studying the responses of endothelial cells under different shear stress states in vitro (Wang et al., 2016).

2.6.2. Advanced methods

The absence of appropriate force-measuring techniques on bacterial cells, has hampered the understanding of the molecular relations that dominate the phenomenon of microbial adhesion (Herman et al., 2015). However, single-molecule force spectroscopy has arisen as a useful set of techniques that successfully evaluate the interactions that govern the mentioned phenomenon, like optical and magnetic tweezers (Addae-Mensah and Wikswo, 2008), bio-membrane force probe, micro-cantilever arrays etc (Neuman and Nagy, 2008). The techniques that follow the above principle can be used to apply force on the bacteria sample but also to measure its shift at the single-molecule level (Neuman and Nagy, 2008). Whereas there is a long list of techniques that manipulate bacteria in the atomic scale, the most useful and broadly studied technique is the Atomic Force Microscopy (Angeloni et al., 2016).

2.6.2.1. Bacterial Force Spectroscopy using Atomic Force Microscopy (AFM)

AFM has been proved to be an extremely beneficial method in biology studies as its major advantage, comparing to other microscopy techniques, is that it can give information on local surface properties, biofilms and bacteria-surface interactions at the same time

(Katsikogianni and Missirlis, 2004). AFM can be used for imaging the individual microbial cells and measuring the interaction forces at microbial surfaces. These forces include above all the above-mentioned (i) van der Waals and (ii) electrostatic forces. Finally, it is a useful tool for the investigation of biofilms and single bacteria mechanical properties (Fang et al., 2000). Despite its major advantage and the numerous reports on the elastic properties of cell structures by means of AFM, an unquestionable, commonly-accepted methodology is needed. A subcategory of AFM is microbial cell force spectroscopy (MCFS). In this technique, special probes are used and developed by immobilizing bacterial cells at the tip of commercial AFM micro-cantilevers. These special modified probes allow the measurement of the different types of cell-surface interactions and adhesion forces (Bowen et al., 2001; Puricelli et al., 2015; Angeloni et al., 2016). Bowen et al., (2001) immobilized individual cells at the end of standard V-shaped AFM tipless cantilevers. The tipless cantilevers used were silicon ultralevers (Thermomicroscopes). The cells in solution were placed on a glass slide and picked up by a small amount of glue (Loctite Glass Bond-Loctite Ltd.) located at the end of an AFM cantilever housed in a micromanipulator. Cell immobilization was facilitated by the use of the micromanipulator (Singer Instruments Ltd.) which allowed the correct location of cells at the apex of the cantilever and ensured that the minimum amount of glue was used. Similarly, Angeloni et al. (2016) based the preparation of bacterial cells colloidal probes on a three-steps procedure: (i) the attachment of a micrometric bead on the cantilever free end; (ii) the chemical modification of the bead surface through substances able to improve cells adhesion; (iii) the transfer of bacterial cells on the bead surfaces. The attachment of the sphere on the AFM cantilever was obtained through the use of a micromanipulator and particular glues, such as epoxy resins or UV-curable glues. The colloidal probe was then functionalized with substances able to increase the bacterial adhesion on the sphere surface, for example polylysine, PEI, or

polydopamine. A single bacterial cell, previously isolated and deposited on a flat substrate, could be picked up by and placed at the apex of the immobilized sphere, using a micromanipulator or the AFM instrumentation. Otherwise, a micromanipulator was used to cover the sphere with a uniform layer of cells.

During the past years many studies to understand the adhesion of living organisms on different surfaces, have measured the mechanical properties of bacteria cells or biofilms using AFM (Katsikogianni and Missirlis, 2004). These mechanical properties include the Young's modulus that can be found in literature as mechanical stiffness or elasticity (Assaly et al., 2012; Zhang et al., 2016). Alternatively, AFM can measure the forces involved in adhesion or cohesion energy to estimate the balance between bacteria growth and bacteria detachment of the various surfaces (Bowen et al., 2001; Ahimou et al., 2007). As the studied sample moves up and down, the deflection of the cantilever can be measured and its analysis can deliver the force data applied. The applied force of the probe to the bacteria sample is plotted as the probe-sample separation distance and a force-distance curve is obtained. The biofilm elasticity and adhesion force can be evaluated using the repulsive section slope of the force-distance curve either on flat surfaces or membranes (Puricelli et al., 2015; Ferrando and Herzberg, 2017).

Ahimou et al. (2007) used AFM to measure the cohesive energy of activated sludge by correlating the volume of the biofilm displaced as a function of the biofilm depth. Puricelli et al. (2015) used AFM and the Hertzian Model in living PC12 and MDA-MB-231 cells, (PC12: pheochromocytoma of the rat adrenal medulla and MDA-MB-231:

human breast adenocarcinoma) in order to show how the Young's modulus is affected under the conditions of a cytoskeleton-targeting drug. Furthermore, they used AFM to point the importance of the finite thickness effect and how essential it is to be corrected. Ferrando and Herzberg (2017) used the Hertzian model as well to measure the Young's modulus in *P. aeruginosa* biofilm and the porosity of reverse osmosis membranes through nanoindentation experiments. The experiments were conducted using a Veeco/Bruker AFM (Multimode with IIIa controller, Bruker Corp., Billerica, MA, USA) in 50 mM NaCl background solution, using a 2.5 μm diameter glass bead probe attached to a 0.06 or 0.07 $N \cdot m^{-1}$ cantilever (Novascan Technologies Inc., Ames, IA, USA). Approach and retraction speeds were each set at 1 $um \cdot s^{-1}$. The Hertzian model was used to calculate Young's modulus from each force curve, assuming a Poisson ratio of 0.5. Elastic indentation responses were extracted from the resulting force vs. separation distance profiles. The biofilms used for the AFM analysis were grown in a rectangular prism flow cell in stationary phase cultures of each of the variants of *P. aeruginosa* PAO1. Assaly et al. (2012) wanted to correlate the biofilm Young's modulus with the wrinkle formation during cell death, and they discovered that the differences that were noticed were due to the difference in extracellular matrix production. Alvarado-Gomez et al. (2018) studied the differences between some biofilm physicochemical properties in single- and mixed-species, formed by bacteria from clinical samples of infected chronic wounds using AFM microscopy and concluded that each bacterium alone formed single layer biofilms, while the mixed-species bacteria formed a multilayer biofilm at the same observation time, a result that marked the importance of a achieving a better understanding of the multispecies-bacteria biofilm adhesion, a milestone that would help in the development of more effective treatments against biofilm formation.

Modification of the cantilever

Cell-probes or bacteria-cell-probes are generated by the modification of commercial silicon (Si) or silicon nitride (SiN) cantilevers, with a spring constant that ranges from 0.01N/m to 0.5 N/m. The cantilever is modified through bacteria cells immobilization on the AFM probe (Zheng et al., 2014). Depending on the specific experiment, the preparation method of the cantilever surface modification is different. Consequently, the final characteristics of the cell probe will be affected by the chosen modification method and, as a result, the operation mode and the data analysis will be also influenced (Angeloni et al., 2016). Unfortunately, up to present there is a lack of a typical process for the production of cell probes. Two kinds of bacterial cell-probes can be categorized as being for attached bacteria, mixed-culture-bacterial cell-probes and single-culture-bacterial cell-probes. One other classification relies on the preparation method of the cantilever (Zheng et al., 2014). The different methods include above all the chemical modification of the surface probes, the attachment of a bacteria-covered microsphere, (colloidal probes) or the not so widely used physical entrapment of cells (Angeloni et al., 2016). Li et al. (2016) used a method that had already been described by Zhu et al. (2012) for the immobilization of A. ferrooxidans to micro-fabricated Si3N4 cantilevers with a spring constant of 0.57 0.03 nN/nm.

Colloidal Probes

The colloidal probes are, as mentioned above, spherical probes that are generated by attaching either bacteria or other microparticles to tipless cantilevers. Colloidal probes are used instead of sharp tips, mainly due to their well-defined geometry. Sharp tips are

widely employed because of their low cost and at the same time their high-resolution potential. These features facilitate the study of the cell mechanical properties and their topography in the nanoscale. One disadvantage that they show is their high cost, however the uniform distribution of stress and strain that is applied in the samples, generally make them great candidates in AFM force measurements (Kappl and Butt, 2002; Neuman and Nagy, 2008). Dagang et al. (2016), used AFM glass colloidal-probes, stainless steel, and cellulose of 20μm to *P. fluorescens* biofilms to evaluate the different adhering behaviour between the above surfaces. On approach, all the colloidal probes experienced a long non-contact phase more than 100 nm in length, possibly due to the steric repulsion by extracellular polymers from the biofilm and hydrophobic effects. Retraction data showed that the adhesion varied from position to position on the biofilm. The mean value of adhesion of glass to the biofilm (48 ± 7 nN) was the greatest, followed by stainless steel (30 ± 7 nN) and cellulose (7.8 ± 0.4 nN). This indicates the involvement of steric repulsion and hydrophobic interactions probably due to EPS in the biofilms. During retraction, glass gave the greatest adhesive force. The method used here allows comparisons between surfaces to which biofilms might adhere, and can be extended to any material for which a colloidal probe can be prepared. Similarly, Erath et al. (2010) used a colloidal probe to determine the contact range of a hard glass surface and measure the forces induced by the probe. The adhesion properties were evaluated by using the Johnson-Kendall-Roberts (JKR) theory. This approach includes first the measurement of the exchange contact area as a function of the induced force. The second part of the JKR approach contains the evaluation of the sample's viscoelastic parameters as well as the thermodynamic work of adhesion. The use of micrometric spherical probes in combination with the development of appropriate algorithms for the automatic application of data analysis in Atomic Force Microscopy, appears to be an optimal way that facilitates the simultaneous measurement

of topographic/mechanical properties on living organisms (cells, bacteria, biofilms), and has the potential of being an extremely useful tool in biology and medicine (Erath et al., 2010; Puricelli et al., 2015).

2.6.2.2. Micromanipulation

Understanding the adhesion and cohesion forces developed in biofilms, especially the forces needed to distort their structure and clean them from the surfaces, is essential for the development of anti-biofouling precautions. In 1992, a micromanipulation technique, to measure the single cell's mechanical strength, was developed by Z. Zhang in the 'School of Chemical Engineering at the University of Birmingham' (Zhang et al, 1992). For the direct measurement of the biofilm adhesive strength on a glass surface, a novel probe with a T-form was developed.

The theoretical principle of that technique at the time was to drag away the biofilm from the glass surface with the probe, and to simultaneously measure the force applied on the biofilm from the probe (Zhang et al, 1992). The biofilm-surface adhesive strength is defined as the work per unit surface that is required, for the biofilms to be removed from the surface (Chen et al., 1998). Since then, several studies for the measurement of adhesion and cohesion forces of biofilms or the measurement of their mechanical properties or single cells have been based in the so mentioned micromanipulation technique (Zhang et al, 1992; Chen et al., 1998; Chen et al., 2005). To study the soiling layers' adhesive and cohesive forces Garrett et al. (2007) developed a modified micromanipulation device. Several studies have been based in the same technique for the direct measurement of the adhesive as well as the cohesive forces of food-fouling-deposits, like tomato paste, milk proteins, tooth- paste, caramel etc. (Liu et al., 2002; Hooper et al., 2006; Liu et al., 2006; Liu et al., 2006; Garret

et al., 2007; Liu et al., 2007). Based on the micromanipulation technique Ali et al., (2015) developed at the University of Cambridge a larger scale, millimanipulation similar technique to investigate the mechanical properties of foods and products with complex structure (Magens et al., 2017).

2.7. Cleaning in Place

As biofilm formation and proliferation affect many aspects both of public health and industrial processes, including contamination in the food and beverage industry (Johansen et al. 1997; Palmer et al., 2007; Goode et al., 2013; Tsiaprazi-Stamou et al., 2019), its elimination is of great importance. In order to control biofilm formation, food industries use routine cleaning processes, including cleaning-in-place (CIP) and cleaning-out-place (COP) systems mainly comprising shear stress generated by fluid flow or mechanical action together with chemical agents (Keener, 2005; Li et al., 2017; Tsiaprazi-Stamou et al., 2019). Effective biofilm cleaning comprises of two distinct phenomena: biofilm removal or/and biofilm deactivation through disinfection (Tsiaprazi-Stamou et al., 2019).

Various studies have focused on studying the detachment kinetics of biofilm from artificial surfaces found in industrial environments, using 'cleaning-in-place' (CIP) systems. Studies on the mechanism that provokes biofilm cleaning from stainless steel substrates, concluded that a combination of hydrodynamic mechanical forces and chemical agents is essential for effective biofilm removal (Lécrigny-Nolf et al, 2000; Blel et al., 2007; Blel et al., 2008; Faille et al., 2013; Bénézech et al, 2018). Lécrigny-Nolf et al. (2000) studied the *Bacillus cereus* spores removal kinetics from stainless steel under shear stress conditions and concluded that the effect of hydrodynamic shear is not linear. Similarly, Blel et al. (2007) studied flow velocity and wall shear stress effect on *Bacillus cereus* spores removal from

stainless steel pipes using NaOH and removal was found to be strongly dependent on both chemical action and hydrodynamic conditions during Cleaning-In-Place (CIP). Sodium hydroxide has shown to be effective in removing proteins and nucleic acids as well as in inactivating most viruses, bacteria, yeasts, fungi, and endotoxins. It is common practice in industrial manufacturing to save time by adding a salt, such as sodium chloride, to the sodium hydroxide solution to combine cleaning with sanitization. As a cleaning agent, sodium hydroxide saponifies fats and dissolves proteins (Block, 1991; Adner et al., 1994).

A later study comparing the mechanical and chemical detachment kinetics of different strains of *Bacillus cereus* from stainless steel coupons. CIP with NaOH under low wall shear stress was found to be more effective than mechanical rinsing with water at higher wall shear stress; however, the result was affected by strains and the spores' surface chemistry (Faille et al., 2013). The role of mechanical vs chemical action on the detachment of *P. fluorescens* biofilm during CIP with NaOH at a pilot-plant scale could be explained with a two-phase kinetics model, where during the 1st phase an instant biofilm removal occurred followed by a slow rate removal during the 2nd phase (Bénézech et al, 2018). According to this study, the shear stress caused the removal of both biofilm and single cells while chemicals mainly cleaned the biofilm during the 1st phase of CIP. They stated that hydrodynamics was responsible for removal of both biofilm and single cells while chemicals mainly disrupted biofilm clusters during the first phase. No complete biofilm removal was observed, suggesting a significant role of the interaction forces between bacteria and substrata in the CIP efficiency. During a CIP procedure of surfaces contaminated with *P. fluorescens* biofilms, the percentage of residual cells first quickly decreased with time. In a few minutes they observed a 5-log reduction. In static conditions, up to two $Logs_{10}$ of

bacteria were detached in 10 min. Under flowing water, similar to what was observed under CIP, a general trend seemed to emerge, with a rapid decrease of the adherent population within the first few 3-5 min of the kinetics, followed by a phase of slow detachment up to 30 min. The initial detachment rate of the biofilm was significantly affected by the wall shear stress as in static condition the removal observed was the lowest. Finally, the influence of hydrodynamic wall shear stresses at different positions of piping elements on the removal of *Bacillus spores* during CIP was investigated and it was found that geometrical changes induced nonhomogeneous distribution of the initial and the residual soil levels (Blel et al., 2008).

As no standard method is still available for the evaluation and the comparison of cleaning agents for CIP processes in the food industry (Ostrov et al., 2016) we can evaluate "biofilm cleaning" by studying the elimination of two distinct parameters, the extracellular polymeric substance (EPS) removal and the bacteria viability. The EPS-removal represents the soil mass of the biofilm and its elimination is substantial for good cleaning practices whereas the bacteria viability signifies the ability of the biofilm's survival and reproduction after cleaning, thus its disinfection is equally crucial as its removal. While routine cleaning in industry comprises of strong alkaline and acidic agents, efficient in CIP of food-processing lines (Antoniou and Frank, 2005; Tsiaprazi-Stamou et al., 2019), this strategy is not always enough for biofilm removal. Also, their safe handling requires the utmost care, and hence milder, safer and more efficient biofilm CIP cleaning agents are desirable (Galié et al., 2018; Tsiaprazi-Stamou et al., 2019).

Research has shown that bacterial cells within biofilms are more resistant in cleaning with antimicrobial agents (Lindsay and Holy, 2006; Tsiaprazi-Stamou et al., 2019). By

forming a biofilm, bacteria protect themselves from host defence, disinfectants, and antibiotics. Bacteria inside biofilms are much more resistant to antimicrobial agents than planktonic forms since bacteria that are unresisting to antimicrobial agents in any way can turn resistant after forming a biofilm (Stoodley et al., 2013; Dincer et al. 2020). Biofilm EPS confers a physical barrier containing numerous anionic and cationic molecules such as proteins, glycoproteins, and glycolipid that can bind charged antimicrobial agents and provide shelter for microorganisms. The adsorption sites of the matrix also limit the transportation of antimicrobial substances (Dincer et al., 2020). Additionally, extracellular DNA (eDNA) is a significant component of the bacterial biofilm matrix that can be obtained endogenously from the outer membrane or from the cell integrity-degraded biofilm microorganisms. eDNA can increase biofilm resistance to certain antimicrobial agents. One of the mechanisms by which the eDNA increases biofilm resistance is that it causes changes in outer membrane because DNA is an anionic molecule; it is able to chelate cations, such as magnesium ions and cause a lowering Mg^{2+} concentration in membrane. Playing a physical role in defence against antibiotics, eDNA has also provided horizontal transfer of antibiotic resistance genes between microorganism cells forming biofilm (Stoodley et al., 2013; Dincer et al., 2020). Furthermore, biofilm bacteria are equipped with a range of stress responses that make them possible to deal with environmental change, such as oxidative stress, unexpected temperature changes, low water activity, deprivation, and DNA damage. These adaptive responses serve to enhance bacterial survivability. Moreover, bacteria interact with neighbours to accomplish collective activities, such as bioluminescence production, biofilm development, and exoenzyme secretion. This cooperation occurs through the quorum sensing mechanism, which is cell-to-cell communication at the molecular level, controlled by chemical signalling molecules called autoinducers. Due to quorum sensing, bacteria can recognize the population density by measuring the

accumulation of signalling molecules that are secreted from members of the community. The accumulation of the signal in the extracellular environment is adequate to activate the response only when the population density is high. Another very important weapon in the biofilm protection against antimicrobial agents are efflux pumps, i.e., membrane proteins that are related to the export of harmful substances from within the bacterial cell into the external environment. They are found in all species of bacteria, and efflux pump genes can be found in bacterial chromosomes or mobile genetic elements, such as plasmids. A wide array of substrates, such as antibiotics, detergents, dyes, toxins, and waste metabolites are extruded by efflux pumps. It is thus seen that biofilms are diverse, resistant and adaptive in common disinfectants or antibiotics (Dincer at al., 2020).

An interesting alternative is the application of enzymes. Since they are biodegradable and show low toxicity, enzymes are considered green countermeasures against biofilm formation (Galié et al., 2018) and they have been used in detergents for biofilm removal in food industry (Furukawa et al., 2010; Tsiaprazi-Stamou et al., 2019). Therefore, proteases (e.g., serine proteases, proteinase K, pepsin and trypsin) and glycosidases (e.g., amylases, dextranase and pectinase) are always the first option for biofilm removal. Pectin methylesterase, for example, is an enzyme capable of reducing biofilm formation in bioreactors. This activity is imperative to the food industry as it can be used as a pre-treatment for the various machines and pipes. Other enzyme activities such as amylases, cellulases, lyases, glycosidases (such as dispersin B) and DNAses, as part of industrial detergents, are commonly used in the food industry as well to remove biofilms (Coughlan et al., 2016). In order to understand the mechanism of enzymatic cleaning against biofilm, Molobela et al. (2010) studied commercial proteases and amylases for their effectiveness in the deformation and detachment of EPS matrix produced by *P. fluorescens*.

Specifically, they tested protease (savinase, everlase and polarzyme) and amylase (Amyloglucosidase and Bacterial Amylase Novo) activity on both biofilms and on extracted EPS. In that study, all enzymes except for the protease polarzyme were proved effective for the degradation of the EPS, with savinase and everlase being the most effective.

Everlase and savinase are protease enzymes developed for the detergent industry that break down protein. These enzymes are made by animals, plants, fungi, and bacteria. Some proteolytic enzymes that may be found in supplements include bromelain, chymotrypsin, ficin, papain, serrapeptase, and trypsin (Molobela et al., 2010). Since the catalytic properties of any enzyme are determined by its three-dimensional structure, which in turn is determined by the linear combination of the constituent amino acids, we can also alter an enzyme's properties by replacing individual amino acids (Robinson, 2015). Detergent enzymes can be made more bleach-stable using this type of protein engineering (known as site-directed mutagenesis). Bleach-stable protein-engineered enzymes have been on the market for a number of years, for example Novozymes' Everlase®. Furthermore, enzymes can be given other useful properties using this technique, for example improved heat stability, higher activity at low temperatures, and reduced dependency on cofactors such as calcium (www.novozymes.com, Enzymes at work).

In other studies (Vickery, 2004; Walker et al., 2007; Tsiaprazi-Stamou et al., 2019) that were investigating the cleaning effectiveness against biofilm, mixtures of enzymes were found more adequate for removing biofilms than single enzyme cleaning treatments.

2.8. Conclusions

Humankind has learned to live side by side with microbes. Bacteria and fungi learn to adapt in our environments and we learn how to fight them and control them. Biofilm adhesion and growth on surfaces is a fraction of this effort, but a crucial one. We need the bacteria in some cases but we have to eliminate them in others. This PhD focuses on the second case: the elimination. As it is a vast field, involving various parameters, the main objectives of this study were:

i. *To understand the biofilm behaviour during cleaning at a fundamental level.* Thus, monoculture biofilms were chosen and studied under basic cleaning conditions. The surfaces chosen in this case were common everyday surfaces, stainless steel and polycarbonate tiles. To comprehend the role of surface modification on biofilm growth and removal, the polycarbonate tiles were also modified using plasma treatment technology.

ii. *To study and investigate the behaviour of biofilm cleaning at the real world.* For that, real-case mixed-microbial biofilm was collected from a food industry site and tested for its cleaning behaviour on stainless steel and polyethylene surfaces with commercial cleaning agents. At the same time, the contribution of enzymes in biofilm cleaning was investigated, as it is believed that they can act as a countermeasure for the elimination of strong chemicals in biofilm control. Consequently, the synergy of amylase, protease and lipase were studied for their action against biofilm.

iii. *To examine the adhesion and cohesion forces of a biofilm relevant substitute under cleaning and non-cleaning conditions on different surfaces.* Therefore, alginic acid was developed and studied on stainless steel and polycarbonate surfaces under air, water, NaOH and HCl conditions. Nonetheless, the role of surface modification under different

pH conditions was evaluated by modifying polycarbonate tiles with different polymeric solutions.

3. MATERIALS AND METHODS

3.1 Summary

This chapter describes the materials and methods used to grow and characterize biofilms and biologically relevant soils found in biofilm extracellular matrix, investigate their adhesive and cohesive strength in relation to surfaces and study their cleaning behaviour. The investigation began with biofilm initial attachment, growth and characterization on various artificial surfaces, which was followed by biofilm removal under different cleaning conditions. For this purpose, a parallel-plate flow chamber was designed and built as a cleaning apparatus, in order to develop a controlled biofilm cleaning protocol.

Two separate cleaning studies have been carried out. In the first one (**Chapter 4**), single-species bacteria biofilms were grown on common industrial and domestic surfaces like stainless steel and polycarbonate, and the cleaning agents that were tested for their cleaning capacity were water at 40^{o}C and NaOH solution (0.1%w/v). In the second study (**Chapter 5**), mixed-microbial biofilm samples were collected from a meat-packaging line and were grown on stainless steel and polyethylene surfaces. In this case the cleaning agents that were chosen to be tested for their cleaning efficiency, were enzymatic formulations that were provided by Itram Hygiene (Vic, Spain). Finally, alginic acid was studied on stainless steel and modified and non-modified polycarbonate surfaces as a representation of the biologically relevant soils contained in the biofilm extracellular polymeric substance (EPS). The aim of this last study (**Chapter 6**) was to evaluate the adhesion and cohesion forces between biologically relevant soils and different hard artificial surfaces; these forces were measured via a micromanipulation technique.

3.2 Introduction

Biofilms are considered the main type of microbial life in nature. They can live and proliferate because they are protected from a self-produced matrix of extracellular polymeric substances (EPS), which gives them consistency and resistance to antibiotics and disinfectants (Katsikogianni and Missirlis, 2004; Flemming et al., 2016). As bacteria choose to grow on available substrates rather than in the surrounding media in order to decrease their energy (Katsikogianni and Missirlis, 2004; Otto et al, 2008), the real problem we are facing, is the study of biofilm growth on surfaces and the actions needed to eliminate it from surfaces. As described in Chapter 2, section 2.7, in order to control biofilm formation, food industries use routine cleaning processes, including cleaning-in-place (CIP) and cleaning-out-place (COP) systems mainly comprising shear stress generated by fluid flow or mechanical action together with chemical agents (Keener, 2005; Li et al., 2017). Effective biofilm cleaning comprises two distinct phenomena: biofilm removal or/and biofilm deactivation through disinfection.

However, to eliminate bacteria, the first step is EPS removal. EPS is mostly water (up to 97%) and contains the structural and functional components of the matrix: soluble, gel-forming polysaccharides, proteins and eDNA, as well as insoluble components such as amyloids, cellulose, fimbriae, pili and flagella (Flemming et al., 2016). From a physicochemical point of view, the removal of biofilms is achieved by using substances that induce detachment by diminishing the cohesiveness of the EPS matrix (Xavier et al., 2005). Thus, understanding the microbial and polymeric interactions with surfaces is essential for the optimum biofilm elimination and removal.

Bacteria exist in the microscale and, hence, advanced monitoring techniques are required to study their behaviour. A well-developed imaging technique capable of visualizing the microbial ultrastructure is confocal laser scanning microscopy (CLSM) which is recognized as a key imaging technique in microbiology (Bucs et al., 2018; Nahar et al. 2018). In this study, CLSM has been extensively used in order to determine the biofilm structure i.e., the biomass thickness, the biovolume and surface coverage, visualized and quantified using ImageJ software. In addition, flow cytometry was used to evaluate the viability of bacteria and an EPS-analysis, based on the measurement of the polysaccharide content before and after any cleaning application, was used to measure the extracellular polymeric substance on biofilm. For maintaining controlled shear stress conditions during cleaning, a parallel-plate flow chamber was designed in order to mimic bench-scale CIP conditions.

Moreover, the adhesive and cohesive strengths of alginic acid, as biologically relevant soils, have been further investigated via micromanipulation. Previous work carried out (Chen *et al.*, 1998; Chen *et al.*, 2005; Garrett *et al.*, 2007) demonstrated the usefulness of micromanipulation in determining the biofilm and biomass adhesion. Additionally, other characterization methods like contact angle measurements and energy-dispersive X-ray spectroscopy/Scanning electron microscopy (EDX/SEM) have been used to determine the surface properties that may affect the cell-surface interactions.

3.3 Material Surfaces, Surface Modification and Substrate Characterization

Several common material surfaces were initially measured for their average work of adhesion and hence their surface energy and wettability: stainless steel (SS), polycarbonate (PC), polypropylene (PRP), Nylon, polytetrafluoroethylene (PTFE), polyethylene terephthalate (PET), borosilicate glass (BG) and hydroxyapatite (HA) (d=1.27mm, Biosurface Technologies Corporation). They were initially cleaned by soaking in 1% (w/v) Virkon solution overnight followed by rinsing with distilled water before soaking in ethanol for 30 minutes. The coupons were then washed with distilled water and dried with compressed air. For the calculation of the work of adhesion of the different surfaces and the evaluation of their hydrophobicity, water contact angle (theta) measurements were held on all the above-mentioned surfaces using a Theta tensiometer contact angle apparatus using deionized water (https://particular.ie/brochures/supplier_brochures_pdf/optical_tensiometers_theta_brochure.pdf). One droplet of water (10μL) was deposited and withdrawn onto a dry surface and the image was recorded over time – this is shown schematically in Figure 3.1.

The contact angle of the surface was determined via analysis of the images using FTA32 software (FTA, UK). Each reported contact angle is the mean of at least five independent measurements. According to the Young- Laplace equation of surface tension, the higher the contact angle of water on the surface, the more hydrophobic is the surface. The work of adhesion was calculated according to the Young-Laplace equation of surface tension

$$W_a = \gamma \cdot (1 + cos\theta) \tag{3.1}$$

Where γ, is the surface tension of water at 25°C.

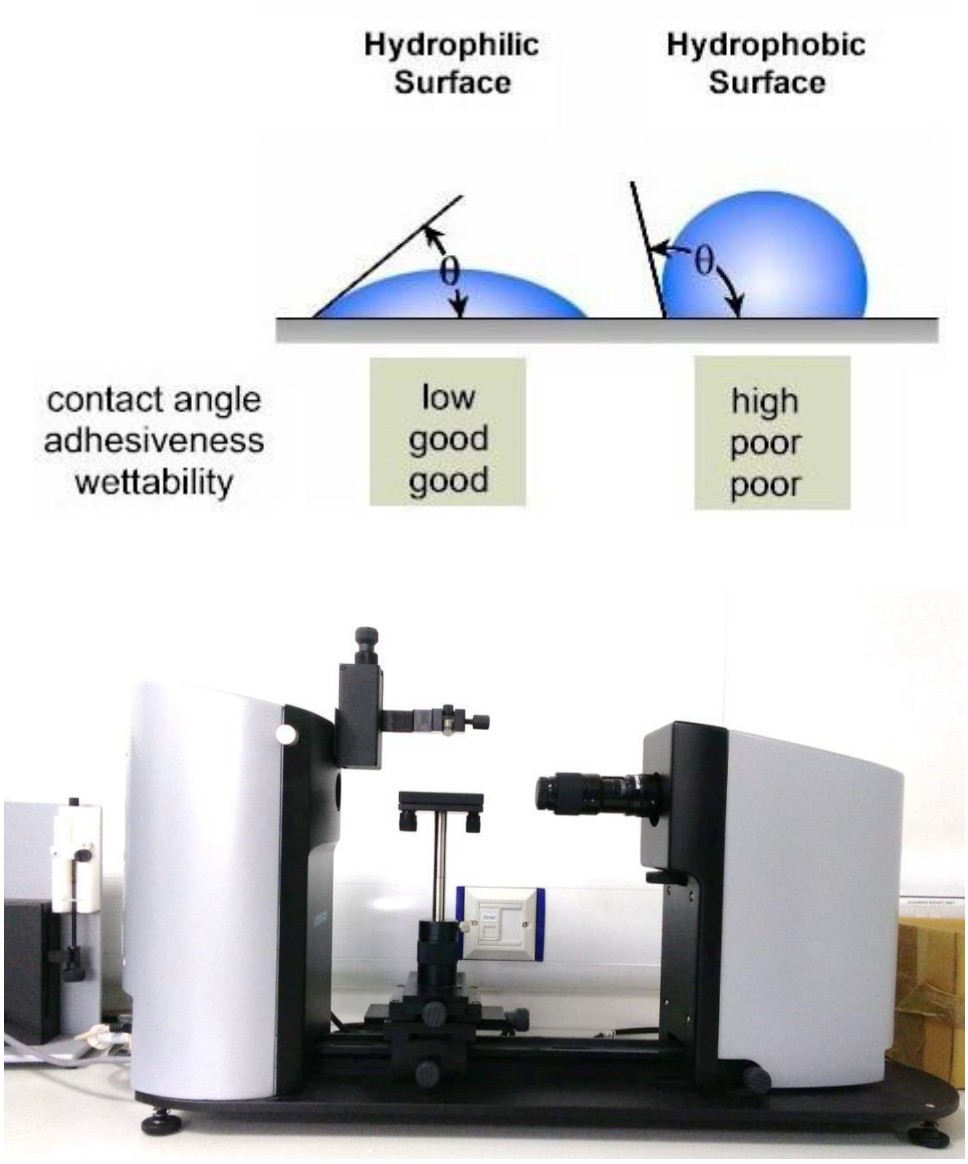

Figure 3.1: (Top image) Representation of water contact angle measurement and evaluation of adhesiveness and wettability. (Bottom image) Theta contact angle tensiometer.

As a result of these preliminary experiments (**Chapter 4, Section 4.4**), stainless steel and polycarbonate surfaces were selected to be studied for their behaviour during biofilm cleaning, as they are the most common materials that are found both in the industrial and the domestic environment. In addition, to evaluate the effect of surface modification on biofilm attachment and hence biofilm cleaning, the polycarbonate surfaces were plasma treated for 5, 10 and 30 minutes, using a Corona discharge (2000) (Földes et al., 2000). After obtaining the average work of adhesion data for the plasma-treated polycarbonate surfaces (**Chapter 4, Section 4.4**), it was decided that 5-minutes plasma treated polycarbonate coupons would also be evaluated for their behaviour during biofilm attachment and biofilm cleaning.

Corona discharge treatment is commonly used to improve the wettability, adhesion, and biocompatibility of a polymeric surface, without affecting the bulk properties (Kelber, 1988; Wypych, 2015). Corona discharge takes place at atmospheric pressure in contrast to low temperature (or cold) plasma that requires vacuum. Corona is a stream of charged particles such as electrons and ions that is accelerated by an electric field. It is generated when a space gap filled with air or other gases is subjected to a sufficiently high voltage to set up a chain reaction of high-velocity particle collisions with neutral molecules resulting in the generation of more ions. Corona discharge has been applied to treat the surface of plastics to render them adherable. In this method, the plastic article is exposed to a corona discharge produced by high-frequency, high-voltage alternating current (Ebnesajjad, 2008). The free electron density in corona discharges is approximately 108 electrons/cm3. Plasmas produced using corona discharges are inherently inhomogeneous and require a narrow space between the electrodes. It has widespread industrial applications including electrophotography, printers, textile processing, and in-powder coating but due to

their inherent nonuniformity, it has limited applications for homogeneous treatments and coating depositions (Wall, 2017).

3.4 Bacterial Organisms and EPS-relative Substances

For the first biofilm cleaning study (**Chapter 4**), two Gram-negative bacteria strains, *P. fluorescens* NCIMB 9046 and *P. putida* ATCC 700008 were chosen as model bacteria in biofilm development. Gram-negative bacteria are more resistant than Gram-positive bacteria, and cause significant morbidity and mortality worldwide (Breijyeh et al., 2020). Both these rod-shaped bacteria strains belong to the Risk category 1 organisms and thus they do not pose high risk to the individual, making them both ideal models for studying biofilms. During the second biofilm cleaning study, performed during a secondment at Itram Higiene in Vic (Spain), mixed-microbial biofilm samples were collected from a meat packaging line. Finally, alginic acid from brown algae (Sigma Aldrich, A2033-250G) was chosen as a biologically relevant soil, as it is a model polysaccharide representing the biofilm extracellular polymeric substance (EPS) (Gordon et al., 2017). This bioorganic compound was chosen as a material to model biofilms because bacterial biofilm adhesion is affected by the extracellular polymeric substances secreted for its protection and survival.

3.5 Culture growth and Biofilm Development

Bacteria growth culture and biofilm development is a procedure that is highly important to be executed aseptically and with sterilized equipment. During the sterilization process the equipment as well as all the nutrient components used in the next procedures, were placed in an autoclave at 121ºC for 15 minutes.

For the first biofilm cleaning study (**Chapter 4**), *Pseudomonas fluorescens* NCIMB 9046 and *Pseudomonas Putida* ATCC 700008 were maintained on tryptone soy agar, TSA, (Oxoid, PO0163) slants, in the dark at 4ºC. Next, using a sterilized loop, a loopful of the slants was aseptically collected and spread on TSA plates. The TSA plates were incubated overnight (24h), at 25ºC for *P. fluorescens* NCIMB 9046 and at 30ºC for *P. putida* ATCC 700008 respectively. A single bacterial colony from the overnight cultures was collected with a loopful and transferred in 100mL of sterile tryptone soy broth (TSB, PanReac AppliChe**,** 413820) solutions of 300mg/L concentration, which were incubated overnight (24 h) at 25ºC and at 30ºC, respectively. Viable bacterial density of the inoculum should equal 10^9 CFU/mL, and may be calculated by Miles & Misra, a serial dilution and bacteria plating method (**Section 3.8.1**).

For the second biofilm cleaning study (**Chapter 5**), swab samples were collected from the surfaces of a meat packaging process line (Vic, Catalonia, Spain) and were incubated overnight at 30ºC in 500mL TSB to a final concentration of 2 x 10^{12} CFU/mL (**Section 3.8.1**) measured by Miles and Misra (data not shown). That was the inoculum that was used next for the biofilm growth on surfaces.

3.5.1 CDC – Biofilm Reactor

For controlled biofilm growth on different surfaces a CDC Biofilm Reactor was selected, as it is intended to serve as an ideal reactor system for researchers interested in growing laboratory biofilms under high shear conditions (BioSurface Technologies Corporation). In this case high shear conditions that are developed in household or industrial environments were aimed to be achieved. The CDC Biofilm Reactor (**Figure 3.2**), is a one-litre glass vessel with an effluent spout at approximately 400mL. It has a polyethylene top that supports eight independent polyethylene coupon holders. Each holder houses three removable coupons of 1.27mm diameter and 3mm thickness (biofilm growth surfaces) for a total of 24 sampling opportunities. A baffled stir bar that was magnetically driven provided continuous mixing of the reactor's bulk fluid, so the coupons experience a consistent high shear from the rotation of the baffled stir bar. The biofilm growth temperature was kept stable by covering the outer part of the reactor with a rubber spiral tube, through which water flowed through at the desired temperature. The CBR can operate as a continuous stirred tank reactor (CSTR), meaning nutrients are continuously pumped into and flow out of the reactor at the same rate.

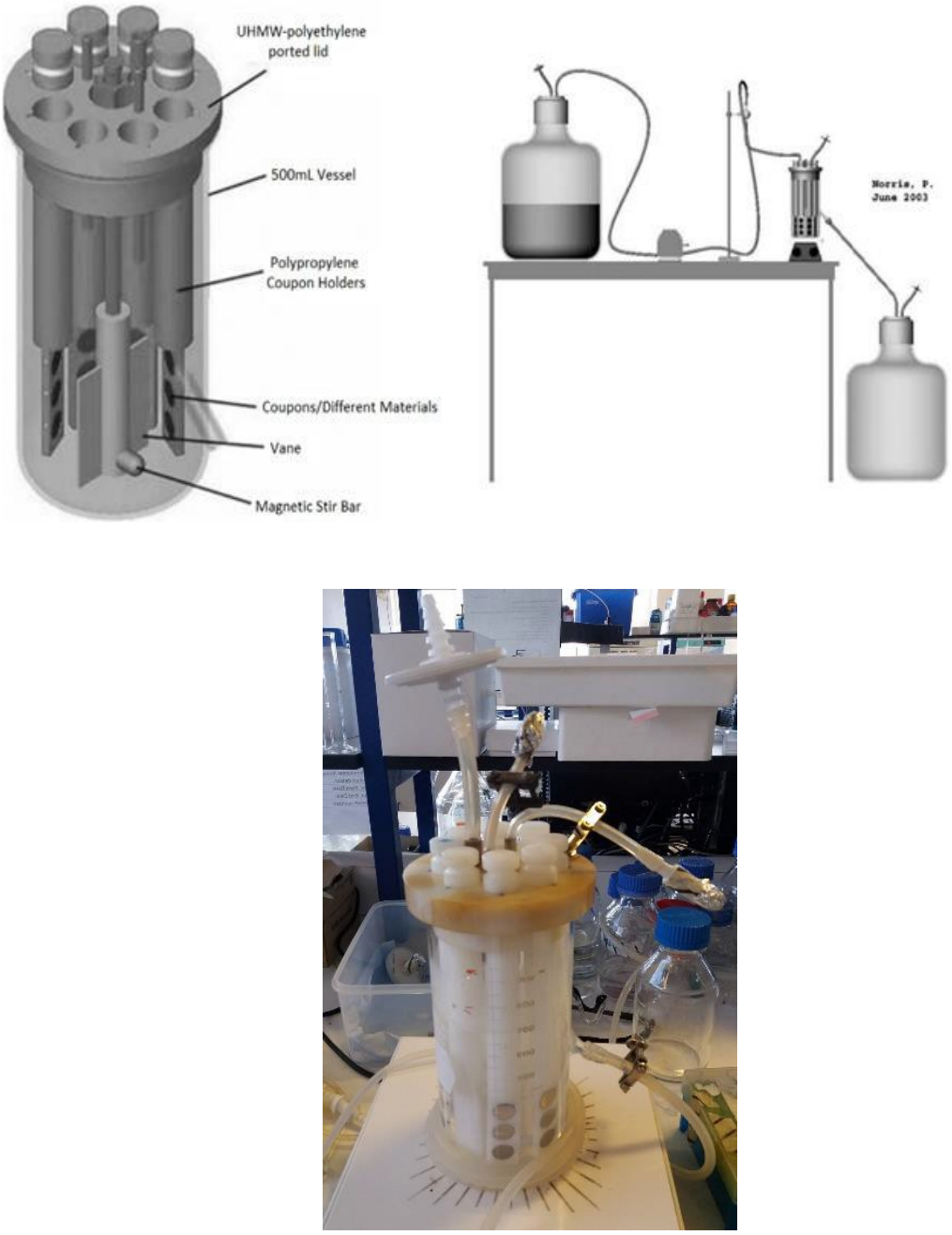

Figure 3.2: (Top image) Schematic representation of the CDC bioreactor and the assembled reactor system. (Bottom image) *P. fluorescens* NCIMB 9046 grown on stainless steel coupons in CDC Bioreactor, 25ºC (ASTM E2562 – 17).

3.5.2 Initial Biofilm Attachment

To study the initial bacteria attachment of *P. fluorescens* and *P. putida* (**Chapter 4**), biofilm was grown on stainless steel, polycarbonate, polypropylene, PET, PTFE, nylon, borosilicate glass and hydroxyapatite coupons. The substrates, bought from the same company as the CDC Bioreactor, were cylinder coupons with diameter 1.27cm and thickness of approximately 3mm (Biosurface Technologies Corporation). They were initially cleaned by soaking in 1% (w/v) Virkon solution overnight followed by rinsing with distilled water before soaking in ethanol for 30 minutes. The coupons were then washed with distilled water, dried with compressed air and placed on the eight independent rods. The rods were placed in the CDC reactor (**Figure 3.2**) with 400 mL of TSB medium (3mg/mL) after having been first autoclaved at 121 °C for 15 min followed by cooling down to room temperature. The closed reactor was then autoclaved again at 121 °C for 15 min and allowed to cool to room temperature. Next, 1mL of *P. fluorescens* inoculum that had been left to incubate overnight at 25ºC as described above was transferred into the CDC reactor. The bacteria concentration of the inoculum was calculated with the Miles and Misra colony forming units method (**Section 3.8.1**) and found to be 10^9 CFU/mL. After 30 minutes of incubation at 25ºC and magnetic stirring the biofilm adhesion process was terminated and the coupons were removed from the reactor and collected for further analysis. The biofilm initial attachment was evaluated using enumeration of bacterial cells in combination with Miles and Misra (**Section 3.8.1**) and Confocal Scanning Laser Microscopy (**Section 3.8.2**). A similar procedure was followed for *P. putida* strain, which was left to incubate at 30ºC for 30 minutes.

3.5.3 Single Bacterial Biofilm Growth

To study the effectiveness of different cleaning processes (**Chapter 4**), *P. fluorescens* NCIMB 9046 and *P. putida* ATCC 700008 biofilms were grown on stainless steel and modified and non-modified polycarbonate surfaces. The substrates, bought from the same company as the CDC Bioreactor, were cylinder coupons with diameter 1.27cm and thickness of approximately 3mm (Biosurface Technologies Corporation). They were initially cleaned by soaking in 1% (w/v) Virkon solution overnight followed by rinsing with distilled water before soaking in ethanol for 30 minutes. The coupons were then washed with distilled water, dried with compressed air and placed on the eight independent rods. The rods were placed in the CDC reactor (**Figure 3.2**) with 400 mL of TSB medium (3mg/mL) after having been autoclaved at 121 °C for 15 min and let cool down to room temperature. The closed reactor was then autoclaved again at 121 °C for 15 min and let cool down to room temperature. Next, 1mL of *Ps. fluorescens* inoculum, that had been left to incubate overnight at 25ºC as described above (**Section 3.5**), was transferred into the CDC reactor (**Figure 3.2**). The bacteria concentration of the inoculum was 1 x 10^9 cells/mL. After 24 hours of incubation at 25ºC and magnetic stirring a continuous flowing system of TSB media was introduced. The flowing system consisted of one carboy filled with 20L of TSB media (1mg/mL) and one empty carboy, both had been autoclaved at 121 °C for 15 min. The first carboy was connected to the input of CDC biofilm reactor and the empty 20L carboy was connected to the output of the reactor, providing the system with fresh media for the next 24 hours at a stable temperature of 25ºC (**Figure 3.2**). After 24 hours the reactors were stopped and the coupons were selected for further cleaning treatment and analysis. A similar procedure was followed for *Ps. Putida* strain, which was left to incubate at 30ºC.

3.5.4 Mixed-Microbial Biofilm Growth

To study the synergistic effect of enzymes against biofilm cleaning from hard surfaces (**Chapter 5**), biofilms were developed on coupon surfaces using cylindrical glass beakers of 2L capacity and 18 cm diameter, named microcosms (**Figure 3.3**). Specifically, for each experiment 36 stainless steel (316L) and 36 polyethylene terephthalate (PET: Polyester, Dacron) coupons (diameter 12.7 mm; BioSurface Technologies Corporation) were placed at the bottom of the microcosms, that were filled with 500mL of Ringers solution (1 tablet in 500ml of distilled water, autoclaved at 121°C for 15 minutes Oxoid, BR0052) and 50mL of Tryptone Soy Broth 3mg/mL (TSB; PanReac AppliChe, 413820). A pump (Eden 105) was placed inside the microcosms to create shear to simulate the dynamic environment of an industrial process line. Next, 2mL of microbial inoculum were transferred in the microcosms to a final concentration of 10^7 CFU/mL. The inoculum was previously prepared from swab samples collected from a meat packaging process line (Vic, Catalonia, Spain) that were incubated overnight at 30ºC in 500mL TSB (3mg/mL) to a final concentration of 2 x 10^{12} CFU/mL. The microcosms were covered with 5 layers of aluminium foil and wrapped with plastic tape, and incubated at 30ºC for 25 days. The volume of the solution reduced due to evaporation so, in order to maintain a constant volume and to avoid modification of the physical-chemical environment due to microbial activity (i.e., pH, oxygen), every 3 days 250mL of the medium was removed from each microcosm and the solution refilled to 500 mL with fresh Ringers solution. The biofilm-colonized stainless steel and polyethylene terephthalate coupons, were removed aseptically, rinsed with sterile PBS (100 mL of 10X PBS to 900 mL of water, Sigma Aldrich P4417) and subsequently used for the CIP enzymatic cleaning experiment.

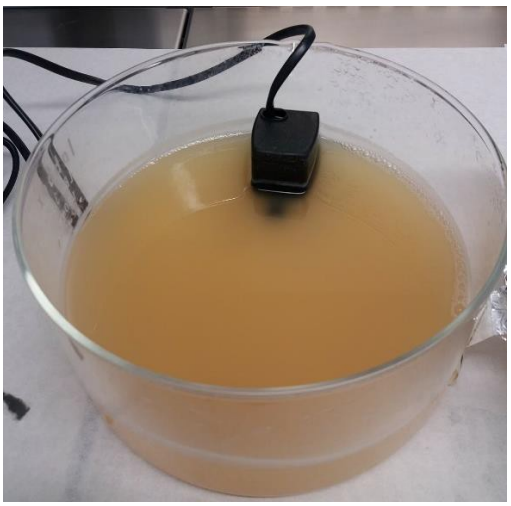

Figure 3.3: Microcosm of 18 cm diameter assembled with an Eden 105 pump to create turbulence in the biofilm growth environment.

3.6 Biofilm removal from surfaces

3.6.1 Design of a parallel-plate chamber

In order to apply a controlled cleaning protocol on biofilm-coated coupon surfaces, a parallel-plate flow chamber was designed to apply a constant and predefined shear stress to the coupons. The goal was to develop a method where the cleaning process would simulate the industrial cleaning procedures in a different scale.

There are very few known cases for which the equation of viscous flow can be solved without approximation; one is the flow of an incompressible fluid between two parallel infinite plates. For this geometry the fluid particles move in the x direction parallel

to the plates, and there is no velocity in the y and z direction (Martines et al., 2004; Munson et al., 1990). In the case of steady flow, the Navier–Stokes equations are easily solved and, if the two plates are fixed, the velocity distribution becomes

$$u_x = \frac{1}{2\mu}\frac{\partial p}{dx}(y^2 - h^2) \tag{3.2}$$

Where μ is the dynamic viscosity of the fluid, p is the hydrodynamic pressure, and h is the half height of the chamber. Equation (**3.2**) shows that the velocity profile between the two fixed plates is parabolic (**Figure 3.4**), i.e., the flow is laminar (characterized by the "slipping motion of layers of fluid over other layers"). In the case of rectangular ducts, such as the flow chamber in this project, the equations cannot so easily be solved, and the solution is more complex. Because of two pair of sidewalls, the velocity profile is a paraboloid (Martines et al., 2004).

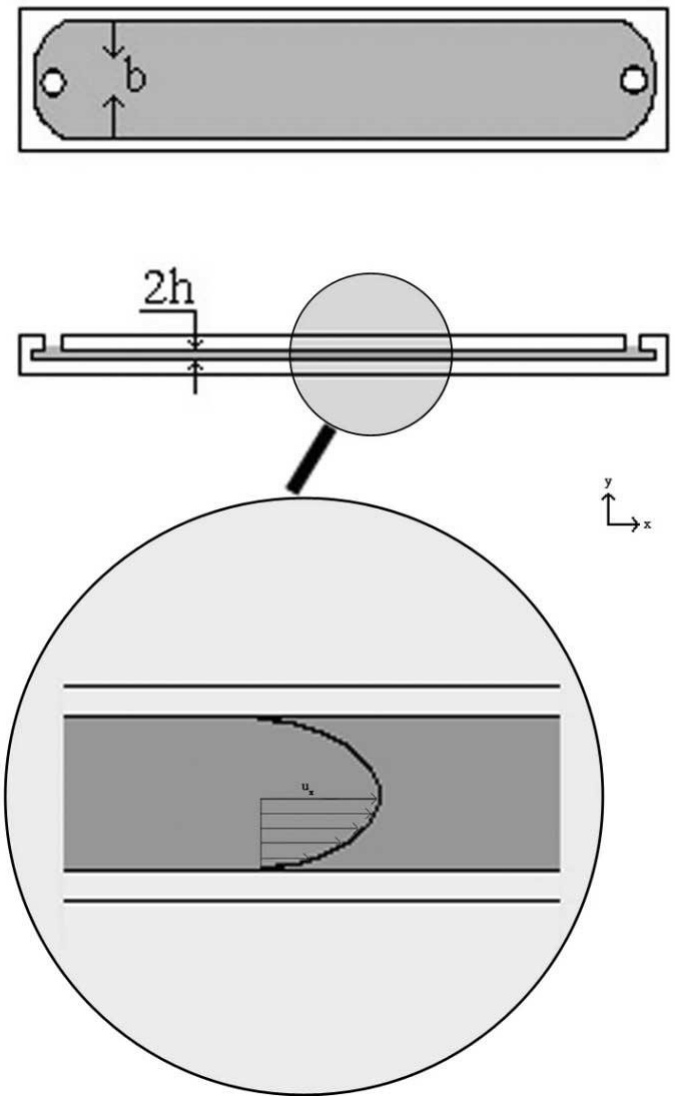

Figure 3.4: Schematic diagram of the flow chamber.

In this chamber the width b, is 23 times greater than the height, so that the two slides have been considered as two infinite (wide) parallel plates. Here, the parallel-plate flow chamber was composed of two stainless steel slides that were considered to act as two infinite parallel plates, and further assumptions were that the fluid was incompressible and Newtonian and that the flow was steady. Three parameters were calculated for the parallel-plate flow chamber (Lane et al., 2012; Martines et al., 2004): (1) The Reynolds number, Re; (2) the entrance length, le and (3) the wall shear stress, τ_w.

Reynolds Number, Re

The calculation of the dimensionless number Re, was selected as a fast and easy way to predict the profile of the flow that is developed in the chamber. The flow profile is generally described as the ratio between the inertial forces and the viscous forces that are present due to the flow (Lane et al., 2012). If *Re* is smaller than 2300, the viscous forces are predominant, so the flow is considered laminar

$$Re = \frac{Dv\rho}{\mu} \tag{3.3}$$

Where ρ is the fluid density, v is the mean velocity of the flow and D, is the hydraulic diameter for rectangular pipes, calculated from the equation

$$D = \frac{4wh}{2(w+h)} \tag{3.4}$$

Where w is the width of the chamber and h the height between the two parallel slides. In order to achieve a well-developed laminar flow, the width of the chamber was 23 times greater than its height (Lane et al., 2012; Martines et al., 2004).

Entrance Length

When the flow enters the chamber, a certain length is needed (so-called entrance length) before it becomes fully developed, i.e. before the velocity profile becomes parabolic. For the calculation of the entrance length of the chamber the equation shown below has been used, where D is the hydraulic diameter (Lane et al., 2012; Martines et al., 2004).

$$l_e = 0.065ReD \tag{3.5}$$

Wall Shear Stress

The wall shear stress was calculated from the equation of the flow rate inside the chamber (Jutila et al., 2007).

$$Q = \frac{wh^2\tau_w}{6\mu} \tag{3.6}$$

Where Q represents the flow rate, τ_w the wall shear stress, w the width of the chamber, h the height of the flow chamber, and μ the viscosity of the flow medium. The parallel plate flow chamber was designed using as a reference fluid water at 40°C. Thus, the physicochemical properties used in all the above equations were used were the following (ThermExcell, 2017):

- Density, ρ = 992.25 kg/m^3
- Viscosity, μ = 0.653 x 10^{-3} kg/(m·s)

For design purposes the width of the chamber was chosen as to be w = 2cm and the flow rate of the water at 40^0C was Q = 0.8 μm^3/s. In order to achieve a well-developed laminar flow, the width of the chamber has to be more than 23 times greater than its height, thus (Martines et al., 2004):

$$\boldsymbol{w \geq 23h \leftrightarrow h \leq \frac{2x10^{-2}}{23} \leftrightarrow h \leq 869.6\mu m}$$

Hence, the height of the parallel-plate flow chamber was chosen as: h = 550 μm. For the flow to be fully developed according to these dimensions the entrance length should be L_e > 0.78cm and thus it was chosen to be 4cm to ensure a fully developed laminar flow (**Fig. 3.5**).

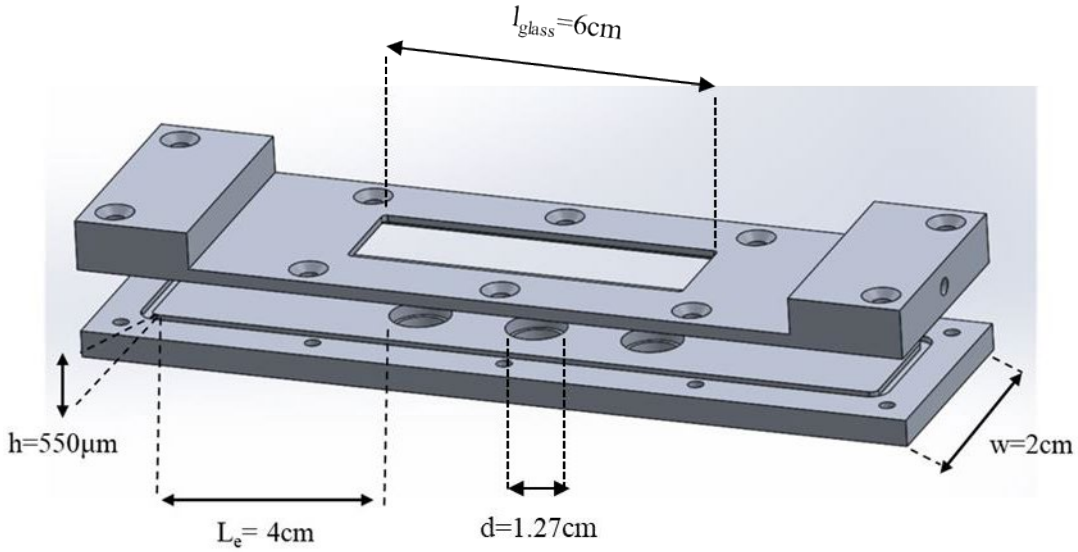

Figure 3.5: Schematic representation of the parallel-plate flow chamber, showing dimensions.

For these dimensions of Width = 2 cm and Height = 550 μm and for water at 40 ºC flow rate Q = 0.8μm^3/s, the wall shear stress is calculated from equation (3.5) as follows:

$$Q = \frac{wh^2\tau_w}{6\mu} \leftrightarrow \tau_w = \frac{6Q\mu}{wh^2} \leftrightarrow$$

$$\tau_w = \frac{6x0.8x10^{-6}x0.653x10^{-3}}{2x10^{-2}x(550x10^{-6})^2} \leftrightarrow$$

$$\tau_w = 0.518\ Pa$$

These equations were used to calculate shear stresses for all of the flows through the chamber.

3.6.2 Cleaning in Place – CIP

To study the effectiveness of different cleaning processes on *P. fluorescens* NCIMB 9046 and *P. putida* ATCC 700008 biofilms on stainless steel and modified and non-modified polycarbonate surfaces (**Chapter 4**), three distinct cleaning in place (CIP) experiments were carried out.

To evaluate the effectiveness of different cleaning processes against the two single-species bacteria strains (**Chapter 4**), three methods were chosen, CIP was performed by using the parallel-plate flow chamber containing triplicate stainless steel and modified and non-modified polycarbonate coupons colonized by biofilm as described above (**Section 3.5.3).** During the first cleaning process (A), water mechanical rinsing at 40ºC was applied in the parallel-plate flow chamber for 30 minutes. In the second cleaning process (B), the coupons were immersed in a glass beaker containing NaOH solution (0.1% w/v) at 40ºC, and no wall shear was applied. Finally, in the third cleaning process (C), NaOH solution (0.1% w/v) at 40ºC was applied in the parallel-plate flow chamber for 30 minutes. The parallel-plate flow chamber operated under stable flow in all the experiments ($Q=0.8\cdot10^{-6}m^3/s$) and the wall shear stress was calculated at 0.518 (N/m^2) for 40ºC.

To evaluate the effectiveness of different enzymes in biofilm removal (**Chapter 5**), CIP comprising of different steps was performed using the parallel-plate flow chamber containing triplicate stainless steel or polyethylene coupons colonized by biofilm as described above (**Section 3.5.4**). During the first cleaning step, enzymatic formulations were applied in flow through the cell for 30 minutes. The formulations applied were not recirculated but were

disposed instead. The initial temperature of the formulation was 55ºC and after the 30 minutes of cleaning process the temperature was 45ºC. In the second step, a commercial disinfectant based on peracetic acid supplied by Itram Hygiene (1% w/w) was applied for 10min at room temperature. Both temperature and exposure time used for the detergents and the disinfectant were as recommended by their manufacturer. The parallel-plate flow chamber operated under stable flow in all the experiments ($Q = 1 \cdot 10^{-6} m^3/s$). The wall shear stress was calculated at 0.129 (N/m^2) for 25ºC and at 0.647 (N/m^2) for 50ºC. The wall shear stress conditions were chosen based on previous references found in literature (Bénézech, T, & Faille, C, 2018).

The different enzymatic products that were tested were prepared using standard enzymatic formulations from Itram Higiene S.L. that contained:

(i) amylase-protease-lipase (Formulation A),

(ii) amylase-protease (Formulation B), and

(iii) amylase-lipase (Formulation C), in combination with a non-foaming Itram enzymatic solution.

The total concentration of enzymes in each formulation was kept constant in all the experiments. The formulations provided by Itram that were used for the preparation of the formulations tested in the experiments had standard concentrations of enzymes and surfactants. Each time the formulation tested (A, B or C) was prepared fresh with the same concentration of the enzyme to be tested. The efficacy of these products was compared to a non-foaming Itram solution without enzymes, which was used as a control.

3.7 Measurement of biofilm residual contamination

3.7.1 Single-Species Biofilms

In the first biofilm cleaning study (**Chapter 4**) to evaluate the effectiveness of biofilm reduction the parameters investigated were:

(i) the bacterial viability using Miles & Misra plating counting technique (**Section 3.8.1**) and

(ii) the percentage (%) of biofilm surface area, biovolume and average biofilm thickness measured from confocal laser scanning microscopy (CLSM) images (**Section 3.8.2**).

All measurements were performed,

(i) before cleaning and

(ii) after cleaning for the different cleaning points.

For each analysis technique and each cleaning point 3 replicates were needed, for each one of the four CIP cleaning processes (Before cleaning, Cleaning process A, Cleaning process B, Cleaning process C) and, thus 24 coupons for each material were initially developed (12 for CLSM and 12 for Miles & Misra).

3.7.2 Mixed-Microbial Biofilm

In the second biofilm cleaning study (**Chapter 5**), in order to monitor the effectiveness of different enzymes in biofilm removal the parameters investigated were:

(i) the percentage (%) of biofilm surface area, biovolume and average biofilm thickness measured from confocal laser scanning microscopy (CLSM) images (**Section 3.8.2**),

(ii) the polysaccharide content in EPS (**Section 3.8.3**) and

(iii) the bacterial viability using Flow Cytometry (**Section 3.8.4**). Complementarily, scanning electron microscopy (SEM) images were obtained to study the microbial biofilm structure (**Section 3.8.5**). All measurements were performed 1) before cleaning, 2) after cleaning with the different enzymatic formulations and 3) after disinfection. For each analysis technique 3 replicates were needed, for each one of the four CIP cleaning processes (Before cleaning, enzymatic formulation, disinfection) and, thus 36 coupons for each material were initially developed (9 for CLSM, 9 for EPS analysis, 9 for flow cytometry and 9 for SEM).

For both studies 1 and 2 (**Chapter 4 and 5**) for all parameters analysed, the effectiveness of biofilm reduction, E_f, was calculated as:

$$E_f(\%) = \frac{|Q_{BC} - Q_{AC}|}{Q_{BC}} * 100 \quad (3.7)$$

Where, Q_{BC} and Q_{AC} are the parameters measured before and after each cleaning step of the process.

3.8 Biofilm Characterization

3.8.1 Miles & Misra

The Miles and Misra method (or surface viable count) is a technique used in microbiology to determine the number of colony forming units (CFU) per mL in a bacterial suspension.

The inoculum is serially diluted by adding 1x of suspension to 9x of Phosphate Buffer Saline (PBS) diluent. When the quantity of bacteria is unknown, dilutions should be made to at least 10^{-8}. Three TSA plates are needed for each dilution series, for statistical reasons an average of at least 3 counts are needed. Plates are divided into equal sectors (**Figure 3.6**). The sectors are labelled with the dilutions.

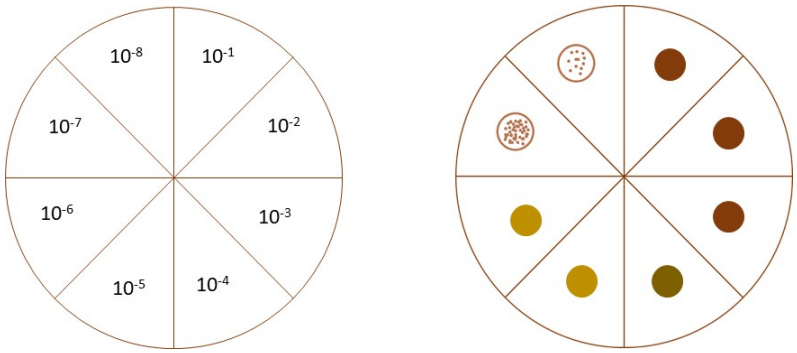

Figure 3.6: Representation of the Miles and Misra plating dilutions.

In each sector, 1 droplet of 20 µl of the appropriate dilution was dropped onto the surface of the agar and the drop was allowed to spread naturally. In the original description of the method a drop from a height of 2.5 cm spread over an area of 1.5-2.0 cm. It is important to avoid touching the surface of the agar with the pipette. The plates were left upright on the bench to dry before inversion and incubation at 25 °C for *P. fluorescens* and at 30ºC for *P. putida* respectively for 18 – 24 hours.

Each sector was observed for growth, high concentrations will give a confluent growth over the area of the drop, or a large number of small/merged colonies. Colonies were counted in the sector where the highest number of full-size discrete colonies can be seen (usually sectors containing between 2-20 colonies are counted). The equation **3.8**. was used to calculate the number of colony forming units (CFU) per ml from the original sample:

$$CFU\ per\ mL = \frac{Average\ number\ of\ colonies\ for\ a\ dilution * dilution\ factor}{volume\ of\ sample\ taken\ (mL)} \Rightarrow$$

$$CFU\ per\ mL = \frac{Average\ number\ of\ colonies\ for\ a\ dilution * dilution\ factor}{20\mu L} \Rightarrow$$

$$CFU\ per\ mL = \frac{Average\ number\ of\ colonies\ for\ a\ dilution * dilution\ factor}{20 * 10^{-3} mL} \Rightarrow$$

CFU per ml = Average number of colonies for a dilution x *50* x *dilution factor*. (3.8)

Enumeration of Adhered Bacterial Cells for Initial Biofilm Attachment

In order to count the bacteria cell concentration on the substrates they needed to be removed from the surfaces into Phosphate Buffer Saline (PBS) diluent. Thus, each surface of interest (stainless steel, polycarbonate, polypropylene, PET, PTFE, nylon, borosilicate

glass and hydroxyapatite coupons) was placed separately inside a sterile plate and was washed twice using sterile PBS (9mL) whilst shaking at 100 rpm using a shaker incubator (Gallencamp Cooled Orbital Incubator, UK) for 1 min to aid the removal of unattached cells. The substrate surface was then wiped using a sterile swab (Fisher Scientific, UK) to help remove the majority of biofilm, and the swab was placed into a sterile tube with the PBS solution (9 mL). Using a pipette, the substrate surfaces were then rinsed with sterile PBS solution (1 mL) which was incorporated into the solution containing the swab, resulting in a total volume of 10mL. The tube was agitated using a vortex mixer for 1 min to ensure that the cells were well dispersed. A series of 10-fold dilutions of each sample were prepared in PBS and six replicate aliquots (10 µL) of each dilution were "spotted" onto TSA plates. The plates were incubated for 24h at 25°C for *P. fluorescens* and at 30°C for *P. putida* respectively and colonies were enumerated using a counting chamber. The visualization of this technique is represented in a schematic diagram (**Figure 3.7**).

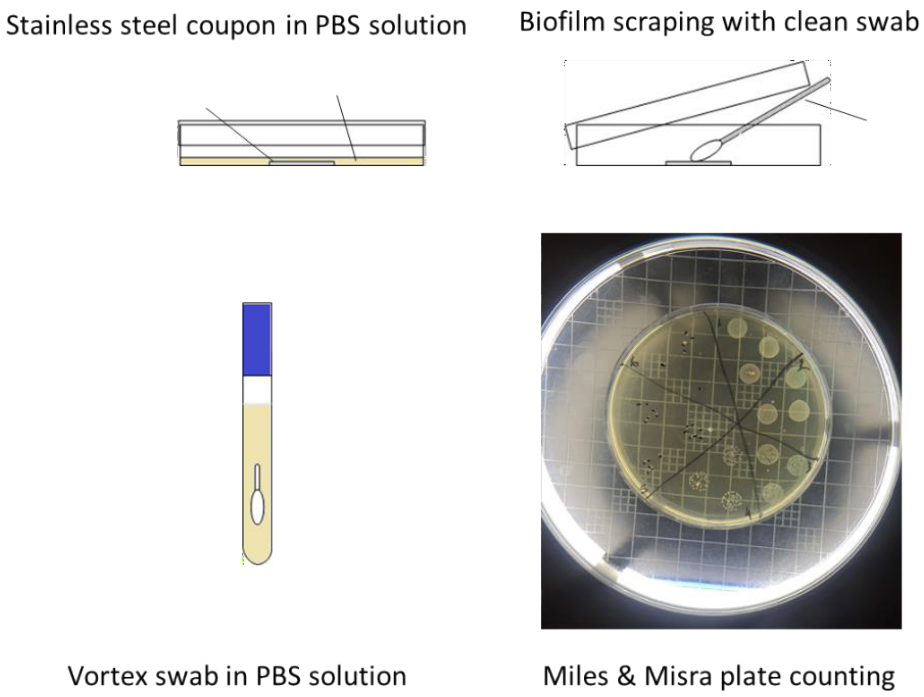

Figure 3.7: Schematic diagram of the methodology of cells enumeration

3.8.2 Biofilm Thickness, Biofilm Surface Area and Biovolume

Multichannel confocal and transmission imaging of the biofilm samples was performed using a multispectral Confocal Leica TCS SP8 microscope. A high-speed module and three light channels and laser lines were used: 405 nm, 488 nm and white laser for 470-670 nm excitation at 592nm. The samples were marked with different fluorophores, depending on the needs of every analysis.

For the initial biofilm attachment (**Chapter 4**), the *P. fluorescens* strain was stained with Acridine Orange (1%w/w) and the *P. putida* strain with DAPI (1%w/w) fluorophores respectively. In each case, for the sample preparation, 15μL of the stain were diluted in phosphate buffer saline. The samples were stained using 60μL of the above solution and were incubated in dark, at room temperature for 10min. The stain was washed with PBS solution and the samples were studied using a 63-magnification oil-lens.

In the case of mixed-microbial biofilms (**Chapter 5**), the samples were marked with SYTO/PI (LIVE/DEAD™ BacLight™ Bacterial Viability Kit, ThermoFischer Scientific) for the live and dead bacterial cells respectively and HCS CellMask™ Blue Stain (ThermoFischer Scientific, H32720) for the EPS bioorganic compounds. For the sample preparation, 15μL of SYTO (1%w/w) and 15μL of PI (1%w/w) were diluted in 1mL of phosphate buffer saline (PBS) solution and 30μL of the lectin (1%w/w) was added. The samples were stained using 60μL of the above solution and were incubated in the dark, at

room temperature for 10min. The stain was washed with PBS solution and the samples were studied using a 63-magnification oil-lens.

For the image acquisition, LAS X Leica software was used with 1024x1024-image resolution, speed 600 and zoom factor 1. For each sample case three replicates were prepared and, in each replicate, images were taken from three random spots on the coupon surface. The 3D biomass information was obtained using a z-stack step of 1μm. This means that once the biofilm was identified on the surface images were collected at the defined spot starting from the top edge of the biofilm and moving every 1μm until the bottom of the biofilm was reached. Image processing and quantification was performed using Fiji (a later version of ImageJ) software along with Comstat2 algorithm, a plugin of ImageJ and Fiji. From the z-stack of the confocal images for each spot the Otsu-threshold plugin and the Skeleton plugin were used in order to collect numerical data from the images (**Figure 3.8**). The volume of the z-stack images represents the biovolume in μm^3 (**Figure 3.9(a)**). The average biofilm thickness represents the average number of z-stack images that were obtained in each sample triplicate (**Figure 3.10**).

Finally, the percentage of the surface area covered with biofilm was calculated by dividing the values of biovolume by the surface area studied and the number of the stacks measured in each case. For example in **Figure 3.9**, two images are observed. To the right (**Figure 3.9 (b)**) is the 2D image that is actually observed over the microscope and shows biofilm EPS (blue), dead (red) and alive (green) bacteria cells of the biofilm. Once the desired biofilm area was found, the microscope camera was moved closer to the surface in order to

examine the biofilm thickness. The Leica software showed at the monitor the exact depth of the camera at each movement. Thus, once the bottom of the biofilm was reached, the user could calculate the biofilm thickness. In this case (**Figure 3.9**) it was 30μm. Next, the camera was moved back to the top edge of the biofilm and was adjusted so as to obtain the information at 1μm intervals across the 30μm depth. The combination of these 30 images is represented as the z-stack of the biofilm at this spot on the coupon (**Figure 3.9(a)**). As the camera was obtaining information on different spots around the coupon, the biofilm thickness could change. Thus, for example at this same coupon (**Figure 3.9**) the biofilm thickness was found 26μm in the second spot of the coupon and 22μm in the third spot of the coupon (not shown here). The average biofilm thickness of that coupon sample was taken as the average of the three mentioned thicknesses and, thus, 22.22μm. In **Figure 3.10** the average thickness (μm) of biofilm is represented as simple columns. Average biofilm thickness is the average height of all columns taken together. The average thickness is presented for the entire observed area of the biomass containing columns. This graph shows that even if there are empty gaps inside the biofilm mass, the average biofilm thickness will be appear the same for two biofilms that are not identical. For this reason it is essential to evaluate other data like biovolume and the surface area covered by biofilm along with the biofilm thickness, in order to collect more representative data about the biofilm architecture.

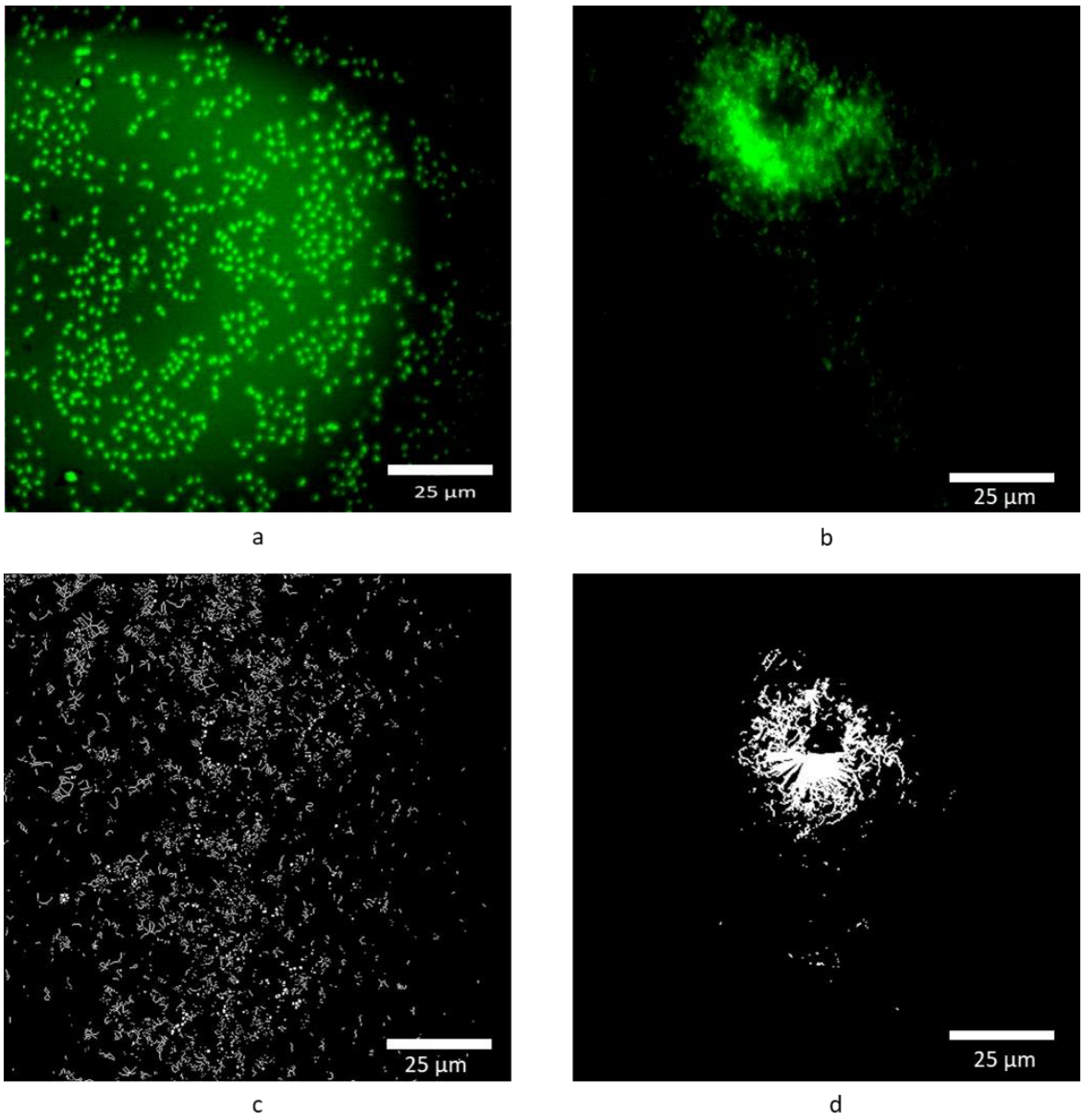

Figure 3.8: a) CLSM image and b) CLSM images (z-stack interval, 1µm) of *P. fluorescens* bacteria, grown in TSB media, under batch phase for 24h, dyed with Acridine Orange (1%w/w), (Image magnification X63). c) "Skeleton" computation of the Otsu-thresholded image a) and d) "Skeleton" computation of the Otsu-thresholded image stack b).

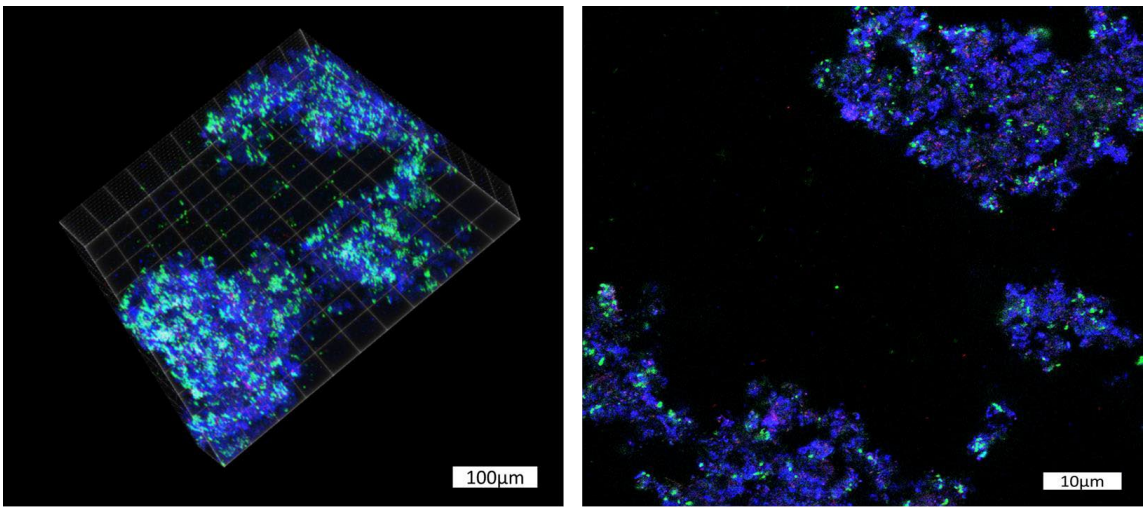

Figure 3.9: a) 3D z-stack images of full-grown biofilm of mixed microbial biofilm. b) 2D Image of EPS (blue-colored), dead (red-colored) and alive (green-colored) singe cell bacteria of a mixed-microbial biofilm.

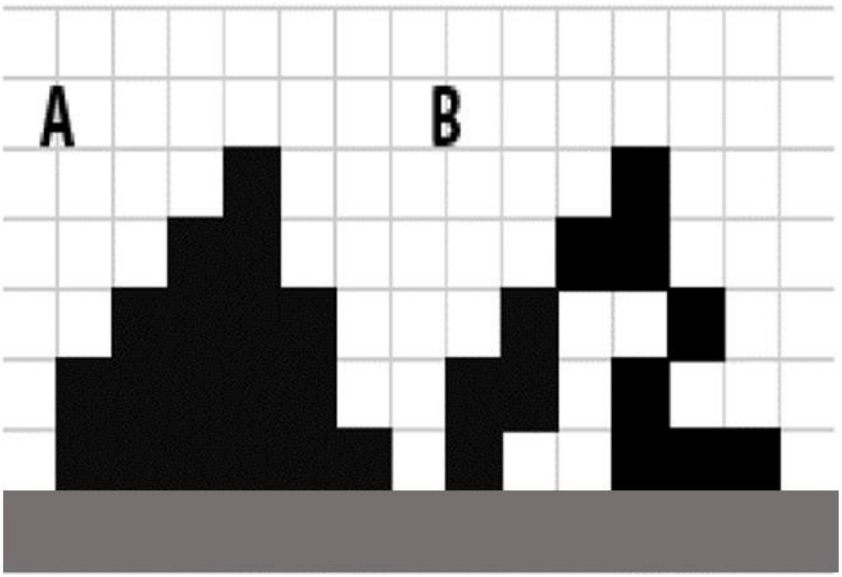

Figure 3.10: The average thickness (µm) is the average height of all columns taken together. The average thickness is presented for the entire observed area of the biomass containing columns.

Finally yet importantly, in all experiments the biovolume, the surface coverage and the average biomass thickness were measured before applying any cleaning process. To compare the results for the different cleaning processes (**Chapter 4**) and enzymatic formulations (**Chapter 5**) the effectiveness of the cleaning was also calculated for all cases (**Section 3.7.2, Equation 3.7**), as the percentage of the reduction of biovolume and surface area coverage respectively.

3.8.3 EPS Analysis

The biofilm EPS was extracted by cation exchange resin (CER) and the content of the polysaccharides was measured as glucose equivalents after digestion (Romani et al., 2008). The cation exchange resin (CER, Dowex® Marathon^{TM} C sodium form, Sigma-Aldrich, 91973-250G-F) was conditioned prior to application for EPS-extraction, following the manufacturer's instructions. The biofilm was scraped off the coupons (sterile silicone scraper, Nunc, Wiesbaden, Germany) into 1ml phosphate buffer (4.49g $Na_2HPO_4 \cdot 12H_2O$, 1.7g KH_2PO_4, adjust to 1L, pH 7) and pipetted into 2ml microtubes (Eppendorf). Then, 0.5 g CER were added to the scraped biofilm and the microtubes were incubated in ice for one hour at 250 rpm agitation. After incubation the particulates of the biofilm were removed from the extract by centrifugation at 12000 x g for 15 minutes at 4^{o}C (Sorvall RC 5B Plus). 500 μL of the supernatant 500 μL of each microtube were pipetted into 10mL glass tubes.

The polysaccharide content of the EPS was determined with the Phenol/H_2SO_4 determination assay developed by Dubois et al. (1956) as phenol can be used for the colorimetric quantification of polysaccharides in the presence of sulphuric acid, as glucose equivalent after digestion. To the 500 µL EPS-extract in a glass-tube, a volume of 12.5 µL phenol solution (80%) was added and the solution was gently mixed. To this tube, 1.25mL of concentrated 95.5% reagent grade H_2SO_4 was added and the glass-tubes were sealed with caps. The samples were left to stand for 10 min and then they were gently shaken and incubated in a water bath for 20 min at 30°C. The developed colour was measured at 485 nm against a reagent blank (U-2000 Spectrophotometer, Hitachi). To calculate the polysaccharide content a glucose calibration curve was built as 500 µL of the prepared glucose standard solutions were used for the phenol-H_2SO_4 assay for the samples. Results were calculated as glucose equivalents per square centimetre of biofilm surface area.

3.8.4 Flow Cytometry

The number of live and dead bacteria was obtained, and the viability of biofilm bacteria evaluated, by flow cytometry. The biofilm was scraped off the coupons with 2 mL of Ringer (1 tablet in 500ml of distilled water, autoclaved at 121°C for 15 minutes Oxoid, BR0052) solution using a cell-scraper and the solutions were vortexed to be homogenized. From the above solution 1ml was added to 4mL of Sodium Pyrophosphate Decahydrate, 99% A.C.S. reagent (50mM) for better disaggregation of the cells, filtered with a 0.2µm pore size filter. The solutions were incubated at 25°C for 15min and sonicated for 10 seconds to avoid disruption of cells. Next, 1ml of the cell suspension was diluted in 9ml of Ringer solution and

the final samples were homogenized by vortexing. For flow cytometry analysis, 400μL from the above solutions were transferred in the sample tubes. Next, 3μL of the BacLight stain (SYTO/PI, in 1:1) were added in the sample tubes, they were vortexed and incubated for 15-30min in the dark at room temperature. To normalize fluorescence data a bead solution (10 μL of 10^6 beads·mL^{-1}, Fisher 1.0μm) was added and the number of live, dead and damaged cells were counted by flow cytometry (FACSCalibur, Becton Dickinson) and the ratio of number of live over number of dead (LIVE/DEAD) bacteria cells were evaluated.

3.8.5 Biofilm morphology

The biofilm morphology was characterized using scanning electron microscopy (SEM). Additionally, scanning electron microscopy was used during the secondment held in Itram, Barcelona, Spain. In this case, the biofilm was grown on stainless steel and polyethylene surfaces for 3 weeks, and the samples were tested 1) before any cleaning application, 2) after the application of the enzymes and 3) after disinfection. For scanning electron microscopy measurements, the samples were fixed with 2.5% (w/v) glutaraldehyde EM grade for 4 hours and stored in 0.1 M cacodylate buffer, pH 7.4 at 4ºC temperature until measurement. Next, they were washed and dehydrated successively in ethanol, dried at the critical point CO2 (Emitech, Alemanya, model K 850 CPD), and evaporated carbon (Emitech, Alemanya, model K950 turbo evaporator). Examinations were carried out with a scanning electron microscope FE-SEM Hitachi, Japan, S-4100. Digital images were collected and processed by Quarz PCI digital software.

3.9 Adhesive & Cohesive strength evaluation

3.9.1 Micromanipulation technique

Understanding the adhesion and cohesion forces developed in biofilms, especially the forces needed to distort their structure and clean them from the surfaces, is essential for the development of anti-biofouling precautions and biofilm cleaning applications. In 1992, a micromanipulation technique, for measuring the mechanical strength of single cells, was developed by Zhibing Zhang in the School of Chemical Engineering at the University of Birmingham (Zhang et al., 1992; Chen et al., 1998). For the direct measurement of the adhesive strength of biofilm on the surface of a glass test stud, a novel probe with a T-form was developed. The theoretical principle of that technique at the time was to drag away a whole biofilm from the surface of the glass test stud with the probe, and to simultaneously measure the force applied on the biofilm from the probe. The adhesive strength among the attached biofilms and the surfaces is defined as the work per unit surface that is required, for the biofilms to be removed from the surface (Chen et al., 2005).

The micromanipulation method is well suited to the removal of layers of any deposit; the probe can be set to travel at a known height about the surface, and the force required to remove the deposit noted. At the same time, the removal process can be observed and recorded (Hooper et al., 2006). Hence, several studies have been based in the same technique for the direct measurement of the adhesive and cohesive forces of food fouling deposits (Liu et al., 2006; Liu et al., 2006; Hooper et al., 2006; Liu et al., 2007), using substrates such as tomato paste, milk proteins, tooth- paste, and caramel. Thus, for the evaluation ofthe adhesive and the

cohesive strength of the biologically relevant soil of alginic acid (Sigma Aldrich, A2033-250G Sigma Aldrich, A2033-250G) this micromanipulation technique was used. The micromanipulation rig (**Figure 3.11**) consists of:

1) Force transducer

2) Computer/Digimatic Indicato (Model ID-C112MB, Mitutoyo Corp. Japan)

3) Fine micromanipulator (Micro instruments, Oxon, UK)

4) T – shaped probe made of stainless steel with dimensions of 30 x 6 x1 mm

5) The stage/ Surface sample sleeve

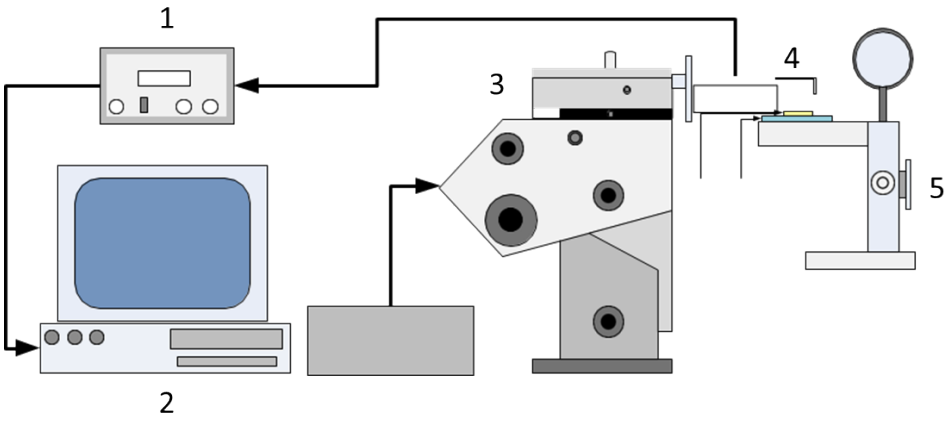

Figure 3.11: Micromanipulation stage that consists of: 1) Power supply and signal conditioner, 2) PC monitor for data collection, 3) Force transducer, 4) T-Shaped probe and 5) Microscopic camera for sample visualization and adjustment.

3.9.2 Calibration of the force transducer

The calibration of the force transducer sensitivity was carried out to ensure the accuracy and the reproducibility of the measurements. Using a method previously described (Chen, 2000; Garrett, 2007), the calibration procedure is summarized as follows. Several pre-weighed pieces of paper were placed on the output tube of the force transducer and the response in volts was measured using a data acquisition program STAT60. The calibrated sensitivity was estimated to be 4.8 N/volts which is close to 5N/volts, the value specified by the manufacturer.

3.9.3 Sample preparation

Alginic acid from Brown Algae 5% w/w (Sigma Aldrich, A2033-250G) was diluted (5%w/w) in water at 40^{o}C, stained with calcofluor white (1%w/w) (Sigma Aldrich, 18909-100ML-F) and left at overnight magnetic stirring, to become a gel. The next day the gel was deposited on the surfaces of interest that were placed on a microscope stage held by the micromanipulator (**Section 3.9.1**). Using the T-shaped probe thin films were developed on stainless steel and polycarbonate rectangles of dimensions 30 mm x 30 mm x 2.9 mm (**Figure 3.12**). The gap between the bottom edge of the T-shaped probe and the surface was adjusted to 100μm by fine-tuning with a digital level indicator (model ID-C112mb. Mitutyo, Corp, Japan). The stainless-steel T-shaped probe was used to pull the deposits horizontally at a constant speed of 1.0 mm/s to create samples of 100μm thickness. After the sample preparation, the adhesion and cohesion force measurements were performed under different conditions, air, water, NaOH (pH 11) and HCl (pH 3). The force exerted on the probe was recorded at 100 Hz by a PC 3D

data acquisition board (Amplicon Liveline, Brighton, UK).

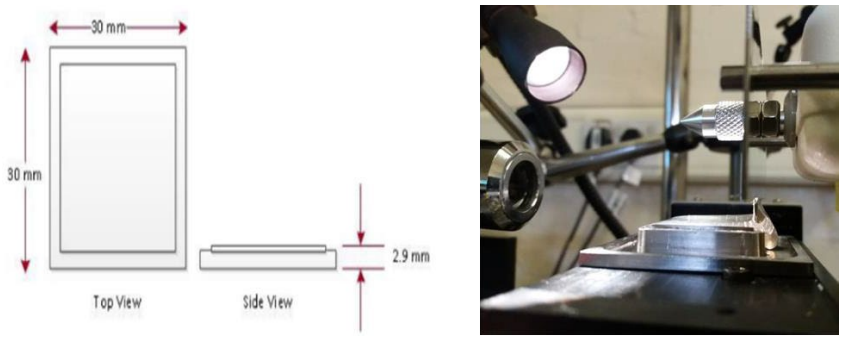

Figure 3.12: (Left) Representation of rectangular samples mounted on the micromanipulation stage. (Right) The development of 100μm thick alginic acid films using the micromanipulation stage.

3.9.4 Analysis of adhesive & cohesive strength

The total work, W (J) done by the applied force, F(t), to remove the deposit may be calculated as the integral of

$$dW = F \cdot dx \tag{3.9}$$

Where, the distance dx is

$$dx = v \cdot dt \tag{3.10}$$

Where v is the probe velocity (m/sec), so that

$$W = \frac{d}{(t_2 - t_1)} \int_{t_1}^{t_2} F dt \tag{3.11}$$

Where d is the side length of the rectangular tile, and t_1 and t_2 the first and last times at which the probe touched the fouled surface. For the case of the adhesive strength

measurements, the force to remove the material from the surface, i.e., leaving nothing left on the surface, the probe was adjusted in order to scrape the alginic acid from the tiles. For the case of the cohesive strength measurements, the force required to break the bonds between elements of the material, the probe was adjusted approximately at 50μm height over the tile.

The apparent adhesive and cohesive strength of a fouling sample, σ (J/m^2), is defined as the work required to remove the sample per unit area from the surface to which it is attached, is then given by:

$$\sigma = \frac{W}{\alpha A} \tag{3.12}$$

Where A (m^2) is the tile surface area, and α is the fraction of that area covered by the sample before any treatment, which is measured by image analysis as described above. This is done by numerical integration of the data set for F (t), as

$$\sigma = \frac{d}{\alpha \cdot \pi \cdot (t_C - t_A) \cdot \frac{d^2}{4}} \int_{t_A}^{t_C} F dt \leftrightarrow$$

$$\sigma = \frac{4}{\alpha \pi d (t_C - t_A)} \cdot \sum_{i=0}^{n-1} \left(\frac{F_{i+1} + F_i}{2} \right) \cdot (t_{i+1} - t_i) \leftrightarrow \tag{3.13}$$

$$\sigma = \frac{0.04}{\pi d (t_C - t_A)} \sum_{i=0}^{n-1} \left(\frac{F_{i+1} + F_i}{2} \right)$$

Where t_{i+1}-t_i is just the time interval between the two measuring data points in the column, in this case, it is 0.01s, and a can be taken as 100% if the sample is wholly removed.

3.10 Conclusions

This chapter presents in detail the methodology that was followed in order to investigate the biofilm cleaning behaviour as well as the adhesion and cohesion forces of biologically relevant soils. To address the aims of this study that are presented in the chapters to follow, these methods were used as described below:

i. *To understand the behaviour of biofilm during cleaning in a fundamental level, as described in Chapter 4, P. fluorescens* and *P. putida* biofilms were grown on stainless steel, polycarbonate and plasma-treated polycarbonate coupon surfaces using a CDC-bioreactor. These surfaces were chosen among eight different common surfaces that were tested for their work of adhesion. They were studied for their cleaning behaviour under shear stress conditions with the parallel-plate flow chamber, designed specifically for this PhD. The conditions tested were water and NaOH solution under shear stress as well as NaOH solution under static conditions. The effectiveness of biofilm cleaning (E_f %) was evaluated by studying three main parameters: (i) the biovolume, (ii) the biofilm surface coverage (%), and (iii) the number of bacteria colony forming units (CFU). For the first two parameters Confocal Scanning Laser Microscopy in combination with ImageJ was used while for the number of CFU the method chosen was Miles & Misra.

ii. *To study and investigate the behaviour of biofilm cleaning in a real-world situation,*

Described in Chapter 5, real-case mixed-microbial biofilm was collected from a food industry and was grown on stainless steel and polyethylene surfaces using a microcosm. They were studied for their cleaning behaviour under shear stress conditions with the parallel-plate flow chamber, designed specifically for this PhD. The conditions tested were three different combinations of amylase, protease and lipase enzymes along with a commercial disinfectant. The effectiveness of biofilm cleaning (E_f %) was evaluated by studying four main parameters: (i) the biovolume, (ii) the biofilm surface coverage (%), (iii) the number of live/dead bacteria and (iv) the EPS-polysaccharide content. For the first two parameters Confocal Scanning Laser Microscopy in combination with ImageJ was used. For the live/dead bacteria the method chosen was Flow Cytometry while an EPS-analysis method based on glucose content was used for the measurement of EPS-polysaccharide content.

iii. *To examine the adhesion and cohesion forces of a biofilm relevant substitute under cleaning and non-cleaning conditions on different surfaces.* Alginic acid was developed and studied on stainless steel and polycarbonate surfaces under air, water, NaOH and HCl conditions. Nonetheless, the role of surface modification under different pH conditions was evaluated by modifying polycarbonate tiles with different polymeric solutions. The method used in all these experiments was the micromanipulation technique as described in Chapter 6.

CHAPTER 4

EFFECT OF SHEAR STRESS ON THE REMOVAL OF *PSEUDOMONAS FLUORESCENS* AND *PSEUDOMONAS PUTIDA* BIOFILM FROM HARD ARTIFICIAL SURFACES

4.1. Summary

As mentioned already in Chapter 3, section 3.8, in this study the removal of *P. fluorescens* NCIMB 9046 and *P. putida* ATCC 700008 biofilms from different surfaces was investigated. It is well documented that biofilm growth can be affected by various environmental conditions (Otto, 2008; Kohila et al., 2013; Abdallah et al., 2014; Colagiorgi et al., 2017), therefore at the earlier stage of this study the biofilm adhesion was examined via confocal laser scanning microscopy (CLSM) and surface viable count (Miles and Misra Method**)** to determine the biofilm abundance on different material surfaces. After 30 minutes of growth at 25 °C for *P. fluorescens* NCIMB 9046 and at 30ºC for *P. putida* the bacteria were found to start their initial attachment on the artificial surfaces. It was found that *P. fluorescens* showed higher percentage of surface coverage comparing to *P. putida* on all surfaces. In terms of different materials, the percentage of the area covered by bacteria was significantly lower on plastic surfaces (PET, PTFE and polypropylene) with lower work of adhesion than on more hydrophilic surfaces like glass, hydroxyapatite and stainless steel.

The biofilm residual contamination was investigated using a parallel-plate flow chamber where three different cleaning conditions were tested on stainless steel, polycarbonate and plasma-treated polycarbonate surfaces: 1) Water mechanical rinsing (CIP with water at 40ºC, τ_{wall}=0.129Pa), 2) Chemical cleaning in static conditions (immersion of the coupons at 40ºC NaOH 0.1%w/w) and 3) Chemical mechanical cleaning (CIP with NaOH 0.1%w/w at 40ºC, τ_{wall}=0.129Pa). To study the biofilm residual contamination the model biofilms were developed inside a CDC bioreactor for 48 hours, 24hrs under batch phase of nutrients and 24hrs under flow phase of nutrients while the temperature was kept stable at 25^{o}C for *P. fluorescens* NCIMB 9046 and at 30^{o}C for *P. putida* ATCC 700008. It was found that the combined CIP procedure with NaOH 0.1%w/w was more effective than the mechanical rinsing with water and the chemical (NaOH static) cleaning processes for all material surfaces. In terms of surfaces, it was seen that stainless steel was cleaned more efficiently compared to polycarbonate and plasma-treated polycarbonate surfaces as well as that the latter material surfaces showed higher work of adhesion. For the different bacteria strains, it was observed that the *P. fluorescens* NCIMB 9046 and the *P. putida* ATCC 700008 biofilms had different structure, as the first one formed islands of bacteria among with EPS, whilst the *P. putida* showed a filamentous structure without a significant quantity of EPS. In terms of biofilm residual contamination, a more distinct biofilm removal was observed *for P. putida* ATCC 700008 than for *P. fluorescens* NCIMB 9046.

4.2. Introduction

As discussed throughout the thesis, biofilms are communities of living microorganisms that can adapt and change their structure according to the environmental conditions, a feature that make them unpredictable and challenging to study (Johansen et al., 1997; Otto, 2008; Flemming et al., 2016). Nonetheless, as discussed in Chapter 2, section 2.7, biofilm elimination is of great concern for various sectors, like the food industry, where day-to-day cleaning with common chemicals is essential for biofilm control (Keener, 2005; Lécrigny-Nolf et al., 2000; Blel et al., 2007; Antoniou and Frank, 2005; Abdallah et al., 2014). Thus, the study of biofilm removal and identification of possible optimum removal conditions is of great importance. To understand the mechanisms that provoke biofilm removal, several studies have tried to model the biofilm detachment kinetics from artificial surfaces. The most important outcome of these studies was that removal is not a straightforward process and its adequate elimination requires the combination of hydrodynamics with chemical agents (Lécrigny-Nolf et al., 2000; Blel et al., 2007; Blel et al., 2008; Faille et al., 2013; Bénézech and Faille, 2018).

Nonetheless, it is essential to consider that a key factor for both biofilm initial attachment and detachment, which plays a key role when defining CIP systems, is the attachment strength of the biofilm to the solid surface where it develops (Donlan, 2002). The physicochemical properties of surfaces and bacteria are important to the biofilm interface and hence its response to cleaning. As already mentioned in Chapter 2, microorganisms are reported to attach more rapidly to hydrophobic, nonpolar surfaces such as Teflon and other plastics than

to hydrophilic materials such as glass or metals (Fletcher and Loeb, 1979; Boonaert et al., 2002; Bayoudh et al., 2005; Guillemot et al., 2006; Detry et al., 2010) while Parkar et al. (2001) reported that surface energy may influence the adhesive strength of cells and bacteria. Cleaning-in-place systems often employ solutions of cleaning agents, which convert the soil or deposit layer to a softer form, promoting erosion or the detachment of the layer from the underlying substrate by modification of the adhesive interactions between the soil and the substrate (Wang et al., 2018). Consequently, the interfacial phenomena between the biofilm and the surface might be important in the choice of the appropriate cleaning agent (Detry et al., 2010), although any relationship made between bacterial adhesion and surface energy must be considered with caution (Boonaert et al., 2002).

Therefore, to understand the biofilm adhesion on surfaces, in this preliminary study the initial bacteria attachment of the bacterial strains *P. fluorescens* NCIMB 9046 and *P. putida* ATCC 700008 on different material surfaces was investigated (**Section 3.3, Section 3.5.2**). Next, to evaluate the biofilm detachment the same bacterial strains were grown on three different material surfaces using three different cleaning processes. The goal was to mimic the Cleaning-In-Place industrial cleaning system using a parallel-plate flow chamber that was designed and built for this study (**Section 3.6.1**).

4.3. Materials and Methods

4.3.1. Material Surfaces, Surface Modification and Substrate Characterization

As described in **Chapter 3, Section 3.3**, several material surfaces were initially measured for their average work of adhesion and surface energy: stainless steel, polycarbonate, polypropylene, Nylon, PTFE, PET, borosilicate glass and hydroxyapatite. According to the results shown at **Section 4.4.1 (Figure 4.3)**, stainless steel and polycarbonate surfaces were selected to be studied for their behaviour during biofilm cleaning, as they are the most common materials that are found both in the industrial and the domestic environment. In addition, to evaluate the effect of surface modification on biofilm attachment and hence biofilm cleaning, the polycarbonate surfaces were plasma treated for 5, 10 and 30 minutes, using a Corona discharge (Oplasma). After obtaining the average work of adhesion data (**Figure 4.4**) for the plasma-treated polycarbonate surfaces (**Section 4.4.1**), it was decided that polycarbonate coupons treated for 5 minutes with plasma would also be evaluated for their behaviour during biofilm attachment and biofilm cleaning, because further plasma treatment did not show significant change in the work of adhesion.

4.3.2. Organisms and growth conditions

As discussed in **Chapter 3, Section 3.4**, *P. fluorescens* NCIMB 9046 and *P. putida* ATCC 700008, Gram-negative bacteria, were chosen as model microorganisms to study the biofilm removal during different cleaning conditions. A loopful from the agar slants was spread

onto TSA agar plates and incubated for 24 h at 25°C for *P. fluorescens* and at 30ºC for *P. putida*. Then using 500 mL flasks, one colony was collected with a loopful and transferred in 100 mL TSB medium that has been autoclaved at 121ºC for 15minutes. The culture was shaken at 150 rpm for 24 h, whilst being maintained at 25 °C for *P. fluorescens* and at 30ºC for *P. putida* until the inoculums reached the stationary phase. For controlled biofilm growth on different surfaces a CDC Biofilm Reactor (CBR) was selected, in order to mimic the high shear conditions that are developed in household or industrial environments, as described in detail in **Chapter 3, Section 3.5.1**.

To study initial bacteria attachment (**Chapter 3, Section 3.5.2**), *P. fluorescens* NCIMB 9046 and *P. putida* ATCC 700008 biofilms were grown on stainless steel, polycarbonate, polypropylene, PET, PTFE, nylon, borosilicate glass and hydroxyapatite coupons. The substrates were cylinder coupons with diameter 1.27cm and thickness of approximately 3mm. They were initially cleaned by soaking in 1% (w/v) Virkon solution overnight followed by rinsing with distilled water before soaking in ethanol for 30 minutes. The coupons were then washed with distilled water, dried with compressed air and placed on the eight independent rods. The rods were placed in the CDC reactor with 400 mL of TSB medium (3mg/mL) after having been autoclaved at 121 °C for 15 min and let cool down to room temperature. The closed reactor was then autoclaved again at 121 °C for 15 min and allowed to cool to room temperature. Next, 1mL of *P. fluorescens* inoculum that had been left to incubate overnight at 25ºC as described above was transferred into the CDC reactor. The bacteria concentration of the inoculum was 1 x 10^6 cells/mL. After 30 minutes of incubation at 25ºC the biofilm adhesion process was terminated and the coupons were collected for further analysis. A similar procedure was followed for *P. putida* strain, which was left to incubate at 30ºC for 30 minutes.

To study the effectiveness of different cleaning processes (**Chapter 3, Section 3.5.3**), *P. fluorescens* NCIMB 9046 and *P. putida* ATCC 700008 biofilms were grown on stainless steel and modified and non-modified polycarbonate surfaces. The substrates were cylinder coupons with diameter 1.27cm and thickness of approximately 3mm. They were initially cleaned by soaking in 1% (w/v) Virkon solution overnight followed by rinsing with distilled water before soaking in ethanol for 30 minutes. The coupons were washed then with distilled water, dried with compressed air and placed on the eight independent rods. The rods were placed in the CDC reactor with 400 mL of TSB medium (3mg/mL) after having been autoclaved at 121 °C for 15 min and allowed to cool to room temperature. The closed reactor was then autoclaved again at 121 °C for 15 min and let cool down to room temperature. Next, 1mL of *Ps. fluorescens* inoculum that had been left to incubate overnight at 25ºC as described above was transferred into the CDC reactor. The bacteria concentration of the inoculum was 1 x 10^9 cells/mL. After 24 hours of incubation at 25ºC a continuous flowing system of TSB media was introduced. The flowing system consisted of one carboy filled with 20L of TSB media (1mg/mL) and one empty carboy that had been both autoclaved at 121 °C for 15 min. The first carboy was connected to the input of CDC biofilm reactor and the empty 20L carboy was connected to the output of the reactor, providing the system with fresh media for the next 24 hours at a stable temperature of 25ºC. After 24 hours the reactors were stopped and the coupons were selected for further cleaning treatment and analysis. A similar procedure was followed for *Ps. Putida* strain, which was left to incubate at 30ºC.

4.3.3. Biofilm Cleaning from Surfaces

To study the *biofilm cleaning from surfaces*, a Cleaning in Place protocol was applied on all surfaces of interest using a parallel-plate flow chamber as a cleaning apparatus. To evaluate the effectiveness of different cleaning processes and conditions, three methods were chosen as described in detail in **Chapter 3, Section 3.6.2**,

i. Cleaning process A: mechanical rinsing with water flowing through the cell at 40ºC such that the wall shear stress $\tau_{wall} = 0.518$ N/m^2.

ii. Cleaning process B: immersion in static solution of NaOH 0.1% w/v at 40ºC and wall shear stress $\tau_{wall} = 0$ N/m^2.

iii. Cleaning process C: CIP process using NaOH 0.1% w/v flowing through the cell at 40ºC such that the wall shear stress $\tau_{wall} = 0.518$ N/m^2.

To evaluate the effectiveness of biofilm reduction, E_f(%) the parameters (**Chapter 3, Section 3.7.2**) investigated were (i) the percentage (%) of the surface area covered by biofilm, (ii) the biovolume and (iii) the average biofilm thickness from confocal laser scanning microscopy (CLSM) images (**Chapter 3, Section 3.8.2**). All measurements were performed (i) before cleaning and (ii) after cleaning with the different cleaning processes. In each experiment *P. fluorescens* or *P. putida* were grown at a different material surface (stainless steel, non-modified polycarbonate and modified polycarbonate). Three replicates of biofilm without any treatment were initially tested. The cleaning processes were performed in three different replicates for different time periods and the biofilm removal was tested. In all cases, the coupons were cleaned for 5, 10, 15, 20 and 30 minutes and biofilm characterizations were performed as

described in detail in **Chapter 3.8**. For biofilm image acquisition Confocal Laser Scanning Microscopy was used to obtain the information on biovolume, biofilm surface area and biofilm thickness in combination with Comstat2 for the calculation of the parameters of interest: (i) percentage (%) of the surface area covered by biofilm, (ii) the biovolume and (iii) the average biofilm thickness.

Finally, for all the parameters analysed, the effectiveness of biofilm reduction, E_f, was calculated as:

$$\boldsymbol{E_f}(\%) = \frac{|\boldsymbol{Q_{BC}} - \boldsymbol{Q_{AC}}|}{\boldsymbol{Q_{BC}}} * \mathbf{100} \qquad (\mathbf{3.7})$$

Where, Q_{BC} and Q_{AC} are the parameters measured before and after the cleaning process.

4.3.4. Measurement of biofilm thickness, surface coverage and volume

As described in **Chapter 3, Section 3.8.2**, multichannel confocal and transmission imaging of the biofilm samples was performed using a multispectral Confocal Leica TCS SP8 microscope. A high-speed module and three light channels and laser lines were used: 405 nm, 488 nm and white laser for 470-670 nm excitation at 592nm. The samples were marked with two different fluorophores, acridine orange for the live bacterial cells of *P. fluorescens* and DAPI for the *P. putida*. The 3D biomass information was obtained using a z-stack step of 1μm and the image processing and quantification was performed using Fiji (ImageJ) (**Chapter 3, Section 3.8.2**).

For all samples, the biovolume, the percentage of the surface area covered with biofilm and the average biomass thickness were calculated. The biovolume (μm^3) represented the total volume of the biofilm, hence the EPS, the dead and the live bacteria. The percentage of the surface area covered with biofilm was calculated by dividing the values with the surface area studied and the number of the stacks measured in each case. Finally the average biomass thickness represented the average number of the z-stacks that were studied in each case. Finally, in all experiments the biovolume, the surface coverage and the average biomass thickness were measured before applying any cleaning process, and, in order to compare the results for the different cleaning processes the effectiveness of the cleaning was also calculated for all cases, as the percentage of the reduction of biovolume and surface area coverage respectively.

4.3.5. Miles and Misra method

As described in detail at **Chapter 3, Section 3.8.1**, for the quantification of bacterial concentration Miles & Misra in combination with enumeration of bacterial cells was used. For this method, a biofilm sample was taken from the coupon surfaces using swabs that were then? placed in sample tubes with phosphate buffer saline (PBS). The tubes were vortexed to extract the bacteria from the swabs and the suspension was serially diluted by adding 10µl to 90µl of PBS. Dilutions were made to 10^{-8}. Next, in three replicates of tryptone soy agar (TSA) plates, divided and labelled with the dilution factor, 1 x 20 µl of the appropriate dilution was dropped onto the surface of the agar and the drop allowed to spread naturally. The plates were left upright on the bench to dry before inversion and incubation for 24 hours at 25 °C for *P. fluorescens* and at 30°C for *P. putida*.

After bacterial counting the following equation was used to calculate the number of

colony forming units (CFU) per ml from the original aliquot / sample:

$$\frac{CFU}{cm^2} = \frac{Average\ number\ of\ colonies\ for\ a\ dilution \times 50 \times dilution\ factor}{Coupon\ surface\ Area} \quad (3.8)$$

4.3.6. Data analysis

The data analysis was performed using analysis of variance (ANOVA) in combination with Tukey's Honestly Significant Differences data comparison system. The one-way ANOVA was used in all analyses to test whether there were significant differences in the data between each treatment and at each cleaning step (enzymatic cleaning and disinfection step) for both surfaces.

4.4. Results

4.4.1. Surface Energy and Initial Biofilm Attachment

From the water contact angle measurements for the different material surfaces, the work of adhesion was calculated according to the Young-Laplace equation (**3.1**) for the contact angle, the surface tension and the work of adhesion. The results for the work of adhesion for the different surfaces show that hydroxyapatite, borosilicate glass and stainless steel have higher work of adhesion rather than plastics (**Figure 4.1**). Stainless steel shows double the work of adhesion when compared to nylon, hydroxyapatite has three times the work of adhesion than polypropylene, while borosilicate glass has work of adhesion 12 times higher than polyethylene. In addition, it was observed that for the plastics, polycarbonate surfaces showed the higher work of adhesion (94.1mN/m), compared to PTFE and Nylon that showed 53.2mN/m and 57.1mN/m

respectively, while polypropylene and polyethylene showed significantly lower work of adhesion, 33.6mN/m and 8.7mN/m correspondingly.

Polycarbonate was thus chosen as a material of interest for further modification and investigation for its biofilm adhesion and cleaning behaviour. Using a corona discharge, polycarbonate coupons were plasma-treated for 5, 10 and 30 minutes to achieve an improvement in their adhesion properties. It was shown that the plasma treatment modification caused an increase in the average work of adhesion of the polycarbonate surfaces. It is remarkable to observe that during the first 5 minutes of the plasma treatment the effect on the work of adhesion was higher compared to the following treatments of 10 and 30 minutes that were not as significant (**Figure 4.2)**.

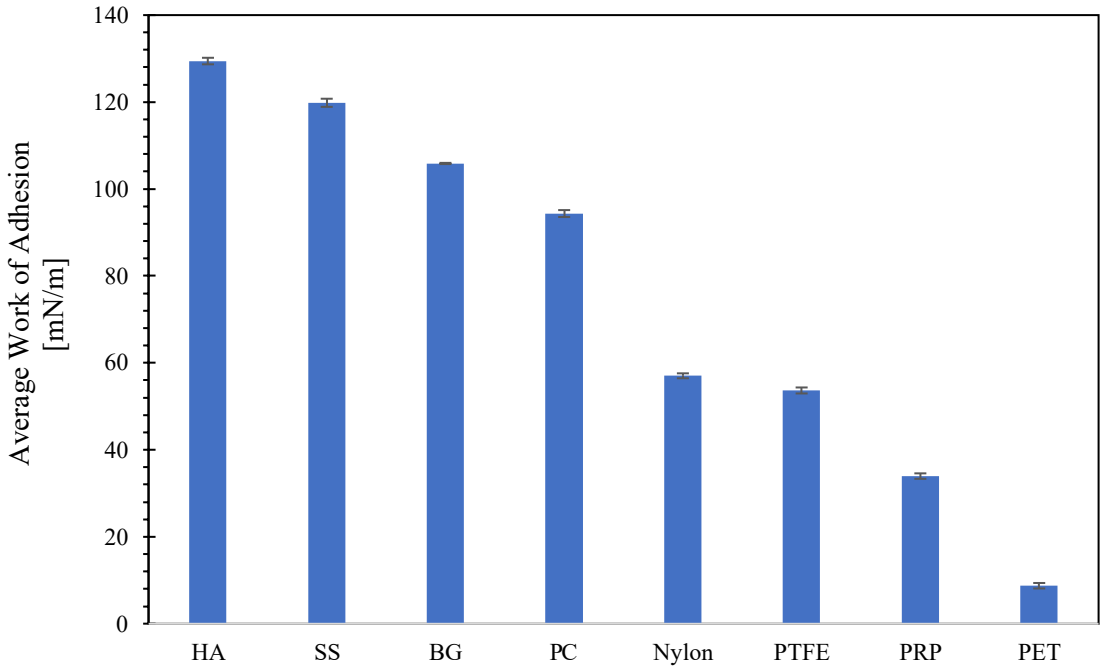

Figure 4.1: Average work of adhesion (mN/m) of Hydroxyapatite (HA), Stainless steel (SS), Borosilicate glass (BG), Polycarbonate (PC), Nylon, Polytetrafluoroethylene (PTFE), Polypropylene (PRP) and Polyethylene Terephthalate (PET). The error bars are the standard deviation of the triplicate repeats for the work of adhesion.

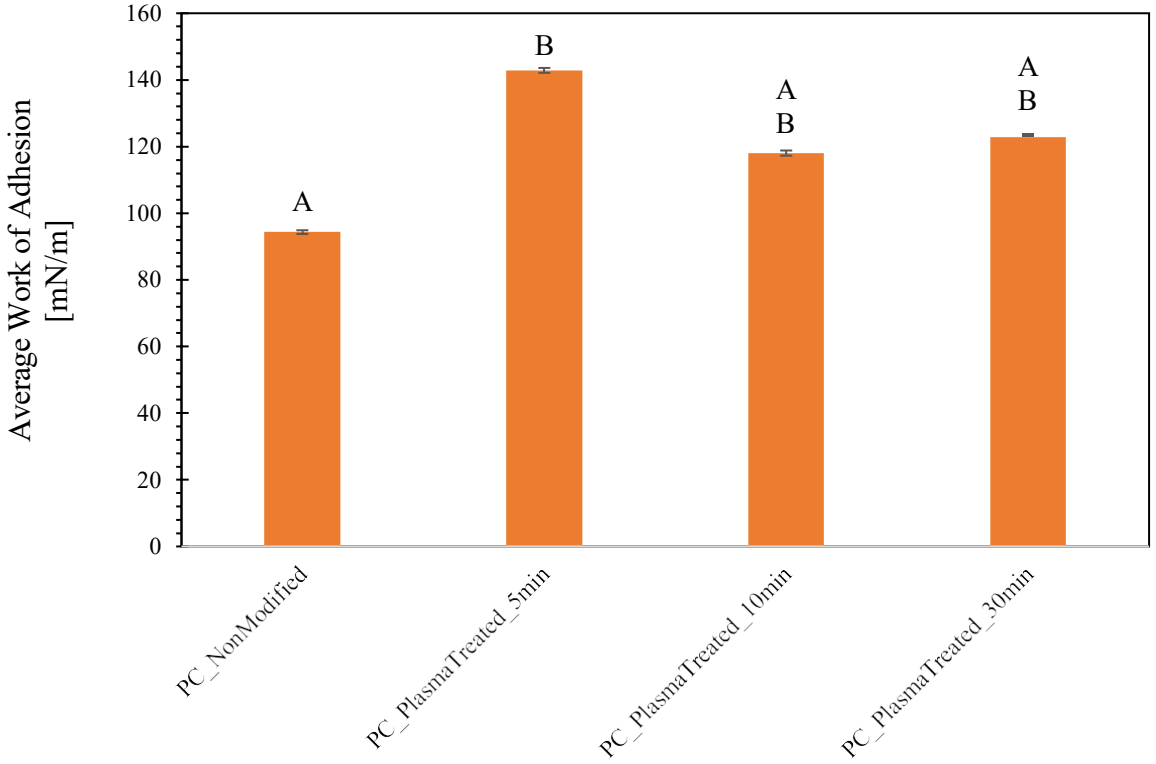

Figure 4.2: Average work of adhesion (mN/m) of non-modified polycarbonate coupons (PC_NonModified) and plasma-treated polycarbonate coupons for different times of treatment: 5 (PC_PlasmaTreated_5min), 10 (PC_PlasmaTreated_10min) and 30 (PC_PlasmaTreated_30min) minutes. The error bars are the standard deviation of the triplicate repeats for the work of adhesion. Capital letters indicate statistically significant different groups at each cleaning step (Tukey's test, $p<0.05$). The same letter indicates no significant difference, i.e., A↮A: no significant difference, one similar letter indicates partial difference, i.e., A↮AB: slightly different and different letter indicates significant difference, while the furthest from control letter A, the most significant the difference, i.e., A↮B: significant difference and A↮C: more significant difference.

In **Figures 4.3** and **4.4**, the log10 (CFU/cm^2) and the percentage of area covered by *P. fluorescens* and *P. Putida* bacteria for the different surfaces are presented. During the initiation of biofilm attachment *P. fluorescens* appeared to be more abundant than *P. putida* bacterial strain, as the $\log_{10}$ (CFU/cm^2) was found higher for *P. fluorescens* (**Fig. 4.3**). Similar results to the biofilm concentration were obtained from the biofilm percentage area coverage (**Fig. 4.4**). It was observed that the area covered by biofilm was remarkably low (lower than 10% for all surfaces) and this phenomenon is believed to have been affected by the short residence time of the coupons inside the reactor. In terms of the different surfaces, it appeared that the plastic surfaces that showed lower work of adhesion (PET, PTFE and polypropylene) and thus lower surface energy, showed also reduced biofilm surface area coverage (**Fig. 4.4**). Interestingly, the polycarbonate coupons surfaces showed higher work of adhesion than the other plastic surfaces and thus increased initial biofilm attachment (2.6 CFU/cm^2 for *P. putida* and 3.4 CFU/cm^2 for *P. fluorescens*), similar to stainless steel (2.6 CFU/cm^2 for *P. putida* and 3.5 CFU/cm^2 for *P. fluorescens*) (**Fig. 4.3**). Analogous results were observed from the biofilm surface coverage data for the two material surfaces as polycarbonate showed 5% for *P. putida* and 5.3% for *P. fluorescens* and stainless steel showed 7% for *P. putida* and 8.3% for *P. fluorescens* respectively. As biofilm adhesion was found to be similar for stainless steel and polycarbonate, they were selected to be further studied for the behaviour during *P. fluorescens* and *P. putida* biofilm cleaning. In addition, due to the fact that polycarbonate surfaces could be easily treated, it was decided to include plasma treated polycarbonate surfaces for 5 minutes in the above substrates of interest. The results of this study are presented in the next section of this chapter.

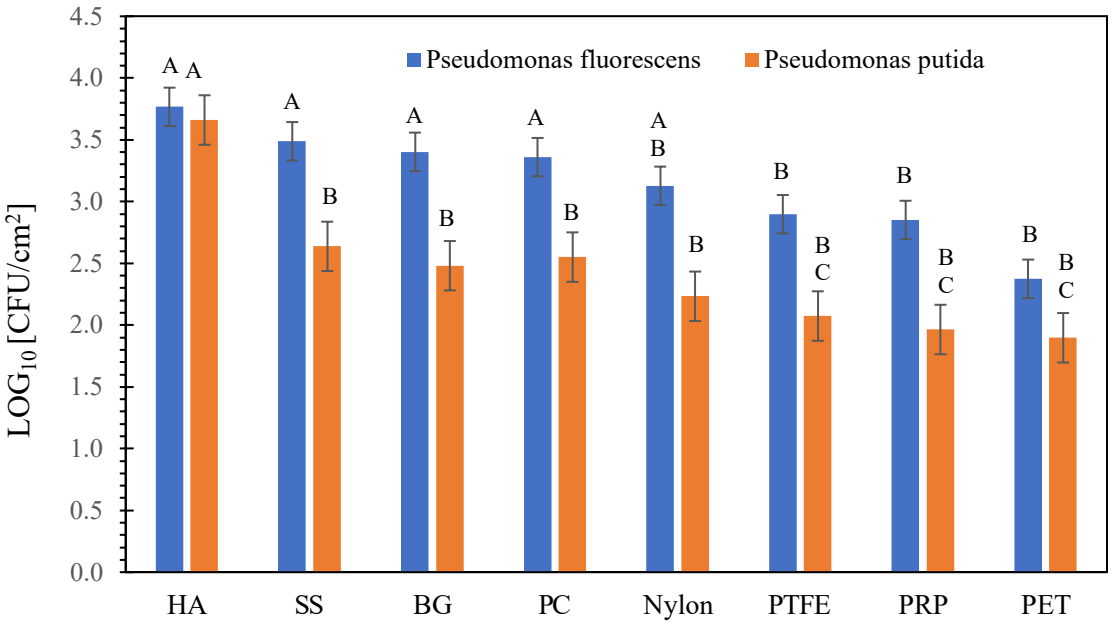

Figure 4.3: *Log*$_{10}$(CFU/*cm*^{2}) of *P. fluorescens* and *P. putida* biofilm initial attachment on Hydroxyapatite (HA), Stainless steel (SS), Borosilicate glass (BG), Polycarbonate (PC), Nylon, Polytetrafluoroethylene (PTFE), Polypropylene (PRP) and Polyethylene Terephthalate (PET). The error bars are the standard deviation of the triplicate's biofilm concentration in log$_{10}$(CFU/cm^2). Capital letters indicate statistically significant different groups at each cleaning step (Tukey's test, $p<0.05$). The same letter indicates no significant difference, i.e., A‡A: no significant difference, one similar letter indicates partial difference, i.e., A‡AB: slightly different and different letter indicates significant difference, while the furthest from control letter A, the most significant the difference, i.e., A‡B: significant difference and A‡C: more significant difference.

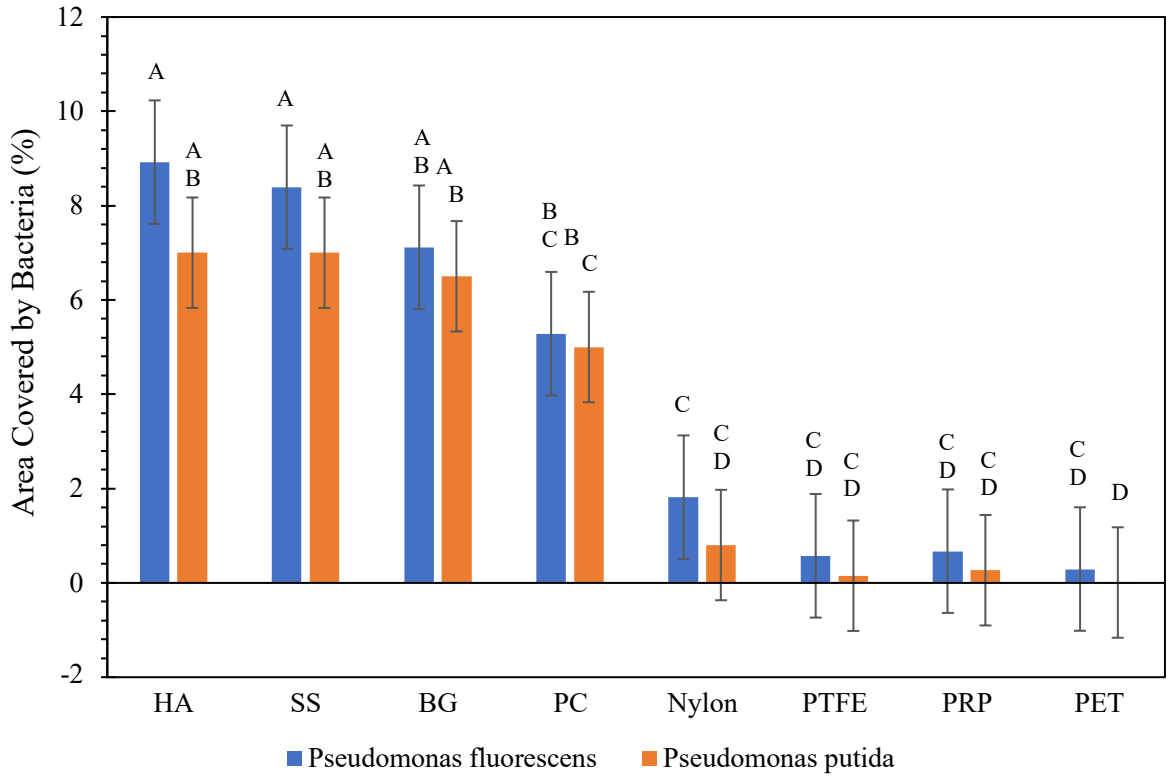

Figure 4.4: Area covered by *P. fluorescens* and *P. putida* bacteria after 30 minutes of fouling for Hydroxyapatite (HA), Stainless steel (SS), Borosilicate glass (BG), Polycarbonate (PC), Nylon, Polytetrafluoroethylene (PTFE), Polypropylene (PRP) and Polyethylene Terephthalate (PET). The error bars are the standard deviation of the triplicate's biofilm surface area (%). Capital letters indicate statistically significant different groups at each cleaning step (Tukey's test, $p<0.05$). The same letter indicates no significant difference, i.e., A↮A: no significant difference, one similar letter indicates partial difference, i.e., A↮AB: slightly different and different letter indicates significant difference, while the furthest from control letter A, the most significant the difference, i.e., A↮B: significant difference and A↮C: more significant difference.

4.4.2. Cleaning of Pseudomonas fluorescens

Prior to any cleaning application, CLSM images showed that all surfaces were covered with *P. fluorescens* NCIMB 9046 biofilm and that the biofilm grown on plasma treated polycarbonate tended to be thicker (19.0±3.6μm in average) compared to stainless steel (6.7±2.1μm in average) but of a similar thickness to polycarbonate (15.1±3.1μm in average). This is similar to the results for the biovolume of *P. fluorescens*; on plasma treated polycarbonate it was found to be (6.5±1.2) $x10^4$ μm^3, on polycarbonate (5.2±1.1) $x10^4$ μm^3 while on stainless steel substrates the biovolume was measured as (2.3±0.7) $x10^4$ μm^3. In addition to the surface coverage data, it was seen that the biofilm grown on plasma treated polycarbonate tended to be more abundant (93.9% biofilm surface area coverage in average) compared to stainless steel and non-treated polycarbonate (69.7% and 68.6% biofilm surface coverage in average) (**Table 4.1**).

Table 4.1. Biovolume (μm^3), Biofilm Surface Coverage (%) and Biofilm thickness of *P. fluorescens* NCIMB 9046 grown on stainless steel (SS), polycarbonate (PC) and plasma treated polycarbonate (PT-PC) prior to any cleaning application. Three replicates were measured at three different spots.

Surface	Biovolume (μm^3)	Biofilm Surface Coverage (%)	Biofilm thickness (μm)
SS	(2.3±0.7) $x10^4$	69.7±3.1	6.7±2.1
PC	(5.2±1.1) $x10^4$	68.6±7.0	15.1±3.1
PT-PC	(6.5±1.2) $x10^4$	93.9±2.11	19.0±3.6

Figure 4.5 shows images from confocal microscopy and Figures 4.6 and 4.7 show graphs of biofilm surface area (%) and biovolume (10^4 μm^3) as a function of time during each cleaning process. In Figure 4.5 it is observed qualitatively that after 30 minutes of cleaning process C, the biofilm surface area coverage on stainless steel is decreased when compared to polycarbonate and plasma-treated polycarbonate. From the kinetics of the cleaning process (**Fig. 4.6**), it was seen in all cleaning processes and surfaces that during the first 30 minutes of cleaning there was a total decrease of biofilm surface area coverage. In the case of the mechanical water rinsing (**Cleaning process A, Fig. 4.6a**), it was seen that for all three surfaces the highest % of biofilm removal occurred in different time points, for stainless steel between 15 and 20 minutes, for polycarbonate between 10 and 15 minutes whereas for plasma treated polycarbonate between 5 and 10 minutes of cleaning. In the case of cleaning process B (**Fig. 4.6b**) the highest % of biofilm removal was observed between 15 and 20 minutes for polycarbonate and plasma treated polycarbonate, while for stainless steel it occurred between 10 and 15 minutes. Last but not least, for cleaning process C (**Fig. 4.6c**) the highest % of biofilm removal occurred between 15 and 20 minutes for all surfaces. As a result, it is believed that for biofilms of this size the most important biomass diminution occurs between 10 and 20 minutes for all surfaces for cleaning process C, which combines chemical cleaning along with shear stress (**Fig. 4.5 and Fig. 4.6c**).

The biovolume of *P. fluorescens* during all cleaning processes was affected similarly to the biofilm surface coverage and the most important biomass diminution occurs between 10 and 20 minutes for all surfaces for all cleaning processes (**Figure 4.7**).

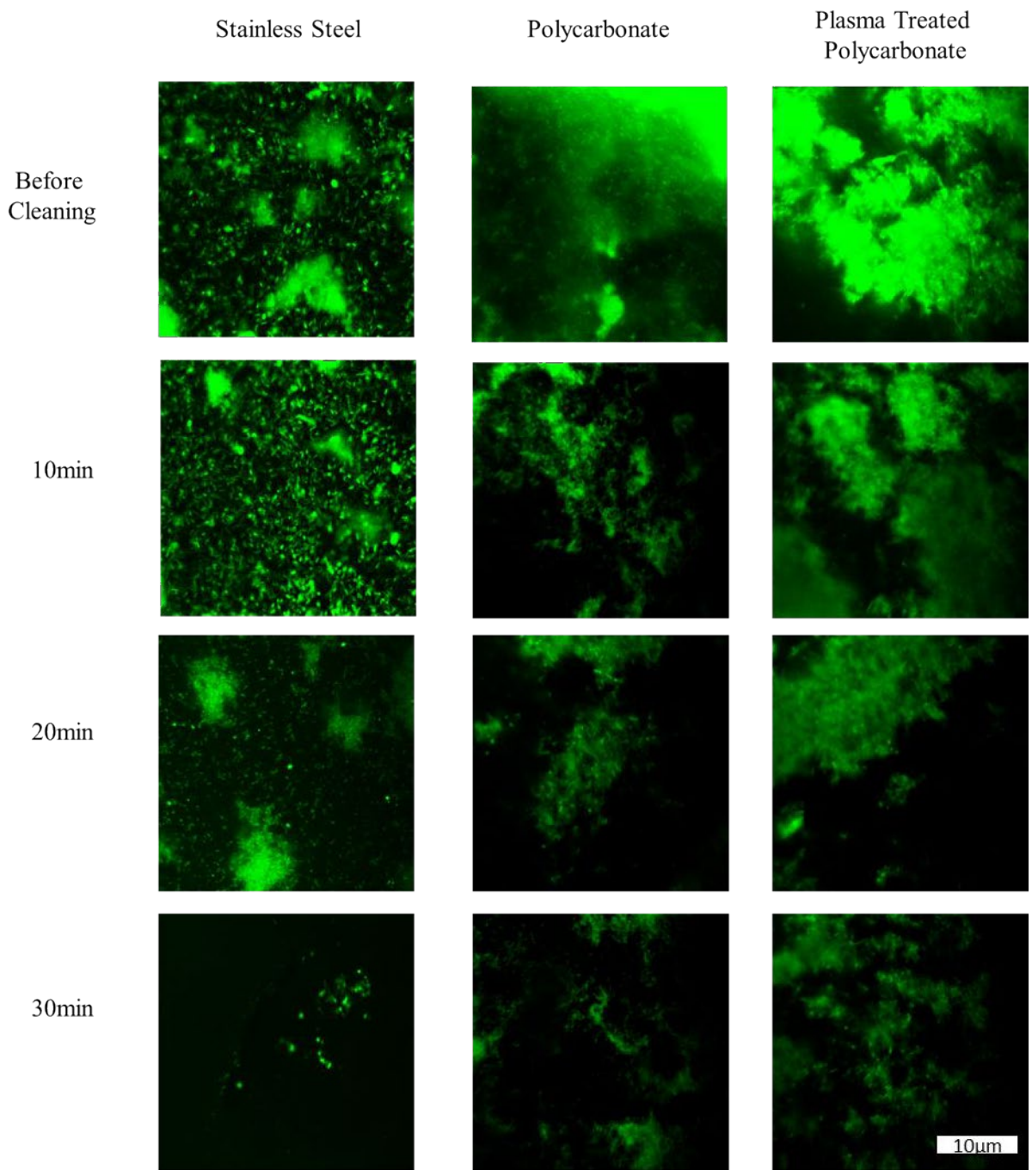

Figure 4.5: Confocal laser scanning microscopy images of the effect of CIP with NaOH (Cleaning Process C) on *P. fluorescens* NCIMB 9046 biofilm grown on stainless steel, polycarbonate and plasma-treated polycarbonate surface coupons before cleaning and after 10, 20 and 30 minutes of cleaning. Biofilm was stained with Acridine Orange (1%w/w). Three replicates were measured at three different spots. One replicate is shown in this case.

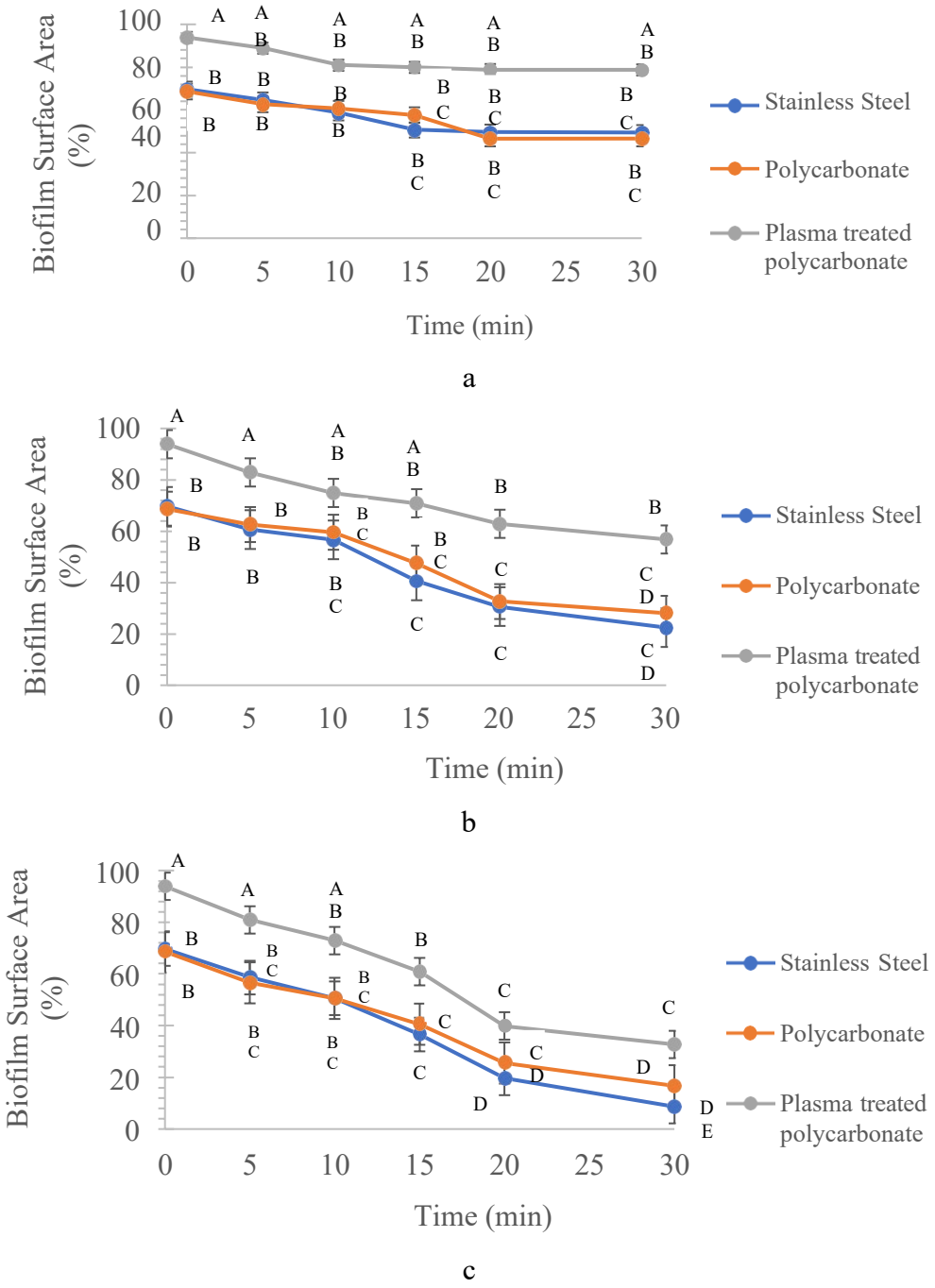

Figure 4.6: Biofilm surface area (expressed as a % of the total surface area) of *P. fluorescens* grown on stainless steel, polycarbonate and plasma-treated polycarbonate surface coupons before cleaning and after 5, 10, 15, 20 and 30 minutes of a) Mechanical rinsing with water (A), b) Immersion in NaOH (B) and c) CIP with NaOH (C). Three replicates measured at three different spots. Error bars are the standard deviation of the triplicate biofilm surface area (%). Capital letters indicate statistically significant different groups at each cleaning step (Tukey's test, $p<0.05$). The same letter indicates no significant difference, i.e., A↮A: no significant difference, one similar letter indicates partial difference, i.e., A↮AB: slightly different and different letter indicates significant difference, while the furthest from control letter A, the most significant the difference, i.e., A↮B: significant difference and A↮C: more significant difference.

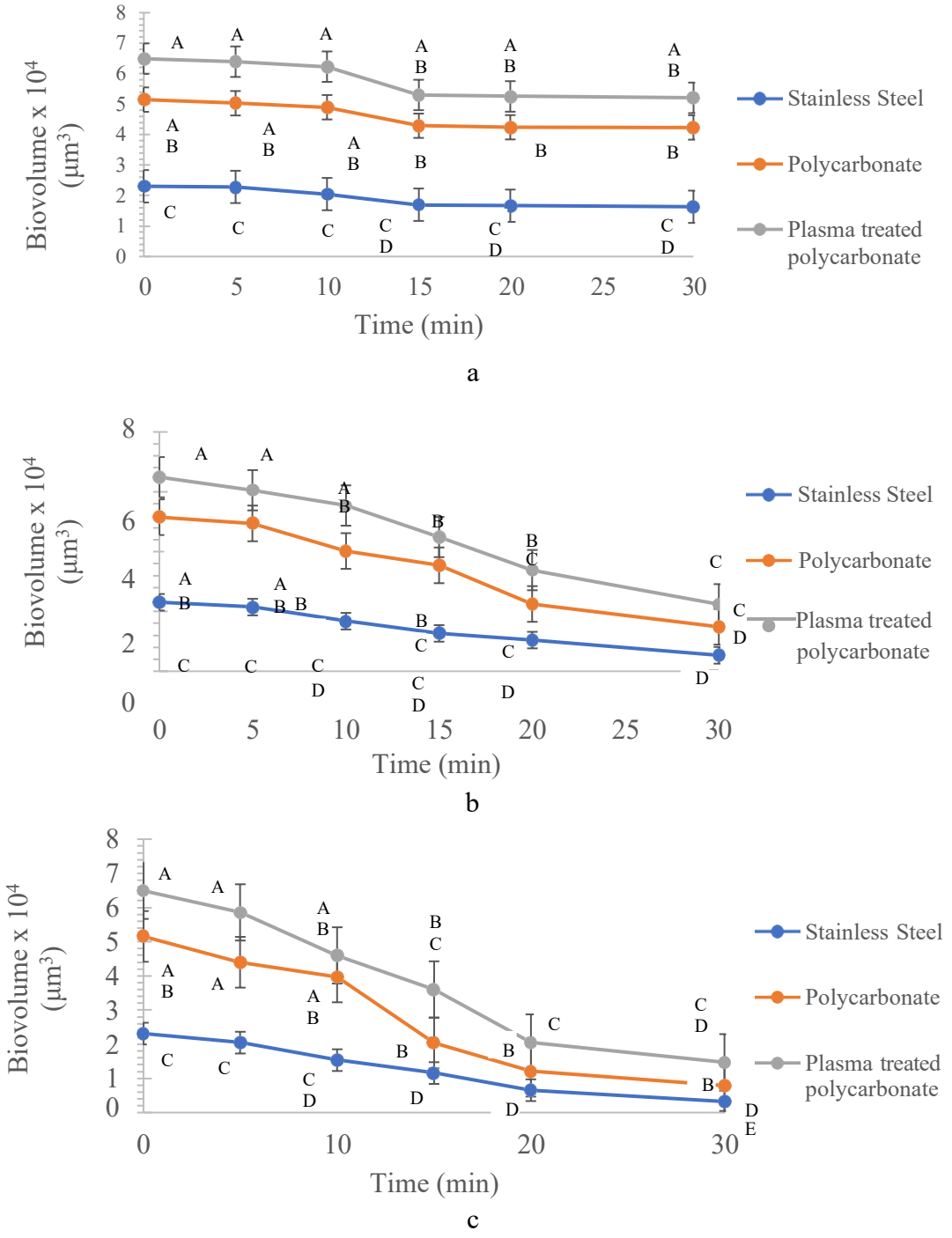

Figure 4.7: Biovolume (µm³) of *P. fluorescens* grown on stainless steel, polycarbonate and plasma-treated polycarbonate surface coupons before cleaning and after 5, 10, 15, 20 and 30 minutes of a) Mechanical rinsing with water (A), b) Immersion in NaOH (B) and c) CIP with NaOH (C). Three replicates were measured at three different spots. The error bars are the standard deviation of the triplicate's biovolume x 10^4 (µm³). Capital letters indicate statistically significant different groups at each cleaning step (Tukey's test, $p<0.05$). The same letter indicates no significant difference, i.e., A⫲A: no significant difference, one similar letter indicates partial difference, i.e., A⫲AB: slightly different and different letter indicates significant difference, while the furthest from control letter A, the most significant the difference, i.e., A⫲B: significant difference and A⫲C: more significant difference.

After 30 minutes of mechanical rinsing with water (**Cleaning Process A, Fig. 4.6a**) a slightly significant decrease of biofilm was seen on all surfaces compared to biofilm prior any cleaning application, as stainless steel showed 49.4%, polycarbonate 46.5% and plasma treated polycarbonate 78.7% of biofilm coverage respectively compared to the initial biofilm coverage, 69.7% for stainless steel, 68.6% 93.9% for polycarbonate and for plasma treated polycarbonate respectively. In the presence of NaOH (**Cleaning Process B, Fig. 4.6b**) an increased removal of the biofilm was observed on all substrates after 30 minutes of cleaning (biofilm coverage, 22.4% for SS, 28.0% for PC and 56.8% for PT-PC correspondingly) in comparison to Cleaning process A. The combination of shear stress and NaOH (**Cleaning Process C, Fig. 4.6c**) showed the most distinct % of biofilm removal at the end of the cleaning process, when compared with cleaning processes A and B, as stainless steel showed 8.6%, polycarbonate 16.7% and plasma treated polycarbonate 32.7% of biofilm coverage respectively. Regardless of the cleaning method, a higher extent of *P. fluorescens* biofilm removal was observed on stainless steel rather than on polycarbonates (**Fig 4.6 & Fig. 4.7**). Furthermore, it was observed that the combination of shear stress and NaOH had an effective result in the biofilm removal for all surfaces (**Fig. 4.6 and Fig. 4.7**), as Cleaning Process C appeared to be the most effective in all cases in terms of absolute values.

Figure 4.8 shows changes in (up) biovolume (μm^3) and (down) biofilm surface coverage (%) after 30 minutes of all cleaning processes in comparison with the data before cleaning for each surface, whereas Figure 4.9 shows the corresponding cleaning efficiency (%). Biovolume and biofilm surface area were considerably reduced during cleaning but the extent of reduction differed depending on the cleaning process and the substrate (**Fig.4.8 and Fig.4.9**). In all surfaces at the end of 30 minutes of cleaning, biovolume was lowest in samples treated by cleaning processes B and C, while cleaning process A did not affect the biovolume of *P.*

fluorescens on the substrates on the same way (**Fig.4.8 and Fig. 4.9**). On stainless steel this resulted in 29.1%, 76.8% and 86.2% biovolume reduction effectiveness on average, for cleaning processes A, B and C respectively (**Fig.4.9 up**). Similarly, for polycarbonate and plasma treated polycarbonate the biovolume reduction effectiveness was found to be 17.8% and 19.7% respectively for cleaning process A, 71.25% and 65.5% for cleaning process B and, 84.7% and 77.4% for cleaning process C (**Fig.4.9 up**). For biofilms grown on stainless steel and polycarbonate, biofilm surface area was reduced in cleaning processes B and C, reaching an effectiveness of cleaning of 67.8% and 87.6% respectively for stainless steel and of 59.2% and 75.6% for polycarbonate. In contrast, for biofilms grown on plasma treated polycarbonate, the biofilm surface area was effectively reduced by 39.5% and 65.2% in cleaning processes B and C correspondingly (**Fig.4.9 down**). As with the biovolume reduction effectiveness data, cleaning process C was observed to have the highest cleaning performance, while cleaning process A did not affect significantly the cleanliness of the surfaces at the end of the 30 minutes cleaning. In terms of surfaces, stainless steel showed the highest reduction effectiveness of biofilm surface area coverage as it was seen in the biovolume data (**Fig. 4.8 down and Fig.4.9 down**).

The biofilm surface coverage data depend on the average biomass thickness (**Chapter 3, Section 3.8.2**) and, though in some cases the total absolute value of biovolume was clearly reduced during the cleaning process, the covered surface area did not change significantly. For example, for polycarbonate surfaces the reduction of biofilm surface area coverage reached 59.2% of effectiveness after 30 minutes of cleaning process B, while the regarding biovolume data of the same cleaning process showed an effectiveness of 71.2% of reduction effectiveness (**Fig.4.9**). More significant is the example of plasma treated polycarbonate that showed a reduction effectiveness of 65.5% in the biovolume data, while only

39.5% in the biofilm surface area coverage data after 30 minutes of cleaning process B (**Fig.4.9**). This result implies that the initial morphology of the biofilms in those cases could contain holes of air in their mass that would not be calculated in the biovolume data however they would be included in the biofilm thickness data (**as shown in Chapter 3, Section 3.8.2, Figure 3.10**). In terms of biofilm adhesion, it can be assumed that the reduced effectiveness of biofilm surface coverage cleaning is a result of the different work of adhesion of the three different material surfaces, as plasma-treated polycarbonate that has the highest work of adhesion, showed also the highest biofilm surface coverage initially. From the initial CLSM image data (**Figure 4.5, Table 4.1**) it appears that polycarbonate and plasma treated polycarbonate were more abundantly covered in biofilm before cleaning, while they also showed higher biovolume values. It is thus believed that biofilm adhesion was stronger in polycarbonate and plasma treated polycarbonate surfaces compared to stainless steel, as the biofilm surface coverage and the biovolume showed reduced effectiveness in these two cases (**Fig. 4.9**).

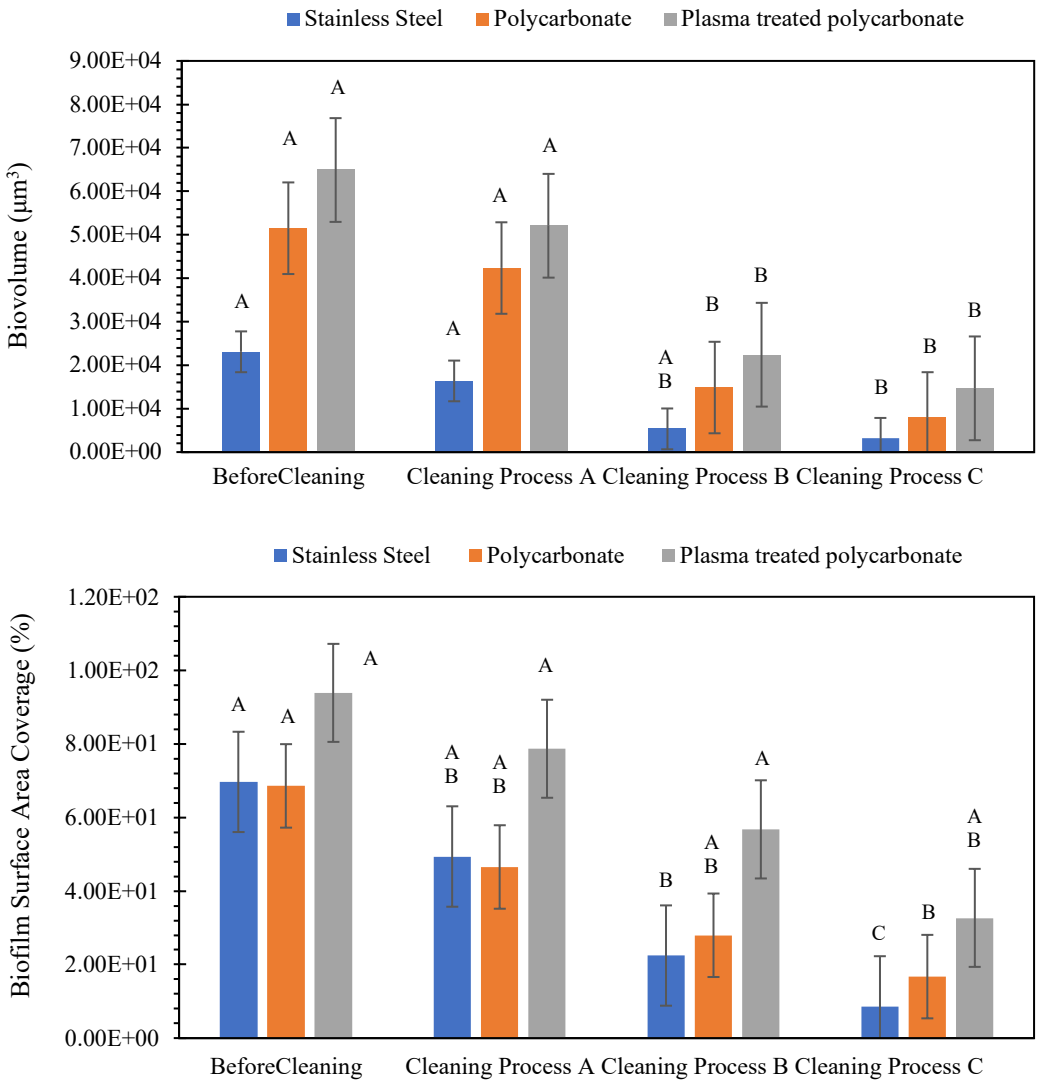

Figure 4.8: Absolute values of up) Biovolume (µm^3) and down) the biofilm surface area covered (%) of *P. Fluorescens* before cleaning and after 30 minutes of all cleaning processes on stainless steel (SS), polycarbonate (PC) and plasma treated polycarbonate (PT-PC) surfaces. Capital letters indicate statistically significant different groups at each cleaning process (Tukey's test, $p<0.05$). The error bars are the standard deviation of the triplicate's a) biovolume x10^4 (µm^3) and b) biofilm surface area (%). The same letter indicates no significant difference, i.e., A‡A: no significant difference, one similar letter indicates partial difference, i.e., A‡AB: slightly different and different letter indicates significant difference, while the furthest from control letter A, the most significant the difference, i.e., A‡B: significant difference and A‡C: more significant difference.

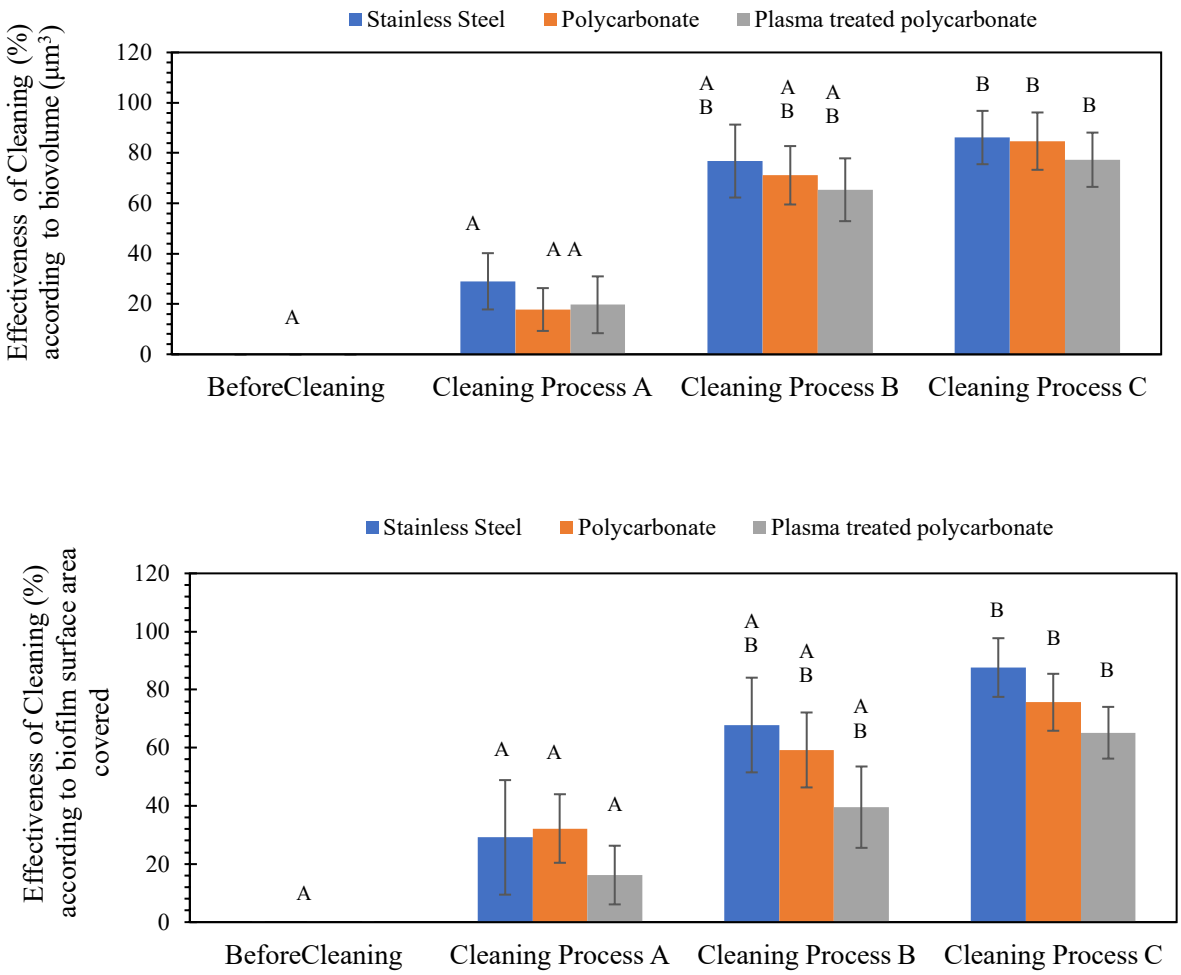

Figure 4.9: Effectiveness of cleaning (%) of *P. fluorescens* according to up) Biovolume (µm^3) and down) the biofilm surface area covered (%) data before cleaning (BC) and after 30 minutes of all cleaning processes on stainless steel (SS), polycarbonate (PC) and plasma treated polycarbonate (PT-PC) surfaces. Three replicates were measured at each of three different spots. The error bars are the standard deviation of the triplicate's effectiveness of cleaning for a) biovolume x10^4 (µm^3) and b) biofilm surface area (%). The same letter indicates no significant difference, i.e., A⧫A: no significant difference, one similar letter indicates partial difference, i.e., A⧫AB: slightly different and different letter indicates significant difference, while the furthest from control letter A, the most significant the difference, i.e., A⧫B: significant difference and A⧫C: more significant difference.

4.4.3 Cleaning of Pseudomonas putida

Prior to any cleaning application, CLSM images (**Figure 4.10**) showed that all surfaces were covered with *P. putida* ATCC 700008 biofilm and that the biofilm grown on plasma treated polycarbonate tended to be thicker (5.9±1.1μm average) than on stainless steel (2.1±0.7μm average) and polycarbonate (4.7±0.9μm average) (**Table 4.2**). In addition, the biovolume on plasma treated polycarbonate was found to be (2.0±0.4) $x10^4$ μm^3, on polycarbonate (1.61±0.3) $x10^4$ μm^3 while on stainless steel substrates the biovolume was measured (7.2±0.2) $x10^3$ μm^3. Moreover, the biofilm surface area coverage data showed that biofilm grown on plasma treated polycarbonate tended to be more abundant (78.4±1.7 % coverage in average) compared to stainless steel and non-treated polycarbonate (57.8±2.4 and 57.3±5.8 in average) (**Table 4.2**).

Table 4.2. Biovolume (μm^3), Biofilm Surface Coverage (%) and Biofilm thickness of *P. putida* ATCC 700008 grown on stainless steel (SS), polycarbonate (PC) and plasma treated polycarbonate (PT-PC) prior to any cleaning application. Three replicates were measured at three different spots.

Surface	Biovolume (μm^3)	Biofilm Surface Coverage (%)	Biofilm thickness (μm)
SS	(7.2±0.2) $x10^3$	57.8±2.4	2.1±0.7
PC	(1.6±0.3) $x10^4$	57.3±5.8	4.7±0.9
PT-PC	(2.0±0.4) $x10^4$	78.4±1.7	5.9±1.1

Figure 4.10 shows images from confocal microscopy and Figures 4.11 and 4.12 show graphs of biofilm surface area (%) and biovolume (10^4 μm^3) as a function of time during the cleaning processes. In Figure 4.10 it was observed qualitatively that after 30 minutes of cleaning

(Cleaning process C), the biofilm surface area coverage on stainless steel was decreased when compared to polycarbonate and plasma-treated polycarbonate. After 30 minutes of mechanical rinsing with water (**Cleaning Process A, Fig. 4.11a**) a small decrease of the biofilm mass was seen on all surfaces, as stainless steel showed 40.9±3.8%, polycarbonate 38.8±7.5% and plasma treated polycarbonate 65.7±0.8% of remaining biofilm surface area coverage respectively. In the presence of NaOH (**Cleaning Process B, Fig.4.11b**) an increased deformation of the biofilm structure was observed on all substrates after 30 minutes of cleaning (resulting biofilm coverage, 18.3±5.7% for SS, 23.2±4.2% for PC and 47.1±1.7% for PT-PC correspondingly), while for the combination of shear stress and NaOH (**Cleaning Process C, Fig.4.11c**) a distinct biofilm removal was viewed at the end of the cleaning process as stainless steel showed 6.7±0.5%, polycarbonate 13.7±2.6% and plasma treated polycarbonate 27.0±2.0% of biofilm coverage respectively.

Table 4.3. Effects of the different cleaning processes A, B and C on *P. fluorescens NCIMB 9046* and *P. putida* ATCC 700008 final biofilm thickness (μm) after 30 minutes of cleaning. Three replicates were measured at three different spots.

Surface	*P. fluorescens* Before cleaning	*P. putida* Before cleaning	Cleaning Process	*P. fluorescens* 30 minutes Cleaning	*P. putida* 30 minutes Cleaning
Stainless Steel	6.7±2.1	2.12±0.7	A	4.8±1.6	1.5±0.5
			B	1.6±0.3	0.5±0.1
			C	1.2±0.5	0.3±0.2
Polycarbonate	15.1±3.1	4.70±0.9	A	12.4±2.1	3.8±0.6
			B	4.4±0.1	1.4±0.1
			C	2.3±0.2	0.7±0.1
Plasma treated polycarbonate	19.0±3.6	5.90±1.1	A	15.3±1.2	4.7±0.4
			B	6.6±0.3	2.1±0.1
			C	4.3±0.2	1.4±0.1

Independently of the cleaning method, a greater effect of cleaning on *P. putida* biofilm removal was observed on stainless steel rather than on polycarbonates from a qualitative point of view (**Figure 4.10**). Furthermore, it was observed that the combination of shear stress and NaOH (**Cleaning Process C, Fig.11b**) had a significant effect on biofilm removal for all surfaces. As for the kinetics of the cleaning process, in contrast to the *P. fluorescens* biofilm, it was seen in all cases that during the first 5 minutes of the cleaning there was a slight but not significant increase of the biofilm surface area coverage (**Figure 4.11**). The biofilm thickness data show that *P. putida* forms thinner biofilms than *P. fluorescens* under the same growth conditions and consequently thinner biofilms after 30 minutes of cleaning with all processes (**Table 4.3**). It is thus believed that for biofilms of this size there might be a rearrangement of the biofilm at the start of cleaning, while the most important biomass diminution occurs between 10 and 20 minutes regardless of the cleaning process (**Figure 4.11**).

Biovolume of *P. putida* during all cleaning processes was affected in the same way as the biofilm surface coverage. An initial increase in the biovolume data was observed which is believed that was due to biofilm swelling at the initiation of the cleaning, which was not significant for all surfaces and all cleaning processes (**Figure 4.12**). After 30 minutes of mechanical rinsing with water (**Fig. 4.12a**) there was a slight effect in the final biovolumes except in the case of stainless-steel surfaces, where the biovolume reduction was more significant. It was observed that during cleaning processes B and C the biofilm removal took place between 5 and 30 minutes of cleaning (**Fig. 4.12b & 4.12c**). Also, biovolume data shows that the cleaning process C, combining the shear stress and the NaOH, resulted in the most significant biofilm removal in absolute values (**Fig. 4.12c**). Finally, it was seen, showing the same trends as the biofilm surface coverage data, that out of all three, stainless steel substrates showed reduced absolute values of biovolume at the end of all cleaning processes (**Figure 4.12**).

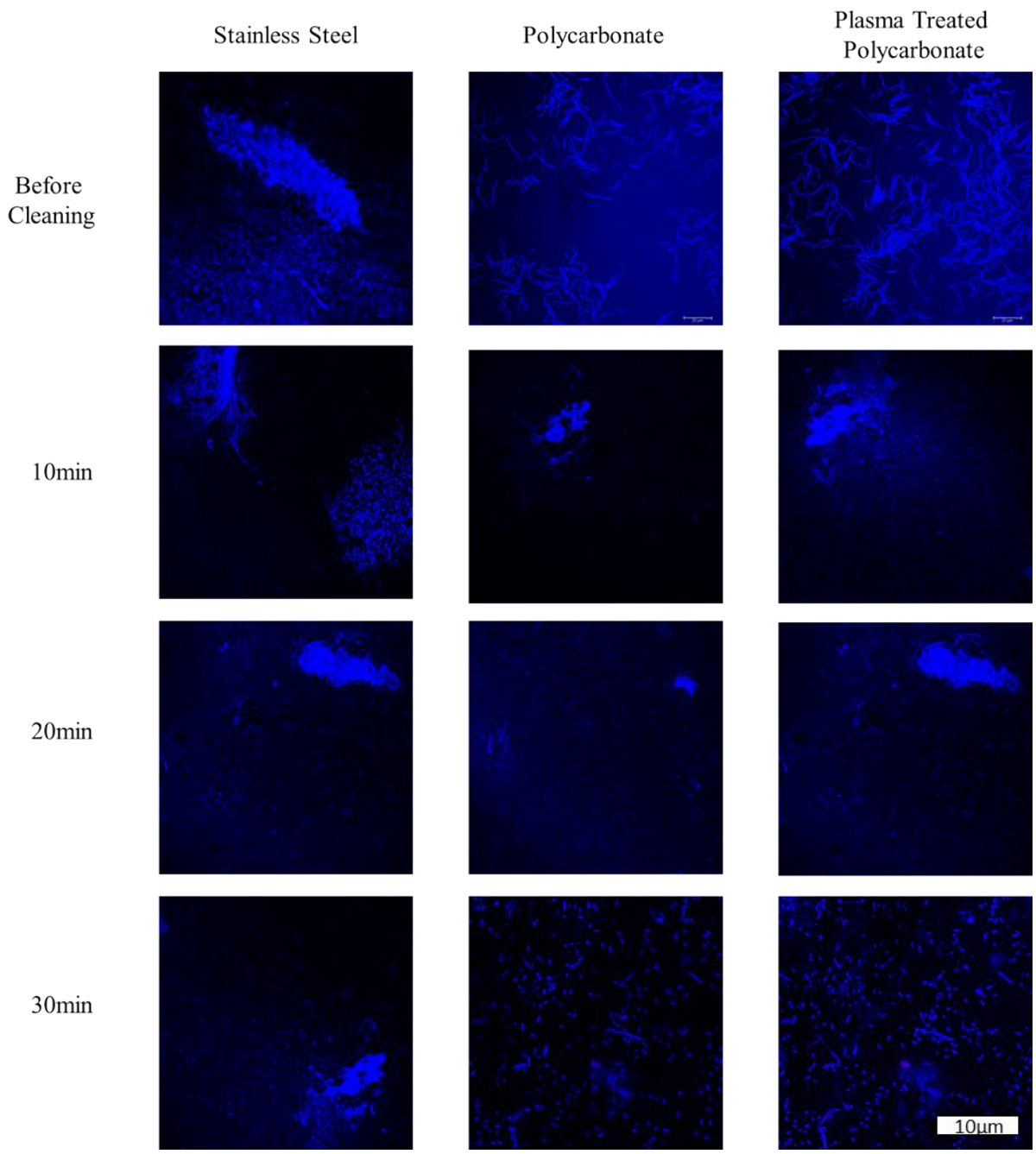

Figure 4.10: Confocal laser scanning microscopy images of the effect of CIP with NaOH (Cleaning Process C) on *P. putida* biofilm grown on stainless steel, polycarbonate and plasma-treated polycarbonate surface coupons before cleaning and after 10, 20 and 30 minutes of cleaning. Biofilm was stained with DAPI (1%w/w). Three replicates were measured at three different spots. One replicate is shown in this case.

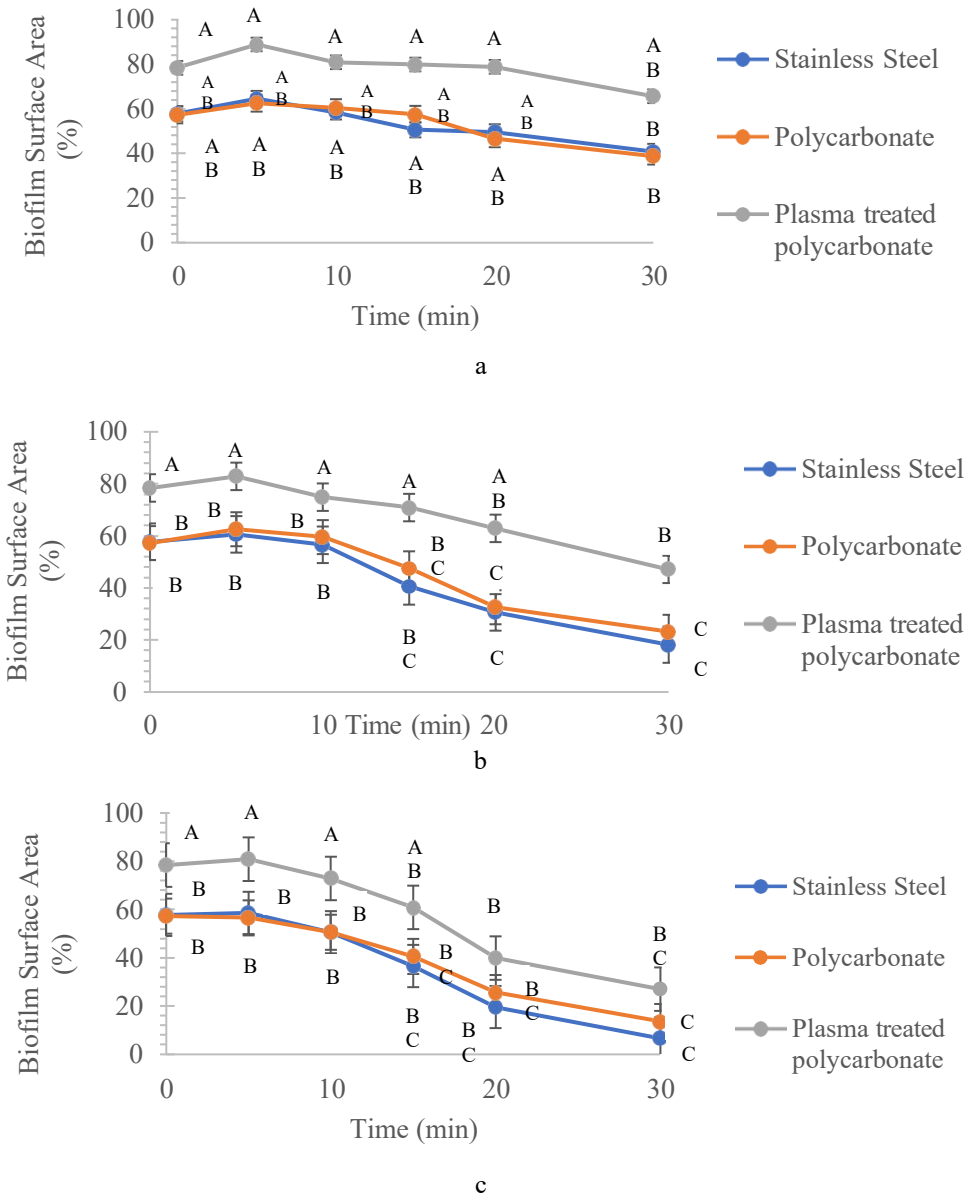

Figure 4.11: Biofilm surface area (expressed as a % of the total surface area) of *P. putida* grown on stainless steel, polycarbonate and plasma-treated polycarbonate surface coupons before cleaning and after 5, 10, 15, 20 and 30 minutes of a) Mechanical rinsing with water (Cleaning Process A), b) Immersion in NaOH (Cleaning Process B) and c) CIP with NaOH (Cleaning Process C). Three replicates were measured at three different spots. The error bars are the standard deviation of the triplicate's biofilm surface area (%). The same letter indicates no significant difference, i.e., A‡A: no significant difference, one similar letter indicates partial difference, i.e., A‡AB: slightly different and different letter indicates significant difference, while the furthest from control letter A, the most significant the difference, i.e., A‡B: significant difference and A‡C: more significant difference.

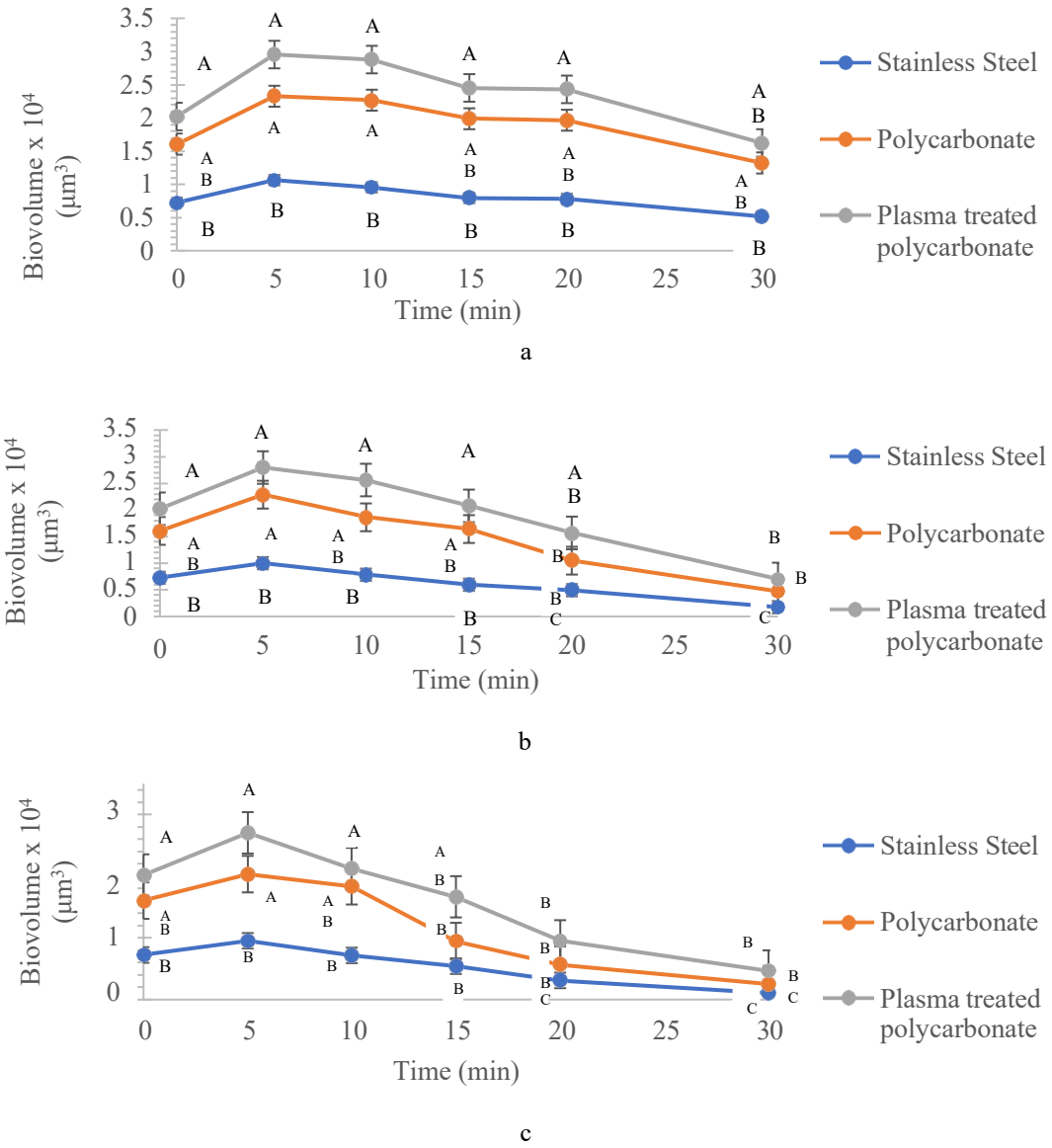

Figure 4.12: Biovolume (µm^3) of *P. putida* grown on stainless steel, polycarbonate and plasma-treated polycarbonate surface coupons before cleaning and after 5, 10, 15, 20 and 30 minutes of a) Mechanical rinsing with water (Cleaning Process A), b) Immersion in NaOH (Cleaning Process B) and c) CIP with NaOH (Cleaning Process C). Three replicates were measured at three different spots. The error bars are the standard deviation of the triplicate's biovolume x10^4 (µm^3). The same letter indicates no significant difference, i.e., A↮A: no significant difference, one similar letter indicates partial difference, i.e., A↮AB: slightly different and different letter indicates significant difference, while the furthest from control letter A, the most significant the difference, i.e., A↮B: significant difference and A↮C: more significant difference.

Figure 4.13 shows changes in (up) biovolume (μm^3) and (down) biofilm surface coverage (%) after 30 minutes of all cleaning processes in comparison with the data before cleaning for each surface, whereas Figure 4.14 shows the corresponding cleaning efficiency (%). Biovolume and biofilm surface area were considerably reduced during the cleaning but the extent of reduction depended on both the cleaning process and the substrate (**Figures 4.13 and 4.14**). For all surfaces at the end of the 30 minutes cleaning, biovolume was lowest in those treated by cleaning processes B and C, while cleaning process A did not significantly affect the biovolume of *P. putida* on all substrates (**Figure 4.13 up**). On stainless steel this resulted in 28.7 ± 12.1%, 76.1 ± 15.0% and 85.3 ± 15.2% biovolume reduction effectiveness in average, for A, B and C respectively (**Figure 4.14 up**). Similarly, for polycarbonate and plasma treated polycarbonate the biovolume reduction effectiveness was 17.7 ± 11.3% and 19.7 ± 10.9% respectively for cleaning process A, 70.8±14.3% and 65.2±18.4% for cleaning process B and, 84.4±15.8% and 77.1±15.3% for cleaning process C (**Figure 4.14 up**).

For biofilms grown on stainless steel and polycarbonate, biofilm surface area was significantly reduced in B and C cleaning processes, reaching a reduction effectiveness of cleaning of 68.4±12.1% and 88.5±11.0% respectively for stainless steel and of 59.5±14.3% and 76.2±13.7% for polycarbonate. In contrast, for biofilms grown on plasma treated polycarbonate, the biofilm surface area was effectively reduced by 40.0±14.6% and 65.6±17.0% in cleaning processes B and C correspondingly (**Figure 4.14**). As with the biovolume reduction effectiveness data, cleaning process C was observed to have the highest performance, while cleaning process A did not significantly affect the cleanliness of the surfaces at the end of the 30 minutes cleaning. In terms of surfaces, stainless steel showed the highest reduction of biofilm surface area coverage and of biovolume data (**Fig. 4.13 and 4.14**).

As already reported for *P. fluorescens* biofilm, the biofilm surface coverage data depend on the average biomass thickness (**Chapter 3, Section 3.8.2, p.68)**, and, though in some cases the total biovolume was clearly reduced during one cleaning process, the covered surface area did not change similarly. For example, in the case of polycarbonate surfaces the biofilm surface area coverage reached 59.5±14.3% of effectiveness during cleaning process B, while the biovolume data of the same cleaning process showed an effectiveness of 70.8±14.3% in cleaning (**Fig. 4.13 and 4.14**). More significant is the example of plasma treated polycarbonate that under the same cleaning conditions (Cleaning process B) showed an effectiveness of 65.2±18.4% from the biovolume data, while only 40.0±14.6% from the biofilm surface area coverage data (**Fig. 4.13 and 4.14**). Interestingly, in the case of polycarbonate coupons that were cleaned with the cleaning process A, the biofilm surface area showed a better effectiveness (32.3±12.7%) than the biovolume effectiveness (17.7±11.3%) (**Fig. 4.13 and 4.14**). This result implies that the biofilm morphology was robust and even though some part of the biofilm mass was removed during cleaning, a significant part of the biofilm remained intact, and thus, the biofilm thickness was not significantly reduced.

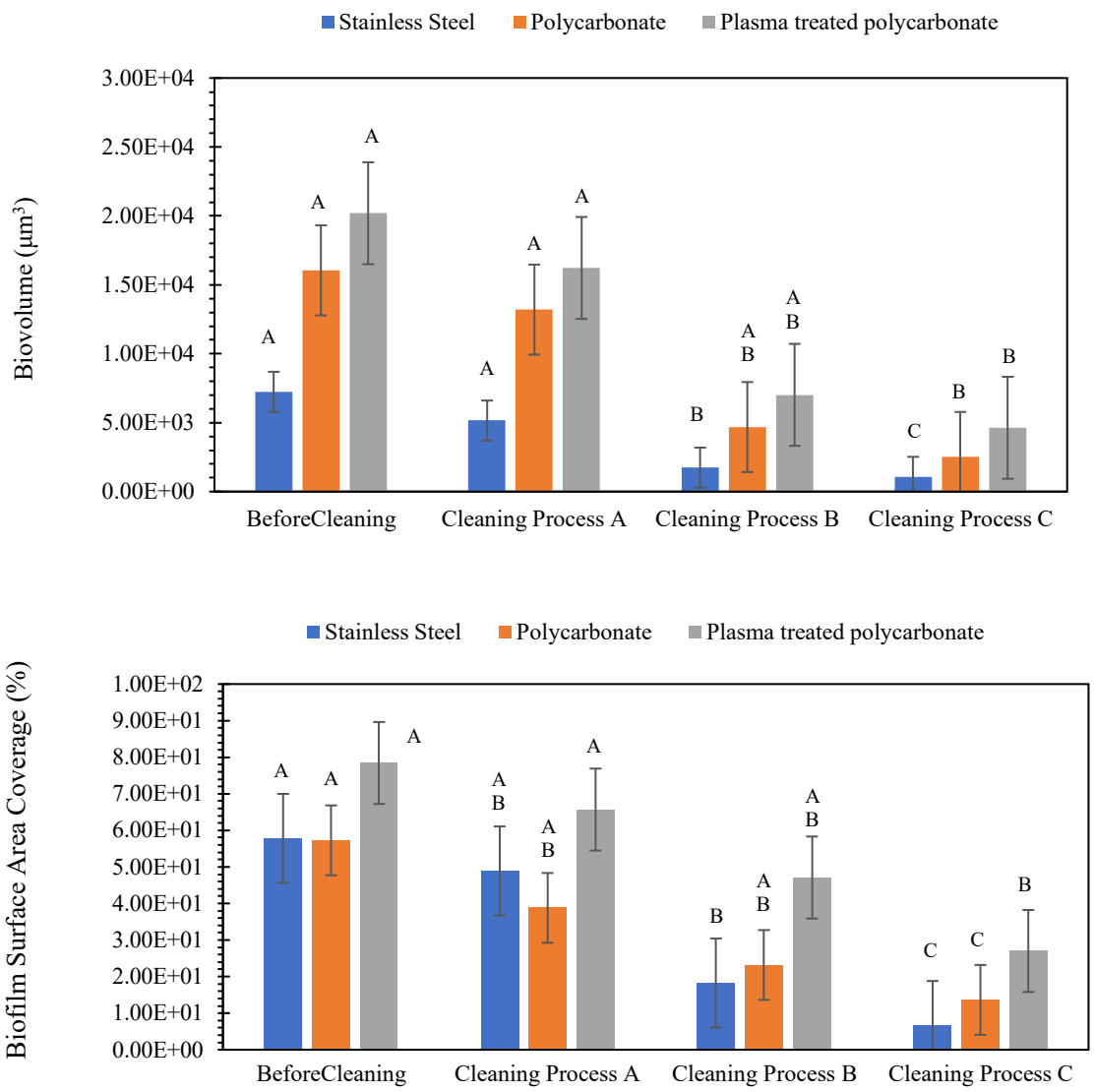

Figure 4.13: Absolute values of up) Biovolume (µm^3) and down) the biofilm surface area covered (%) of *P. Putida* before cleaning and after 30 minutes of all cleaning processes on stainless steel (SS), polycarbonate (PC) and plasma treated polycarbonate (PT-PC) surfaces. Capital letters indicate statistically significant different groups at each cleaning process (Tukey's test, $p<0.05$). The error bars are the standard deviation of the triplicate's a) biovolume x10^4 (µm^3) and b) biofilm surface area (%). The same letter indicates no significant difference, i.e., A‡A: no significant difference, one similar letter indicates partial difference, i.e., A‡AB: slightly different and different letter indicates significant difference, while the furthest from control letter A, the most significant the difference, i.e., A‡B: significant difference and A‡C: more significant difference.

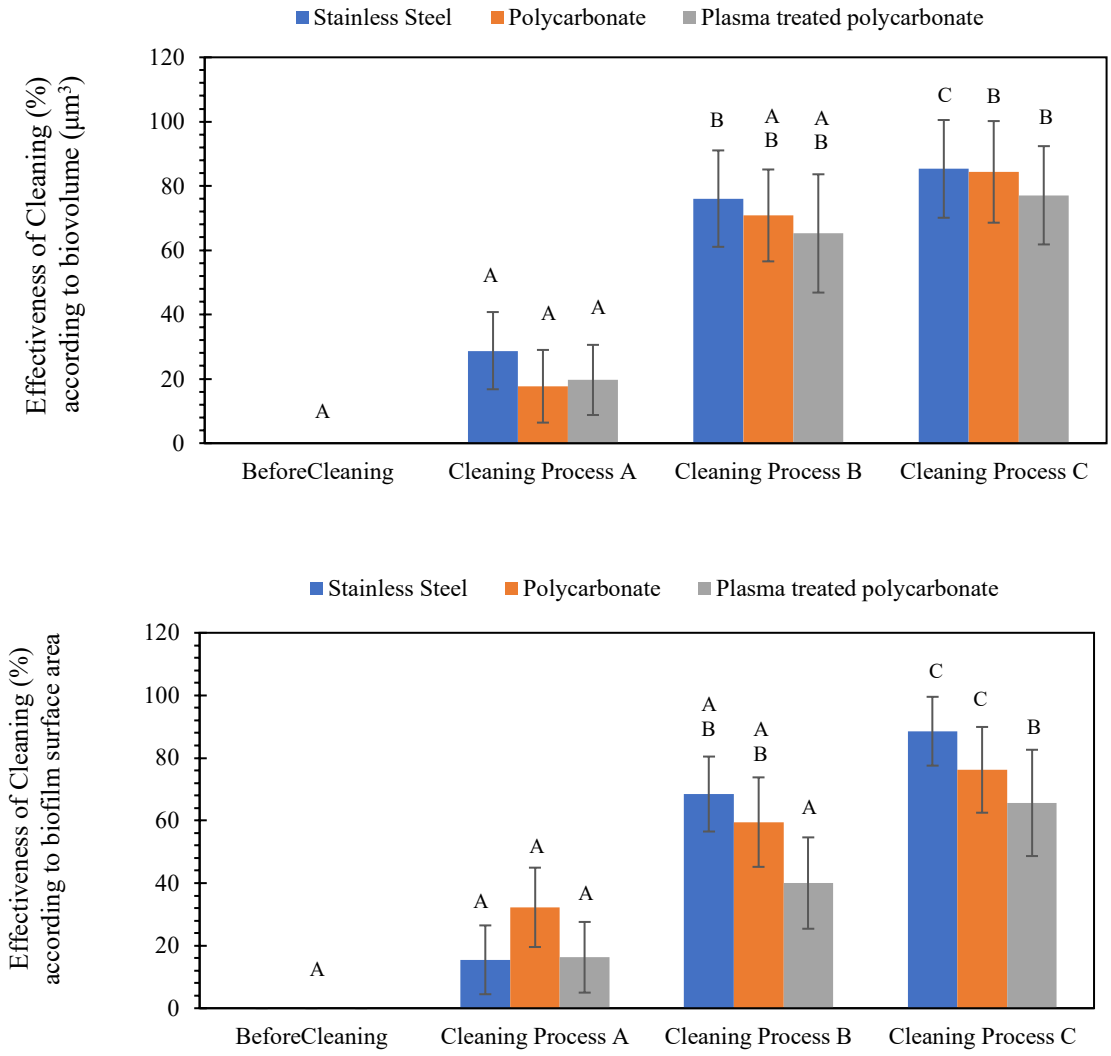

Figure 4.14: Effectiveness of cleaning (%) of *P. putida* according to up) Biovolume (µm^3) and down) the biofilm surface area covered (%) data before cleaning (BC) and after 30 minutes of all cleaning processes on stainless steel (SS), polycarbonate (PC) and plasma treated polycarbonate (PT-PC) surfaces. Three replicates were measured at each of three different spots. The error bars are the standard deviation of the triplicate's effectiveness of cleaning for a) biovolume x10^4 (µm^3) and b) biofilm surface area (%). The same letter indicates no significant difference, i.e., A↮A: no significant difference, one similar letter indicates partial difference, i.e., A↮AB: slightly different and different letter indicates significant difference, while the furthest from control letter A, the most significant the difference, i.e., A↮B: significant difference and A↮C: more significant difference.

4.5. Discussion

Bacteria express adhesion proteins on the surface of planktonic organisms and eventually cells that are not washed away will fast adapt to their local environment and will cause irreversible biofilm attachment on surfaces (Stoodley et al., 2013; Harriott, 2019). Biofilm growth is of great concern for various sectors, like the food industry. Biofilm on surfaces of food-processing plants could lead to food-borne illness outbreaks since day-to-day cleaning with common chemicals is not always efficient for biofilm control. (Lindsay and Holy, 2006; Walker et al., 2007; Galié et al., 2018; Santos et al., 2018). Studies on the mechanism that provokes biofilm cleaning from stainless steel substrates, the most common material surface viewed in the food industry, concluded that the combination of hydrodynamic mechanical forces and chemical agents is essential for effective biofilm removal (Lécrigny-Nolf et al, 2000; Levièvre et al., 2001; Levièvre et al., 2002; Faille et al., 2013; Awad et al., 2018; Bénézech et al, 2018). Thus, this study was focused on studying the biofilm removal of *P. fluorescens* and *P. putida* from stainless steel, polycarbonate and plasma-treated polycarbonate surfaces during three distinct cleaning processes, monitored in different time points of the cleaning.

In all, it was observed that biofilm growth was successful on all surfaces and all cleaning processes resulted in biofilm removal. Cleaning process C, combining the NaOH action with the shear stress forces, caused the higher reduction in both the parameters studied, biovolume and biofilm surface coverage. As a cleaning agent, sodium hydroxide saponifies fats and dissolves proteins and is a common cleaning practise in industrial manufacturing sites (Block, 1991; Adner et al., 1994). It is believed that the combined CIP method weakened the adhesive and cohesive forces of the EPS organic compounds and removed the biofilm from the surfaces

better than the other two cleaning processes that were without the action of NaOH (cleaning process A) or the shear from the hydrodynamic conditions (cleaning process B) respectively. These results agree with current literature, as indicatively, *Bacillus cereus* spores removal from stainless steel pipes using NaOH studied by Levièvre et al. (2001) was found to be strongly dependent on both chemical action and hydrodynamic conditions during CIP, while Faille et al. (2013) concluded that for *Bacillus cereus* detachment from stainless steel coupons, CIP with NaOH under low wall shear stress was found to be more effective than mechanical rinsing with water at higher wall shear stress.

When comparing the three surfaces, it was observed that the biofilm structure was different according to the bacteria strain. In general, *P. fluorescens* formed thicker and more robust biofilms on all surfaces compared to *P. putida*, which showed thinner biofilms with filamentous structure. Between the three surfaces, stainless steel had the thinnest biofilms initially while the biofilm grown on polycarbonate showed similar data for the surface coverage but greater thickness and biovolume. In contrast, plasma-treated polycarbonate that exhibited high work of adhesion, showed increased biofilm surface coverage, biofilm thickness as well as biovolume for both bacteria strains. This result agrees with the current literature on antifouling coatings, where research shows that hydrophobic surfaces show better antifouling activity than hydrophilic ones (Yin et al. 2016, Dong et al., 2021). Moreover, in terms of different cleaning performance, it was shown that stainless steel was cleaned more successfully than polycarbonate and plasma-treated polycarbonate coupons.

The increased biovolume and average biomass thickness on polycarbonate surfaces

compared to stainless steel played an important role in their difference in cleaning efficacy. As mentioned in literature, this contrast between stainless steel and plasma-treated polycarbonate is caused by the difference of their physicochemical properties, ie., their roughness, chemical composition and surface energy that affects both the initial biofilm structure and, their cleanability (Fletcher and Loeb 1979; Detry et al., 2007; Detry et al., 2010). Surface energy, otherwise known as work of adhesion, is one of the parameters believed to play a key role in biofilm adhesion (Katsikogianni and Misirlis, 2004), as biofilm has a tendency to grow on substrates that have surface energy close to its own (Detry et al., 2010). Thus, the work of adhesion that was observed on the plasma-treated polycarbonate substrates might have aided the stronger attachment of the bacteria on the surfaces, which lead to the reduced cleanability of the surface.

For *P. putida* the slight increase during the initial part of the cleaning was not predicted, as it was expected that even on the first point of biofilm cleaning there would be an immediate reduction in all parameters. However, it was seen in literature that instant swelling could be observed at the initial disruption of the EPS during cleaning (Zhang et al., 2017; Zhao et al., 2017; Galie et al. 2018). Moreover, Lécrigny-Nolf et al. (2000) concluded that the effect of shear stress in *Bacillus cereus* spores removal is not linear, while Levièvre et al. (2002) assumed that the cleaning process combines removal and deposition, and thus an instant increase in the biofilm parameters might be observed when monitoring cleaning. Finally yet importantly, Bénézech et al. (2018), explained the detachment of *P. fluorescens* biofilm during CIP with NaOH with a two-phase kinetics model, initiated by an instant removal occurred during the 1st phase followed by a slow rate during the 2nd phase, indicating that biofilm cleaning is not linear but instead more sophisticated and probably consists of more distinct phases.

4.6. Conclusions

In this chapter the investigation of biofilm morphology during cleaning using CLSM indicates that biofilm removal was strongly influenced by the cleaning conditions. The combined CIP procedure with NaOH 0.1%w/w was more effective than the mechanical rinsing with water and the chemical (NaOH static) cleaning processes for all material surfaces. In terms of surfaces, it was seen that stainless steel was cleaned more efficiently compared to polycarbonate and plasma-treated polycarbonate surfaces as well as that the latter material surfaces showed higher work of adhesion.

The interactions between three different material surfaces and biofilm development showed that *P. fluorescens* developed higher percentage of surface coverage comparing to *P. putida* on all surfaces. In terms of different materials, the percentage of the area covered by bacteria was significantly lower on plastic surfaces (PET, PTFE and polypropylene) with lower work of adhesion than on more hydrophilic surfaces like glass, hydroxyapatite and stainless steel.

For the different bacteria strains, it was observed that the *P. fluorescens* NCIMB 9046 and the *P. putida* ATCC 700008 biofilms had different structure, as the first one formed islands of bacteria among with EPS, whilst the *P. putida* showed a filamentous structure. As no stain for the biofilm EPS was used it is difficult to see differences in the EPS structures between *P. fluorescens* and *P. putida*. In terms of biofilm residual contamination for cleaning process C, a

more distinct biofilm removal was observed *for P. putida* ATCC 700008 than for *P. fluorescens* NCIMB 9046, as in the end of the 30 minutes cleaning both biofilm surface coverage and biovolume absolute values were lower for all surfaces. However, during the *P. putida* cleaning an unexcepted instant increase was observed in biofilm mass, indicating that biofilm cleaning might strongly depend on the different strains with different type of EPS and that a universal biofilm cleaning mechanism is not possible to be predicted.

This chapter has showed the development of an easy and reliable method for quantifying the effectiveness of biofilm cleaning. To evaluate the data in a multi parameter scale different bacteria strain, material surfaces and cleaning methods were chosen. The parallel-plate flow chamber was proved to be an easy and accurate essay in order to clean three replicates simultaneously, while the cleaning parameters of temperature, shear stress, cleaning agents concentration can be kept stable. Next, by using the same method, it was interesting to investigate the effect of enzymatic cleaning products in a real case, mixed microbial biofilm that was obtained from a meat processing line. The design of the experiments, methodology and the relevant results are discussed in Chapter 5.

1

CHAPTER 5: THE SYNERGISTIC EFFECT OF ENZYMATIC DETERGENT ON BIOFILM CLEANING FROM DIFFERENT ARTIFICIAL SURFACES

5.1. Summary

In Chapter 4 the need to understand the mechanisms involved in the biofilm removal from solid artificial surfaces was discussed. Additionally, the development of an easy and reliable biofilm cleaning monitoring technique was evaluated by measuring the biofilm removal of single microbial biofilms of *P. fluorescens* and *P. putida* strains from artificial surfaces.

In this chapter the removal of real mixed-microbial biofilm from common artificial surfaces was investigated using commercial enzymatic detergents and disinfectants used in the food industry, a sector where biofilm growth is a significant contamination source. Enzymes are considered green countermeasures against biofilm formation due to their biodegradability and low toxicity, features that make them a useful tool in the food industry. In this study, the synergistic effect of enzymes was studied against biofilm cleaning from hard surfaces. A mixed-microbial sample was sourced from a meat packaging line and biofilm was grown under high shear conditions on stainless steel and polyethylene surfaces. The model cleaning-in-place (CIP) parallel-plate flow chamber (**Chapter 3, Section 3.6.1**) was used for firstly, the enzymatic cleaning and secondly, a disinfection step. The cleaning effectiveness was evaluated in response to different formulations containing non-foaming commercial surfactants among with amylase, protease and lipase at neutral pH. The formulation combining all three enzymes was proved the most effective, showing a synergy essential for the deformation of biofilm structure and consequently the better

disinfection for both material surfaces.

Initially, mixed-microbial biofilm was obtained from a meat packaging line and was grown on stainless-steel and polyethylene coupons in microcosms (**Chapter 3, Section 3.5.4**). The aim of the experiments reported in this chapter was to evaluate the effectiveness of different enzymes in biofilm removal. For this reason, CIP comprising of different steps was performed by using the parallel-plate flow chamber with stainless steel or polyethylene coupons already colonized by biofilm (**Chapter 3, Section 3.6.2**).

To evaluate the effectiveness of biofilm reduction the parameters investigated were

(i) the percentage (%) of the area covered by biofilm, biovolume and average biofilm thickness measured using confocal laser scanning microscopy (CLSM) images (**Chapter 3, Section 3.8.2**),

(ii) the polysaccharide content in EPS measured in glucose equivalents (**Chapter 3, Section 3.8.3**) and

(iii) the bacterial viability (**Chapter 3, Section 3.8.4**).

In addition, scanning electron microscopy (SEM) images were obtained to study the microbial biofilm structure (**Chapter 3, Section 3.8.5**). All measurements were performed 1) before cleaning, 2) after cleaning with the different enzymatic formulations and 3) after disinfection. For all parameters analyzed, the effectiveness of biofilm reduction, $E_{f,}$ was calculated as described in detail in Chapter 3, section 3.7.2.

5.2. Introduction – Defining biofilm cleaning

As discussed in previous chapters, biofilms are complex microbial ecosystems formed by one or more species immersed in an extracellular matrix of different compositions depending on the type of food manufacturing environment and the colonizing species (Galié et al., 2018). Fouling of food process plant surfaces and the subsequent cleaning needed is a significant industrial problem, both in terms of hygiene and costs (Goode et al., 2013). Thus, biofilm cleaning is of great importance and, as biofilm is a multifaceted substance, it is extremely challenging to give a specific definition on "biofilm cleaning".

According to Goode et al. (2013), biofilm is considered a "microbial and gel-like film that needs to be removed in part by water and in part by chemical.", whereas Charlton (2008) separates biofilms from other types of soil as: (i) they are composed of living organisms constantly interacting with the environment; (ii) the cells inhabit a wide range of microenvironments in the biofilm; (iii) the cells exhibit a wide range of physiological states and engage in specific biofilm-related processes; and (iv) the cells are embedded in a complex matrix of organic and inorganic compounds.

To control biofilm formation, food industries use routine cleaning processes, including cleaning-in-place (CIP) and cleaning-out-place (COP) systems mainly comprising shear stress together with chemical agents (Keener, 2005; Li et al., 2017). To understand the mechanisms that result in biofilm removal, several studies have tried to model the biofilm detachment kinetics from artificial surfaces. The most important outcome was to demonstrate that it is not a straightforward process and adequate elimination of biofilm requires a

combination of hydrodynamics with chemical agents (Lécrigny-Nolf et al., 2000; Blel et al., 2007; Faille et al., 2013; Bénézech and Faille, 2018), as shown also in Chapter 4.

As there is no standard method available for evaluating and comparing cleaning agents for use in CIP procedures in the food industry (Ostrov et al., 2016) we can evaluate "biofilm cleaning" by studying the elimination of two distinct parameters, the extracellular polymeric substance (EPS) removal and the bacteria viability. The EPS-removal represents the soil mass of the biofilm and its elimination is substantial for good cleaning practices whereas the bacteria viability signifies the ability of the biofilm's survival and reproduction after cleaning, thus its disinfection is equally crucial as its removal. While routine cleaning in industry uses strong alkaline and acidic agents, efficient in CIP of food-processing lines (Antoniou and Frank, 2005), this strategy is not always enough for biofilm removal. Also, the safe handling of food industrial surfaces requires the utmost care, and hence milder, safer and more efficient biofilm CIP cleaning agents are desirable (Galié et al., 2018).

Research has shown that bacterial cells within biofilms are physiologically distinct from their planktonic counterparts and, for this reason, are more resistant to cleaning (Lindsay and Holy, 2006). An interesting alternative to strong alkaline and acidic agents is the application of enzymes. Since they are biodegradable and show low toxicity, enzymes are considered green countermeasures against biofilm formation (Galié et al., 2018) and they have been used in detergents for biofilm removal in food industry (Furukawa et al., 2010). In order to understand the mechanism of enzymatic cleaning against biofilm, Molobela et al. (2010) studied commercial proteases and amylases for their effectiveness in the deformation and detachment of EPS matrix produced by *P. fluorescens*. In that study, all enzymes except for the protease polarzyme were proved effective for the degradation of the EPS, with savinase

and everlase being the most effective. In other studies (Vickery, 2004; Walker et al., 2007) that were investigating the cleaning effectiveness against biofilm, mixtures of enzymes were found more adequate for removing biofilms than single enzyme cleaning treatments.

In order to eliminate biofilm, a key component is the EPS matrix, which is mostly water (up to 97%) and contains the structural and functional components of the matrix: soluble, gel-forming polysaccharides, proteins and eDNA, as well as insoluble components such as amyloids, cellulose, fimbriae, pili and flagella (Flemming et al., 2016). Although little is known about the interactions between enzymes and EPS, it is found that polysaccharases, polysaccharide lyases, and to some extent proteases, disrupt the EPS structure (Sutherland, 2001; Vickery, 2004). From a physicochemical point of view, the removal of biofilms is achieved by using substances that induce detachment by diminishing the cohesiveness of the EPS matrix (Xavier et al., 2005), and enzymes have been proved as such (Augustin et al., 2004; Vickery, 2004; Xavier et al., 2005). Along with chemical agents, enzymes are categorised as detachment-promoting agents (DPAs) comprising a diversity of mechanisms that are not fully characterized (Vickery, 2004; Xavier et al., 2005; Palmer et al., 2007). What is suggested is that they destroy the physical integrity of EPS by weakening the structural bonds in proteins, carbohydrates and lipids making up the structures of the EPS through the degradation process (Melo and Bott, 1997; Furukawa et al., 2010; Lequette et al., 2010; Molobela et al., 2010).

In this study, the activity of enzymes in different formulations against a mixed-microbial biofilm sourced from a meat packaging line was evaluated using a model CIP system on stainless steel and polyethylene surfaces – these surfaces are similar to those used in the plant. As these two material surfaces are widely used in industry, the first objective was

to examine whether there would be a difference in their cleanability against biofilm. Moreover, the synergistic effect of three enzymes, amylase, protease and lipase, was investigated in combination with non-foaming surfactants in neutral pH. The hypothesis was that the combination of the enzymes would be more effective against biofilm but the goal was to explore whether there were significant differences between their cleaning efficacies.

5.3. Materials and Methods

5.3.1. Biofilm Growth

To study the synergistic effect of enzymes against biofilm cleaning from hard surfaces, biofilms were developed in microcosms under shear stress conditions, on stainless steel and polyethylene coupon surfaces (**Chapter 3, Section 3.5.4**). The mixed-microbial inoculum used for the biofilm development was previously prepared from swab samples that were collected from a meat packaging process line (Vic, Catalonia, Spain). The microcosms were covered with aluminum foil and wrapped with plastic tape, and incubated at 30ºC for 25 days. The volume of the solution was reduced due to evaporation and, in order to maintain a constant volume and to avoid modification of the physical-chemical environment due to microbial activity (i.e. pH, oxygen), every 3 days 250mL of the medium was removed from each microcosm and replaced to 500 mL with fresh Ringers solution. The biofilm colonized stainless steel and polyethylene coupons, were removed aseptically, rinsed with sterile PBS water and subsequently used for the CIP enzymatic cleaning experiment.

5.3.2. Cleaning-in-Place (CIP) protocol

To evaluate the effectiveness of different enzymes in biofilm removal, CIP comprising of different steps was performed by using the parallel-plate flow chamber (**Chapter 3, Section 3.6.1**) containing triplicate stainless steel or polyethylene coupons colonized by biofilm as described above.

During the first cleaning step, enzymatic formulations were applied for 30 minutes (**Chapter 3, Section 3.6.2**). The initial temperature of the formulation was 55ºC and after the 30 minutes of cleaning process the temperature was 45ºC. In the second step, a commercial disinfectant based on peracetic acid (1% w/w) was applied for 10min at room temperature. Both temperature and exposure time used for the detergents and the disinfectant were recommended by their manufacturer.

The parallel-plate flow chamber operated under stable flow in all the experiments ($Q = 1 \times 10^{-6}\ m^3/s$). The wall shear stress was calculated at 0.129 (N/m^2) for 25ºC and at 0.647 (N/m^2) for 50ºC. The different enzymatic products that were tested were prepared by the author using standard enzymatic formulations from Itram Higiene S.L. company that contained 1) amylase-protease-lipase (Formulation A), 2) amylase-protease (Formulation B), and 3) amylase-lipase (Formulation C), in combination with a non-foaming Itram enzymatic solution. The total concentration of enzymes in each formulation was kept constant in all the experiments. The formulations provided by Itram that were used for the preparation of the formulations tested in the experiments had standard concentrations of enzymes and surfactants. Each time the formulation tested (A, B or C) was prepared fresh by the authors with the same concentration of the enzyme to be tested. The efficacy of these products was

compared to a non-foaming Itram solution without enzymes, which was used as a control. In each experiment a different formulation (control, A, B and C) was tested in combination with a disinfection process on freshly grown biofilms. Three replicates of biofilm without any treatment were initially tested. The enzymatic detergent treatments were performed in six different replicates and three of them were tested. Finally, the disinfection process was performed in three remaining replicates that had been treated with the enzymatic formulations and they were also tested using the same analysis techniques.

In this biofilm cleaning study, as described in **Chapter 3, Section 3.7.2**, in order to monitor the effectiveness of different enzymes in biofilm removal the parameters investigated were 1) the percentage (%) of biofilm surface area, biovolume and average biofilm thickness from confocal laser scanning microscopy (CLSM) images (**Chapter 3, Section 3.8.2**), 2) the polysaccharide content in EPS (**Chapter 3, Section 3.8.3**) and 3) the bacteria viability using Flow Cytometry (**Chapter 3, Section 3.8.4**). In addition, scanning electron microscopy (SEM) images were obtained to study the microbial biofilm structure (**Chapter 3, Section 3.8.5**). All measurements were performed 1) before cleaning, 2) after cleaning with the different enzymatic formulations and 3) after disinfection.

For all parameters analyzed, the effectiveness of biofilm reduction, E_f, was calculated using the equation 3.7 described at **Chapter 3, Section 3.7.2**, as:

$$E_f(\%) = \frac{|Q_{BC} - Q_{AC}|}{Q_{BC}} * 100 \qquad (3.7)$$

Where, Q_{BC} and Q_{AC} are the parameters measured before and after each cleaning step of the process.

5.3.3. Biofilm Thickness, Biofilm Surface Area and Biovolume

In order to measure the biofilm thickness, the biofilm surface area and the biovolume, after each cleaning step for the different enzymatic formulations, Confocal Laser Scanning Microscopy (**Chapter 3, Section 3.8.2**) was used. After collecting the biofilm thickness, the biofilm surfaced area and the biovolume data, biofilm reduction was calculated using the equation 3.6 presented above (**Chapter 3, Section 3.7.2**).

5.3.4. Polysaccharide content in biofilm using EPS Analysis

In order to evaluate the polysaccharide content of biofilm after each cleaning step for the different enzymatic formulation, the biofilm EPS was extracted by cation exchange resin (CER) and the content of the polysaccharides was measured as glucose equivalents after digestion (Romani et al., 2008), as it is well described in **Chapter 3, Section 3.8.3**. After collecting the EPS data, the biofilm reduction was calculated using the equation 3.6 presented above (**Chapter 3, Section 3.7.2**).

5.3.5. Bacteria Viability using Flow Cytometry

In order to measure the bacteria viability, after each cleaning step for the different enzymatic formulation, Flow Cytometry (**Chapter 3, Section 3.8.4**) was used to obtain the number of live and dead bacteria and the viability of biofilm bacteria was evaluated. After

collecting the EPS data, the biofilm reduction was calculated using the equation 3.6 presented above (**Chapter 3, Section 3.7.2**).

5.3.6. Biofilm morphology

The biofilm morphology was characterized using scanning electron microscopy (**Chapter 3, Section 3.8.5**). The biofilm samples were tested qualitatively 1) before any cleaning application, 2) after the application of the enzymes and 3) after disinfection**.**

5.3.7. Data Analysis

The data analysis was performed using analysis of variance (ANOVA) in combination with Tukey's Honestly Significant Differences data comparison system. The one-way ANOVA was used in all analyses to test whether there were significant differences in the data between each treatment and at each cleaning step (enzymatic cleaning and disinfection step) for both surfaces.

5.4. Results

5.4.1. Bacterial Viability measured by Flow Cytometry

Before any cleaning application no significant differences were observed between treatments ($p>0.05$) for bacterial viability (**Table 5.1**), but initial values of LIVE/DEAD cells were higher for PET (2.89 in average) than for SS grown biofilms (0.68 in average) (**Figure 5.1**). After enzymatic cleaning and the disinfection step, all enzymatic formulations, A, B and

C caused a significant reduction in bacterial viability ($p<0.05$) when compared with the control that depended on the enzyme formulation and the substrate (**Table 5.1, Figure 5.1**). Formulations A and C significantly reduced the bacterial viability in biofilms grown on SS (82.9% and 73.5% reduction effectiveness in average, for A and C respectively), while formulations B and C reduced 25% of bacterial viability and formulation A reduced 82.6% of bacterial viability for biofilms grown on PET (**Table 5.2, Fig. 5.1**). Differences between treatments after disinfection were the same as those observed after enzymatic cleaning (**Table 5.2, Fig. 5.1**). The most effective formulation for both surfaces, that caused a clear reduction of the bacterial viability over cleaning, was formulation A that contained all three enzymes evaluated in this study, amylase-protease-lipase. Over the first step of enzymatic cleaning for polyethylene terephthalate surfaces, amylase-lipase (C) and amylase-protease (B) combinations caused similar effects on the bacterial viability, while after the disinfection step the formulation C had a bigger effect on the bacterial viability than formulation B. On the contrary, on stainless steel surfaces, the presence of protease (B) and lipase (C) showed a more distinct cleaning behaviour, with the latter being clearly more effective (**Table 5.2, Fig. 5.1)**.

Table 5.1. Effects of enzymatic cleaning and disinfection treatments on bacterial viability. Significance (probability, p) after one-way Anova analyses is indicated. All contrasts of the A, B, and C treatments with the Control were significant ($p<0.0001$, not shown). Three replicates were measured at three different spots.

Surface	Parameter	Contrast	Enzymatic Cleaning	Disinfection
SS	Bacteria Viability	A vs B	**<0.0001**	**0.000**
		B vs C	**<0.0001**	**0.001**
		C vs A	0.268	0.079
PET		A vs B	**0.039**	**0.001**
		B vs C	**0.047**	**0.004**
		C vs A	0.987	0.205

Table 5.2. Effects of cleaning with enzymatic detergent and disinfection treatments on bacteria viability and on EPS-polysaccharide content. Effectiveness of biofilm reduction ($E_{f,}$ %) is indicated. Three replicates were measured at three different spots.

Surface	Parameter	Formulation	Enzymatic cleaning (%)	Disinfection (%)
SS	Bacteria Viability	Control	10.6	17.4
		A	82.9	92.1
		B	14.4	27.9
		C	73.5	82.0
PET		Control	8.6	16.9
		A	82.6	90.8
		B	26.8	36.1
		C	34.6	63.7

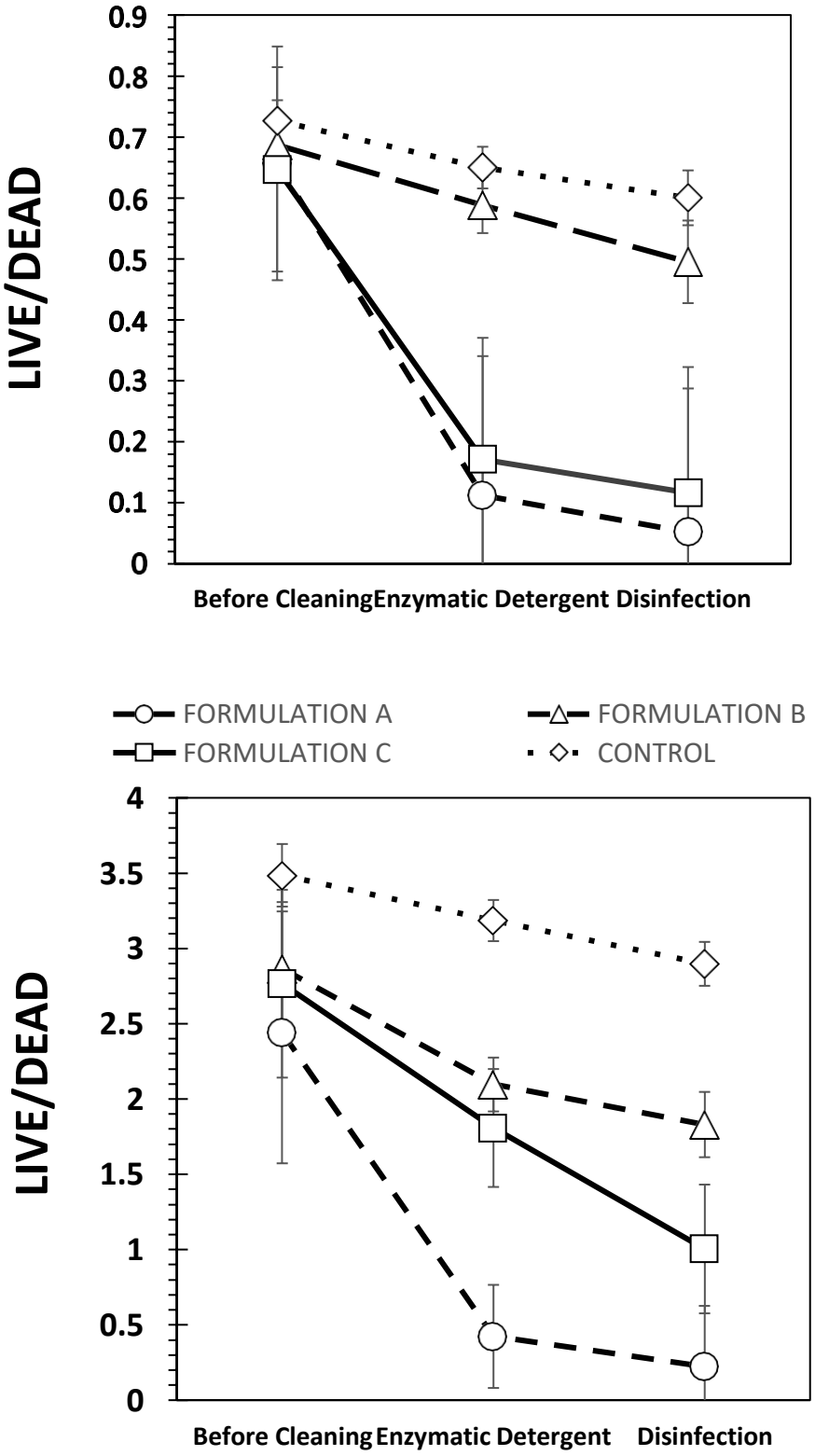

Figure 5.1: Bacterial viability measured by flow cytometry as a ratio of LIVE/DEAD bacteria/cm^2 during cleaning steps on (up) stainless steel (SS) and (down) polyethylene terephthalate surfaces (PET).

5.4.2. Polysaccharide content in biofilm EPS

The EPS-polysaccharide content showed no significant differences between treatments before cleaning ($p>0.05$) and biofilms grown on both surfaces had similar contents (4.02μg/cm^2 and 3.81μg/cm^2 in average for SS and PET, respectively). Similarly to the bacterial viability data, formulation A caused the most significant EPS-polysaccharide reduction (**Table 5.3, Fig.5.2**)**.** For biofilms grown on SS, the three formulations had a similar effect on EPS-polysaccharide content, reducing around 45% and 50% after enzymatic cleaning and disinfection, respectively (**Table 5.4, Fig. 5.2**). For SS surfaces there were no significant differences between enzymatic treatments A, B and C (Tukey's test, $p>0.05$) but all three were significantly different from the control ($p<0.05$) (**Table 5.3**). For biofilms grown on PET, the EPS-polysaccharide content was significantly reduced (81%) after enzymatic cleaning with formulation A, the EPS content being significantly different in A to that in B and control treatments (Anova, $p<0.05$, Table 5.3, Fig. 5.2). After disinfection, EPS reduction slightly increased in A (up to 96%) and also occurred in C (61.4%) and the EPS content was significantly different between the three enzymatic treatments ($p<0.05$) and also different form the control treatment (**Table 5.3, Table 5.4, Figure 5.2**).

Table 5.3. Effects of enzymatic cleaning and disinfection treatments on bacterial viability and EPS-polysaccharide content. Significance (probability, p) after one-way Anova analyses is indicated. All contrasts of the A, B, and C treatments with the Control were significant ($p<0.0001$, not shown).

Surface	Parameter	Contrast	Enzymatic Cleaning	Disinfection
SS	EPS-polysaccharide content	A vs B	0.103	0.795
		B vs C	0.147	0.952
		C vs A	0.957	0.932
PET		A vs B	**0.011**	**0.032**
		B vs C	0.308	**0.001**
		C vs A	0.071	**0.001**

Table 5.4. Effects of cleaning with enzymatic detergent and disinfection treatments on bacteria viability and on EPS-polysaccharide content. Effectiveness of biofilm reduction (E_f, %) is indicated.

Surface	Parameter	Formulation	Enzymatic cleaning (%)	Disinfection (%)
SS	EPS-polysaccharide content	Control	4.4	8.7
		A	45.0	55.9
		B	43.6	51.2
		C	41.0	43.9
PET		Control	4.4	8.8
		A	81.2	96.0
		B	7.2	10.7
		C	31.8	61.4

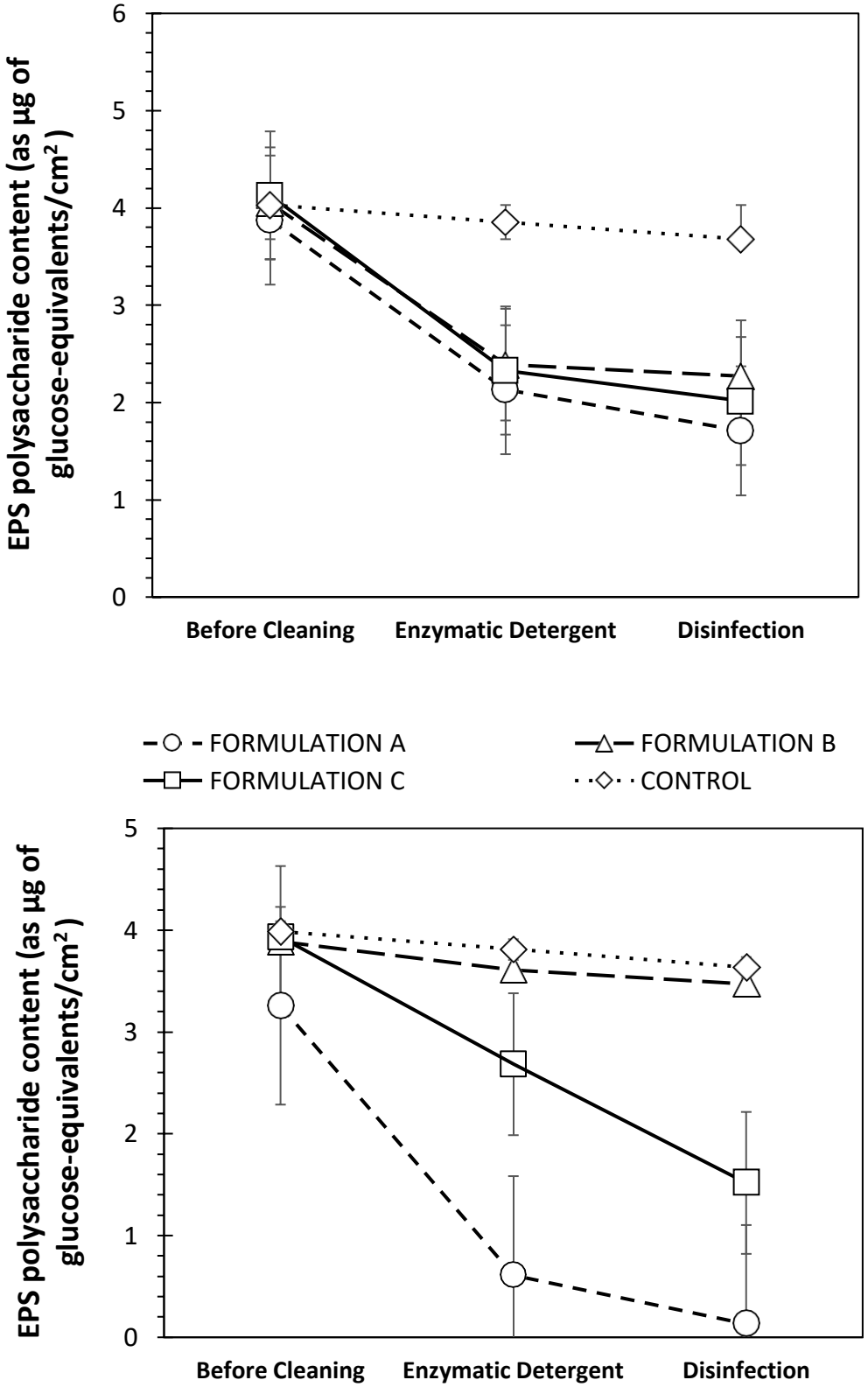

Figure 5.2: EPS polysaccharide content (as µg of glucose-equivalents/cm^2) during cleaning on a) stainless steel (SS) and b) polyethylene terephthalate surfaces (PET).

5.4.3. Biovolume, Biofilm Surface Area & Biofilm Thickness

Prior to any cleaning application, CLSM images showed that both surfaces were covered with biofilm and that the biofilm grown on polyethylene terephthalate tended to be thicker (46.4μm in average) compared to stainless steel (32.5μm in average) (**Table 5.5, Fig. 5.3a & Fig. 5.4a**). In the presence of all three enzymes amylase-protease-lipase (formulation A) a distinct deformation of the biofilm structure was observed on both substrates (biofilm thickness after cleaning, 20.1μm for SS and 25.9μm for PET), (**Table 5.5, Fig. 5.3d & Fig. 5.4d)**, while the formulation containing amylase-protease (B) was not that effective (biofilm thickness after cleaning, 28.6μm for SS and 36μm for PET), (**Table 5.5, Fig. 5.3f & Fig. 5.4f**) and the one, containing amylase-lipase (C), had a greater effect on biofilm removal on stainless steel (24.4μm) than on polyethylene terephthalate (33.6μm) (**Table 5.5, Fig. 5.3h & Fig.5.4h**). Furthermore, it was observed that the synergetic effect of all three enzymes (formulation A) had a significant effect in the viability of bacteria for both surfaces (**Fig. 5.3d & Fig. 5.4d**), a result that is in agreement with the observations from the flow cytometry data (**Table 5.2, Fig. 5.1**).

Table 5.5. Effects of cleaning with enzymatic detergent and disinfection treatments on biofilm average thickness. Three replicates have been studied at three different points

	Formulation	Before Cleaning (μm)	Enzymatic cleaning (μm)	Disinfection (μm)
SS	Control	35.8±5.4	30.9±2.9	27.3±5.1
	A	27.3±3.2	20.1±3.4	16.4±2.4
	B	30.9±3.4	28.6±5.1	20.3±4.1
	C	35.8±3.4	24.4±3.1	15.1±3.0
	Average	**32.5±3.9**	**26±3.6**	**19.8±3.7**
PET	Control	49.8±7.4	40.8±6.4	35.0±5.0
	A	49.8±6.8	25.9±4.3	24.2±4.2
	B	40.8±5.2	36.0±4.9	31.2±4.8
	C	45.0±6.4	33.6±5.0	25.3±3.7
	Average	**46.4±6.5**	**34.0±5.2**	**28.9±4.4**

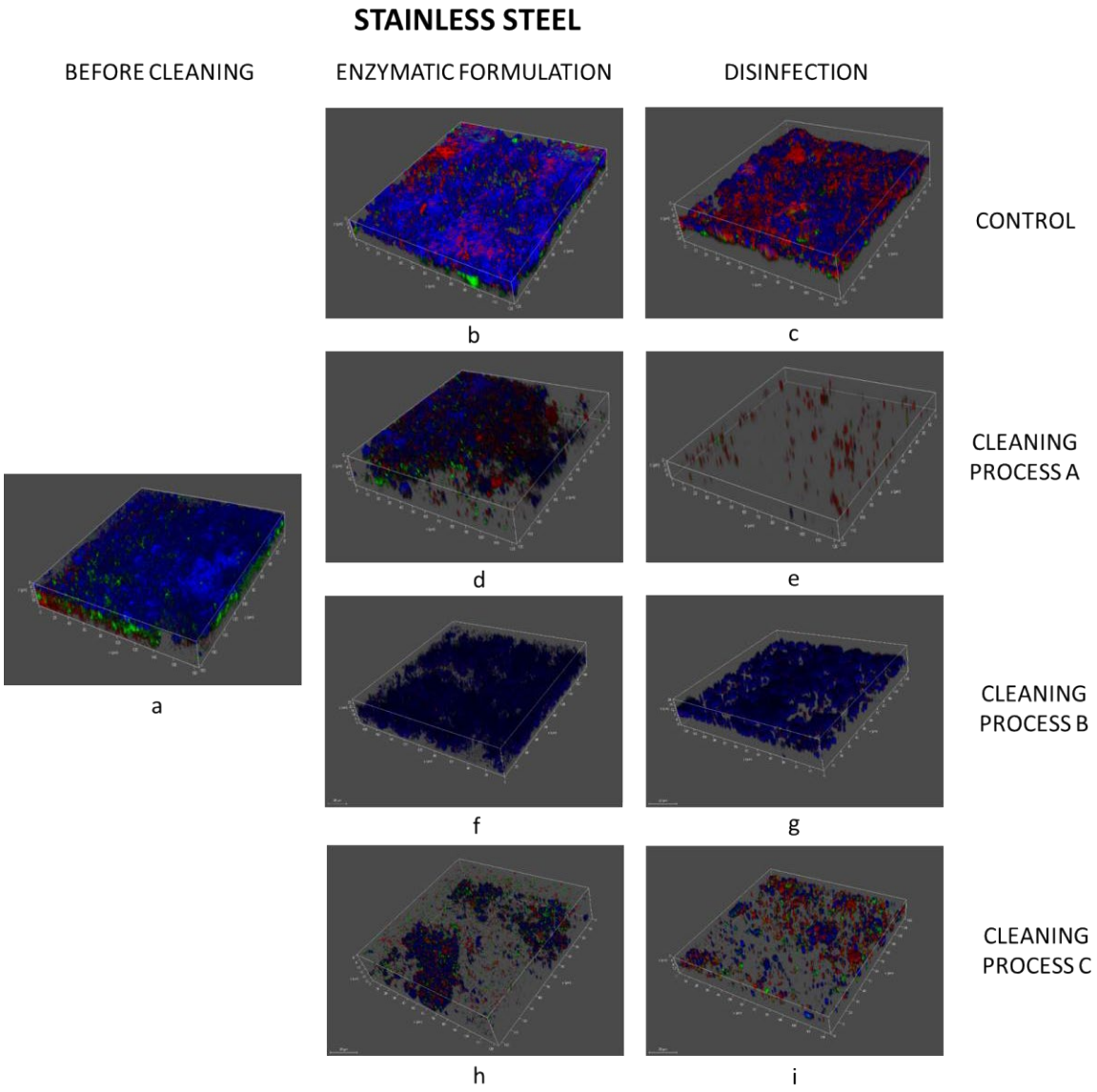

Figure 5.3: Confocal laser scanning microscopy images of the effect of different enzymatic formulations and the following disinfection step on 25-days-old biofilm grown on stainless steel surface coupons. a) before cleaning, b) control, c) control after the following disinfection step, d) formulation A, e) formulation A after the following disinfection step, f) formulation B, g) formulation B after the following disinfection step, h) formulation C and i) formulation C after the following disinfection step. Blue colour represents EPS-polymers (stained with HCS CellMask™ Blue Stain 1%w/w), green colour live bacteria (SYTO, 1%w/w) and red colour dead bacteria (stained with PI, 1%w/w).

After the disinfection step, the biofilm that was treated with the control formulation remained intact with only a part of dead bacteria (**red colour Fig. 5.3c & Fig.5.4c**) existing on the outer EPS matrix for SS, while in the case of PET not all the live biofilm bacteria were deactivated. On the contrary, for surfaces that had been cleaned using the combination of the three enzymes (formulation A) a significant reduction of biofilm was observed after the disinfection step for both surfaces and especially for stainless steel, the majority of the biomass assemblies had been removed from the substrate (**Table 5.5, Fig.5.3e & Fig.5.4e**). Interestingly, the enzymatic formulation that contained amylase-lipase (C) was also proved effective, as although the biomass was not completely removed the majority of bacteria appeared to be dead (**Table 5.5, Fig.5.3i & Fig.5.4i**). Finally, the formulation containing amylase-protease (B) was the least effective as a very small portion of the biofilm was either removed or deactivated (**Table 5.5, Figure 5.3g & Fig.5.4g**).

When comparing the biofilm cleaning behaviour between the two surfaces it seems that stainless steel showed better results than PET in all cases (**Figure 5.3 & Figure 5.4**). On PET surface coupons thicker biofilm was initially grown (**Table 5.5**) and regardless from the cleaning method the biofilm was harder to be removed (**Table 5.5**) or, in agreement with flow cytometry data, deactivated in comparison to stainless steel (**Figure 5.1 & Figure 5.4**). Especially in the cleaning process B on PET coupons little or no effect was observed (**Figure 5.4f and 5.4g**).

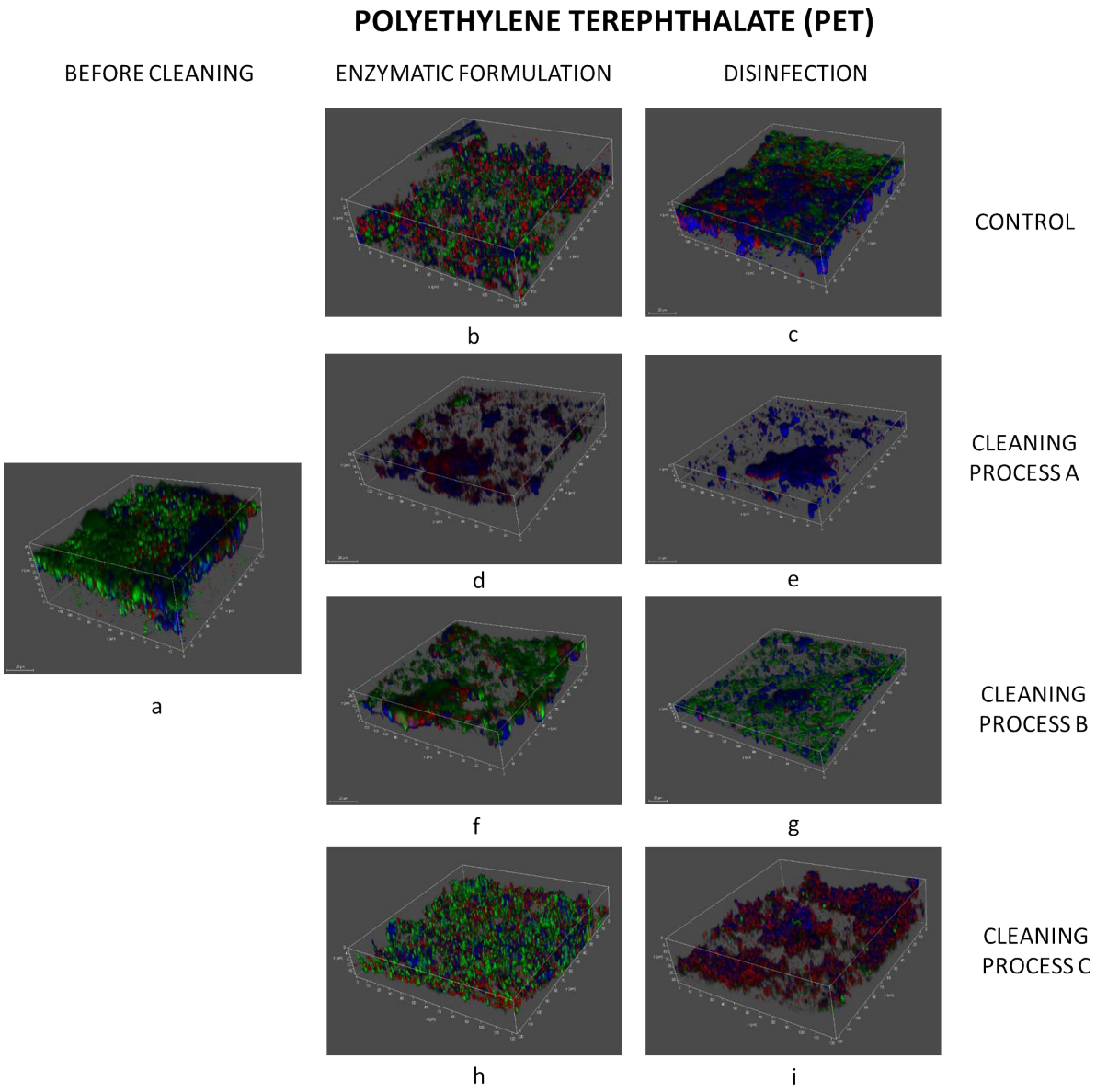

Figure 5.4: Confocal laser scanning microscopy images of the effect of different enzymatic formulations and the following disinfection step on 25-days-old biofilm grown on polyethylene terephthalate (PET) surface coupons. a) before cleaning, b) control, c) control after the following disinfection step, d) formulation A, e) formulation A after the following disinfection step, f) formulation B, g) formulation B after the following disinfection step, h) formulation C and i) formulation C after the following disinfection step. Blue colour represents EPS-polymers (stained with HCS CellMask™ Blue Stain 1%w/w), green colour live bacteria (SYTO, 1%w/w) and red colour dead bacteria (stained with PI, 1%w/w).

Biovolume and biofilm surface area were considerably reduced during the cleaning but reduction differed depending on the enzymatic treatments and surface (**Figure 5.5**). In stainless steel grown biofilms, biovolume was lowest in those cleaned by enzymatic formulations A and B before the disinfection step. However, after the disinfection step the biovolume also decreased in coupons treated with formulation C (**Figure 5.5**). This resulted in 77.1, 59.2 and 66% biovolume reduction effectiveness in average, for A, B and C respectively after the enzymatic formulations (**Figure 5.6**). Thus, for biofilms grown on SS biovolume was significantly reduced in A and C formulations. For biofilms grown on PET, cleaning with formulation B reduced biovolume by 21.8% while formulation A and C significantly reduced 80.2% and 49.5% respectively of biovolume (**Figure 5.6**). Differences between treatments after disinfection were the same as those observed after enzymatic cleaning in all cases (**Table 5.5, Fig. 5.5**).

Similarly, biofilm surface coverage was significantly reduced in formulations A and C, and especially in the SS surfaces (39.2% and 58.0% effectiveness in average for A and C), reaching an effectiveness of 87.5% and 80.5% for A and C after the disinfection step (**Figure 5.6**). As described in **Chapter 3, Section 3.8.2 (p.68)**, the biofilm surface coverage data depend on the average biomass thickness and, though in some cases the total biovolume was clearly reduced during the cleaning process, the covered surface area did not change significantly. For example, for polyethylene terephthalate surfaces cleaned using amylase-protease (B) showed a lower percentage of covered surface area than those cleaned with amylase-lipase (C); however, the biovolume values were higher (**Figure 5.5**). Thus, as expected, they had also higher average thickness than those cleaned with formulation C (**Table 5.5**). Consequently, the effectiveness of cleaning for the same surface was different for the biovolume and the covered surface area data.

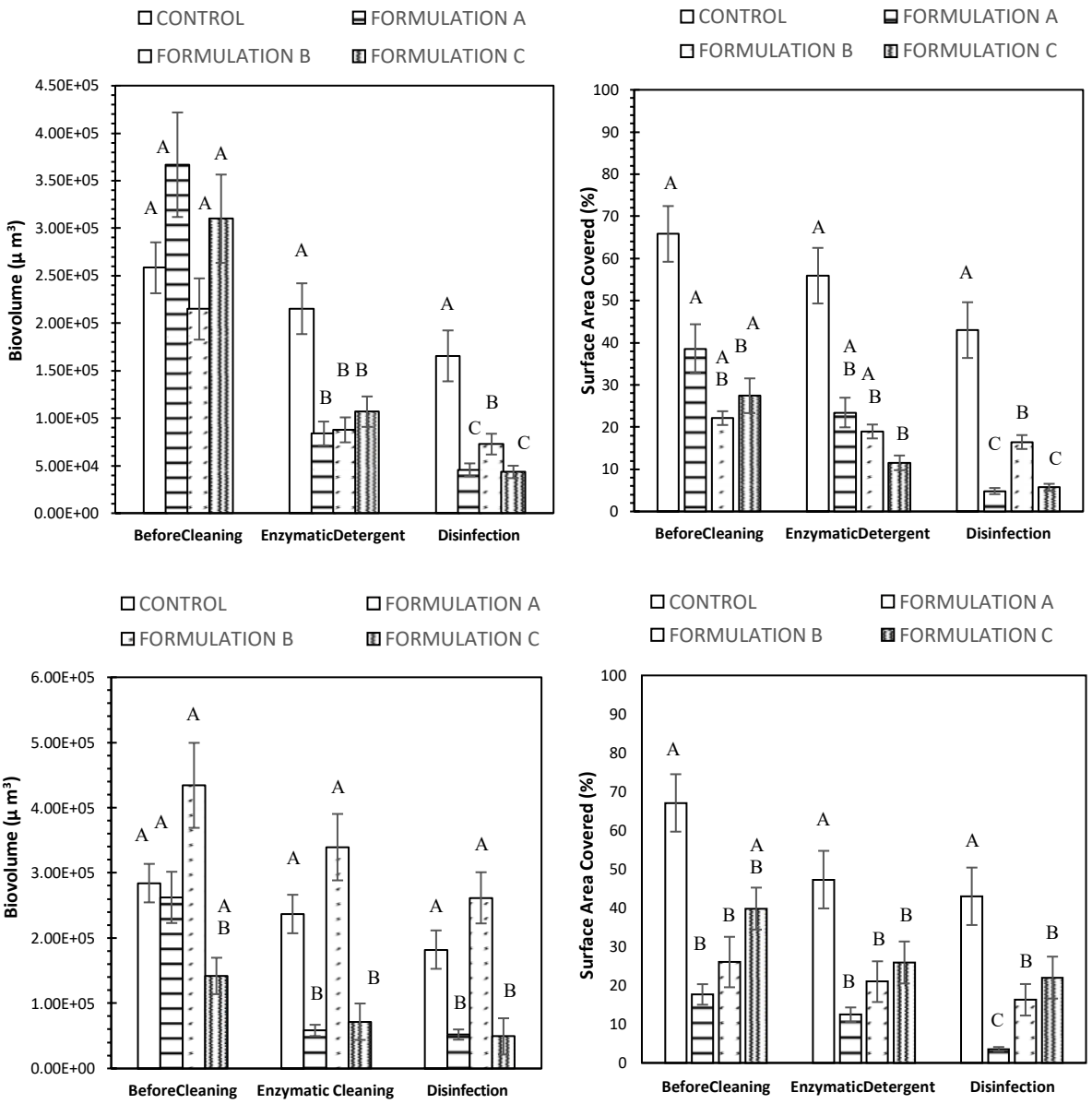

Figure 5.5: Biovolume (μm^3) and the surface area covered (%) by biofilm during enzymatic cleaning with the different enzymatic formulations and after the disinfection step for up) stainless steel (SS) and down) polyethylene terephthalate (PET) surfaces. Capital letters indicate statistically significant different groups at each cleaning step (Tukey's test, $p<0.05$). The same letter indicates no significant difference, i.e., A‡A: no significant difference, one similar letter indicates partial difference, i.e., A‡AB: slightly different and different letter indicates significant difference, while the furthest from control letter A, the most significant the difference, i.e., A‡B: significant difference and A‡C: more significant difference.

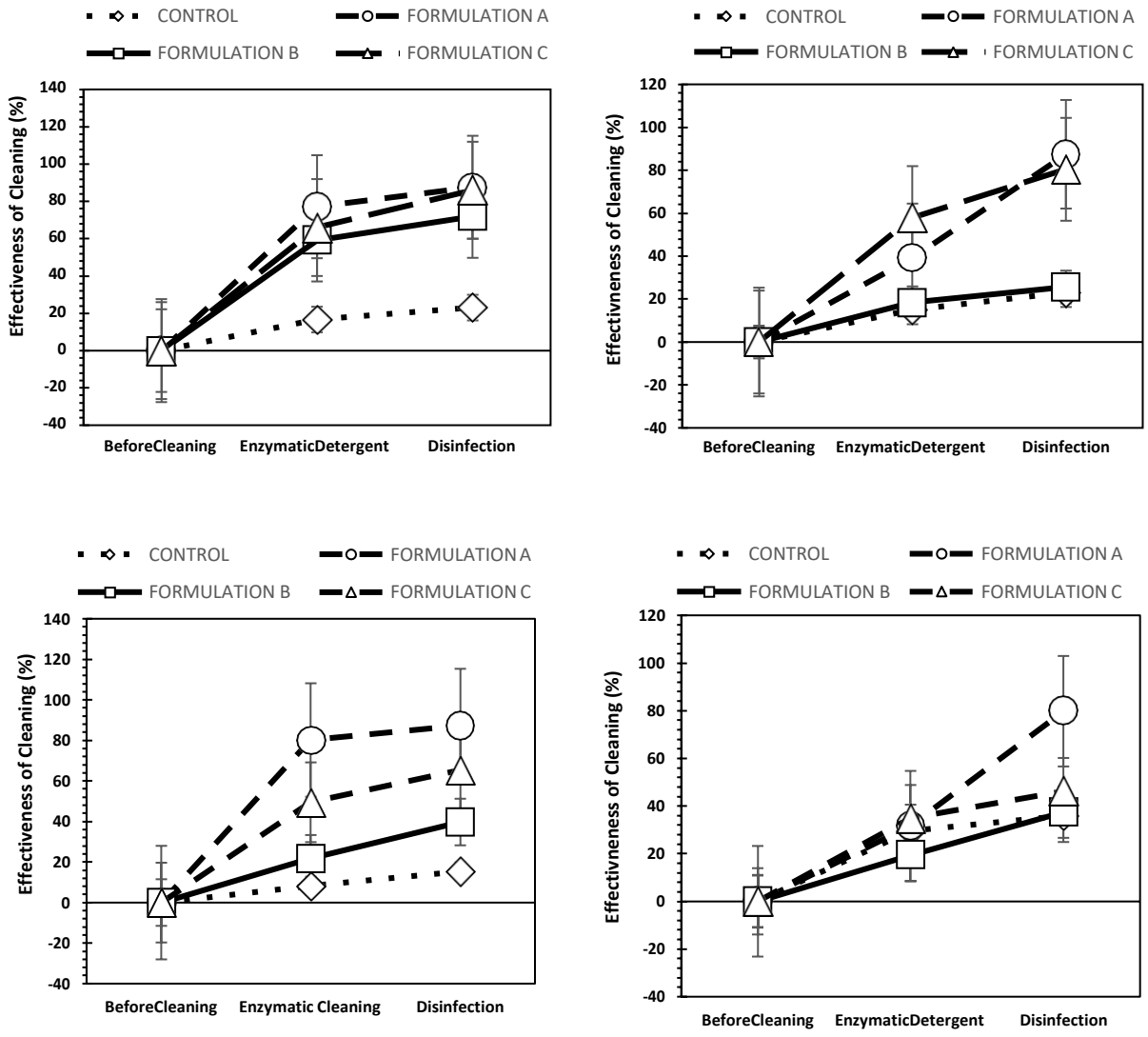

Figure 5.6: Effectiveness of cleaning (%) calculated from data for the biovolume and the surface area covered (%) by biofilm during enzymatic cleaning (i) with the different enzymatic formulations and (ii) after the disinfection step for up) stainless steel (SS) and down) polyethylene terephthalate (PET) surfaces. Capital letters indicate statistically significant different groups at each cleaning step (Tukey's test, $p<0.05$). The same letter indicates no significant difference, i.e., A‡A: no significant difference, one similar letter indicates partial difference, i.e., A‡AB: slightly different and different letter indicates significant difference, while the furthest from control letter A, the most significant the difference, i.e., A‡B: significant difference and A‡C: more significant difference.

5.4.4. Biofilm structure on different artificial substrates

The biofilm structure was investigated using SEM and a distinct difference was observed in the biofilm geometry between the stainless steel and the polyethylene terephthalate substrates (**Figure 5.7**). On stainless steel the biofilm formed ring-shaped structures with diameter of 6-7μm, whilst on polyethylene terephthalate the EPS created a random network of organic compounds where bacteria were attached. In addition, the microbial biofilm was composed by bacteria of different shape and size that, along with the EPS organic compounds, formed small and large aggregates on both surfaces.

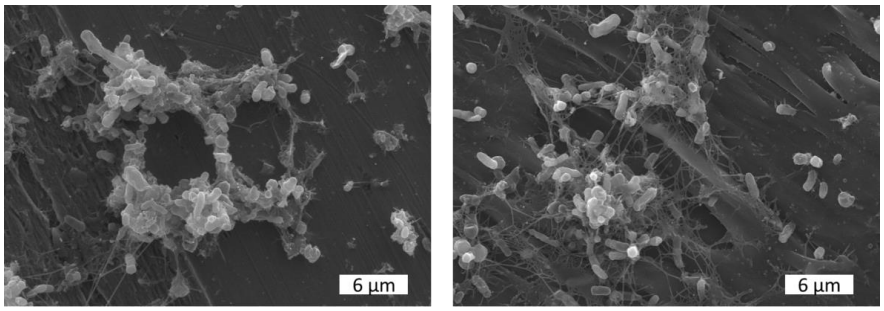

Figure 5.7: Scanning electron microscopy images of 25-days-old biofilm grown on a) stainless steel b) and polyethylene terephthalate surface coupons before cleaning.

Next, similarly to the previous analyses, the effect of different enzymatic formulations, A, B and C on stainless steel and polyethylene terephthalate coupons was studied (**Figure 5.8**). In the first step of the cleaning with amylase-protease-lipase (Formulation A), a distinct disruption of the biofilm structure was seen on both surfaces. It was evident that the combination of the three enzymes and the surfactants provoked the decomposition of the EPS components and spherical assemblies of biomass were formed (**Figures 5.8e and 5.8f**). Formulations containing amylase-protease (B) and amylase-lipase (C) did not change the biofilm structure in the same way as formulation A, as there was no sign of spherical assemblies (**Figures 5.8g – 5.10j**).

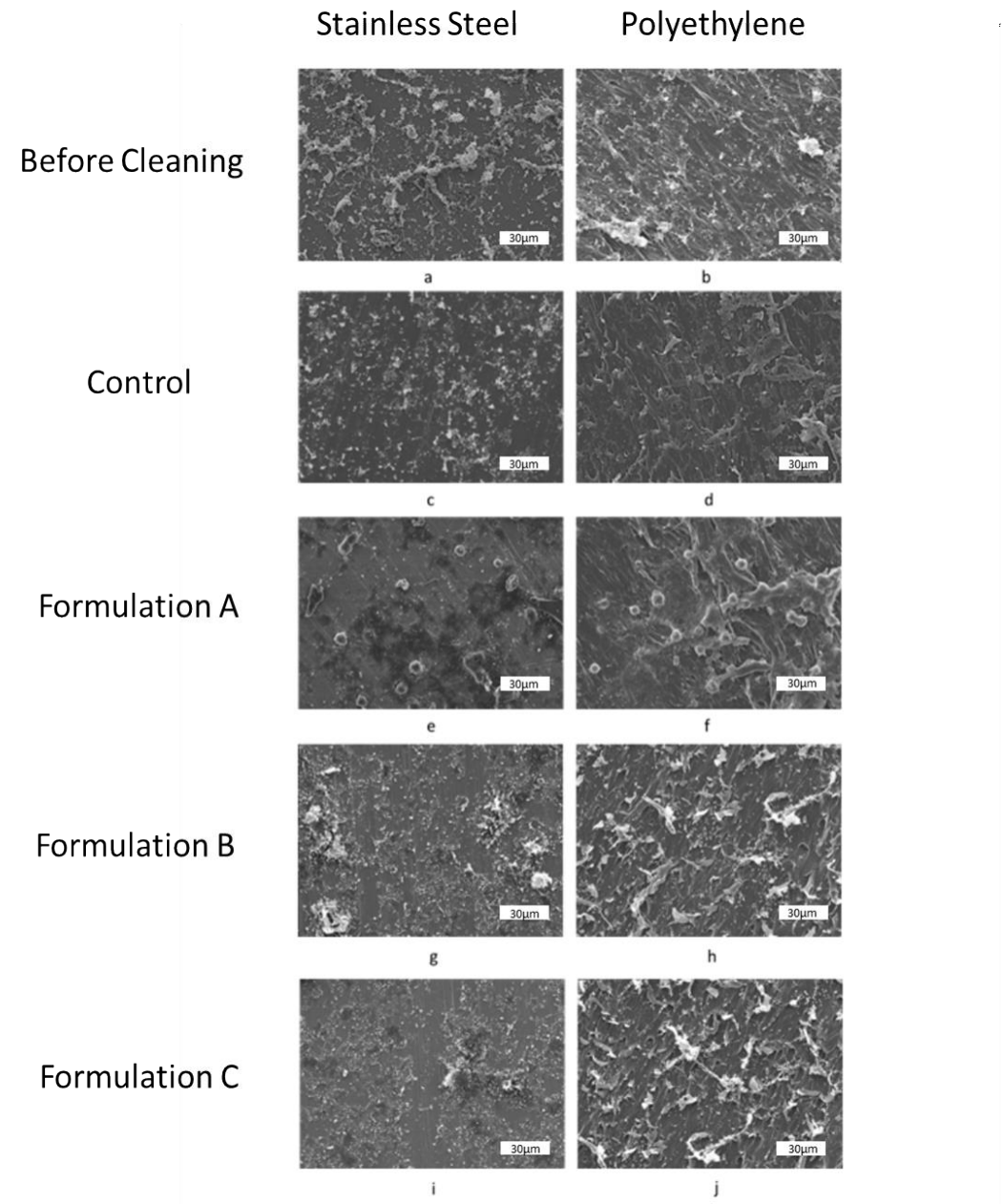

Figure 5.8: Scanning electron microscopy images of the effect of different enzymatic formulations on 25-days-old biofilm grown on stainless steel and polyethylene terephthalate (PET) surface coupons. a) stainless steel before cleaning, b) PET before cleaning, c) control on stainless steel, d) control on PET, e) formulation A on stainless steel, f) formulation A on PET, g) formulation B on stainless steel, h) formulation B on PET, i) formulation C on stainless steel and j) formulation C on PET.

After the disinfection step (**Fig. 5.9**), a significant reduction of EPS was observed on both surfaces, although on stainless steel it seemed that most of the biofilm had been removed (**Fig. 5.9e & 5.9f**). In contrast, the formulations containing amylase-protease (B) and amylase-lipase (C) respectively appeared to be less effective than formulation A, as even after the disinfection step there was a significant amount of biomass remained on both surfaces (**Fig. 5.9g – 5.9j**). It could be concluded that formulation A, containing amylase-protease-lipase was the most effective in biofilm cleaning.

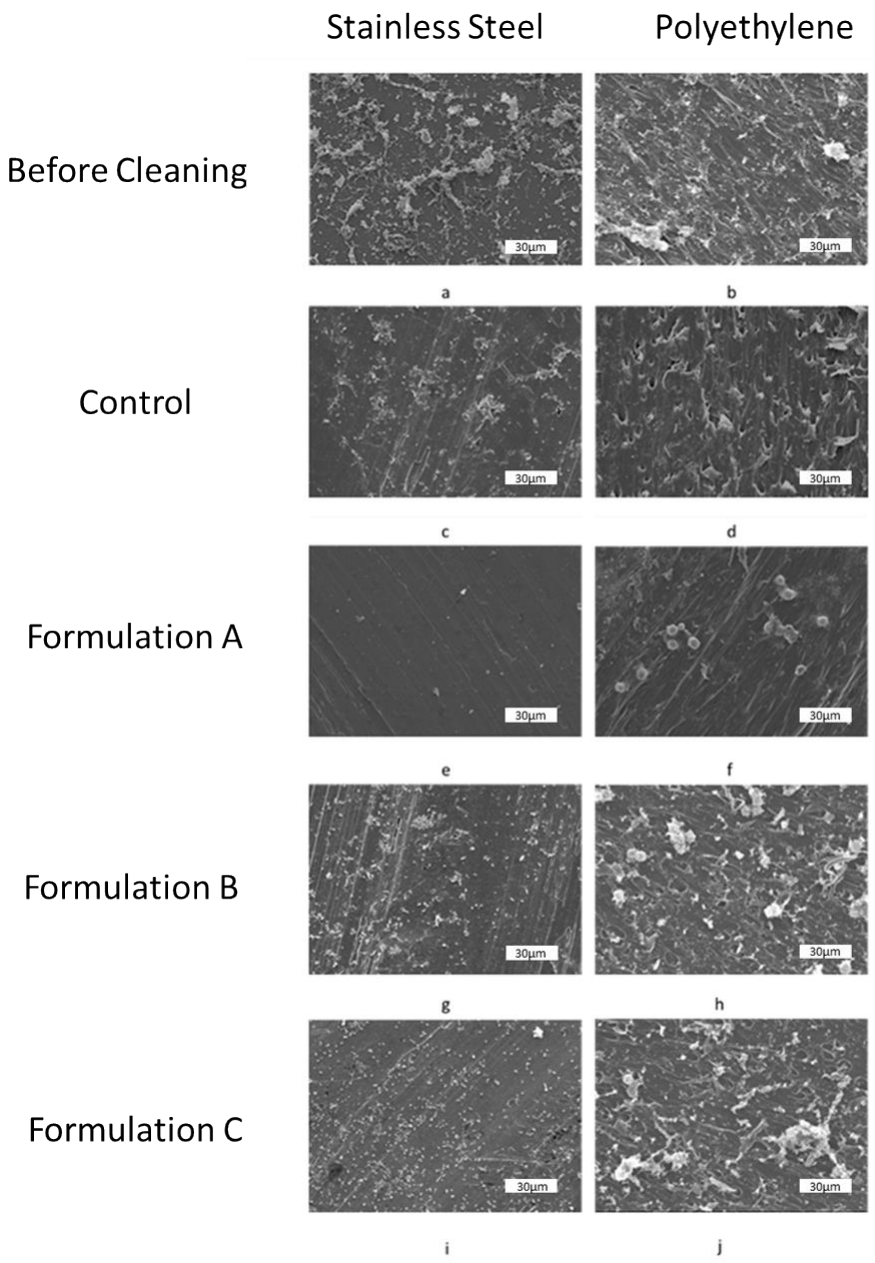

Figure 5.9: Scanning electron microscopy images of the effect of the disinfection step after cleaning with different enzymatic formulations on 25-days-old biofilm grown on stainless steel and polyethylene terephthalate (PET) surface coupons. a) stainless steel before cleaning, b) PET before cleaning, c) control – surfactants without enzymes on stainless steel, d) control – surfactants without enzymes on PET, e) amylase/lipase/protease on stainless steel, f) amylase/lipase/protease on PET, g) amylase/protease on stainless steel, h) amylase/protease on PET, i) amylase/lipase on stainless steel and j) amylase/lipase on PET.

5.5 Discussion

By forming biofilms, bacteria protect themselves from host defence, disinfectants, and antibiotics, as they are much more resistant to environmental stresses than in their planktonic forms (Stoodley et al., 2013; Dincer et al. 2020). The key difference between planktonic bacteria and biofilms is the extracellular polymeric substance, widely referred as EPS and also known as glycocalyx (Harriot et al., 2019). Biofilm EPS, occupying approximately 90% of the biofilm, confers a physical barrier containing numerous ionic molecules such as proteins, glycoproteins, and glycolipid that can bind charged antimicrobial agents and provide shelter for microorganisms. that limit the transportation of antimicrobial substances (Stoodley et al., 2013; Dincer et al., 2020). Biofilm control is of great concern for various sectors, like the food industry, where day-to-day cleaning with common chemicals is not always efficient for biofilm elimination and knowing the biofilm EPS composition is key in order to choose the appropriate agent for its removal (Molobela et al., 2010). Detergent enzymes developed for the detergent industry are countermeasures against strong chemicals that might be dangerous for the food industry, for example Novozymes' Everlase®. Furthermore, enzymes can be given useful properties for example improved heat stability, higher activity at low temperatures, and reduced dependency on cofactors such as calcium (www.novozymes.com, Enzymes at work; Tsiaprazi-Stamou et al., 2019). Thus, enzymes like protease and amylase, have gained attention as alternative agents that could destroy the EPS matrix and attack bacterial cells (Vickery, 2004; Xavier et al., 2005; Lindsay and Holy, 2006; Walker et al., 2007; Galié et al., 2018; Tsiaprazi-Stamou et al., 2019). Moreover, in a study of Kiran et al. (2014) it was suggested that lipases were between 90% and 95% effective in biofilm destruction and, hence, protease, amylase and lipase were chosen in this study as the enzymes of interest against a mixed-microbial biofilm obtained from a meat packaging

process line.

In all, it was observed that enzymes were highly efficient in biofilm cleaning and that the synergistic effect of all enzymes was essential for the most complete deformation of the biofilm structure and consequently the better disinfection of the surface. Formulation A, containing all three enzymes, caused the higher reduction in all the parameters studied, biovolume, surface coverage, bacterial viability and polysaccharide content in the biofilm. It is believed that the combination of the three enzymes weakened the adhesive and cohesive forces of the EPS organic compounds and removed the biofilm from the surfaces more efficiently than the other two formulations that were missing the enzymes of lipase (formulation B) and protease (formulation C) respectively. As reported by Flemming et al. (2007), an increasing number of components have been identified in EPS, but many are yet to be identified and information about their localization and stability is not well known. Also, regardless of the bacteria species, the EPS composition will depend on the medium that the biofilm is grown, a feature that makes them widely unpredictable (Molobela et al., 2010). The mechanism by which enzymes destroy the physical integrity of the EPS is through weakening the adhesion proteins, carbohydrate and lipid making up the structures of the EPS through the degradation process (Molobela et al., 2010; Harriot et al., 2019). Furthermore, it was suggested by Lequette at al., (2014) that a combination of enzymes targeting several components of EPS, surfactants, dispersing and chelating agents would be an efficient alternative to chemical cleaning agents. It is thus believed that the efficiency of formulation A that contained all three enzymes, amylase-protease-lipase, may be due to the broad-spectrum activity in degrading a variety of EPS compounds.

The fact that the least efficient agent was formulation B, containing amylase and

protease, to an extent conflicts with the literature where protease has been widely studied and proved many times the most effective enzyme in biofilm cleaning (Vickery, 2004; Walker et al., 2007; Lequette et al., 2010; Molobela et al., 2010). However, these studies were focused on single species bacterial biofilms, whereas here the effectiveness of enzymatic cleaning was studied against a mixed-microbial biofilm. Additionally, Donlan (2002) indicated that biofilm EPS may be hydrophilic or hydrophobic depending on its structural components, which are mostly polysaccharides and proteins, followed by lipids, DNA etc. (Sutherland, 2001; Czaczykand Myszka, 2007; Flemming et al, 2007; Flemming et al., 2016). Consequently, it was expected that amylase, which is degrading polysaccharides, and protease, which can degrade proteins (Molobela et al., 2010), would be the most effective enzymes against biofilm EPS. In this case, it was shown that the presence of lipase in the enzymatic formulations A and C was decisive in biofilm deformation and subsequently better disinfection as shown by the biovolume and the bacterial viability reduction in Figures 5.5 and 5.1 It is thus believed that the stereochemistry of the polysaccharides, the proteins and the lipids in the EPS biomass, played a crucial role in the cohesive strength developed in their structure and, consequently, their decomposition by the appropriate enzymes. Results suggest that the complex chemistry and elegant three-dimensional structure of the EPS may necessarily need the combination of enzymes with distinct targets and that especially some lipids may play a key structural role (Harriot et al., 2019).

When comparing the two material surfaces, it was initially observed that the biofilm structure was different. On stainless steel, the biofilm was thinner while the biofilm grown on polyethylene terephthalate showed greater bacterial viability and increased biovolume, and both of them had similar biofilm surface area covered and EPS-polysaccharide content.

Moreover, in terms of different cleaning behaviour, it was shown that stainless steel was cleaned more successfully than polyethylene terephthalate. It is thought that the increased biovolume and average biomass thickness on polyethylene terephthalate surfaces compared to stainless steel played an important role in their difference in cleaning efficacy. In addition, the higher bacterial viability that was observed on polyethylene terephthalate might have aided the stronger attachment of the bacteria on the surfaces, which lead to the reduced cleanability of the surface. As mentioned in the literature, it is believed that this distinct contrast between the two surfaces is caused by the variation on their physicochemical properties, i.e., their roughness, chemical composition and surface energy that affects their fouling activity, initial biofilm structure and, hence, determines their cleanability (Fletcher and Loeb 1979; Detry et al., 2007; Detry et al., 2010; Yin et al., 2016; Don et al., 2021). Surface energy, otherwise known as work of adhesion, is one of the parameters believed to play a key role in biofilm adhesion (Katsikogianni and Missirlis, 2004), as biofilm tends to grow on substrates that have surface energy close to its own (Detry et al., 2010).

The different cleaning behaviour of the three formulations on polyethylene terephthalate surfaces against polysaccharide reduction was unexpected, as all three formulations contained the same concentration of amylase and surfactants. Results suggest that the physical chemistry of the interfaces between the surface, the surfactants and the enzymes in the formulations might have played a significant role in biofilm cleaning. In this study, the hydrophobicity/hydrophilicity of the biofilm, the enzymatic detergent and the material surface, was not specifically analysed. However, measuring the hydrophobicity/hydrophilicity of the interfaces involved might work as a useful tool in improving the biofilm cleaning process, as it is important to understand the phenomena that occur on the interfaces between the biofilm, the cleaning agent and the material surface, a

multidimensional problem that needs to take into account several parameters.

Moreover, it was confirmed that the disinfection process was relevant for the final cleaning of the surfaces, as, although most reduction occurred due to the enzymatic cleaning, there was a further biofilm elimination between the enzymatic cleaning and the disinfection step as especially shown by the biovolume and surface coverage results. Finally, yet importantly, from the biovolume and biofilm surface area parameters, it was observed that the disinfection process was not competent without the initial enzymatic cleaning (control treatment), which is another indication that the presence of the enzymes was responsible for breaking the organic compounds of the EPS and made bacteria more vulnerable against the disinfectant in the second step of cleaning.

5.6 Conclusions

The microscopic observation of changes in biofilm structure using SEM and confocal analyses indicated that enzymes were very effective in biofilm removal, especially on stainless steel surfaces. It was observed that the combination of enzymes was more efficient than formulations based in a single enzyme regardless of surfaces (stainless steel and polyethylene terephthalate). The treatment with formulation combining amylase, protease and lipase, effectively decreased the total biofilm mass, the bacteria viability and the polysaccharide content in the biofilm. Moreover, it was observed that surfaces differed in initial biofilm growth and this needs to be considered in consequent different cleaning patterns.

This chapter was dedicated to the evaluation of the cleaning method developed and described in Chapter 4 in a real-case scenario. The mixed-microbial biofilm sample was collected from an everyday industrial surface and was tested for its cleaning behavior using commercially available agents. The next goal was to investigate the phenomenon of biofilm attachment and removal as an effect of the physicochemical forces developed between the biofilm-substrate interphase.

CHAPTER 6: THE EFFECTIVENESS OF BIOFILM CLEANING AS A RELATION TO BIOFILM EPS-DERIVED FORCES

6.1. Summary

Previous chapters have shown that the biofilm cleaning between various surfaces can show a different behaviour as biofilm can adhere to the different surfaces in different ways through EPS. EPS is generally comprised of soluble, gel-forming polysaccharides, proteins and eDNA, as well as insoluble components such as amyloids, cellulose, fimbriae, pili and flagella - so we need to understand the forces between EPS and surfaces. Furthermore, surface modification can play a significant role in the prevention of biofilm adhesion and consequently the achievement of more effective cleaning. Last but not least, the different environment conditions are expected to change the adhesion forces between the biofilm and the surfaces. For this reason, the goal of this study was to measure directly the adhesion and cohesion forces that are developed between biofilms and surfaces while in air or under simulations of cleaning conditions like water and different pH solutions. The method for measuring forces at this level, developed at the university of Birmingham by Zhang et al at (1992) is the micromanipulation method. However, as it was difficult to study biofilm EPS under this system due to accuracy limitations of the optical monitoring, an alternative for biofilms was chosen to be studied instead. Thus, alginic acid, a polysaccharide that has been found in the *Pseudomonas aeruginosa* biofilms (Gordon et al., 2017) was chosen as an alternative material. Several polymers were studied as material for polycarbonate surface modification under two different pH conditions (3 and 11) and the adhesion and cohesion forces of alginic acid were measured under air, water, NaOH and HCl solutions.

6.2. Introduction

As discussed in previous Chapters, microorganisms can live and proliferate as planktonic cells or they can attach to surfaces, where they grow as highly organized multicellular communities, known as biofilms (Otto, 2008). In biofilms, planktonic bacteria are embedded in self-produced matrix of extracellular polymeric substances (EPS) that promote surface adhesion (Gordon et al. 2017) and give biofilms consistency and resistance to antibiotics and disinfectants (Katsikogianni and Missirlis, 2004; Flemming et al., 2016). This extracellular matrix, also known as glycocalyx, is the hallmark of biofilm communities. The mature biofilm is a complex and elegant three-dimensional structure consists of proteins, glycoproteins, and glycolipid that can bind charged antimicrobial agents and provide shelter for microorganisms (Harriott M., 2019; Dincer et al., 2020). In some types of bacteria like *Pseudomonas aeruginosa*, their honeycomb 3D structure EPS (Stoodley et al., 2013) contains Pel, Psl polysaccharides and alginate or alginic acid (Gordon et al., 2017), materials that have been found both to stimulate biofilm formation and provide the mature biofilm with mechanical stability (Nahar et al., 2018). Alginic acid is a binary copolymer of 1,4-linked α-L-guluronic acid (G) and β-D mannuronic acid (M) that is present in the EPS that surrounds several bacteria species such as the genus of *Pseudomonas* (Grządka and Matusiak, 2017). It is an anionic polysaccharide that possesses carboxyl, ether and hydroxyl groups and it appears to be a material of interest when it comes to biofilms.

Biofilm formation affects many aspects of public health and industrial processes (Johansen et al. 1997; Palmer et al., 2007; Goode et al., 2013), by forming human pathogens that can grow on substrates, such as stainless steel, polyethylene, wood, glass, polypropylene, rubber, etc. (Kohila et al., 2013; Abdallah et al., 2014; Colagiorgi et al., 2017). Goode et al. (2013) review and classify biofilm deposits in food processing, where cleanliness is of great

importance, and consider the effectiveness of cleaning essential. Several studies focus on evaluating the effectiveness of cleaning biofilm from stainless steel surfaces of different geometries, from piping elements to plates (Faille et al., 2013; Li et al., 2017; Bénézech & Faille, 2018). The general outcome of those studies was that the parameters that affect the efficacy of any cleaning procedure are the flow velocity of the surfactant-based solution, the wall shear stress that is developed by flow, the effect of temperature, time and parameters like the pH of the solution (Goode et al., 2013). Chapter 5 has shown the efficacy of enzymes against biofilm cleaning from hard stainless steel and polyethylene terephthalate surfaces (published as Tsiaprazi-Stamou et al., 2019). The results of Chapter 5 indicated that the combination of the different enzymes as well as the material surfaces played a key role in the cleaning performance. Therefore, the detachment of biofilms from a surface is a multidimensional problem that is governed by the physical and chemical forces that appear in the interfaces.

To understand the phenomena that result in biofilm detachment it is essential to study the problem from its initial step and focus on biofilm attachment followed by proliferation - also known as biofilm adhesion. Understanding the adhesion and cohesion forces within biofilms, especially those needed to distort their structure and clean them from the surfaces, is essential for the development of anti-biofouling precautions and effective cleaning strategies. To our knowledge there are no studies devoted to surface cleanability from biofilms in relation to their adhesive and cohesive strength.

A key factor for biofilm detachment and thus playing a role when defining cleaning systems is its attachment strength to the solid surface where it develops (Donlan, 2002). The physicochemical properties of surfaces and bacteria are important to the biofilm

interface and hence its response to cleaning. Microorganisms are reported to attach more rapidly to hydrophobic, nonpolar surfaces such as Teflon and other plastics than to hydrophilic materials such as glass or metals (Fletcher and Loeb, 1979; Boonaert et al., 2002; Bayoudh et al., 2005; Guillemot et al., 2006; Detry et al., 2010). However, Flint et al. (2000) reported that bacteria of *Streptococcus thermophilus* (H) and *Streptococcus waiu* (sp. nov) would adhere more easily to hydrophilic substrates, while Parkar et al. (2001) showed that bacterial adhesion and surface energy showed no correlation on stainless steel although surface energy may influence the adhesive strength of cells and bacteria. Consequently, interfacial phenomena between biofilms and the surface might be important in the choice of the appropriate cleaning agent (Detry et al., 2010), although any relationship made between bacterial adhesion and surface energy must thus be considered with caution as there is no clear correlation found in literature (Boonaert et al., 2002; Achinas, Charalampogiannis and Euverink, 2019). Even though results might be similar it is very difficult to draw a conclusion and compare the materials used in relation to their surface characteristics, as many parameters like the bacteria strain, the biofilm growth stage and the age of the surface.

Cationic polymers with quaternary ammonium groups have been investigated and are considered to have high antibacterial activity (Beyth et al., 2012; Nelson et al., 2017; Pal et al., 2018). The antibacterial action of these materials relies on their positive charge (Nelson et al., 2017) that can interact with the negatively charged groups in the bacterial membrane and cause a disinfectant effect. Beyth et al. (2012) found that a structure – activity relationship of the polymers creates antibacterial surfaces, with a combination of long, positively charged and moderately hydrophobic polymeric chains. Furthermore, the length of the polymeric chain enhances the attraction of the positive charge towards the bacteria and amplifies any bacteriostatic activity (Pal et al., 2018). Hence in this study, to prevent initial bacterial

development and attachment on artificial surfaces, a method of polymeric coating was investigated and Poly-(2-ethyl-2-oxazoline), DADMAC (high and low MW) and Lupasol were used for the chemical surface modification of polycarbonate tiles. Poly-(2-ethyl-2-oxazoline) is a high charge density cationic polymer (Lee et al., 2011) that has been studied as coating on silver and gold nanoparticles with antibacterial activity (Lee et al., 2011; Raweewan, T. and Rawiwan L., 2015) and it has also been used as a flocculating agent as well as an enzyme immobilizer agent, which has been proved to make Gram-negative bacteria permeable to hydrophobic antibiotics and to surfactants (Helander et al., 1998). DADMAC (diallylmethylammonium chloride) consists of cyclic unit and positively charged quaternary ammonium groups in individual molecules that has been investigated for its bacteriostatic properties (Pal et al., 2018).

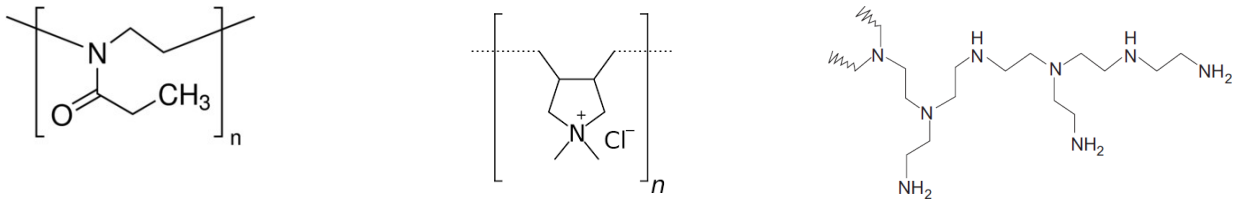

a) b) c)

Figure 6.1: Chemical structure of a) Poly-(2-ethyl-2-oxazoline), b) DADMAC and c) Lupasol

The aim of this work was to understand the phenomenon of initial biofilm growth on different material surfaces, and thus the adhesive and cohesive strength of alginic acid on several material substrates were investigated, as a replacement for biofilm. Additionally, to understand the cleaning efficacy of alginic acid from the surfaces, the effect of water, NaOH (pH 11) and HCl (pH 3) on both the adhesive and cohesive strength was studied. Surfaces of interest that are abundant in the industrial and the household environment were stainless steel, and modified and non-modified polycarbonate tiles. For the direct measurement of the adhesive

and cohesive strength of alginic acid from the so mentioned surfaces, the micromanipulation technique was used.

6.3. Materials & Methods

6.3.1. Surface Modification

Anionic (Poly-(2-ethyl-2-oxazoline) and cationic polymers (DADMAC (high and low MW) and Lupasol) were used for the chemical surface modification of rectangular polycarbonate tiles of 30mm length size and 2.9mm thickness. The polymer solutions (1%w/w) were prepared by diluting the polymers at room temperature water and left in magnetic stirring for 3 hours. The pH of the solutions was adjusted to pH 11 using NaOH solution (pH 12) and to pH 3 using HCl solution (pH 2). Different pH solutions were chosen in order to examine the solubility of the polymers and the effect they would cause on the surface properties, the adhesion and the cohesion of the alginic acid on them. The polycarbonate tiles were first sonicated for 15 minutes in ethanol solution (99%) and then for 15 minutes in distilled water. Next, the tiles were left overnight in the polymer solutions and the next day the surface characterization measurements were performed (**Figure 6.2**).

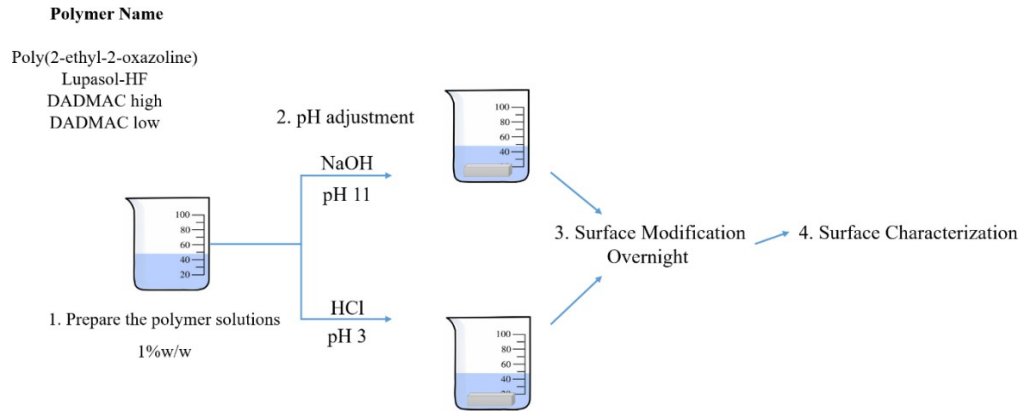

Figure 6.2: Visualization of polycarbonate tiles surface modification with polymers.

6.3.2. Water Contact Angle Measurement – Surface Energy

A theta optical tensiometer – contact angle meter was used for the measurement of the water contact angle with the surfaces and hence the calculation of the average surface energy or the work of adhesion. For the calculation of the work of adhesion of the different surfaces and the evaluation of their hydrophobicity the model of Young-Laplace for the surface tension was used. According to the Young- Laplace equation of surface tension, the higher the contact angle of water on the surface, the more hydrophobic is the surface. The work of adhesion was calculated according to the Young-Laplace equation of surface tension

$$W_a = \gamma \cdot (1 + cos\theta) \quad (6.1)$$

Where γ, is the surface tension of water at 25^oC and θ is the contact angle of the water and the surface. The work of adhesion was measured in mN/m.

6.3.3. Sample Preparation

Alginic acid (Sigma Aldrich, A2033-250G) 5% w/w was diluted in water (5%w/w) at 40ºC that had been stained with calcofluor white (1%w/w), a fluorescent blue dye that generally binds to cellulose and chitin (Sigma Aldrich, 18909). The solution was left stirring overnight, to turn as alginate gel the next morning. The next day thin films of alginate gel were developed on the surfaces of interest using a stainless steel, T-shaped probe which was mounted on a three-dimensional micromanipulator (Micro Instrument, Oxon UK) connected to an automated motor.

The micromanipulation technique was developed by Zhang et al. (1992) for measuring the mechanical strength of single cells at the University of Birmingham. This method has been developed in a number of ways to study different systems. For direct measurement of the adhesive strength of biofilm on a glass surface, a novel T-shaped probe was developed. The principle of the method at the time was to drag away a whole biofilm from the surface of the glass test stud with the probe, and measure the force needed for the removal. The adhesive strength among the attached biofilms and the surfaces is defined as the work per unit area required to remove the biofilm from the surface (Chen at al., 1998). Several measurements of adhesion and cohesion of biofilms or the measurement of their mechanical properties or single cells have been made using this method (Zhang et al., 1992; Chen at al., 1998; Chen at al., 2005).

To study the adhesive and cohesive forces within soiling layers Garrett et al. (2007) developed a modified micromanipulation device. Several studies have used the technique for the direct measurement of the adhesive and cohesive forces of fouling deposits, such as dairy soils (Liu et al., 2002; Hooper et al., 2006; Liu et al., 2007).

Thus, for the sample preparation, the gap between the bottom edge of the T-shaped probe and the surface was adjusted to 100μm using a side camera. The stainless-steel T-shaped probe was then used to pull the deposits horizontally at a constant speed of 1.0 mm/s to create samples of 100μm thickness. The deposits were immediately tested for their adhesive and cohesive properties under the different conditions: air, water, NaOH solution (1%w/w) and HCl solution (1%w/w).

6.3.4. Micromanipulation

The same micromanipulation rig used for the sample preparation was used to measure the adhesive and cohesive strength of the fouling deposit using a T-shape probe. The probe was connected to the output aperture of a transducer (Digital gauge, FHS, Sauter Germany) mounted on a three-dimensional micromanipulator (Micro Instrument, Oxon UK).

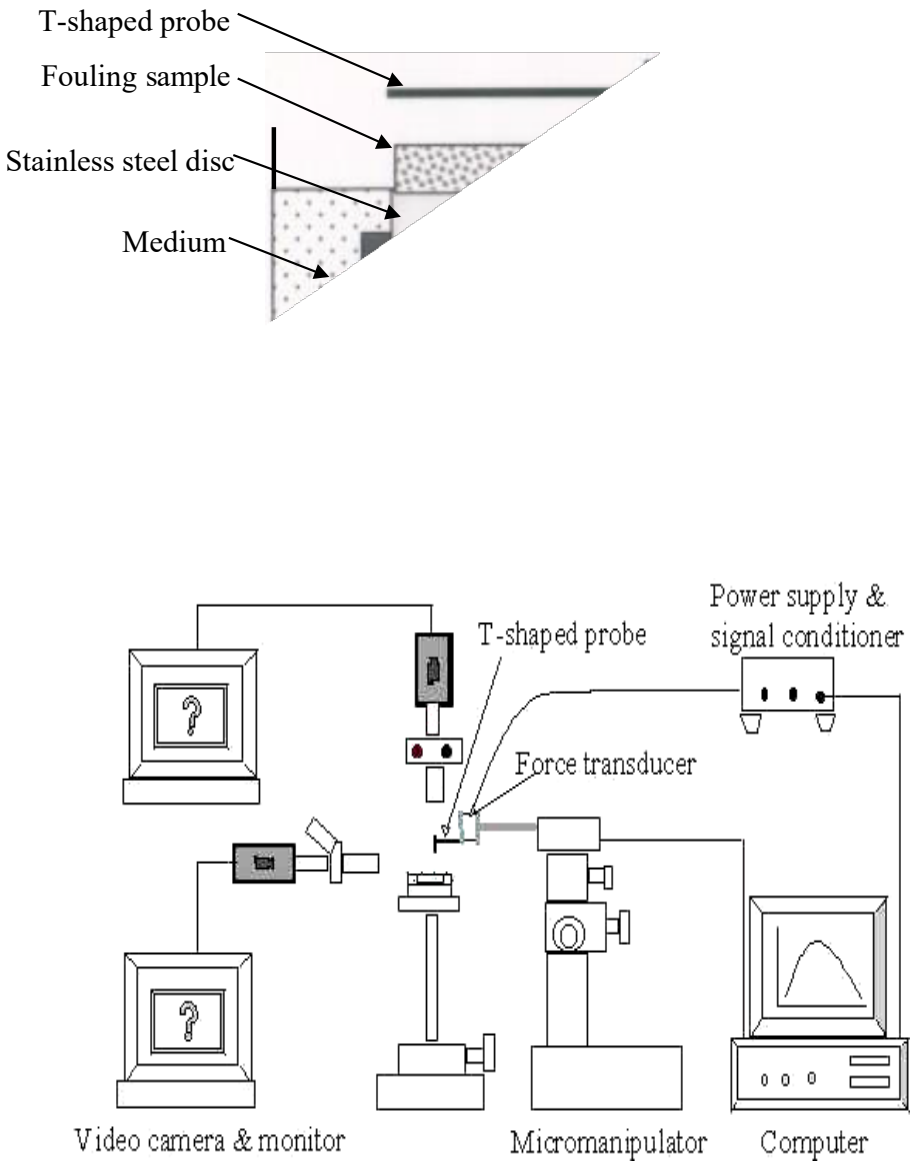

Figure 6.3: (Up) Schematic of the T-shaped probe, fouling sample and stainless-steel disc. (Down) Schematic of the Micromanipulation rig. (Taken from Liu et al., 2002).

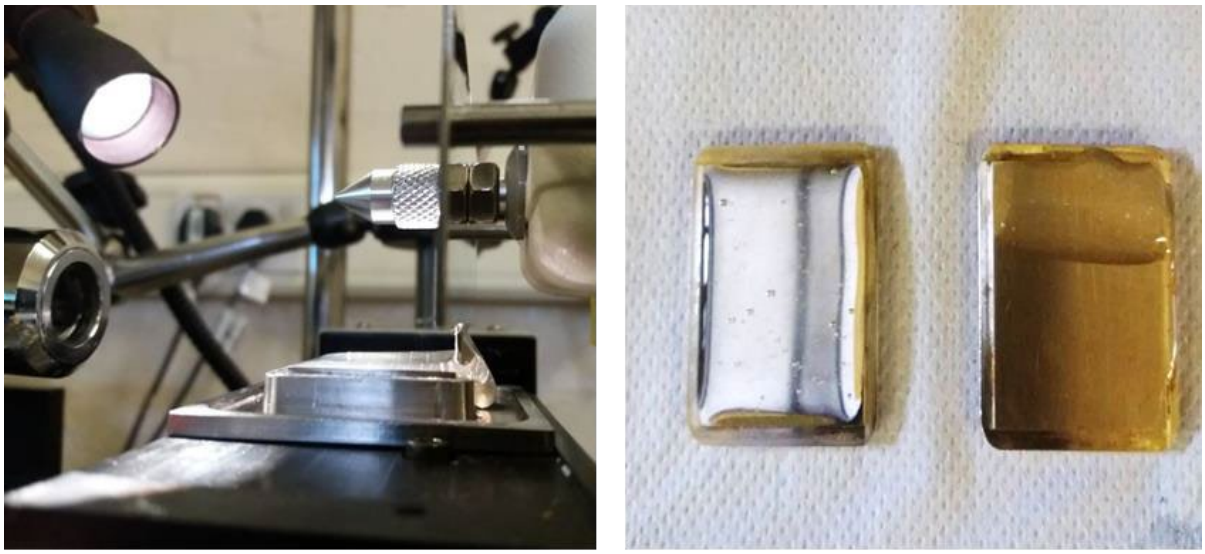

a b

Figure 6.4: a) Side view of the probe pulling the sample from the surface and b) Alginic acid on coupon surfaces before and after adhesion measurement.

After sample preparation, the adhesion and cohesion force measurements were performed under four different conditions as mentioned above, in which the alginate layer was (i) in air, (ii) submerged in water, (iii) submerged in NaOH solution (1%w/w, pH 11) and (iv) submerged in HCl solution (1%w/w, pH 3).

For cases (ii) – (iv), a rectangular vessel with stainless-steel base and glass walls was designed and developed to adjust the dimensions of the micromanipulation rig. The sample surfaces were locked to the bottom of the vessel using dual-lock tape and the vessel was mounted on the rig. Using the side camera, the T-shaped probe was adjusted to the desired height and the vessel was filled with the appropriate solution in each case (ii)-(iv). The adhesion and cohesion measurements were performed immediately after sample loading in the vessel. Two types of measurement were conducted, adhesive and cohesive strength measurements.

For *adhesive strength* measurements, the force to remove the material from the surface, i.e., leaving nothing left on the surface, the probe was adjusted in order to scrape the alginic acid from the tiles. For *cohesive strength* measurements, the force required to break the bonds between elements of the material, the probe was adjusted approximately at 50μm height over the tile. Adhesive and cohesive strength was measured in σ (J/m^2) and work of adhesion in mN/m. The ratio is 1 mN/m = 0.001 J/m^2.

The total work, W (J) done by the applied force, F(t), to remove the deposit may be calculated as the integral of

$$dW = F \cdot dx \tag{6.2}$$

Where, the distance *dx* is

$$dx = v \cdot dt \tag{6.3}$$

Where *v* is the probe velocity (m/s), so that

$$W = \frac{l}{(t_2 - t_1)} \int_{t_1}^{t_2} F dt \tag{6.4}$$

Where *l* is the length of the rectangular tile, and t_1 and t_2 the first and last times at which the probe touched the fouled surface. The apparent strength of a fouling sample, σ (J/m^2), is defined as the work required to remove the sample per unit area from the surface to which it is attached, is then given by:

$$\sigma = \frac{W}{aA} \tag{6.5}$$

Where *A* (m^2) is the tile surface area, covered by the alginate gel and *a*=1 in all our cases.

6.3.5. Data analysis

The data analysis was performed using analysis of variance (ANOVA) in combination with Tukey's Honestly Significant Differences data comparison system. The one-way ANOVA was used in all analyses to test whether there were significant differences in the data between the adhesive and cohesive strength measured under air and under each cleaning condition for all the surfaces.

6.4. Results

6.4.1. *Surface Energy*

The chemical surface modification with the polymeric solutions affected the average work of adhesion for the polycarbonate substrates (**Figure 6.5**). In general, the surface modification increased both the hydrophilicity and the average work of adhesion of the substrates for both pH conditions, pH 3 and pH 11. More specifically, under acidic conditions (pH 3) the lowest increase on the work of adhesion was shown on DADMAC of low molecular weight (5.8% increase, absolute value 99.6±8.7 mN/m) and the highest work of adhesion for Lupasol (33.9% increase, absolute value 131.4±7.6 mN/m) (**Figure 6.5**). Similarly, under basic conditions (pH 11) the polymer that caused the most significant increase on the work of adhesion was Lupasol (43.3% increase, absolute value 134.9±6.6 mN/m), while the one that had no significant effect was DADMAC of low molecular weight (12.3% increase, absolute value 105.7±8.3 mN/m) (**Figure 6.5**). Untreated polycarbonate surfaces showed the lowest work of adhesion and stainless-steel surfaces' work of adhesion was closest to the surfaces that had been modified with Poly-(2-ethyl-2-oxazoline) under acidic conditions (107.0±4.5 mN/m) and under basic conditions (112.8±4.3 mN/m) (**Figure 6.5**).

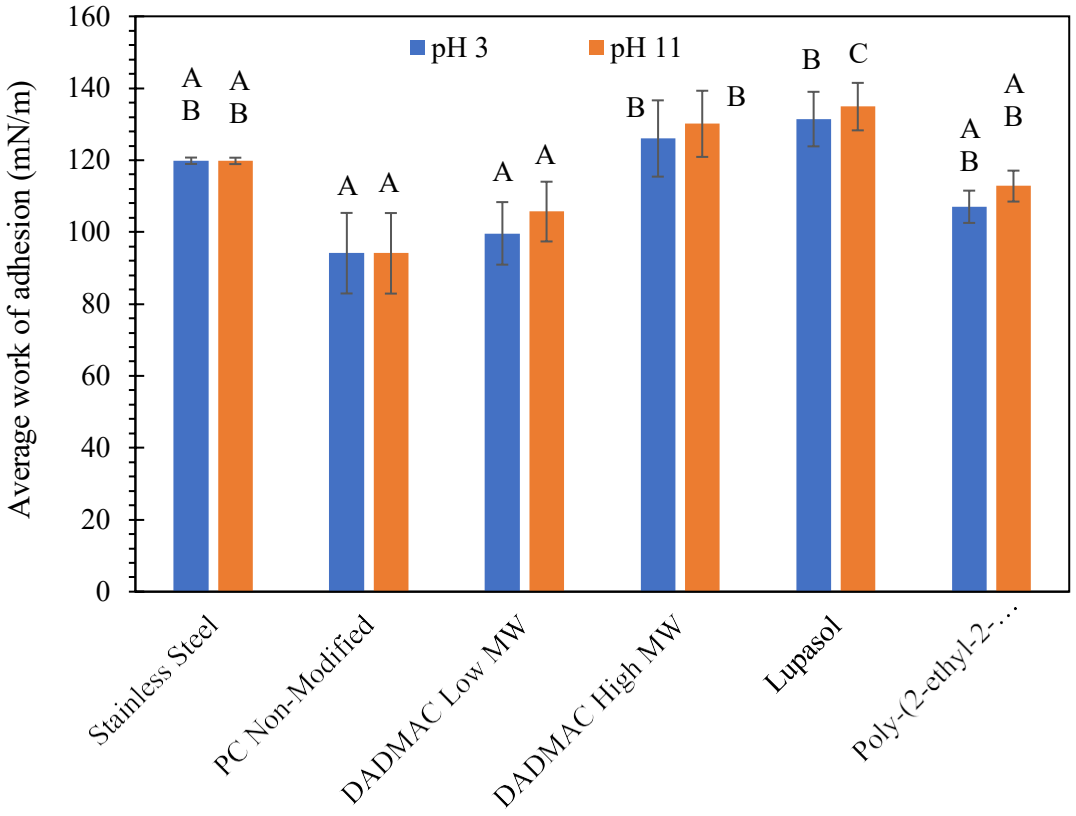

Figure 6.5: Average work of adhesion (mN/m) for modified and unmodified surfaces under different pH conditions. Three replicates were examined for each material surface at each pH condition. The error bars are the standard deviation of the triplicates work of adhesion. Capital letters indicate statistically significant different groups at each cleaning step (Tukey's test, $p<0.05$). The same letter indicates no significant difference, i.e., AłA: no significant difference, one similar letter indicates partial difference, i.e., AłAB: slightly different and different letter indicates significant difference, while the furthest from control letter A, the most significant the difference, i.e., AłB: significant difference and AłC: more significant difference.

6.4.2. Adhesive & Cohesive Strength in Air

As mentioned above, the adhesive strength is the force needed to remove the alginic acid from the surface measured in (J/m^2). The cohesive strength (J/m^2) is the force required to break the bonds between elements of the alginic acid, to cause a fracture on the deposit. For this reason, in the first case the probe was adjusted in order to touch the upper surface of the tile and scrape the deposit, leaving nothing left on the surface after the measurement. Similarly, in the second case the probe was adjusted at 50μm height above the upper surface of the tile and scrape the deposit, leaving a fraction of the deposit on the surface. The initial height of the deposit was 100μm and thus for the cohesive strength measurements the probe was set to cut in the middle of the deposit's height.

Figure 6.6 shows the adhesive and cohesive strengths for all the surfaces under air. In all surfaces of interest, the adhesive strength of alginic acid was higher than its cohesive strength under air. For the different surfaces, the adhesive strength of alginic acid was always higher for the polycarbonate tiles than for the stainless steel before any surface treatment. However, after the surface modification the adhesive strength was decreased for all polymers and at both pH values, 3 and 11 (**Fig. 6.6**). After the surface modification performed at pH 11, DADMAC (high MW), DADMAC (low MW) and Lupasol had a similar effect in the decrease of adhesive strength while Poly-(2-ethyl-2-oxazoline) caused the most significant reduction in the adhesive strength of the alginic acid (92.2±1.2 J/m^2) (**Fig. 6.6**). Equally, for the surface modification performed at pH 3, a similar decrease of the adhesive strength of alginic acid was observed, since Poly-(2-ethyl-2-oxazoline) caused the most significant reduction (98.2±0.5 J/m^2) (**Figure 6.6**).

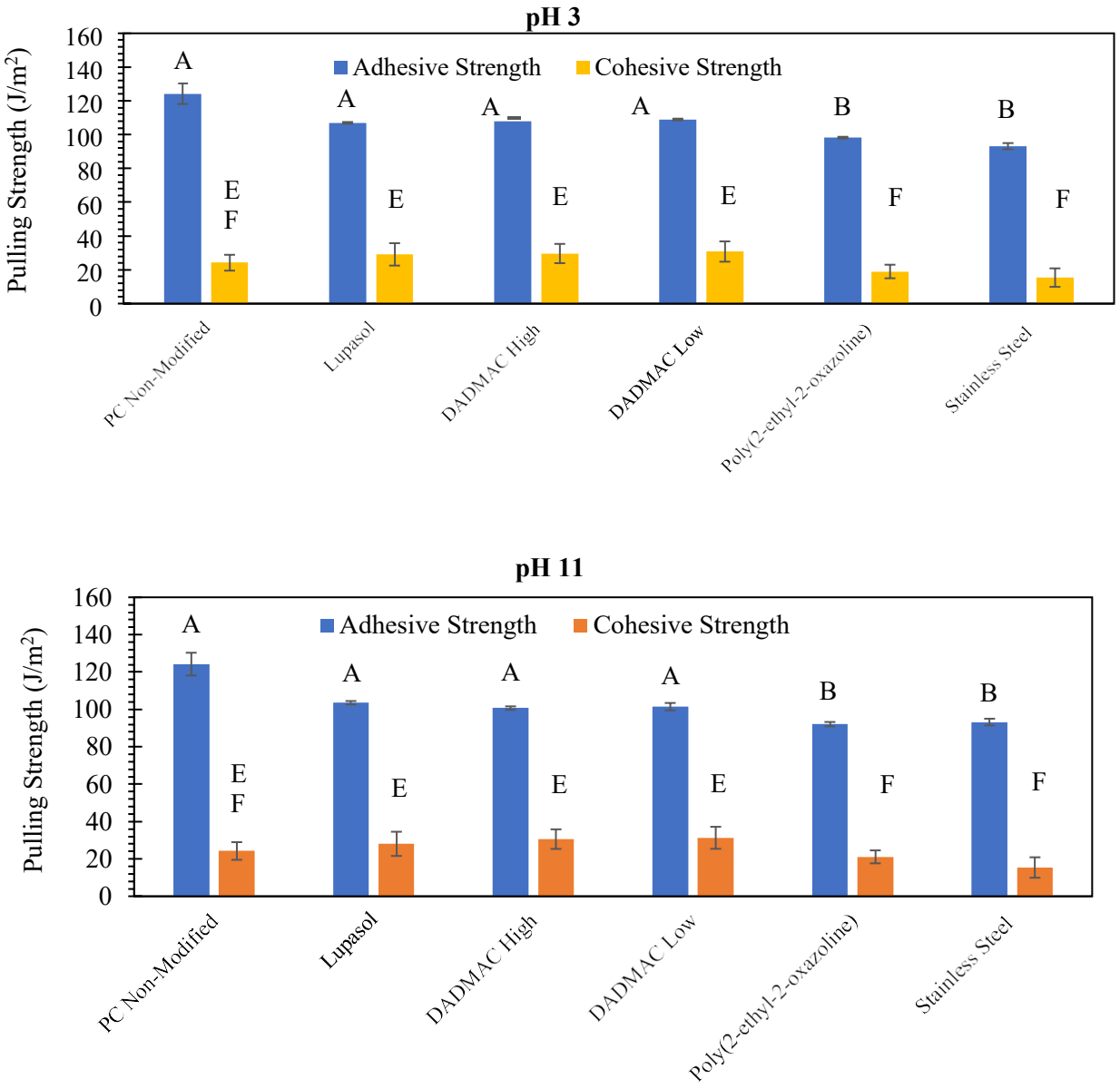

Figure 6.6: Adhesive and cohesive strength for modified and unmodified surfaces (at pH 3 and pH 11 solutions) under air. The error bars are the standard deviation of the triplicates' adhesive and cohesive strength respectively. Capital letters indicate statistically significant different groups at each cleaning step (Tukey's test, $p<0.05$). The same letter indicates no significant difference, i.e., AłA: no significant difference, one similar letter indicates partial difference, i.e., AłAB: slightly different and different letter indicates significant difference, while the furthest from control letter A, the most significant the difference, i.e., AłB: significant difference and AłC: more significant difference.

Figure 6.6 shows that in all cases the cohesive strength is significantly less than the adhesive strength. Cohesive strength might be expected to be similar for all tiles, as the system is being studied for fracture within the deposit. However, cohesive strength varied between different surfaces at both pH values ranging from 15.4 ± 5.5 J/m^2 to 31.3 ± 6.0 J/m^2 for surfaces modified at pH 11 and from 15.4 ± 5.5 J/m^2 to 30.9 ± 6.0 J/m^2 for the surface modifications that occurred at pH 3 conditions. The cohesive force is thus a factor of four less than the adhesive force in all cases. As cutting the deposit in half is a more complex technical problem than scraping the surface clean, it was felt possible that the height of the T-shape probe might not have been exactly 50μm in all experiments.

To identify possible reasons for the measured different probe results, it was decided to compare the alginic mass removed by the T-Shape probe on the cohesive strength measurements under different probe heights. For this reason, additional experiments were performed as described: The tile was weighed before the experiment (W_B), and then the T-shape probe was adjusted between 10μm-90μm over the upper surface of the tile. The probe then passed over the surface and the cohesive strength was measured in air. The tile was then weighed after the measurement (W_A). In that way the mass scraped away on the probe could be calculated easily (W_P).

$$W_P = W_B - W_A \tag{6.6}$$

It was seen that as the mass remaining on the probe, W_P, increased the cohesive strength also increased (**Figure 6.7a**). Figure 6.7b shows the average cohesive force measured on stainless steel as a function of the probe height over the surface. It is observed that as the cut height decreases the measured cohesive strength is increased, as a result of the force being measured being the sum of the breakage of deposit-deposit bonds and the subsequent dragging

of the deposit off the surface onto the probe. At a height of 50 μm, a change in the height of ca. 10 μm makes a change of about 10 J/m^2 in the measured cohesive strength. Thus, it is believed that the accuracy limit of the probe height caused the significant difference that was observed in the previous measurements. This demonstrates the limitations of the micromanipulation rig at this scale – an alternative was designed but was not completed within the time available for the thesis, and is discussed in Chapter 7.

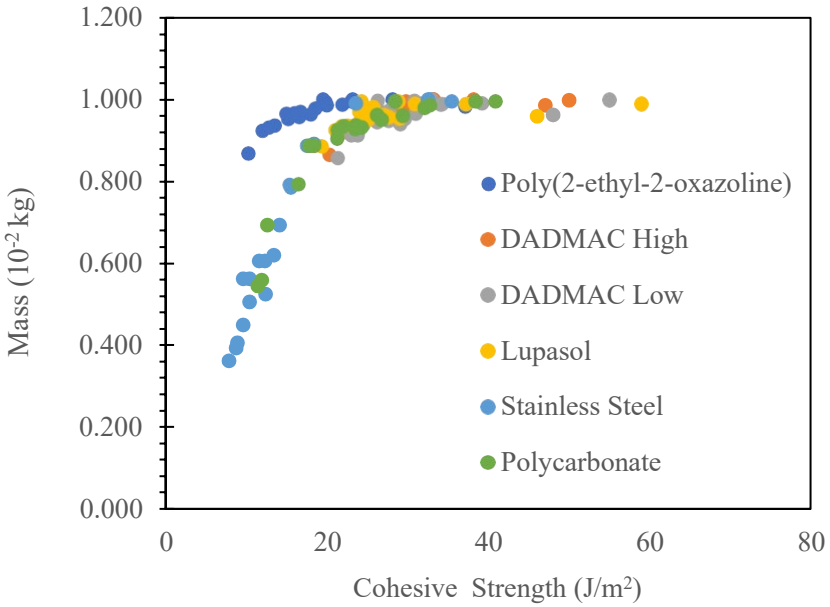

a

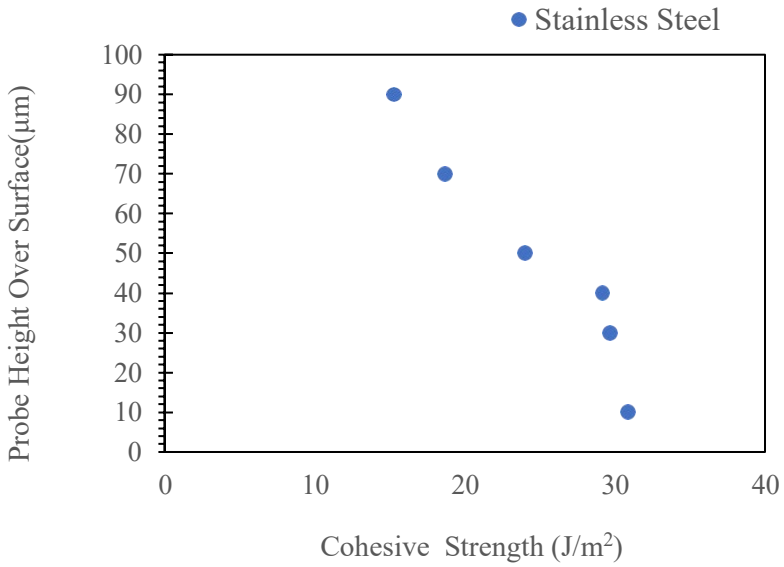

b

Figure 6.7: a) Cohesive strength (J/m^2) of alginic acid measured on all surfaces of interest as a function of the weight of deposit left on the probe (10^{-2}kg). b) Cohesive strength (J/m^2) of alginic acid measured on stainless steel as a function of the probe height over the surface (µm).

6.4.3. Adhesive & Cohesive Strength in Water

Both the adhesive and the cohesive strength of alginic acid for water and NaOH solutions significantly decreased on all surfaces (**Table 6.1, Figure 6.8**). Moreover, in the case of water conditions, no significant difference was observed among the surfaces for either the adhesive or the cohesive strength. In contrast, under NaOH solution of pH 11 it was observed that two polymers, Lupasol and Poly-(2-ethyl-2-oxazoline) caused a significant decrease in the adhesive strength of alginic acid from 11.6±0.5 J/m^2 to 1.8±0.2 J/m^2 and 3.1±0.2 J/m^2 respectively (**Figure 6.8**). As with water, the cohesive strength of alginic acid under NaOH solution did not show any significant difference between the surfaces of interest (**Table 6.1**). It is believed that there was a swelling noticed in the alginic acid during its immersion to NaOH. The experiment did not intend to identify the effects of water over NaOH in the morphology of the alginic acid, though it would be an interesting next step if the setup of the micromanipulation could be upgraded with a high-definition microscopic camera.

Similarly, in the case of surfaces that were chemically modified at pH 3, the adhesive and cohesive strength of the alginic acid decreased under both water and HCl solutions (**Table 6.1, Figure 6.8**). The effect of the adhesive and the cohesive strength under water was the same and no significant difference was observed between the surfaces of interest (**Table 6.1, Figure 6.8**). However, under HCl solution for surfaces that had been modified under pH 3 conditions, it was observed during the experiment that the physical properties of the alginic acid immediately changed, as it became more dense and rigid. Consequently, it was seen that the cohesive strength of the alginic acid increased and the adhesive strength decreased for all surfaces (**Table 6.1, Figure 6.8**). Finally yet importantly, similarly to the case of water as expected, the cohesive strength of alginic acid under HCl solution showed no significant difference between the surfaces studied as it varies between 33.6±0.5 J/m^2 and 35.9±0.5 J/m^2

for the surfaces studied (**Table 6.1)**. It is believed that the highly acidic environment had an immediate effect in the alginic acid dehydration, yet again it would be interesting as a next step to actually collect microscopic data of the effect of water, NaOH and HCl on the alginic acid.

Table 6.1: Cohesive strength for unmodified, modified surfaces (prepared at pH 11) under water, and NaOH solutions (1%w/w) and modified surfaces (prepared at pH 3) under water, and HCl solutions (1%w/w). Three replicates were examined for each material surface at each pH condition. The error bars are the standard deviation of the triplicates' adhesive and cohesive strength respectively.

Surfaces	**Cohesive Strength (J/m^2) (Surfaces modified at pH 3)**		**Cohesive Strength (J/m^2) (Surfaces modified at pH 11)**	
	Water	HCl	**Water**	**NaOH**
Stainless Steel	4.5±0.1	34.8±0.6	4.5±0.1	2.4±0.2
PC Non-Modified	4.8±0.3	35.9±0.5	4.8±0.3	2.4±0.1
DADMAC Low MW	4.4±0.1	34.5±0.6	3.7±0.3	2.4±0.2
DADMAC High MW	4.4±0.1	33.9±0.6	3.7±0.4	2.4±0.1
Lupasol	4.3±0.1	33.8±0.5	3.5±0.4	2.4±0.2
Poly-(2-ethyl-2-oxazoline)	4.4±0.1	33.6±0.5	4.0±0.3	1.9±0.2

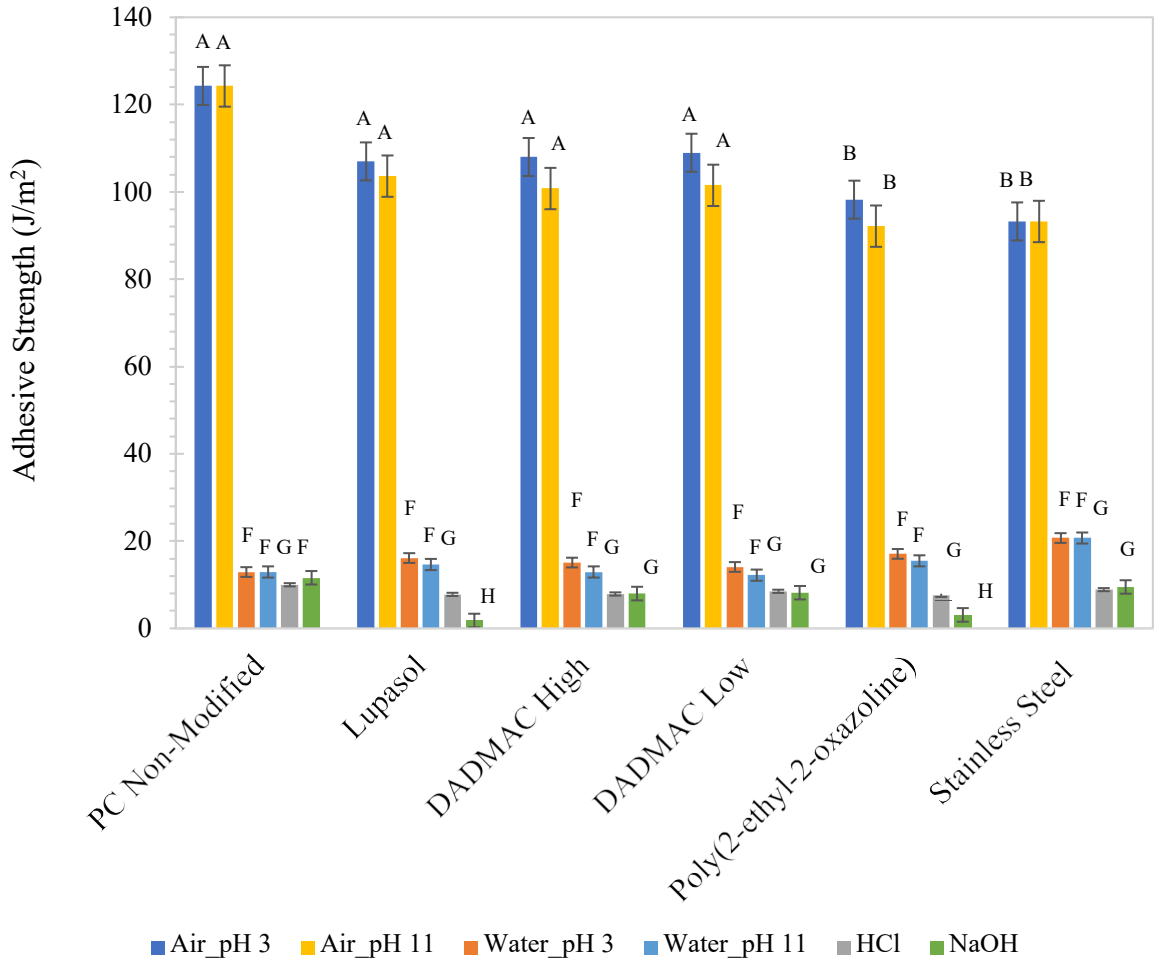

Figure 6.8: Adhesive strength for modified and unmodified surfaces (under different pH conditions) under water, HCl and NaOH solutions. The error bars are the standard deviation of the triplicates' adhesive and cohesive strength respectively. Capital letters indicate statistically significant different groups at each cleaning step (Tukey's test, $p<0.05$). The same letter indicates no significant difference, i.e., A≠A: no significant difference, one similar letter indicates partial difference, i.e., A≠AB: slightly different and different letter indicates significant difference, while the furthest from control letter A, the most significant the difference, i.e., A≠B: significant difference and A≠C: more significant difference.

6.5. Discussion

As biofilm formation is a phenomenon that affects many aspects of public health and industrial processes (Johansen et al. 1997; Palmer et al., 2007; Goode et al., 2013), biofilm attachment has been widely studied and investigated over the years. Boulané-Petermann (1996) concluded that the processes governing bacterial adhesion are physicochemical and depend on the properties of the stainless steel, the bacterium and the surrounding liquid medium. Katsikogianni et al. (2005) reviewed that bacterial adhesion is a complicated process initiated by a physicochemical interaction phase that is followed by a biochemical step. They categorized the techniques used in estimating bacteria–material interactions as those that utilize flow against the adhered bacteria and measuring the percentage of the detached bacteria, and those that manipulate single bacteria in various configurations which lend themselves to more specific force application and provide the basis for theoretical analysis of the receptor–ligand interactions. Nonetheless, as biofilms are highly organized communities composed by planktonic bacteria in an extracellular polymeric matrix (Otto, 2008) that provides mechanical stability and protection against cleaning agents (Flemming et al., 2016; Gordon et al., 2017), biofilm detachment and cleaning is a challenging problem to investigate and solve.

To understand the mechanisms that enhance biofilm removal, several studies have tried to model detachment kinetics of biofilms from artificial surfaces. The most important outcome was the observation that removal is not a straightforward process and that adequate elimination requires the combination of hydrodynamic force coupled with chemical agents (Lécrigny-Nolf et al., 2000; Blel et al., 2007; Faille et al., 2013; Bénézech and Faille, 2018). However, to our knowledge, there are no studies that correlate the biofilm removal with their adhesion forces and eventually their attachment on surfaces. Thus, in this study, alginic acid an anionic polysaccharide that appears to be a material of interest when it comes to biofilms (Grządka and

Matusiak, 2017), was chosen as a model material to replace biofilm for a better control of its parameters. The aim was to investigate the adhesive and cohesive force of the alginic acid on different material surfaces and under different cleaning conditions, as an effort to correlate the effect of biofilm forces in its cleaning performance from artificial substrates. For this reason, the adhesive and cohesive strength of alginic acid was studied as a control under air and then in three cleaning conditions 1) water, 2) NaOH solution (1%w/w, pH 11) and 3) HCl solution (1%w/w, pH 3). Surfaces of interest that are abundant in the industrial and the household environment were stainless steel, and modified and non-modified polycarbonate tiles. It was interesting to investigate the effect of surface modification on biofilm attachment by using cationic polymers with quaternary ammonium groups that have been investigated and are considered to have high antibacterial activity (Beyth et al., 2012; Nelson et al., 2017; Pal et al., 2018). The antibacterial action of these materials relies on their positive charge (Nelson et al., 2017) that can interact with the negatively charged groups in the bacterial membrane and cause a disinfectant effect.

First, it was seen that the polymer surface modification caused a transformation in the physicochemical properties of the substrates. On the one hand the average work of adhesion, thus the wettability of the surfaces, was increased, which is believed that played a key role in the increase of the adhesive force of the alginic acid on the chemically modified surfaces. On the other hand, the average roughness was simultaneously decreased, a phenomenon that probably affected the average surface area of the interphase between the alginic acid, the material surface and the aqueous media in all the cleaning-condition cases. Finally yet importantly, it was observed that the pH did not play a significant role in the surface modification or in the adhesive and cohesive forces of the alginic acid in all cases.

For the direct measurement of the adhesive and cohesive strength of alginic acid from the so mentioned surfaces, the micromanipulation technique was used. Firstly, it was seen that both the adhesive and cohesive strength of alginic acid when measured on air depended strongly on the substrate. As expected, alginic acid was attached more easily to hydrophobic, nonpolar surfaces such as polycarbonate and other plastics than to hydrophilic materials such as stainless steel (Boulané-Petermann, 1996). Secondly, it was observed that for all surfaces the adhesive strength of alginic acid decreased under all cleaning conditions, water, NaOH solution and HCl solution.

When the tiles were introduced in the aquatic solutions the adhesive strength decreased substantially. The highest difference was observed on the tiles that had been modified using Lupasol (pH 11) where the initial adhesive strength under air was 103.6±0.9 J/m^2 but decreased to 1.8±0.2 J/m^2 under NaOH solution. Similarly, the tiles that had been modified using Poly-(2-ethyl-2-oxazoline) (pH 11) showed an initial adhesive strength of 92.2±1.2 J/m^2 that reduced to 3.1±0.2 J/m^2 under NaOH solution. It is believed that the highly charged cationic polymeric chains of both Poly-(2-ethyl-2-oxazoline) and Lupasol in combination with NaOH, were responsible for influencing the permeability and eventually the adhesive strength of alginic acid. Moreover, the lowest difference on adhesive strength was observed on stainless steel that was introduced in water. In this case the adhesive strength was measured as 93.2±1.8 J/m^2 and as 20.7±6.6 J/m^2 in water.

Furthermore, it was observed that the cohesive strength of alginic acid did not depend on the material surface but mostly on the surrounding cleaning medium, whether that was water, NaOH solution or HCl solution. For water and NaOH it was seen that the cohesive strength of alginic acid was decreased (4.03±0.06 J/m^2 and 2.3±0.02 J/m^2 respectively), whilst

in the case of HCl solution it was increased (34.3±1.6 J/m^2). It is thought that the low pH of HCl solution caused the dehydration of the alginic acid that influenced its cohesive strength. Acid induced transformation of the bulk physical properties of rigidness and mechanical stability of the alginic acid, resulted in the reduction of the adhesive strength respectfully.

6.6. Conclusions

The micromanipulation results of this study indicate that the material of the substrate plays a crucial role in the cohesive force as well as the development of the adhesive force in the interphase with the alginic acid. However, during cleaning conditions it appears that for the cohesive strength what is more important is the nature of the aqueous medium rather than the substrate of interest. Moreover, it was seen that during acidic conditions the cohesive strength of alginic acid increases, while in water and in NaOH solution it decreases. Nonetheless, the adhesive strength declines during cleaning conditions, water, NaOH (pH 11) and HCl solutions (pH 3) and depends highly on the surface. Furthermore, the polymer surface modification of the polycarbonate surfaces had a significant impact on the adhesive strength of the alginic acid in all cases. Of great interest were two polymers, Lupasol and Poly-(2-ethyl-2-oxazoline), as they caused the most important reduction in the adhesive strength of the alginic acid. It is thus believed that further research of those two polymers would give interesting answers for the development of cleaning strategies against biofilm.

CHAPTER 7: OVERALL CONCLUSIONS AND NEXT STEPS

7.1. Overall Conclusions

This project thesis was dedicated in investigating new ways to measure biofilm adhesion and cohesion forces according to different chemistries of modified and non-modified surfaces, as a contribution in the broader goal of BIOCLEAN – "BIOfilm management and CLEANing by leveraging fundamental understanding of biological, chemical and physical combined approaches". Biofilms are challenging to control and their growing resistance in common antimicrobial agents is a severe problem of the 21st century. BIOCLEAN projects, as this thesis, were built in order to understand the physics, biology and chemistry of bacteria, biofilm, cleaning agents and surfaces, on the interphases and in bulk.

The first objective of the present study was to examine the biofilm cleaning behaviour from different material surfaces that have wide applications in domestic areas and industrial sites. Quantification of bacterial detachment from common artificial surfaces is very important in order to determine the effectiveness of several biofilm cleaning agents. For evaluating the effectiveness of biofilm cleaning from the surfaces, there was a need for the development of an easy and reliable method in order to evaluate the effectiveness of biofilm cleaning. Thus, the parallel plate flow chamber was designed and built in a way so that three replicates could be evaluated at a time. Biofilm cleaning was initially monitored via confocal laser scanning microscopy using single species of bacteria under a variety of conditions.

From the range of conditions studied, it was observed that combined CIP procedure with NaOH 0.1%w/w was the most effective cleaning process for all material surfaces. Additionally, in terms of surfaces, it was seen that stainless steel was cleaned more efficiently compared to polycarbonate and plasma-treated polycarbonate surfaces, and that the latter material surfaces showed higher work of adhesion, a parameter that generally increases the fouling of surfaces according to literature. Between the two bacteria strains studied, *P. fluorescens* developed higher percentage of surface coverage compared to *P. putida*, due to their different structure and biofilm development. Consequently, *P. putida* biofilm was removed more easily from all material surfaces. However, the instant swelling during *P. putida* biofilm cleaning, indicates that there is a strong relation of biofilm strain and cleaning behaviour, which is believed is related to the different EPS development of different bacteria strains.

After gaining fundamental knowledge on single-bacteria biofilm cleaning behaviour and the evaluation of the cleaning efficiency method developed, a mixed-microbial biofilm was collected from the "real world". An industrial environment of a meat-packaging line in Spain was the place of interest in order to collect samples from common everyday surfaces and grow a real case biofilm. At this point the biofilm removal was investigated by using commercial, ecologically friendly enzymatic cleaning products as a substitute for the chemical agents studied in the single-bacteria work. The synergistic effect of amylase, protease and lipase on the effectiveness of biofilm cleaning was studied by evaluating four different parameters: biovolume, surface coverage, bacterial viability and polysaccharide content. By using a combination of microscopy techniques (CLSM, SEM), flow cytometry and a polysaccharide extraction technique, the biofilm residual contamination over cleaning was monitored. In order to develop a correlation between these techniques, a quantitative

assessment of cell detachment is required and thus the effectiveness of cleaning has been tested in all cases.

In all, it was observed that enzymes could be highly efficient in biofilm cleaning and the most complete deformation of the biofilm structure, and consequently the better disinfection of the surface, required the synergistic effect of all enzymes. Formulation A, containing all three enzymes, caused the highest reduction in all the parameters studied. It is believed that the combination of the three enzymes weakened the adhesive and cohesive forces of the EPS organic compounds and removed the biofilm from the surfaces more efficiently than the other two formulations that were missing lipase (formulation B) and protease (formulation C) enzymes respectively. As EPS regulates biofilm adhesion on surfaces, it is believed that the efficiency of formulation A that contained all three enzymes may be due to its broad-spectrum activity in degrading a variety of EPS compounds. However, EPS biofilm formation depends on the growth medium, which is a fact that creates yet another parameter in the choice of the biofilm cleaning agents according to the industry.

Biofilms on the two material surfaces used in the enzyme cleaning work had significantly different structures. On stainless steel, the biofilm was smaller in thickness while the biofilm grown on polyethylene terephthalate showed greater bacterial viability and higher biovolume, while both surfaces showed similar biofilm surface area covered and EPS-polysaccharide content. An additional overall observation was that stainless steel was cleaned more successfully than polyethylene terephthalate. It is thought that the increased biovolume and average biomass thickness on polyethylene terephthalate surfaces compared to stainless steel played an important role in their difference in cleaning efficacy. In addition,

the higher bacterial viability observed on polyethylene terephthalate might have aided stronger attachment properties, which led to the reduced cleanability of the surface.

The different cleaning behaviour of the three formulations on polyethylene terephthalate surfaces against polysaccharide reduction was an indication that effective cleaning it is not only a matter of enzyme concentration. However, it is believed the physical chemistry of the interfaces between the surface, the surfactants and the enzymes in the formulations as well as the biofilm geometry at the nanoscale might play a significant role in EPS breakage and eventually biofilm cleaning. Finally yet importantly, it was confirmed that disinfection was crucial for effective biofilm cleaning; incomplete disinfection of the control surfaces that were not treated with enzymes shows that the combination of the processes is essential for successful biofilm cleaning.

The overall conclusions of the two biofilm studies, both the single-species and mixed-species bacteria, were two: First, it was observed in all cases that stainless steel surfaces showed increased cleaning efficiency against plastics (polycarbonate, plasma-treated polycarbonate and PET), regardless of the biofilm type or the cleaning agent. This is an important conclusion that contributes to current literature, which will allow industries to choose their working surfaces accordingly, while taking into account parameters of cost, efficiency and biofilm cleaning behaviour. The second conclusion was that the combined chemistry along with mechanical stress would benefit in the cleaning efficiency of all surfaces, again regardless of the biofilm type and cleaning agent. This is a general conclusion which shows that agents with a broader spectrum of cleaning efficacy would be more beneficial for everyday industrial use, although, again the selective choice of specific

biofilm cleaning agents would save costs and increase cleaning efficiency.

Finally, after collecting information on the biofilm cleaning behaviour the goal was to directly measure adhesion and cohesion forces in the biofilm matrix. For this study a micromanipulation technique was used. It is difficult to measure the forces required to disrupt biofilm, as it is a sensitive and challenging material to measure forces, and the micromanipulation rig available for this study showed limitations at the microscale needed for biofilm monitoring. As a result, alginic acid was chosen as a biologically relevant soil that is abundant in EPS of some of the *Pseudomonas* genus biofilms. The work undertaken in this project aimed to develop new understanding of biofilms via investigation of their adhesive and cohesive strengths on different substrates and the effects of surface modification on those strengths, as an effort to correlate the effect of biofilm forces in its cleaning performance from artificial substrates. For this reason, the adhesive and cohesive strength of alginic acid was studied, first as a control under air and then under three cleaning conditions; 1) water, 2) NaOH solution (pH 11) and 3) HCl solution (pH 3). Surfaces of interest that are abundant in the industrial and the household environment were used, both stainless-steel, and modified and non-modified polycarbonate tiles. The effect of surface modification on biofilm attachment was studied by using four polymers that are considered to show antibacterial activity: DADMAC of high and low molecular weight, Lupasol and Poly-(2-ethyl-2-oxazoline).

The micromanipulation results indicate that the material of the substrate plays a crucial role in the cohesive force as well as the development of the adhesive force in the interphase with the alginic acid. As expected, alginic acid attached more easily to

hydrophobic, nonpolar surfaces such as polycarbonate and other plastics than to hydrophilic materials such as stainless steel. However, under cleaning conditions it appears that, for the cohesive strength, what is more important is the nature of the aqueous medium rather than the substrate of interest. It was seen that during acidic conditions the cohesive strength of alginic acid increases, while in water and in NaOH solution it decreases. Nonetheless, the adhesive strength declines during cleaning conditions, water, NaOH (pH 11) and HCl solutions (pH 3) and depends highly on the surface. Furthermore, the polymer surface modification of the polycarbonate surfaces had a significant impact on the adhesive strength of the alginic acid in all cases. Of great interest were two polymers, Lupasol and Poly-(2-ethyl-2-oxazoline), as they caused the most important reduction in the adhesive strength of the alginic acid. It is thus believed that further research of those two polymers would give interesting answers for the development of cleaning strategies against biofilm.

7.2. Future recommendations

By looking at the conclusions of the three studies several interesting ideas are born. Since the results from all studies have been very promising the next goal would be to expand the experiments through the combination of the relevant conditions. The direct measurement of adhesion forces of grown biofilms on surfaces is the most important next step in the understanding of biofilm cleaning behaviour according to surfaces. The micromanipulation system tested in Chapter 6 can be used at the micron-mm scale to measure model biofilms, but is not well suited to measurements at the micron scale that would be needed to study real biofilms. The first step in future work would thus be the development of a new biofilm scraper base plate that can be connected to a more advanced micromanipulation rig with a

more sensitive probe. This system would allow measurement of forces at the microscale, and include an optics system that would facilitate the instant visualization of biofilms during measurements. An initial system has been designed but was not completed in the research.

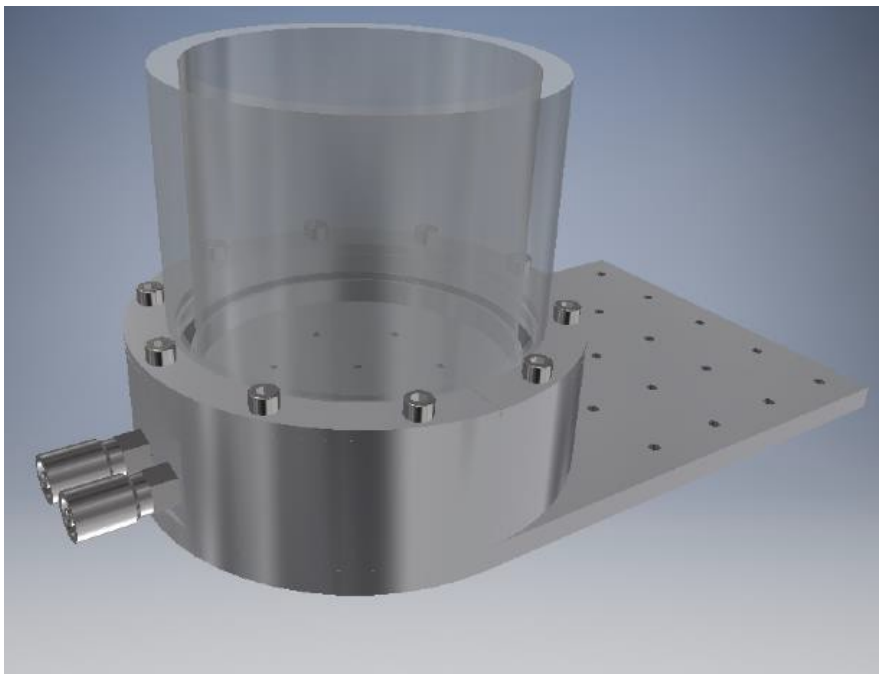

Figure 7.1: Representation of the new advanced biofilm scraper plate base.

The idea is simply that inside a polycarbonate vessel as shown in **Figure 7.1** a rotating coupon holder would be mounted for placing 6 coupons for measurement. The biofilms can be grown on the coupons using the CDC bioreactor as described in Chapter 4. As it appears in **Figure 7.2**, the vessel is a double-wall stainless steel to which a polycarbonate transparent tube-like tank is attached. Through the double-wall vessel, water can be circulated in order to achieve desired temperatures for cleaning conditions. Any cleaning fluid that needs to be tested can be placed in the vessel. The strength of any biofilm in the system can be tested using a probe. Unlike the T-shaped probe used in the micromanipulation experiments, the

new probe has a small diameter so that it can be pushed into and through the biofilm. It's diameter size and accuracy are a matter of further investigation. Over the biofilm scraper base a high-definition fluorescence microscope camera could be used to visualize the probe as it contacts the film.

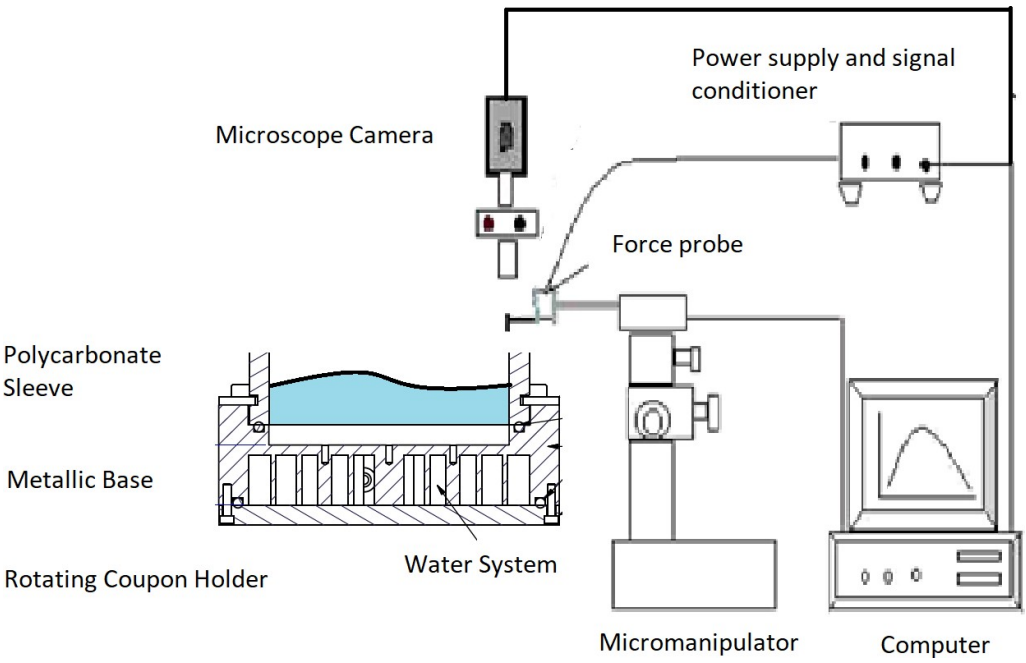

Figure 7.2: Schematic representation of the system

This type of equipment would enable to measure the adhesion forces between surface and bacterial films while they will be placed inside different cleaning formulations. Some of these experiments that are recommended are:

1) Study the adhesion of *P. fluorescens* and *P. putida* on stainless steel, polycarbonate and modified polycarbonate surfaces with Lupasol and Poly-(2-ethyl-2-oxazoline) polymers in single enzymatic formulations.

2) Study the adhesion of *P. fluorescens* and *P. putida* grown on stainless steel, polycarbonate and modified polycarbonate surfaces with Lupasol and Poly-(2-ethyl-2-oxazoline) polymers in water, NaOH and different enzymatic formulations.

3) Study the adhesion forces of any kind of real case biofilm grown on industrial surfaces of individual interest in water, NaOH and different enzymatic formulations and disinfectants.

These are some of the examples that would contribute to the knowledge acquired by this thesis. Such a device could be used accordingly to the individual interest for all kinds of biofilms, surfaces and cleaning agents combined. Also, it could be used for more fundamental microbiological studies such as the mechanisms through which the enzymes degrade the EPS proteins, polysaccharides and lipids, as a further step in the development of new eco-friendly detergents in biofilm management and cleaning.

Overall, this thesis has demonstrated how biofilms can be grown and quantified in a number of ways, using both lab-grown and industrial biofilms as well as model systems, and a variety of measurement methods. It is clear that measurements of biofilm structure and strength can be used to select suitable chemicals to minimize the effects of the biofilm. Given the ubiquity of biofilms in a wide variety of fields, such measurements will have practical as well as academic value.

8. REFERENCES

Abdallah, M., Benoliel, C., Drider, D., Dhulster, P., and Chihib, N.-E. (2014). 'Biofilm formation and persistence on abiotic surfaces in the context of food and medical environments', *Archives of Microbiology*, 196(7), p.453–472.

Achinas, S., Charalampogiannis, N. and Euverink, G., (2019). 'A Brief Recap of Microbial Adhesion and Biofilms', *Applied Sciences*, 9(14), p.2801.

Addae-Mensah, K. A., Wikswo, J. P. (2008). 'Measurement Techniques for Cellular Biomechanics *In Vitro'*, *Experimental Biology and Medicine*, 233(7), p.792-809.

Adner, N., Sofer, G. (1994). Biotechnology Product Validation, part 3: Chromatography Cleaning Validation. *Biopharm* 7, 44–48.

Ahimou, F., Semmens, M. J., Novak, P. J., Haugstad, G. (2007). 'Biofilm Cohesiveness Measurement Using a Novel Atomic Force Microscopy Methodology', *Applied and Environmental Microbiology*, 73(9), p.2897- 2904.

Akhtar, N., Bowen, J., Asteriadou, K., Robbins, P., Zhang, Z., & Fryer, P. (2010). 'Matching the nano- to the meso-scale: Measuring deposit- surface interactions with atomic force microscopy and micromanipulation', *Food and Bioproducts Processing*, 88(4), 341-348.

Ali, A., DeAth, D., Gibson, D., Parkin, J., Alam, Z., Ward, G., & Wilson, D. I. (2015). 'Development of a 'millimanipulation' device to study the removal of soft solid fouling

layers from solid substrates and its application to cooked lard deposits', *Food and Bioproducts Processing*, 93, 256-268.

Alvarado-Gomez, E., Perez-Diaz, M., Valdez-Perez, D., Ruiz-Garcia, J., Magaña-Aquino, M., Martinez-Castañon, G. and Martinez-Gutierrez, F. (2018). 'Adhesion forces of biofilms developed in vitro from clinical strains of skin wounds', *Materials Science and Engineering: C,* 82, p.336-344.

Angeloni, L., Passeri, D. (2016). 'A Review on Microbial Cells Force Spectroscopy by Using Atomic Force Microscopy', *Nanoscience and Nanometrology*, 2(1), p.30-40.

Araújo, E. A., de Andrade, N. J., da Silva, L. H. M., de Carvalho, A. F., de S Silva, C. A., Ramos, A. M. (2010). 'Control of microbial adhesion as a strategy for food and bioprocess technology', *Food and Bioprocess Technology*, 3(3), p.321-332.

Asally, M., Kittisopikul, M., Ru, P., Du, Y., Hu, Z., aatay, T., Sel, G. M. (2012). 'Localized cell death focuses mechanical forces during 3D patterning in a biofilm', *Proceedings of the National Academy of Sciences*, 109(46), p.18891-18896.

Baier, RE (2006). 'Surface behaviour of biomaterials: *The theta surface* for biocompatibility', *Journal of Materials Science: Materials in Medicine*, 17(11), 1057–1062.

Bayoudh, S., Ponsonnet, L., Ben Ouada, H., Bakhrouf, A., and Othmane, A. (2005). 'Bacterial detachment from hydrophilic and hydrophobic surfaces using a microjet impingement', *Colloids and Surfaces A: Physicochemical and Engineering Aspects.,* 266,

(1-3), p.160–167.

Bayoudh, S., Othmane, A., Mora, L., Ouada, H. B. (2009). 'Assessing bacterial adhesion using DLVO and XDLVO theories and the jet impingement technique', *Colloids and Surfaces B: Biointerfaces,* 73, (1), p.1-9.

Beauvais A, Schmidt C, Guadagnini S, Roux P, Perret E, et al. (2007) An extracellular matrix glues together the aerial-grown hyphae of Aspergillus fumigatus. *Cellular Microbiology* 9, p. 1588–1600.

Bénézech, T., and Faille, C. (2018). 'Two-phase kinetics of biofilm removal during CIP. Respective roles of mechanical and chemical effects on the detachment of single cells vs cell clusters from a *Pseudomonas fluorescens* biofilm', *Journal of Food Engineering*, 219, p.121-128.

Beyth, N., I. Yudovin-Farber, E.i. Weiss, and A.j. Domb. (2012). 'Antimicrobial Nanoparticles in Restorative Composites', in Subramani, K., Ahmed, W. (ed.) In Micro and Nano Technologies, *Emerging Nanotechnologies in Dentistry*, p. 35-47, William Andrew Publishing.

Blel, W., Bénézech, T., Legentilhomme, P., Legrand, J., & Gentil-Lelièvre, C. L. (2007). 'Effect of flow arrangement on the removal of Bacillus spores from stainless steel equipment surfaces during a Cleaning In Place procedure', *Chemical Engineering Science*, 62(14), p.3798-3808.

Blel, W., Legentilhomme, P., Legrand, J., Bénézech, T., & Gentil-Lelièvre, C. L. (2008). 'Hygienic design: Effect of hydrodynamics on the cleanability of a food processing line', *AIChE Journal*, 54(10), p.2553-2566.

Block, S. S. (1991). 'Disinfection, sterilization, and preservation', Philadelphia: Lea & Febiger.

Boonaert, C. J. P., Dufrene, Y., and Rouxhet, P. G. (2003). 'Adhesion (primary) of microorganisms onto surfaces', *Encyclopedia Environmental Microbiology.* Bitton G., (ed.), p. 113–132, John Wiley, NY.

Boulané-Petermann, L. (1996). 'Processes of bioadhesion on stainless steel surfaces and cleanability: A review with special reference to the food industry', *Biofouling: The Journal of Bioadhesion and Biofilm Research*, 10(4), p.275-300.

Bowen, W. R., Lovitt, R. W., Wright, C. J. (2001). 'Atomic Force Microscopy Study of the Adhesion of *Saccharomyces cerevisiae'*, *Journal of Colloid and Interface Science*, 237(1), p.54-61.

Breijyeh, Z., Jubeh, B. and Karaman, R. (2020). 'Resistance of Gram-Negative Bacteria to Current Antibacterial Agents and Approaches to Resolve It', *Molecules*, 25(6), 1340.

Bucs, S., Farhat, N., Kruithof, J., Picioreanu, C., van Loosdrecht, M. and Vrouwenvelder, J., (2018). 'Review on strategies for biofouling mitigation in spiral wound membrane systems', *Desalination*, 434, p.189-197.

Busscher, H. J., Weerkamp, A. H., van der Mei, H. C., Van Pelt, A. W., de Jong, H. P.,

Arends, J. (1984). 'Measurement of the surface free energy of bacterial cell surfaces and its relevance for adhesion', *Applied and Environmental Microbiology*, 48(5), p.980-983.

Chapalain, A., Rossignol, G., Lesouhaitier, O., Merieau, A., Gruffaz, C., Guerillon, J. (2008). 'Comparative study of 7 fluorescent pseudomonad clinical isolates', *Canadian Journal of Microbiology,* 54(1), p.19–27.

Chaudhury M. K., Finlay J. A., Chung J. Y., Callow M.E., Callow J. E. (2005). 'The influence of elastic modulus and thickness on the release of the soft-fouling green alga *Ulva linza* (syn. *Enteromorpha linza*) from poly(dimethylsiloxane) (PDMS) model networks', *Biofouling: The Journal of Bioadhesion and Biofilm Research,* 21(1), p. 41 – 48.

Chen, M., Zhang, Z. and Bott T. (1998). 'Direct measurement of the adhesive strength of biofilms in pipes by micromanipulation', *Biotechnology Techniques*, 12, p.875-880.

Chen, M., Zhang, Z., & Bott, T. (2005). 'Effects of operating conditions on the adhesive strength of *Pseudomonas fluorescens* biofilms in tubes', *Colloids and Surfaces B: Biointerfaces*, 43(2), p.61-71.

Chia, T. W. R., Nguyen, V. T., McMeekin, T., Fegan, N. and Dykes, G. A. (2011). 'Stochasticity of Bacterial Attachment and Its Predictability by the Extended Derjaguin-Landau-Verwey-Overbeek Theory', *Applied and Environmental Microbiology*, 77(11), p.3757–3764.

Choi, N. C. Choi, J. W., Kwon, K. S., Lee, S. G. and Lee, S. (2017). 'Quantifying bacterial attachment and detachment using leaching solutions of various ionic strengths after bacterial

pulse', *AMB Express,* 7, p.38.

Cohen, B., Pinkas, O., Foox, M., and Zilberman, M.. (2013). 'Gelatin–Alginate Novel Tissue Adhesives and Their Formulation–Strength Effects', *Acta Biomaterialia* 9 (11), p.9004–9011.

Colagiorgi, A., Bruini, I., Di Ciccio, P. A., Zanardi, E., Ghidini, S., and Ianieri, A. (2017). '*Listeria monocytogenes* Biofilms in the Wonderland of Food Industry', *Pathogens,* 6(3), p.41.

Coughlan, L. M., Cotter, P. D., Hill, C., and Álvarez-Ordóñez, A. (2016). New weapons to fight old enemies: novel strategies for the (bio)control of bacterial biofilms in the food industry. *Front. Microbiol.* 7:1641.

Dagang, W. W., Bowen, J., OKeeffe, J., Robbins, P. T., Zhang, Z. (2016). 'Adhesion of *Pseudomonas fluorescens* biofilms to glass, stainless steel and cellulose', *Biotechnology Letters*, 38(5), p.787-792.

Dincer, S., Uslu, F.M. and Delik, A. (2020). Antibiotic Resistance in Biofilm. *Bacterial Biofilms*. [online] Available at: https://www.intechopen.com/books/bacterial-biofilms/antibiotic-resistance-in-biofilm.

De La Fuente, L., Montanes, E., Meng, Y., Li, Y., Burr, T. J., Hoch, H. C., Wu, M. (2007). 'Assessing Adhesion Forces of Type I and Type IV Pili of *Xylella fastidiosa* Bacteria by Use of a Microfluidic Flow Chamber', *Applied and Environmental Microbiology*, 73(8), p.2690-2696.

Derjaguin, B., Landau, L. (1993). 'Theory of the stability of strongly charged lyophobic sols and of the adhesion of strongly charged particles in solutions of electrolytes', *Progress in Surface Science*, 43(1-4), p.30-59.

Detry, J.G., Sindic, M., & Deroanne, C. (2010). 'Hygiene and Cleanability: A Focus on Surfaces', *Critical Reviews in Food Science and Nutrition*, 50(7), p.583-604.

Donlan, R. M. (2002). 'Biofilms: Microbial Life on Surfaces', *Emerging Infectious Diseases,* 8(9), p.881-890.

Dong, W., Li, B., Wei, J., Tian, N., Liang, W. and Zhang, J. (2021). Environmentally friendly, durable and transparent anti-fouling coatings applicable onto various substrates. *Journal of Colloid and Interface Science*, 591, pp.429–439.

Doyle, S. P., Kjellebergbcd, Rice, A.S., Liang, Y., Seviour, T., Kundukad, R. B. (2016). 'Mechanical properties of the superficial biofilm layer determine the architecture of biofilms', *Soft Matter*, 12, p.5718-5726.

Drehlich, J., Tormoen, G. W., and Beach, E. R. (2004). 'Determination of solid surface tension from particle-substrate pull-off forces measured with the atomic force microscope', *Journal of Colloid and Interface Science,* 280(2), p.484-497.

Drury, J. L., Dennis, R. G., Mooney, D. J. (2004). 'The tensile properties of alginate hydrogels', *Biomaterials*, 25(16), p.3187-3199.

Ebnesajjad, S. (2008). 'Adhesives technology handbook' Norwich, Ny: William Andrew Pub, p. 37-46.

Elias, S. and Banin, E. (2012). 'Multi-species biofilms: Living with friendly neighbors', *FEMS Microbiology Reviews* 36, p. 990–1004.

Erath, J., Schmidt, S., Fery, A. (2010). 'Characterization of adhesion phenomena and contact of surfaces by soft colloidal probe AFM', *Soft Matter*, 6(7), p.1432-1437.

Faille, C., Bénézech, T., Blel, W., Ronse, A., Ronse, G., Clarisse, M., and Slomianny, C. (2013). 'Role of mechanical vs. chemical action in the removal of adherent Bacillus spores during CIP procedures', *Food Microbiology*, 33(2), p.149-157.

Fang, Herbert H. P., Chan, K. Y. and Xu, L. C. (2000). 'Quantification of bacterial adhesion forces using atomic force microscopy (AFM)', *Journal of Microbiological Methods*, 40, (1), p.89–97.

Ferrando, D., Ziemba, C., Herzberg, M. (2017). 'Revisiting interrelated effects of extracellular polysaccharides during biofouling of reverse osmosis membranes: Viscoelastic properties and biofilm enhanced osmotic pressure', *Journal of Membrane Science*, 523, p.394-401.

Flemming, H., Wingender, J., Szewzyk, U., Steinberg, P., Rice, S. A., & Kjelleberg, S. (2016). 'Biofilms: An emergent form of bacterial life', *Nature Reviews Microbiology*, 14(9), p.563-575.

Fletcher, M., & Loeb, G. (1979). 'Influence of substratum characteristics on the attachment of a marine pseudomonad to solid surfaces', *Applied and Environmental Microbiology*, 37(1), p.459-469.

Flint, S. H., Brooks, J. D., and Bremer, P. J. (2000). 'Properties of the stainless steel substrate, influencing the adhesion of thermo-resistant streptococci', *Journal of Food Engineering,* 43(4), p.235–242.

Földes, E., Tóth, A., Kálmán, E., Fekete, E. and Tomasovszky–Bobák, A., (2000). 'Surface changes of corona-discharge-treated polyethylene films', *Journal of Applied Polymer Science*, 76(10), p.1529-1541.

Frank, J. F., and Chmielewski, R. (2001). 'Influence of Surface Finish on the Cleanability of Stainless Steel', *Journal of Food Protection*, 64(8), p.1178-1182.

Galié, S., García-Gutiérrez, C., Miguélez, E.M., Villar, C.J. and Lombó, F. (2018). Biofilms in the Food Industry: Health Aspects and Control Methods. *Frontiers in Microbiology*, 9.

Garrett, T. R., Bhakoo, M., & Zhang, Z. (2007). 'Characterization of bacterial adhesion and removal in a flow chamber by micromanipulation measurements', *Biotechnology Letters*, 30(3), p.427-433.

Good, R. J. (1993). 'Contact angle, wetting, and adhesion: A critical review', In: Contact Angle, Wettability and Adhesion, Mittal, K. S., Ed., VSP, Philadelphia. 336.

Goode, K. R., Asteriadou, K., Robbins, P. T., & Fryer, P. J. (2013). 'Fouling and Cleaning Studies in the Food and Beverage Industry Classified by Cleaning Type', *Comprehensive Reviews in Food Science and Food Safety*, 12(2), p.121-143.

Goode, K., R., Christian, G., K., & Fryer, P. J. (2016). 'Improving the Cleaning of Heat Exchangers', Huub Lelieveld, H., Holah, j., and Gabrić, D. (ed.), In Woodhead Publishing Series in Food Science, Technology and Nutrition, *Handbook of Hygiene Control in the Food Industry (Second Edition)*, Woodhead Publishing, p.465-489.

Gordon, V. D., David-Fields, M., Kovach, K., Rodesney, C.A. (2017). 'Biofilms and mechanics: a review of experimental techniques and findings', *Journal of Physics D: Applied Physics*, 50(22), article id 223002.

Gottenbos, B., Mei, H. C. V. D., Busscher, H. J. (2000). 'Initial adhesion and surface growth of *Staphylococcus epidermidis* and *Pseudomonas aeruginosa* on biomedical polymers', *Journal of Biomedical Materials Research*, 50(2), p.208-214.

Grządka, E., and J. Matusiak. (2017). 'The Effect of Ionic and Non-Ionic Surfactants and PH on the Stability, Adsorption and Electrokinetic Properties of the Alginic Acid/Alumina System', *Carbohydrate Polymers,* 175, p.192–98.

Guillemot, G., Vaca-Medina, G., Martin-Yken, H., Vernhet, A., Schmitz, P., and Mercier-Bonin, M. (2006). 'Shear-flow induced detachment of *Saccharomyces cerevisiae* from stainless steel: Influence of yeast and solid surface properties', *Colloid and Surfaces B: Biointerfaces,* 49(2), p.126–135.

Guzel, M., Afsar, Y., Akdogan, D., Moncheva, P., Hristova, P., and Erdem, G. (2018). 'Evaluation of metallo-beta-lactamase production in multiple antibiotic resistant *Pseudomonas* spp. and *Acinetobacter baumannii* strains', *Biotechnology and Biotechnological Equipment,* 32(5), p.1285–1290.

Harriott, M.M. (2019). Biofilms and Antibiotics. *Reference Module in Biomedical Sciences*.

Helander, I. M., K. Latva-Kala, and K. Lounatmaa. (1998). 'Permeabilizing action of polyethyleneimine on Salmonella typhimurium involves disruption of the outer membrane and interactions with lipopolysaccharide', *Microbiology* 144(2), p.385-390.

Hermansson, M. (1999). 'The DLVO theory in microbial adhesion', *Colloids and Surfaces B: Biointerfaces,* 14(1-4), p.105–119.

Herrera, J. J. R., Cabo, M. L., Gonzlez, A., Pazos, I., Pastoriza, L. (2007). 'Adhesion and detachment kinetics of several strains of *Staphylococcus aureus* subsp. *aureus* under three different experimental conditions', *Food Microbiology*, 24(6), p.585-591.

Hochmuth, R. M., Mohandas, N., Blackshear, P. L. (1973). 'Measurement of the elastic modulus for red cell membrane using a fluid mechanical technique', *Biophysical Journal*, 13(8), p.747-762.

Høiby N, Bjarnsholt T, Givskov M, Molin S, Ciofu O. (2010). 'Antibiotic resistance of bacterial biofilms', *International Journal of Antimicrobial Agents*, 35(4), p.322-32.

Hooper, R., Liu, W., Fryer, P., Paterson, W., Wilson, D., & Zhang, Z. (2006). 'Comparative Studies of Fluid Dynamic Gauging and a Micromanipulation Probe for Strength Measurements', *Food and Bioproducts Processing*, 84(4), p.353-358.

Herman-Bausier, P., Formosa-Dague, C., Feuillie, C., Valotteau, C., Dufrêne, Y. F. (2017). 'Forces guiding staphylococcal adhesion', *Journal of structural biology*, 197(1), p.65-69.

Hung, C.-C., Santschi, P.H. and Gillow, J.B. (2005). ''Isolation and characterization of extracellular polysaccharides produced by *Pseudomonas fluorescens* Biovar II'', *Carbohydrate Polymers*, 61(2), pp.141–147.

Ichinose, Y., Taguchi, F., and Mukaihara, T. (2013). 'Pathogenicity and virulence factors of *Pseudomonas syringae*', *Journal of General Plant Pathology,* 79, p.285–296.

Jiang S., Cao, Z. (2010). 'Ultralow-Fouling, Functionalizable, and Hydrolyzable Zwitterionic Materials and Their Derivatives for Biological Applications', *Advanced Materials*, 22(9), p.920-932.

Johansen, C., Falholt, P. and Gram, L. (1997). 'Enzymatic Removal and Disinfection of Bacterial Biofilms', *Applied and Environmental Microbiology*, 63 (9), p.3724–3728.

Jucker, B. A., Zehnder, A. J., Harms, H. (1998). 'Quantification of Polymer Interactions in Bacterial Adhesion', *Environmental Science and Technology*, 32(19), p.2909-2915.

Jutila M.A., Walcheck B., Bargatze R., Palecanda A. (2007). 'Measurement of Neutrophil

Adhesion under Conditions Mimicking Blood Flow', *Neutrophil Methods and Protocols, Methods in Molecular Biology*, 412, p.239–256.

Kappl, M., Butt, H. J. (2002). 'The Colloidal Probe Technique and Its Application to Adhesion Force Measurements', *Particle & Particle Systems Characterization*, 19(3), p.129-143.

Katsikogianni, M., Missirlis, Y. F. (2004). 'Concise review of mechanisms of bacterial adhesion to biomaterials and of techniques used in estimating bacteria-material interactions', *European Cells & Materials*, 8(3), p.37-57.

Kelber, J.A. (1988). 'Plasma Treatment of Polymers for Improved Adhesion', *MRS Proceedings*, 119.

Kirov M., S. (2003). 'Bacteria that express lateral flagella enable dissection of the multifunctional roles of flagella in pathogenesis', *FEMS Microbiology Letters,* 224 (2), p.151-159.

Kohila, V., Susha, T., Prabhawathia, V. Boobalana, T., Shilpa, N., S., Mukesh, D. (2013). 'In vitro biocompatibility of modified polycarbonate as a biomaterial', *Colloids and Surfaces B: Biointerfaces*, 108, p.191–198.

Krishnan S., Ayothi R., Hexemer A., Finlay J., Sohn K., Perry R., Ober C.K., Kramer E.J., Callow M.E., Callow J.A., Fischer D.A. (2006). 'Anti-Biofouling Properties of Comb-Like Block Copolymer with Amphiphilic Side-Chains', *Langmuir* 22(11), p.5075-5086.

Kuramitsu HK, He X, Lux R, Anderson MH, and Shi W (2007). 'Interspecies interactions within oral microbial communities', *Microbiology and Molecular Biology Reviews* 71, p. 653–670

Kwon, K. W., Choi, S. S., Kim, B., Lee, S. N., Park, M. C., Kim, P., Suh, K. Y. (2006). 'A microfluidic flow sensor for measuring cell adhesion', *In Sensors, 2006. 5th IEEE Conference on (pp. 105-108).*

Lane, W., Jantzen, A., Carlon, T., Jamiolkowski, R., Grenet, J., Ley, M., Haseltine, J., Galinat, L., Lin, F., Allen, J., Truskey, G. and Achneck, H., (2012). 'Parallel-plate Flow Chamber and Continuous Flow Circuit to Evaluate Endothelial Progenitor Cells under Laminar Flow Shear Stress', *Journal of Visualized Experiments*, 59, p.3349.

Lee, H., J., Lee, S., G., Oh, E., J., Chung, H., Y., Han, S., I., Kim, E., J., Seo, S., Y., Ghim, H., D., Yeum, J., H., and Choi J., H., (2011). 'Antimicrobial Polyethyleneimine-silver Nanoparticles in a Stable Colloidal Dispersion', *Colloids and Surfaces B: Biointerfaces,* 88(1), p.505-511.

Lelieveld, H. L., Mostert, M. A., & Holah, J. T. (2005). *Handbook of hygiene control in the food industry. Boca Raton: CRC Press*.

Levine, S., Dube, G. P. (1939). 'Interaction between two hydrophobic colloidal particles, using the approximate Debye-Huckel theory. I. General properties', *Transactions of the Faraday Society*, 35, p.1125–1141.

Li, G., Miles, N., J., Wu, T., & Hall, P. (2017). 'Large eddy simulation and Reynolds-averaged Navier-Stokes based modelling of geometrically induced swirl flows applied for the better understanding of Clean-In-Place procedures', *Food and Bioproducts Processing*, 104, p.77-93.

Li, Q., Wang, Q., Zhu, J., Zhou, S., Gan, M., Jiang, H., Sand, W. (2016). 'Effect of Extracellular Polymeric Substances on Surface Properties and Attachment Behavior of Acidithiobacillus ferrooxidans', *Minerals*, 6(4), p.100.

Liu, H., Fang, H., P. (2003). 'Extraction of extracellular polymeric substances (EPS) of sludge', *Biotechnology*, 95, p. 249-256.

Liu, W., Aziz, N., Zhang, Z., & Fryer, P. (2007). 'Quantification of the cleaning of egg albumin deposits using micromanipulation and direct observation techniques', *Journal of Food Engineering*, 78(1), p.217-224.

Liu, W., Christian, G., Zhang, Z., & Fryer, P. (2002). 'Development and Use of a Micromanipulation Technique for Measuring the Force Required to Disrupt and Remove Fouling Deposits', *Food and Bioproducts Processing*, 80(4), p.286-291.

Liu, W., Fryer, P., Zhang, Z., Zhao, Q., & Liu, Y. (2006). 'Identification of cohesive and adhesive effects in the cleaning of food fouling deposits', *Innovative Food Science & Emerging Technologies*, 7(4), p.263-269.

Liu, W., Zhang, Z., & Fryer, P. (2006). 'Identification and modelling of different removal

modes in the cleaning of a model food deposit', *Chemical Engineering Science*, 61(22), p.7528-7534.

Lu, H., Koo, L. Y., Wang, W. M., Lauffenburger, D. A., Griffith, L. G., Jensen, K. F. (2004). 'Microfluidic Shear Devices for Quantitative Analysis of Cell Adhesion', *Analytical chemistry*, 76(18), p.5257-5264.

Mack, D. (1999). 'Molecular mechanisms of Staphylococcus epidermidis biofilm formation', *Journal of Hospital Infection*, 43, p.113-125.

Magens, O. M., Liu, Y., Hofmans, J. F., Nelissen, J. A., & Wilson, D. I. (2017). 'Adhesion and cleaning of foods with complex structure: Effect of oil content and fluoropolymer coating characteristics on the detachment of cake from baking surfaces', *Journal of Food Engineering*, 197, p.48-59.

Marshall, K. C., Stout, R., Mitchell, R. (1971). 'Mechanism of the Initial Events in the Sorption of Marine Bacteria to Surfaces', *Microbiology*, 68(3), p.337-348.

Martines, E., McGhee, K., Wilkinson, C., & Curtis, A. (2004). 'A parallel-plate flow chamber to study initial cell adhesion on a nanofeatured surface', *IEEE Transactions on Nanobioscience*, 3(2), p.90-95.

Mayer, C., Moritz, R., Kirschner, C., Borchard, W., Maibaum, R., Wingender, J., Flemming, H. C. (1999). 'The role of intermolecular interactions: studies on model systems for bacterial biofilms', *International Journal of Biological Macromolecules*, 26(1), p.3-16.

Michalski, M. C., Desobry, S., Mousavi, M., and Hardy, J. (1998). 'Prediction of mass residues on food-contact surfaces from edible oils and their emulsions', *Journal of Food Engineering,* 37(3), p.271-291.

Missirlis, Y. F., Spiliotis, A. D. (2002). 'Assessment of techniques used in calculating cell material interactions', *Biomolecular Engineering*, 19(2), p.287-294.

Molobela, I. P., Cloete, T. E. and Beukes, M. (2010). 'Protease and amylase enzymes for biofilm removal and degradation of extracellular polymeric substances (EPS) produced by *Pseudomonas fluorescens* bacteria', *African Journal of Microbiology Research* 4(14), p. 1515-1524.

Morra, M., Cassinelli, C. (1996). 'Staphylococcus epidermidis adhesion to films deposited from hydroxyethylmethacrylate plasma', *Journal of Biomedical Materials Research Part A*, 31(2), p.149-155

Munson, B., Young, D. F. and Okiishi, T. H. (1990). *Fundamentals of Fluid Mechanics*, 3rd ed. New York: Wiley.

Nahar, S., Mizan, M., Ha, A. and Ha, S., (2018). 'Advances and Future Prospects of Enzyme-Based Biofilm Prevention Approaches in the Food Industry', *Comprehensive Reviews in Food Science and Food Safety,* 17(6), p.1484-1502.

Nelson V., A. and Rodríguez-Hernández, J.. (2017). 'Antimicrobial Polymeric

Nanostructures', in Ficai A. and Grumezescu, A., M. (ed.), In Micro and Nano Technologies, *Nanostructures for Antimicrobial Therapy*, Elsevier, p.85-115.

Neuman, K. C., Nagy, A. (2008). 'Single-molecule force spectroscopy: optical tweezers, magnetic tweezers and atomic force microscopy', *Nature methods*, 5(6), p.491.

Ober, C. (2017). 'Fifty years of the Baier curve: progress in understanding antifouling coatings', *Green Materials*, 5(1), p.1–3.

Ong, Y. L., Razatos, A., Georgiou, G., Sharma, M. M. (1999). 'Adhesion Forces between E. coli bacteria and biomaterial surfaces', *Langmuir*, 15(8), p.2719-2725.

Orgaz, B., Kives, J., Pedregosa, A., M., Monistrol, I., F., Laborda, F., SanJose, C. (2006). 'Bacterial biofilms removal using fungal enzymes' *Enzymatic Microbial Technology*, 40, p. 51-56.

Otto, K. (2008). 'Biophysical approaches to study the dynamic process of bacterial adhesion', *Research in microbiology*, 159(6), p.415-422

Palmer, J., Flint, S., & Brooks, J. (2007). 'Bacterial cell attachment, the beginning of a biofilm', *Journal of Industrial Microbiology & Biotechnology*, 34(9), p.577-588.

Parkar, S. G., Flint, S. H., Palmer, J. S., and Brooks, J. D. (2001). 'Factors influencing attachment of thermophilic bacilli to stainless steel', *Journal of Applied Microbiology,* 90(6), p.901–908.

Peters BM, Jabra-Rizk MA, O'may GA, Costerton JW, and Shirtliff ME (2012)

‘Polymicrobial interactions: Impact on pathogenesis and human disease’, *Clinical Microbiology Reviews* 25, p. 193–213.

Planinsek, O., Trojak, A., and Srcic, S. (2001). ‘The dispersive component of the surface free energy of powders assessed using inverse gas chromatography and contact angle measurements’, *International Journal of Pharmaceutics,* 221(1–2), p.211-217.

Puricelli, L., Galluzzi, M., Schulte, C., Podest, A., Milani, P. (2015). ‘Nanomechanical and topographical imaging of living cells by atomic force microscopy with colloidal probes’, *Review of Scientific Instruments*, 86(3), 033705.

Quintieri L., Fanelli F., Zühlke D., Caputo L., Logrieco A.F., Albrecht D. and Riedel K. (2020). ‘Biofilm and Pathogenesis-Related Proteins in the Foodborne *P. fluorescens* ITEM 17298 With Distinctive Phenotypes During Cold Storage’, *Frontiers in Microbiology,* 11, p.991.

Raposo, A., Pérez, E., de Faria, C. T., Ferrús, M. A., and Carrascosa, C. (2017). ‘Food spoilage by *Pseudomonas* spp.—an overview’, in *Food Borne Pathogens and Antibiotic Resistance*, ed. O. V. Singh (Hoboken, NJ: John Wiley & Sons), p.41–58.

Raweewan, T. and Rawiwan L. (2015). ‘Competitive binding of polyethyleneimine-coated gold nanoparticles to enzymes and bacteria: a key mechanism for low-level colorimetric detection of gram-positive and gram-negative bacteria’, *Microchimica Acta,* 183(1), p.389-96.

Robinson, P.K. (2015). Enzymes: principles and biotechnological applications. *Essays In Biochemistry*, 59(0), pp.59–75.

Santini, J. T., Cima, M. J., Langer, R. (1999). 'A controlled-release microchip', *Nature*, 397, p.335-338.

Sharma, D., Misba, L. & Khan, A.U. (2019). 'Antibiotics versus biofilm: an emerging battleground in microbial communities', *Antimicrobial Resistance & Infection Control,* 8, article No 76.

Sharma, P. K., Hanumantha Rao, K. (2003). 'Adhesion of Paenibacillus polymyxa on chalcopyrite and pyrite: surface thermodynamics and extended DLVO theory', *Colloids and Surfaces B: Biointerfaces,* 29(1), p.21- 38.

Siebold, A., Walliser, A., Nardin, M., Oppliger, M., and Schultz, J. (1997). 'Capillary Rise for Thermodynamic Characterization of Solid Particle Surface', *Journal of Colloid and Interface Science,* 186(1), p.60-70.

Simoes, M., de Carvalho, H., Pereira, M., O., Viera, M., J. (2003). 'Studies on the behaviour of *Pseudomonas fluorescens* biofilms after Ortho-phthalaldehyde treatment' *Biofouling*, 3, p. 151-157.

Stoodley, P., Hall-Stoodley, L., Costerton, B., DeMeo, P., Shirtliff, M., Gawalt, E. and Kathju, S. (2013). Biofilms, Biomaterials, and Device-Related Infections. *Handbook of Polymer Applications in Medicine and Medical Devices*, pp.77–101.

ThermExcel, 2003-2019, France, [accessed 2017 Apr 30] Messe, J. Y. https://www.thermexcel.com/english/tables/eau_atm.htm

Tsiaprazi-Stampou, A., Ylla Monfort, I., Romani, A. M., Bakalis, S. and Gkatzionis, K. (2019). 'The synergistic effect of enzymatic detergents on biofilm cleaning from different surfaces', *Biofouling*, 35, (8), p.883-899.

Verwey, E. J. W., Overbeek, J. Th. G. (1948). 'Theory of the Stability of Lyophobic Colloids', *The Journal of Physical and Colloid Chemistry, Amsterdam: Elsevier*, 51 (3), p.631–636.

Wall, G. (2017). Functionalised Cardiovascular Stents, p.155-198.

Wang, Y. X., Xiang, C., Liu, B., Zhu, Y., Luan, Y., Liu, S. T., Qin, K. R. (2016). 'A multi-component parallel-plate flow chamber system for studying the effect of exercise-induced wall shear stress on endothelial cells', *BioMedical Engineering OnLine*, 15(2), Article No 154.

Wang, B., Ye, Z., Xu, Q., Liu, H., Lin, Q., Chen, H. and Nan, K. (2016). 'Construction of a temperature-responsive terpolymer coating with recyclable bactericidal and self-cleaning antimicrobial properties', *Biomaterial Science*, 4(12), 1731-1741.

Weigel L., M., Donlan R., M., Shin D., H., Jensen B., Clark N., C., et al. (2007). 'High-level vancomycin-resistant Staphylococcus aureus isolates associated with a polymicrobial biofilm'. *Antimicrobial Agents and Chemotherapy* 51, p. 231–238.

Weinman C. J., Finlay J. A., Park D., Paik M.Y., Krishnan S., Sundaram H.S., Dimitriou M., Sohn K.E., Callow M.E., Callow J.A., Handlin D. L., Willis C.L., Kramer E.J., Ober C.K. (2009). 'ABC Triblock Surface-Active Block Copolymers with Grafted Ethoxylated Fluoroalkyl Amphiphilic Side Chains for Marine Anti-Fouling/Fouling-Release Applications', *Langmuir*, 25(20), p.12266-12274.

Wypych, G. (2015). PVC Degradation and Stabilization (Third Edition). Pages 215-226, 7.

Yamamoto R, Noiri Y, Yamaguchi M, Asahi Y, Maezono H, Kuboniwa M, et al. (2013). 'The *sinR* Ortholog PGN_0088 Encodes a Transcriptional Regulator That Inhibits Polysaccharide Synthesis in *Porphyromonas gingivalis* ATCC 33277 Biofilms', *PLOS ONE,* 8(2), Article No 56017.

Yin, J. L., Mei, M. L., Li, Q. L., Xia, R., Zhang, Z. H. and Chu, C. H. (2016). 'Self-cleaning and antibiofouling enamel surface by slippery liquid-infused technique', *Scientific Reports* 6, Article No 25924.

Yuehuei H. An, and Richard J. Friedman. (1998). 'Concise review of mechanisms of bacterial adhesion to biomaterial surfaces', *Journal of Biomedical Materials Research*, 43(3), p.338–348.

Zhang, Z., Ferenczi, M., & Thomas, C. (1992). 'A micromanipulation technique with a theoretical cell model for determining mechanical properties of single mammalian cells', *Chemical Engineering Science*, 47(6), p.1347-1354.

Zeng, G., Müller, T. and Meyer R. L. Meyer. (2014). 'Single-Cell Force Spectroscopy of Bacteria Enabled by Naturally Derived Proteins', *Langmuir*, 30(14), p.4019−4025.

Zhu, J., Li, Q., Jiao, W., Jiang, H., Sand, W., Xia, J., Chai, L. (2012). 'Adhesion forces between cells of *Acidithiobacillus ferrooxidans*, *Acidithiobacillus thiooxidans* or *Leptospirillum ferrooxidans* and chalcopyrite', *Colloids and Surfaces B: Biointerfaces*, 94, p.95-100.

Zeriouh, O., Marco-Rocamora, A., Reinoso-Moreno, J. V., López-Rosales, L., García-Camacho, F., Molina-Grima, E. (2019). 'New insights into developing antibiofouling surfaces for industrial photobioreactors', *Biotechnology and Bioengineering*, 116(9), p.2212–2222.

Zisman, W. A. and Fowkes, F. (1964). 'Contact Angle, Wettability, and Adhesion. Advances in Chemistry', *Washington*, *American Chemical Society*, 43, p.1–51.